Proceedings of the

Electroporation based Technologies and Treatments

International SCIENTIFIC WORKSHOP and POSTGRADUATE COURSE

Ljubljana, Slovenia
November 15-21, 2015

ISBN 978-961-243-293-5

9 789612 432935

Proceedings of the Workshop is also available in PDF format at *2015.ebtt.org/proceedings*

Electroporation based Technologies and Treatments 2015

EUROPEAN COOPERATION IN SCIENCE AND TECHNOLOGY

November 15-21, 2015
Ljubljana, Slovenia

LEA EBAM

Proceedings of the

Electroporation based Technologies and Treatments

International SCIENTIFIC WORKSHOP and POSTGRADUATE COURSE

Edited by:

Peter Kramar
Damijan Miklavčič
Lluis M. Mir

Organised by:

University of Ljubljana
Faculty of Electrical Engineering

Institute of Oncology, Ljubljana

Supported by:

Bioelectrochemical Society
Le Centre national de la recherche scientifique
Laboratory for Telecomunications LTFE

BEHLKE
BIA Separations
FuG Elektronik
IGEA
Intracel
Iskra Medical
Kemomed
Leroy Biotech

Course conducted in the scope of EBAM European Associated Laboratory (LEA)

www.ebtt.org

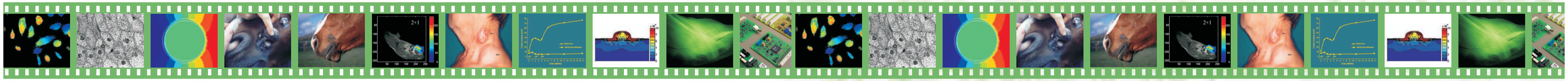

LEA EBAM

cost
EUROPEAN COOPERATION
IN SCIENCE AND TECHNOLOGY

B E S
The Bioelectrochemical Society

LIFE

cnrs

BEHLKE
HIGH-TECH IN HIGH VOLTAGE

BIA separations

fug

IGEA
CLINICAL BIOPHYSICS

INTRACEL
Electroporation by ABBOTSBURY

IskraMedical

KEMOMED
BRINGING SOLUTIONS

leroy
BIOTECH

2nd World Congress on Electroporation and Pulsed Electric Fields
In Biology, Medicine, Food & Environmental Technologies

Norfolk, Virginia USA **September 24-28, 2017**

Tentative topics of the World Congress 2017

- Basics, biology of electroporation
- Basics, modeling of electroporation including MD studies
- Technology for PEF and large treatment capacities
- Technology for electric pulses for research and medical applications
- Medical applications (ECT, IRE, GET)
- Food industry applications
- Environmental applications
- Micro and Nanotechnologies (single cell electroporation, microfluidics …)

November 15-21, 2015
Ljubljana, Slovenia

Proceedings of the

COST TD1104

Electroporation-Based Technologies and Treatments

International SCIENTIFIC WORKSHOP and POSTGRADUATE COURSE

Edited by:
Peter Kramar
Damijan Miklavčič
Lluis M. Mir

Organised by:
University of Ljubljana
Faculty of Electrical Engineering

Institute of Oncology, Ljubljana

Organising committee:
Chair:
Peter Kramar
Members:
Matej Kranjc, Lea Vukanović,
Tadeja Forjanič

Supported by:
Bioelectrochemical Society
Le Centre national de la recherche scientifique
Laboratory for Telecomunications LTFE
BEHLKE
BIA Separations
FuG Elektronik
IGEA
Intracel
Iskra Medical
Kemomed
Leroy Biotech

Course conducted in the scope of EBAM European Associated Laboratory (LEA).

www.ebtt.org

CIP - Kataložni zapis o publikaciji
Narodna in univerzitetna knjižnica, Ljubljana

602.621(082)
577.352.4(082)

PROCEEDINGS of the electroporation based technologies and treatments : international scientific workshop and postgraduate course, November 15-21, 2015, Ljubljana, Slovenia / organised by University of Ljubljana, Faculty of Electrical Engineering [and] Institute of Oncology, Ljubljana ; edited by Peter Kramar, Damijan Miklavčič, Lluis M. Mir. - 1. izd. - Ljubljana : Založba FE, 2015

ISBN 978-961-243-293-5
1. Kramar, Peter, 1977- 2. Fakulteta za elektrotehniko (Ljubljana) 3. Onkološki inštitut (Ljubljana)
281882624

Založnik: Založba FE, Ljubljana
Izdajatelj: UL Fakuleta za elektrotehniko, Ljubljana
Urednik: prof. dr. Sašo Tomažič

Natisnil: Tiskarna Bori
Naklada: 90 izvodov
1. izdaja

Welcome note

Dear Colleagues,

Dear Students,

The idea of organizing the Workshop and Postgraduate Course on Electroporation Based Technologies and Treatments at the University of Ljubljana had been developing for several years. After preliminary discussions, the Workshop and Course was organised for the first time in 2003. In twelve years the Course has been attended by 508 participants coming from 31 different countries. And this year again we can say with great pleasure: “with participation of many of the world leading experts in the field”.

The aim of the lectures at this Workshop and Course is to provide the participants with sufficient theoretical background and practical knowledge to allow them to use electroporation effectively in their working environments.

It also needs to be emphasized that all written contributions collected in this proceeding have been peer-reviewed and then thoroughly edited by Peter Kramar. We thank all authors, reviewers and editors. Finally, we would like to express our sincere thanks to colleagues working in our and collaborating laboratories for their lectures and for the preparation of the practical trainings delivered during the course, to the agencies that have been sponsoring our research work for years, and to Slovenian Research Agency, Centre National de la Recherche Scientifique (CNRS) and to the Bioelectrochemical Society. We also would like to thank BEHLKE (Germany), BIA Separations (Slovenia), FuG Elektronik (Germany), Igea (Italy), Intracel (UK) Iskra Medical (Slovenia), Kemomed (Slovenia), and Leroy Biotech (France), whose financial support allowed us to assist many students participating in this Workshop and Course. The course is conducted in the scope of the LEA EBAM (European Associated Laboratory on the Pulsed Electric Fields Applications in Biology and Medicine). Finally it needs to be stressed that EBTT also became a training school of the COST TD1104 action which covers part of expenses and provides grants for students.

Thank you for participating in our Workshop and Course. We sincerely hope that you will benefit from being with us both socially and professionally.

Sincerely Yours,

Damijan Miklavčič and Lluis M. Mir

COST (European Cooperation in Science and Technology) is a pan-European intergovernmental framework. Its mission is to enable break-through scientific and technological developments leading to new concepts and products and thereby contribute to strengthening Europe's research and innovation capacities.

It allows researchers, engineers and scholars to jointly develop their own ideas and take new initiatives across all fields of science and technology, while promoting multi- and interdisciplinary approaches. COST aims at fostering a better integration of less research intensive countries to the knowledge hubs of the European Research Area. The COST Association, an International not-for-profit Association under Belgian Law, integrates all management, governing and administrative 10 functions necessary for the operation of the framework. The COST Association has currently 36 Member Countries. www.cost.eu

This Proceedings is based upon work from COST Action TD1104, supported by COST (European Cooperation in Science and Technology)

EUROPEAN COOPERATION
IN SCIENCE AND TECHNOLOGY

COST is supported by the EU Framework Programme Horizon 2020

LECTURERS' ABSTRACTS

Resting and Induced Transmembrane Voltage

Tadej Kotnik
University of Ljubljana, Faculty of Electrical Engineering, Ljubljana, Slovenia

Abstract: Under physiological conditions, a resting voltage in the range of tens of millivolts is continually present on the cell plasma membrane. An exposure of the cell to an external electric field induces an additional component of transmembrane voltage, proportional to the strength of the external field and superimposing onto the resting component for the duration of the exposure. Unlike the resting voltage, the induced voltage varies with position, and also depends on the shape of the cell and its orientation with respect to the electric field. In cell suspensions, it also depends on the volume fraction occupied by the cells. There is a delay between the external field and the voltage induced by it, typically somewhat below a microsecond, but larger when cells are suspended in a low-conductivity medium. As a consequence of this delay, for exposures to electric fields with frequencies above 1 MHz, or to electric pulses with durations below 1 μs, the amplitude of the induced voltage starts to decrease with further increase of the field frequency or further decrease of the pulse duration. With field frequencies approaching the gigahertz range, or with pulse durations in the nanosecond range, this attenuation becomes so pronounced that the voltages induced on organelle membranes in the cell interior become comparable, and can even exceed the voltage induced on the plasma membrane.

THE CELL AND ITS PLASMA MEMBRANE

A biological cell can be considered from various aspects. We will skip the most usual description, that of a biologist, and focus on two more technical ones, electrical and geometrical.

From the electrical point of view, a cell can roughly be described as an electrolyte (the cytoplasm) surrounded by an electrically insulating shell (the plasma membrane). Physiologically, the exterior of the cell also resemble an electrolyte. If a cell is exposed to an external electric field under such conditions, in its very vicinity the field concentrates within the membrane. This results in an electric potential difference across the membrane, termed the *induced transmembrane voltage*, which superimposes onto the *resting transmembrane voltage* typically present under physiological conditions. Transmembrane voltage can affect the functioning of voltage-gated membrane channels, initiate the action potentials, stimulate cardiac cells, and when sufficiently large, it also leads to cell membrane electroporation, with the porated membrane regions closely correlated with the regions of the highest induced transmembrane voltage [1].

With rapidly time-varying electric fields, such as waves with frequencies in the megahertz range or higher, or electric pulses with durations in the submicrosecond range, both the membrane and its surroundings have to be treated as materials with both a non-zero electric conductivity and a non-zero dielectric permittivity.

From the geometrical point of view, the cell can be characterized as a geometric body (the cytoplasm) surrounded by a shell of uniform thickness (the membrane). For suspended cells, the simplest model of the cell is a sphere surrounded by a spherical shell. For augmented generality, the sphere can be replaced by a spheroid (or an ellipsoid), but in this case, the requirement of uniform thickness complicates the description of the shell substantially. If its inner surface is a spheroid or an ellipsoid, its outer surface lacks a simple geometrical characterization, and vice versa.[1] Fortunately, this complication does not affect the steady-state voltage induced on the plasma membrane of such cells, which can still be determined analytically.

Spheres, spheroids, and ellipsoids may be reasonable models for suspended cells, but not for cells in tissues. No simple geometrical body can model a typical cell in a tissue, and furthermore every cell generally differs in its shape from the rest. With irregular geometries and/or with cells close to each other, the induced voltage cannot be determined analytically, and thus cannot be formulated as an explicit function. This deprives us of some of the insight available from explicit expressions, but using modern computers and numerical methods, the voltage induced on each particular irregular cell can still be determined quite accurately.

RESTING TRANSMEMBRANE VOLTAGE

Under physiological conditions, a voltage in the range of –90 mV up to –40 mV is always present on the cell membrane [2,3]. This voltage is caused by a

[1] This can be visualized in two dimensions by drawing an ellipse, and then trying to draw a closed curve everywhere equidistant to the ellipse. This curve is not an ellipse, and if one is content with an approximation, the task is actually easier to accomplish by hand than with basic drawing programs on a computer.

minute deficit of positive ions in the cytoplasm relative to the negative ones, which is a consequence of the transport of specific ions across the membrane. The most important actors in this transport are: (i) the Na-K pumps, which export Na^+ ions out of the cell and simultaneously import K^+ ions into the cell; and (ii) the K leak channels, through which K^+ ions can flow across the membrane in both directions. The resting transmembrane voltage reflects the electrochemical equilibrium of the action of these two mechanisms, and perhaps the easiest way to explain the occurrence of this voltage is to describe how the equilibrium is reached.

The Na-K pump works in cycles. In a single cycle, it exports three Na^+ ions out of the cell and imports two K^+ ions into it. This generates a small deficit of positive ions in the cytoplasm and a gradient of electric potential, which draws positive ions into the cell, and negative ions out of the cell. But at the same time, the pump also generates concentration gradients of Na^+ and K^+, which draw the Na^+ ions into the cell, and the K^+ ions out of the cell. The K^+ ions are the only ones that possess a significant mechanism of passive transport through the membrane, namely the K leak channels, and through these the K^+ ions are driven towards the equilibration of the electrical and the concentration gradient. When this equilibrium is reached, the electrical gradient across the membrane determines the resting transmembrane voltage, which is continually present on the membrane.

The unbalanced ions responsible for the resting transmembrane voltage represent a very small fraction of all the ions in the cytoplasm, so that the osmotic pressure difference generated by this imbalance is negligible. Also, the membrane acts as a charged capacitor, with the unbalanced ions accumulating close to its surface, so that the cytoplasm can in general be viewed as electrically neutral.

INDUCED TRANSMEMBRANE VOLTAGE

When a biological cell is placed into an electric field, this leads to a local distortion of the field in the cell and its vicinity. As outlined in the introductory section of this paper, due to the low membrane conductivity, in the vicinity of the cell the field is concentrated in the cell membrane, where it is several orders of magnitude larger than in the cytoplasm and outside the cell. This results in a so-called induced transmembrane voltage, which superimposes to the resting component. In the following subsections, we describe in more detail the transmembrane voltage induced on cells of various shapes and under various conditions. In each considered case, the principles of superposition allow to obtain the complete transmembrane voltage by adding the resting component to the induced one.

Spherical cells

For an exposure to a DC homogeneous electric field, the voltage induced on the cell membrane is determined by solving Laplace's equation. Although biological cells are not perfect spheres, in theoretical treatments they are usually considered as such. For the first approximation, the plasma membrane can also be treated as nonconductive. Under these assumptions, the induced transmembrane voltage $\Delta\Phi_m$ is given by a formula often referred to as the (steady-state) Schwan's equation [4],

$$\Delta\Phi_m = \frac{3}{2} ER\cos\theta\,, \tag{1}$$

where E is the electric field in the region where the cell is situated, R is the cell radius, and θ is the angle measured from the center of the cell with respect to the direction of the field. voltage is proportional to the applied electric field and to the cell radius. Furthermore, it has extremal values at the points where the field is perpendicular to the membrane, i.e. at $\theta = 0°$ and $\theta = 180°$ (the "poles" of the cell), and in-between these poles it varies proportionally to the cosine of θ (see Fig. 1, dashed).

The value of $\Delta\Phi_m$ given by Eq. (1) is typically established several μs after the onset of the electric field. With exposures to a DC field lasting hundreds of microseconds or more, this formula can safely be applied to yield the maximal, steady-state value of the induced transmembrane voltage. To describe the transient behavior during the initial microseconds, one uses the first-order Schwan's equation [5],

$$\Delta\Phi_m = \frac{3}{2} ER\cos\theta\left(1-\exp(-t/\tau_m)\right), \tag{2}$$

where τ_m is the time constant of membrane charging,

$$\tau_m = \frac{R\,\varepsilon_m}{2d\,\dfrac{\sigma_i\sigma_e}{\sigma_i+2\sigma_e}+R\sigma_m} \tag{3}$$

with σ_i, σ_m and σ_e the conductivities of the cytoplasm, cell membrane, and extracellular medium, respectively, ε_m the dielectric permittivity of the membrane, d the membrane thickness, and R again the cell radius.

In certain experiments *in vitro*, where artificial extracellular media with conductivities substantially lower than physiological are used, the factor 3/2 in Eqns. (1) and (2) decreases in value, as described in detail in [6]. But generally, Eqns. (2) and (3) are applicable to exposures to sine (AC) electric fields with frequencies below 1 MHz, and to rectangular electric pulses longer than 1 μs.

To determine the voltage induced by even higher field frequencies or even shorter pulses, the dielectric permittivities of the electrolytes on both sides of the membrane also have to be accounted for. This leads to a further generalization of Eqns. (2) and (3) to a second-order model [7-9], and the results it yields will be outlined in the last section of this paper.

Spheroidal and ellipsoidal cells

Another direction of generalization is to assume a cell shape more general than that of a sphere. The most straightforward generalization is to a spheroid (a geometrical body obtained by rotating an ellipse around one of its radii, so that one of its orthogonal projections is a sphere, and the other two are the same ellipse) and further to an ellipsoid (a geometrical body in which each of its three orthogonal projections is a different ellipse). To obtain the analogues of Schwan's equation for such cells, one solves Laplace's equation in spheroidal and ellipsoidal coordinates, respectively [10-12]. Besides the fact that this solution is by itself somewhat more intricate than the one in spherical coordinates, the generalization of the shape invokes two additional complications outlined in the next two paragraphs.

A description of a cell is geometrically realistic if the thickness of its membrane is uniform. This is the case if the membrane represents the space between two concentric spheres, but not with two confocal spheroids or ellipsoids. As a result, the thickness of the membrane modeled in spheroidal or ellipsoidal coordinates is necessarily nonuniform. By solving Laplace's equation in these coordinates, we thus obtain the spatial distribution of the electric potential in a nonrealistic setting. However, under the assumption that the membrane conductivity is zero, the induced transmembrane voltage obtained in this manner is still realistic. Namely, the shielding of the cytoplasm is then complete, and hence the electric potential everywhere inside the cytoplasm is constant. Therefore, the geometry of the inner surface of the membrane does not affect the potential distribution outside the cell, which is the same as if the cell would be a homogeneous non-conductive body of the same shape.[2] A more rigorous discussion of the validity of this approach can be found in [10]. Fig. 1 compares the transmembrane voltage induced on two spheroids with the axis of rotational symmetry aligned with the direction of the field, and that induced on a sphere.

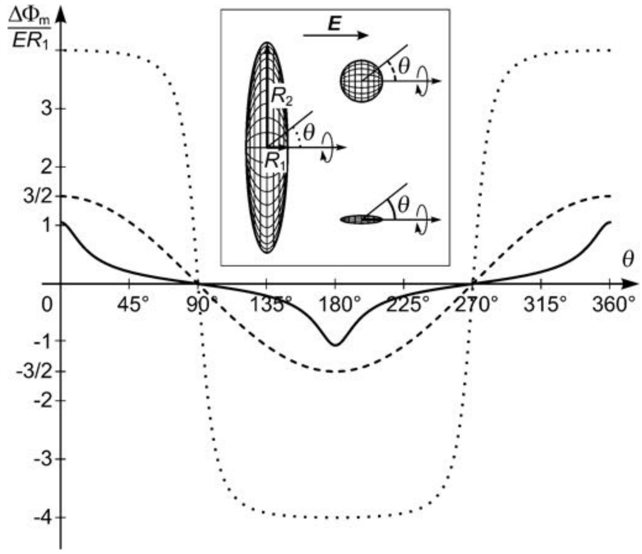

Figure 1: Normalized steady-state $\Delta\Phi_m$ as a function of the polar angle θ for spheroidal cells with the axis of rotational symmetry aligned with the direction of the field. Solid: a prolate spheroidal cell with $R_2 = 0.2 \times R_1$. Dashed: a spherical cell, $R_2 = R_1 = R$. Dotted: an oblate spheroidal cell with $R_2 = 5 \times R_1$.

For nonspherical cells, it is generally more revealing to express $\Delta\Phi_m$ as a function of the arc length than as a function of the angle θ (for a sphere, the two quantities are directly proportional). For uniformity, the normalized version of the arc length is used, denoted by *p* and increasing from 0 to 1 equidistantly along the arc of the membrane. This is illustrated in Fig. 2 for the cells for which $\Delta\Phi_m(\theta)$ is shown in Fig. 1, and all the plots of $\Delta\Phi_m$ on nonspherical cells will henceforth be presented in this manner.

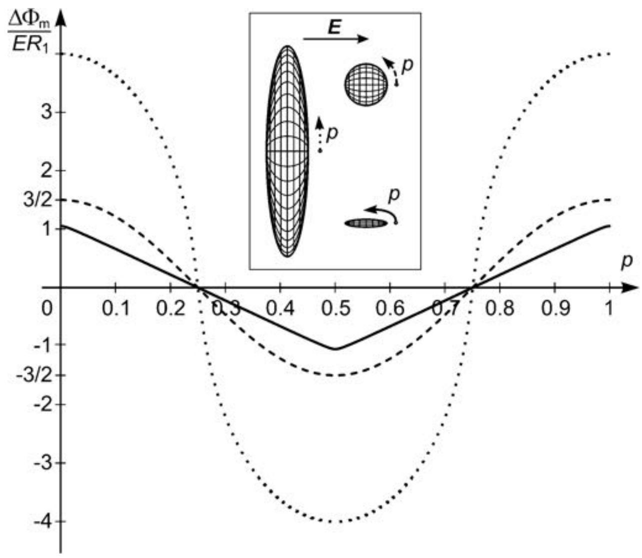

Figure 2: Normalized steady-state $\Delta\Phi_m$ as a function of the normalized arc length *p* for spheroidal cells with the axis of rotational symmetry aligned with the direction of the field. Solid: a prolate spheroidal cell with $R_2 = 0.2 \times R_1$. Dashed: a spherical cell, $R_2 = R_1 = R$. Dotted: an oblate spheroidal cell with $R_2 = 5 \times R_1$.

[2] As a rough analogy, when a stone is placed into a water stream, the streamlines outside the stone are the same regardless of the stone's interior composition. Due to the fact that stone is impermeable to water, only its outer shape matters in this respect. Similarly, when the membrane is nonconductive, or "impermeable to electric current", only the outer shape of the cell affects the current density and the potential distribution outside the cell.

The second complication of generalizing the cell shape from a sphere to a spheroid or an ellipsoid is that the induced voltage now also becomes dependent on the orientation of the cell with respect to the electric field. To deal with this, one decomposes the field vector into the components parallel to the axes of the spheroid or the ellipsoid, and writes the induced voltage as a corresponding linear combination of the voltages induced for each of the three coaxial orientations [11,12]. Figs. 3 and 4 show the effect of rotation of two different spheroids with respect to the direction of the field.

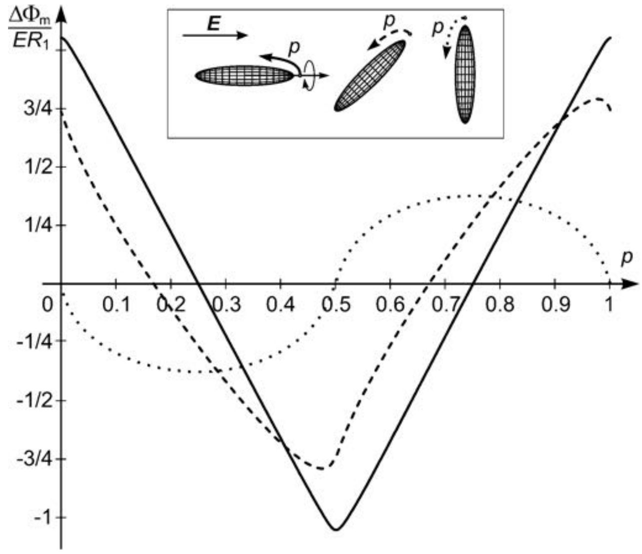

Figure 3: Normalized steady-state $\Delta\Phi_m(p)$ for a prolate spheroidal cell with $R_2 = 0.2 \times R_1$. Solid: axis of rotational symmetry (ARS) aligned with the field. Dashed: ARS at 45° with respect to the field. Dotted: ARS perpendicular to the field.

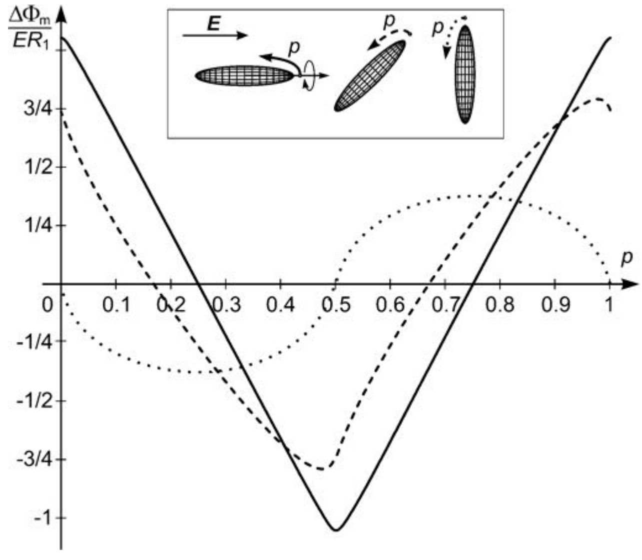

Figure 4: Normalized steady-state $\Delta\Phi_m(p)$ for an oblate spheroidal cell with $R_2 = 5 \times R_1$. Solid: axis of rotational symmetry (ARS) aligned with the field. Dashed: ARS at 45° with respect to the field. Dotted: ARS perpendicular to the field.

Irregularly shaped cells

For a cell having an irregular shape, the induced transmembrane voltage cannot be determined exactly, as for such a geometry Laplace's equation is not solvable analytically. Using modern computers and finite-elements tools such as COMSOL Multiphysics, the voltage induced on a given irregular cell can still be determined numerically, as described in detail in [13,14]. While the results obtained in this manner are quite accurate, they are only applicable to the particular cell shape for which they were computed. Fig. 5 shows examples of two cells growing in a Petri dish and the voltages induced on their membranes.

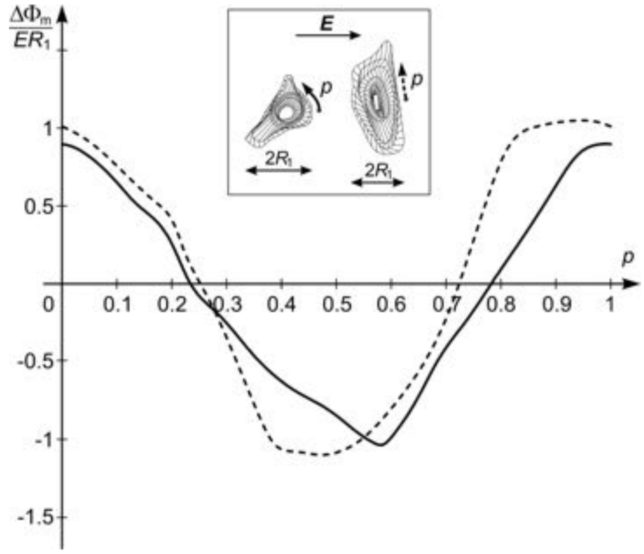

Figure 5: Normalized steady-state $\Delta\Phi_m(p)$ for two irregularly shaped cells growing on the flat surface of a Petri dish.

Cells in dense suspensions

In dilute cell suspensions, the distance between the cells is much larger than the cells themselves, and the local field outside each cell is practically unaffected by the presence of other cells. Thus, for cells representing less than 1 % of the suspension volume (for a spherical cell with a radius of 10 μm, this means up to 2 million cells/ml), the deviation of the actual induced transmembrane voltage from one predicted by Schwan's equation is negligible. However, as the volume fraction occupied by the cells gets larger, the distortion of the local field around each cell by the presence of other cells in the vicinity becomes more pronounced, and the prediction yielded by Schwan's equation less realistic (Fig. 6). For volume fractions over ten percent, as well as for clusters and lattices of cells, one has to use appropriate numerical or approximate analytical solutions for a reliable analysis of the induced transmembrane voltage [15,16]. Regardless of the volume fraction they occupy, as long as the cells are suspended, they are floating freely, and their arrangement is rather uniform. Asymptotically, this would correspond to a face-centered cubic lattice, and this lattice is also the most appropriate for the analysis of the transmembrane voltage induced on cells in suspension.

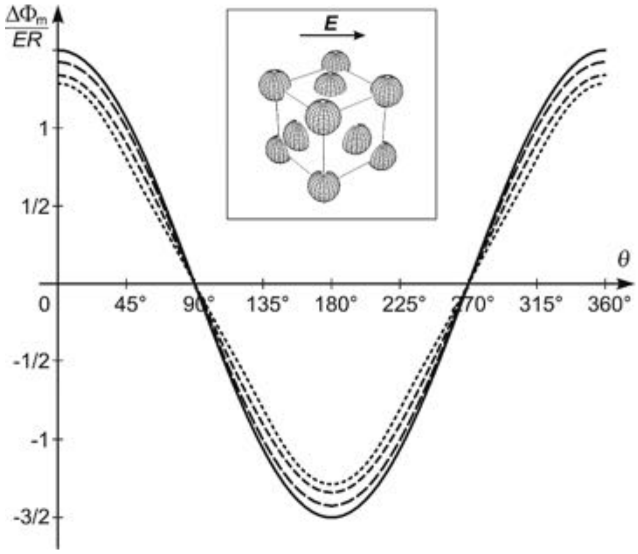

Figure 6: Normalized steady-state $\Delta\Phi_m(\theta)$ for spherical cells in suspensions of various densities (intercellular distances). Solid: The analytical result for a single cell as given by Eq. (1). Dashed: numerical results for cells arranged in a face-centered cubic lattice and occupying (with decreasing dash size) 10%, 30%, and 50% of the total suspension volume.

For even larger volume fractions of the cells, the electrical properties of the suspension start to resemble that of a tissue, but only to a certain extent. The arrangement of cells in tissues does not necessarily resemble a face-centered lattice, since cells can form specific structures (e.g. layers). In addition, cells in tissues can be directly electrically coupled (e.g. through gap junctions). These and other specific features of the interactions between cells in tissues and electric fields will be considered in more detail in the paper that follows this one.

High field frequencies and very short pulses

The time constant of membrane charging (τ_m) given by Eq. (3) implies that there is a delay between the time courses of the external field and the voltage induced by this field. As mentioned above, τ_m (and thus the delay) is somewhat below a microsecond under physiological conditions, but can be larger when cells are suspended in a low-conductivity medium. For alternating (AC) fields with the oscillation period much longer than τ_m, as well as for rectangular pulses much longer than τ_m, the amplitude of the induced voltage remains unaffected. However, for AC fields with the period comparable or shorter than τ_m, as well as for pulses shorter than τ_m, the amplitude of the induced voltage starts to decrease.

To illustrate how the amplitude of the induced transmembrane voltage gets attenuated as the frequency of the AC field increases, we plot the normalized amplitude of the induced voltage as a function of the field frequency. For a spherical cell, the plot obtained is shown in Fig. 6. The low-frequency plateau and the downward slope that follows are both described by the first-order Schwan's equation, but the high-frequency plateau is only described by the second-order model [7-9], in which all electric conductivities and dielectric permittivities are accounted for.

With field frequencies approaching the GHz range, or with pulse durations in the nanosecond range, the attenuation of the voltage induced on the cell plasma membrane becomes so pronounced that this voltage becomes comparable to the voltage induced on organelle membranes in the cell interior. In certain circumstances, particularly if the organelle interior is electrically more conductive than the cytosol, or if the organelle membrane has a lower dielectric permittivity than the cell membrane, the voltage induced on the membrane of this organelle can temporarily even exceed the voltage induced on the plasma membrane [17]. In principle, this could provide a theoretical explanation for a number of recent reports that very short and intense electric pulses (tens of ns, millions or tens of millions of V/m) can also induce electroporation of organelle membranes [18-20].

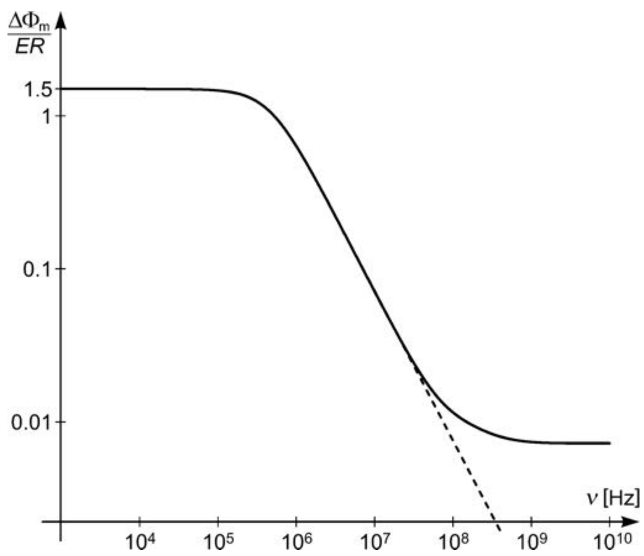

Figure 7: The amplitude of normalized steady-state $\Delta\Phi_m$ as a function of the frequency of the AC field. The dashed curve shows the first-order, and the solid curve the second-order Schwan's equation. Note that both axes are logarithmic.

REFERENCES

[1] T. Kotnik, G. Pucihar, D. Miklavčič. Induced transmembrane voltage and its correlation with electroporation-mediated molecular transport. *J. Membrane Biol.* 236: 3-13, 2010.

[2] K.S. Cole. *Membranes, Ions and Impulses*. University of California Press, Berkeley, USA, 1972.

[3] H.L. Atwood, W.A. Mackay. *Essentials of Neurophysiology*. BC Decker, Toronto, Canada, 1989.

[4] H.P. Schwan. Electrical properties of tissue and cell suspensions. *Adv. Biol. Med. Phys.* 5: 147-209, 1957.

[5] H. Pauly, H.P. Schwan. Über die Impedanz einer Suspension von kugelförmigen Teilchen mit einer Schale. *Z. Naturforsch.* 14B: 125-131, 1959.

[6] T. Kotnik, F. Bobanović, D. Miklavčič. Sensitivity of transmembrane voltage induced by applied electric fields — a theoretical analysis. *Bioelectrochem. Bioenerg.* 43: 285-291, 1997.

[7] C. Grosse, H.P. Schwan. Cellular membrane potentials induced by alternating fields. *Biophys. J.* 63: 1632-1642, 1992.

[8] T. Kotnik, D. Miklavčič, T. Slivnik. Time course of transmembrane voltage induced by time-varying electric fields — a method for theoretical analysis and its application. *Bioelectrochem. Bioenerg.* 45: 3-16, 1998.

[9] T. Kotnik, D. Miklavčič. Second-order model of membrane electric field induced by alternating external electric fields. *IEEE Trans. Biomed. Eng.* 47: 1074-1081, 2000.

[10] T. Kotnik, D. Miklavčič. Analytical description of transmembrane voltage induced by electric fields on spheroidal cells. *Biophys. J.* 79: 670-679, 2000.

[11] J. Gimsa, D. Wachner. Analytical description of the transmembrane voltage induced on arbitrarily oriented ellipsoidal and cylindrical cells. *Biophys. J.* 81: 1888-1896, 2001.

[12] B. Valič, M. Golzio, M. Pavlin, A. Schatz, C. Faurie, B. Gabriel, J. Teissié, M.P. Rols, D. Miklavčič. Effect of electric field induced transmembrane potential on spheroidal cells: theory and experiment. *Eur. Biophys. J.* 32: 519-528, 2003.

[13] G. Pucihar, T. Kotnik, B. Valič, D. Miklavčič. Numerical determination of the transmembrane voltage induced on irregularly shaped cells. *Annals Biomed. Eng.* 34: 642-652, 2006.

[14] G. Pucihar, D. Miklavčič, T. Kotnik. A time-dependent numerical model of transmembrane voltage inducement and electroporation of irregularly shaped cells. *IEEE T. Biomed. Eng.* 56: 1491-1501, 2009.

[15] R. Susil, D. Šemrov, D. Miklavčič. Electric field induced transmembrane potential depends on cell density and organization. *Electro. Magnetobiol.* 17: 391-399, 1998.

[16] M. Pavlin, N. Pavšelj, D. Miklavčič. Dependence of induced transmembrane potential on cell density, arrangement, and cell position inside a cell system. *IEEE Trans. Biomed. Eng.* 49: 605-612, 2002.

[17] T. Kotnik, D. Miklavčič. Theoretical evaluation of voltage inducement on internal membranes of biological cells exposed to electric fields. *Biophys. J.* 90: 480-491, 2006.

[18] K.H. Schoenbach, S.J. Beebe, E.S. Buescher. Intracellular effect of ultrashort electrical pulses. Bioelectromagnetics 22: 440-448, 2001.

[19] S.J. Beebe, P.M. Fox, L.J. Rec, E.L. Willis, K.H. Schoenbach. Nanosecond, high-intensity pulsed electric fields induce apoptosis in human cells. *FASEB J.* 17: 1493-1495, 2003.

[20] E. Tekle, H. Oubrahim, S.M. Dzekunov, J.F. Kolb, K.H. Schoenbach, P. B. Chock. Selective field effects on intracellular vacuoles and vesicle membranes with nanosecond electric pulses. *Biophys. J.* 89: 274-284, 2005.

ACKNOWLEDGEMENT

This work was supported by the Ministry of Higher Education, Science and Technology of the Republic of Slovenia. Research conducted in the scope of the EBAM European Associated Laboratory (LEA).

Tadej Kotnik was born in Ljubljana, Slovenia, in 1972. He received a Ph.D. in Biophysics from University Paris XI and a Ph.D. in Electrical Engineering from the University of Ljubljana, both in 2000. He is currently a Full Professor and the Vice-dean for Research at the Faculty of Electrical Engineering of the University of Ljubljana. His research interests include membrane electrodynamics, theoretical and experimental study of related biophysical phenomena, particularly membrane electroporation and gene electrotransfer.

Tadej Kotnik is the first author of 21 articles in SCI-ranked jour¬nals cited over 650 times to date excluding self-citations. His h-index is 22. In 2001 he received the Galvani Prize of the Bioelectrochemical Society.

NOTES

Electric Properties of Tissues and their Changes during Electroporation

Damijan Miklavčič, Nataša Pavšelj

University of Ljubljana, Faculty of Electrical Engineering, Ljubljana, Slovenia

Abstract: Passive electric properties of biological tissues such as permittivity and conductivity are important in applied problems of electroporation. The current densities and pathways resulting from an applied electrical pulse are dictated to a large extent by the relative permittivity and conductivity of biological tissues. We briefly present some theoretical basis for the current conduction in biologic materials and factors affecting the measurement of tissue dielectric properties that need to be taken into account when designing the measurement procedure. Large discrepancies between the data reported by different researchers are found in the literature. These are due to factors such as different measuring techniques used, the fact that macroscopic tissue properties show inhomogeneity, dispersions, anisotropy, nonlinearity, as well as temperature dependence and changes over time. Furthermore, when biological tissue is exposed to a high electric field, changes in their electric properties occur.

INTRODUCTION

The electrical properties of biological tissues and cell suspensions have been of interest for over a century. They determine the pathways of current flow through the body and are thus very important in the analysis of a wide range of biomedical applications. On a more fundamental level, knowledge of these electrical properties can lead to the understanding of the underlying, basic biological processes. To analyze the response of a tissue to electric stimulus, data on the conductivities and relative permittivities of the tissues or organs are needed. A microscopic description of the response is complicated by the variety of cell shapes and their distribution inside the tissue as well as the different properties of the extracellular media. Therefore, a macroscopic approach is most often used to characterize field distributions in biological systems. Moreover, even on a macroscopic level the electrical properties are complicated. They can depend on the tissue orientation relative to the applied field (directional anisotropy), the frequency of the applied field (the tissue is neither a perfect dielectric nor a perfect conductor) or they can be time and space dependent (e.g., changes in tissue conductivity during electroporation) [1]-[3].

BIOLOGICAL MATERIALS IN THE ELECTRIC FIELD

The electrical properties of any material, including biological tissue can be broadly separated into two categories: conducting and insulating. In a conductor the electric charges move freely in response to the application of an electric field whereas in an insulator (dielectric) the charges are fixed and not free to move – the current does not flow.

If a conductor is placed in an electric field, charges will move within the conductor until the resulting internal field is zero. In the case of an insulator, there are no free charges so net migration of charge does not occur. In polar materials, the positive and negative charge centers in the molecules (e.g. water) do not coincide. An applied field, E_0, tends to orient the dipoles and produces a field inside the dielectric, E_p, which opposes the applied field. This process is called polarization [4]. Most materials contain a combination of dipoles and free charges. Thus the electric field is reduced in any material relative to its free-space value. The resulting internal field inside the material, E, is then

$$E = E_0 - E_p$$

The resulting internal field is lowered by a significant amount relative to the applied field if the material is an insulator and is essentially zero for a good conductor. This reduction is characterized by a factor ε_r, which is called the relative permittivity or dielectric constant, according to

$$E = \frac{E_0}{\varepsilon_r}$$

In practice, most materials, including biological tissue, actually display some characteristics of both, insulators and conductors, because they contain dipoles as well as charges which can move, but in a restricted manner.

On a macroscopic level we describe the material as having a permittivity, ε, and a conductivity, σ. The permittivity characterizes the material’s ability to trap or store charge or to rotate molecular dipoles whereas the conductivity describes its ability to transport charge. The permittivity also helps to determine the speed of light in a material so that free space has a permittivity ε_0 =8.85 x 10-12 F/m. For other media:

$$\varepsilon = \varepsilon_r \varepsilon_0$$

The energy stored per unit volume in a material, u, and the power dissipated per unit volume, p, are:

$$u = \frac{\varepsilon E^2}{2} \qquad p = \frac{\sigma E^2}{2}$$

Consider a sample of material which has a thickness, d, and cross-sectional area, A (Figure 1).

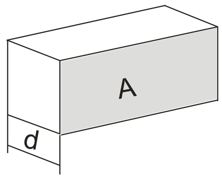

Figure 1: A considered theoretical small part of a material.

If the material is an insulator, then we treat the sample as a capacitor with capacitance (C); if it is a conductor, then we treat it as a conductor with conductance (G):

$$C = \varepsilon \cdot A/d \qquad G = \sigma \cdot A/d$$

A simple model for a real material, such as tissue, would be a parallel combination of the capacitor and conductor. If a constant (DC) voltage V is applied across this parallel combination, then a conduction current I_C = GV will flow and an amount of charge Q=CV will be stored. However, if an alternating (AC) voltage was applied to the combination:

$$V(t)=V_0\cos(\omega t)$$

The charge on the capacitor plates is now changing with frequency f. We characterize this flow as a displacement current:

$$I_d = dQ/dt = -\omega C V_0 \sin(\omega t)$$

The total current flowing through the material is the sum of the conduction and displacement currents, which are 90° apart in phase. The total current is $I = I_c + I_d$, hence

$$I = GV + C \cdot dV/dt = (\sigma + i\omega\varepsilon) A \cdot V/d$$

The actual material, then, can be characterized as having an admittance, Y*, given by:

$$Y^* = G + i\omega C = (A/d)(\sigma + i\omega\varepsilon)$$

where * indicates a complex-valued quantity. In terms of material properties we define a corresponding, complex-valued conductivity

$$\sigma^* = (\sigma + i\omega\varepsilon)$$

Describing a material in terms of its admittance emphasizes its ability to transport current. Alternatively, we could emphasize its ability to restrict the flow of current by considering its impedance Z*=1/Y*, or for a pure conductance, its resistance, R=1/G.

We can also denote total current as:

$$I = (\varepsilon_r - i\sigma/\omega\varepsilon_0) i\omega\varepsilon_0 A/d = C\frac{dV}{dt}$$

We can define a complex-valued, relative permittivity:

$$\varepsilon^* = \varepsilon_r - \frac{i\sigma}{\omega\varepsilon_0} = \varepsilon_r' - i\varepsilon_r''$$

with $\varepsilon_r' = \varepsilon_r$ and $\varepsilon_r'' = \sigma/(\omega\varepsilon_0)$. The complex conductivity and complex permittivity are related by:

$$\sigma^* = i\omega\varepsilon^* = i\omega\varepsilon_0\varepsilon_r^*$$

We can consider the conductivity of a material as a measure of the ability of its charge to be transported throughout its volume in a response to the applied electric field. Similarly, its permittivity is a measure of the ability of its dipoles to rotate or its charge to be stored in response to the applied field. Note that if the permittivity and conductivity of the material are constant, the displacement current will increase with frequency whereas the conduction current does not change. At low frequencies the material will behave like a conductor, but capacitive effects will become more important at higher frequencies. For most materials, however, σ* and ε* are frequency-dependent. Such a variation is called dispersion and is due to the dielectric relaxation – the delay in molecular polarization following changing electric field in a material. Biological tissues exhibit several different dispersions over a wide range of frequencies [4].

Dispersions can be understood in terms of the orientation of the dipoles and the motion of the charge carriers. At relatively low frequencies it is relatively easy for the dipoles to orient in response to the change in applied field whereas the charge carriers travel larger distances over which there is a greater opportunity for trapping at a defect or interface like cell membrane [5]. The permittivity is relatively high and the conductivity is relatively low. As the frequency increases, the dipoles are less able to follow the changes in the applied field and the corresponding polarization disappears. In contrast, the charge carriers travel shorter distances during each half-cycle and are less likely to be trapped. As frequency increases, the permittivity decreases and, because trapping becomes less important, the conductivity increases. In a heterogeneous material, such as biological tissue, several dispersions are observed as illustrated in Figure 2. In short, alpha dispersion in the kilohertz range is due to cell membrane effects such as gated channels and ionic diffusion and is the first of the dispersions to disappear with tissue death. Beta dispersion can be observed around the megahertz range due to the capacitive charging of cell membranes. Above beta dispersion the impedance of cell membranes drops drastically, allowing the electric current to pass through not only extracellular, but also intracellular space. This dispersion is particularly interesting as it is also apparent in the conductivity of the material. The last, gamma dispersion (above the gigahertz range) is due to dipolar mechanisms of water molecules in the material.

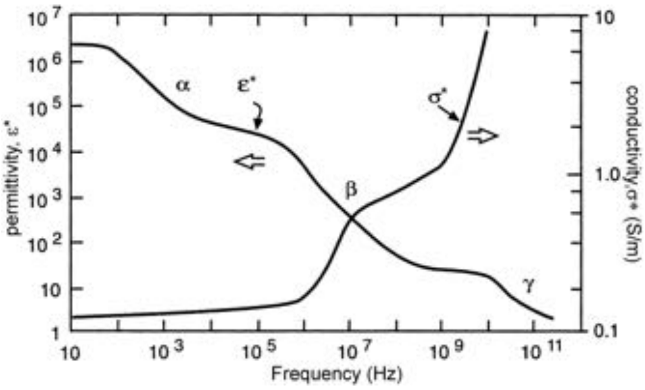

Figure 2: Typical frequency dependence of the complex permittivity and complex conductivity of a heterogeneous material such as biological tissue.

DIELECTRIC MEASUREMENTS OF TISSUES

There is a large discrepancy between data on electrical properties of biological materials found in the literature. The measurement of tissue dielectric properties can be complicated due to several factors, such as tissue inhomogeneity, anisotropy, the physiological state of the tissue, seasonal, age and disease-linked changes and electrode polarization [1].

Inhomogeneity of tissues

Tissue is a highly inhomogeneous material. The cell itself is comprised of an insulating membrane enclosing a conductive cytosol. A suspension of cells can be regarded at low frequencies simply as nonconducting inclusions in a conducting fluid [6]. The insulation is provided by the cell membrane. At frequencies in the MHz range capacitive coupling across this membrane becomes more important, allowing the electric current to pass not only around the cell, but also through it. In tissue, the cells are surrounded by an extracellular matrix, which can be extensive, as in the case of bone, or minimal, as in the case of epithelial tissue. Tissue does not contain cells of a single size and function. The tissue is perfused with blood and linked to the central nervous system by neurons. It is thus difficult to extrapolate from the dielectric properties of a cell suspension to those of an intact tissue.

Anisotropy of tissues

Some biological materials, such as bone and skeletal muscle, are anisotropic. Therefore, when referring to measured conductivity and permittivity values, one needs to include data on the orientation of the electrodes relative to the major axis of the tissue; e.g., longitudinal, transversal or a combination of both. For example, muscles are composed of fibers, very large individual cells aligned in the direction of muscle contraction. Electrical conduction along the length of the fiber is significantly easier than conduction in the direction perpendicular to the fibers. Therefore, muscle tissue manifests typical anisotropic electric properties. The longitudinal conductivity is significantly higher than the transverse conductivity (can be up to 8 times higher).

Moreover, tissue anisotropy is frequency dependent. Namely, if the frequency of the current is high enough, the anisotropic properties disappear. Specifically for muscle tissue, that happens in the MHz frequency range, i.e. at beta dispersion.

Physiological factors and changes of tissue

Any changes in tissue physiology should produce changes in the tissue electrical properties. This principle has been used to identify and/or monitor the presence of various illnesses or conditions [7].

Tumors generally have higher water content than normal cells because of cellular necrosis but also irregular and fenestrated vascularization. Higher conductivity of tumors in the MHz frequency range could lead to their selective targeting by radio-frequency hyperthermia treatment. In addition, there may be differences in the membrane structure. Also, fat is a poorer conductor of electricity than water. Changes in the percentage of body fat or water are reflected in tissue impedance changes [7].

Further, tissue death or excision results in significant changes in electrical properties. Tissue metabolism decreases after the tissue has been excised and often the temperature falls. If the tissue is supported by temperature maintenance and perfusion systems, the tissue may be stabilized for a limited period of time in a living state *in vitro* (*ex vivo*). If the tissue is not supported, however, irreversible changes will occur, followed by cell and tissue death. For these reasons considerable caution must be taken in the interpretation of electrical measurements which were performed on excised tissues.

The electrical properties of tissue also depend on its temperature. The mobility of the ions which transport the current increases with the temperature as the viscosity of the extracellular fluid decreases. The rapid increase of conductivity with temperature was suggested to be used e.g. to monitor the progress of hyperthermia treatment. Also, possible other changes, such as cell swelling and edema, or blood flow occlusion, all affect tissue properties.

Electrode polarization

Electrode polarization is a manifestation of molecular charge organization which occurs at the tissue/sample-electrode interface in the presence of water molecules and hydrated ions. The effect increases with increasing sample conductivity.

In a cell suspension a counterion layer can form at each electrode. The potential drop in this layer reduces the electric field available to drive charge transport in the bulk suspension, resulting in apparently lower suspension conductivity. As the frequency increases, the counterion layer is less able to follow the changes in the applied signal, the potential drop at the sample-electrode interface decreases, and the apparent conductivity of the suspension increases. Thus electrode polarization is more pronounced at lower frequencies.

The process is more complicated in tissue. Insertion of electrodes can first cause the release of electrolytes due to trauma from the surrounding tissue and later the development of a poorly-conductive wound region may occur. This region can shield part of the electrode from the ionic current and thus reduce the polarization effects compared to an ionic solution equivalent in conductivity to the intracellular fluid.

The material of the electrode plays an important part in determining its polarization impedance, the relative importance of which decreases with increasing frequency. It is considered a good practice to measure tissue impedance *in-vivo* after waiting a sufficient time for the electrode polarization processes to stabilize. A typical time might be on the order of thirty minutes.

Two different electrode set-ups are used to measure the electric properties of biological materials; the two-electrode and the four-electrode method.

Two-electrode method: Suitable for alternating current (AC) measurements. Cannot be used as such for direct current (DC) measurements because of the electrode polarization, which consequently gives incorrect results for the conductivity of the sample between the electrodes. For AC measurements the frequency range over which electrode polarization is important depends to some extent on the system being measured and the electrode material. For cell suspensions it is important up to nearly 100 kHz whereas for tissue measured *in vivo* it is significant only up to about 1 kHz. By varying the separation of the electrodes, the contribution of the electrode polarization can be determined and eliminated.

Four-electrode method: Can be used for both DC and AC measurements. Two pairs of electrodes are used: the outer, current electrodes and the inner, voltage electrodes. The current from the source passes through the sample. Voltage electrodes of known separation are placed in the sample between the current electrodes. By measuring the current as the voltage drop across a resistor in series with the sample and the voltage drop across the inner electrodes, one can determine the conductivity of the sample between the inner electrodes. The advantage of this method is that the polarization on the current electrodes has no influence on the voltage difference between the voltage electrodes. Polarization at the voltage electrodes is negligible for both DC and AC due to the high input impedance of the measurement system.

ELECTRICAL RESPONSE OF TISSUE TO ELECTRIC FIELD

Changes in tissue conductivity have been observed *in vivo* if the tissue is subjected to a high enough electric field. Having said that, we can use the dielectric properties of liver and try to calculate the theoretical electrical response to a short rectangular voltage pulse having the duration of 100 µs and the rise time of 1 µs (typical pulse parameters used for electrochemotherapy). We used the parallel RC circuit to model the electrical response of the tissue (see Figure 3).

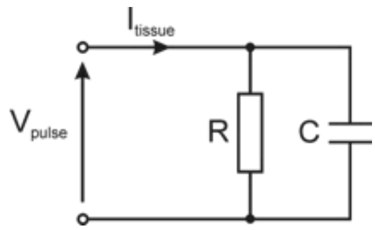

Figure 3: Parallel RC circuit: a theoretical representation of tissue response to electic pulses.

The complications arise from the facts that i) the pulse parameters (the pulse duration, the rise and the fall time) determine the span of its frequency spectrum and ii) the tissue conductivity and permittivity are frequency dependent. The obtained response for the first pulse is presented in Figure 4. At the onset of voltage pulse, capacitive transient displacement current is observed. As membranes charge, voltage across them rises and the measured current decreases. Soon steady state is reached and current stabilizes through the conductance of extracellular fluid. Since the model describing dielectric dispersions is linear, change of the applied voltage proportionally scales the amplitude of the current.

We can compare this calculated response with the measured response on rat liver *in vivo* for the same pulse as above and different pulse amplitudes spanning up to electroporative field strengths (Figure 5) [8]. For the lowest applied voltage we can see a good agreement with calculated response. As the field intensity is increased, the electrical response of tissue is no longer linear and increase of conductivity during the pulse is observed. Measuring the passive electrical properties of electroporated tissues could provide real time feedback on the outcome of the treatment [8], [9].

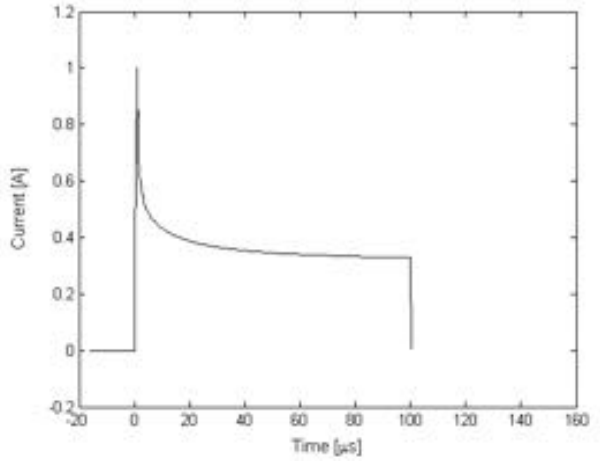

Figure 4: Calculated tissue response during delivery of rectangular voltage pulse with the duration of 100 µs having the rise time of 1 µs and the amplitude of 120 V. Plate electrodes with 4.4 mm interelectrode distance were assumed.

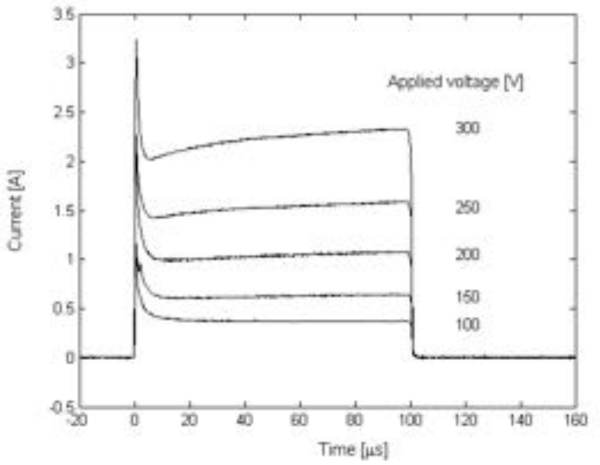

Figure 5: Measured tissue response during delivery of 100 µs rectangular pulses of different amplitudes to rat liver *in vivo*. Adapted from Cukjati *et al.* [8]. Pulses were generated using Jouan GHT1287B; plate electrodes with 4.4 mm interelectrode distance were used.

The measured response is consistent with the hypothesis that the bulk tissue conductivity should also increase measurably since on a cellular level electroporation causes the increase of membrane conductance [10]-[14]. In measuring *ex vivo* tissue and phantom tissue made of gel like material [15] using MREIT we were able to demonstrate that electric conductivity changes due to membrane electroporation are amplitude dependent and occur in tissue only but not in phantom tissue. It is not clear, however, to which value tissue conductivity increases as a consequence of plasma membrane electroporation. It has been stipulated that this could be close to the value in beta dispersion range [16].

Further, in applications where electric pulses to skin or tissues underneath (such as subcutaneous tumor) are applied externally, through skin, one might expect high (too high) voltage amplitudes needed in order to breach the highly resistive skin tissue and permeabilize tissues underneath. Namely, tissues between the electrodes can be seen as serially connected resistors. Applying voltage on such a circuit (voltage divider) causes the voltage to be distributed between the resistors proportionally to their resistivities [17]. Upon applying electric pulses, almost the entire applied voltage thus rests across the most resistive (least conductive) tissue, in our case skin. That means a very high electric field in skin tissue, while the electric field in other tissues stays too low for a successful cell electroporation. If our goal is the electrochemotherapy of the underlying tumor, one might wonder how a successful electrochemotherapy of subcutaneous tumors is possible when external plate electrodes are used. The answer lies in the increase in bulk conductivities of tissues during electroporation, a phenomenon that was also observed *in vivo*. This conductivity increase leads to a changed electric field distribution, which exposes the tumor to an electric field high enough for a successful cell membrane permeabilization [18]. To further support this hypothesis, we described this process with a numerical model, taking into account the changes of tissue bulk electrical properties during the electroporation. In Figure 6 six steps of the electroporation process in the subcutaneous tumor model for the voltage of 1000 V between the electrodes are shown. The electric field distribution is shown in V/cm. Step 0 denotes the electric field distribution as it was just before the electroporation process started, thus when all the tissues still had their initial conductivities. When the voltage is applied to the electrodes, the electric field is distributed in the tissue according to conductivity ratios of the tissues in the model. The field strength is the highest in the tissues with the lowest conductivity, where the voltage drop is the largest, and the voltage gradient the highest. In our case, almost the entire voltage drop occurs in the skin layer which has a conductivity of about 10-100 times lower than the tissues lying underneath.

If we look at the last step of the sequential analysis, step 5, at 1000 V (Figure 6) the tumor is entirely permeabilized, in some areas the electric field is also above the irreversible threshold.

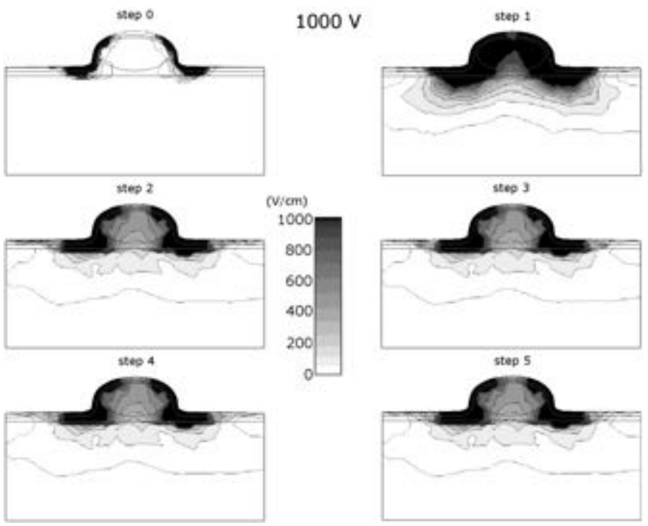

Figure 6: Six steps of the sequential analysis of the electroporation process in the subcutaneous tumor model at 1000 V between two plate electrodes with distance of 8 mm [18]. Time intervals between steps are in general not uniform. Different steps follow a chronological order but do not have an exact time value associated with them. The electric field distribution is shown in V/cm.

A similar situation can be encountered when applying electric pulses on a skin fold with external plate electrodes as a method to enhance *in vivo* gene transfection in skin [19]. Skin consists of three main layers: epidermis, dermis and subcutaneous tissue (Figure 7). Skin epidermis is made up of different layers, but the one that defines its electrical properties the most is the outermost layer, the stratum corneum. Although very thin (typically around 20 μm), it contributes a great deal to the electrical properties of skin. Its conductivity is three to four orders of magnitude lower than the conductivities of deeper skin layers. Again, when electric pulses are applied on skin fold through external plate electrodes, almost the entire applied voltage rests across the stratum corneum, which causes a very high electric field in that layer, while the electric field in deeper layers of skin – the layers targeted for gene transfection – stays too low. Similarly as in the case of subcutaneous tumors, the increase in bulk conductivities of skin layers during electroporation exposes the skin layers below stratum corneum to an electric field high enough for a successful permeabilization [20].

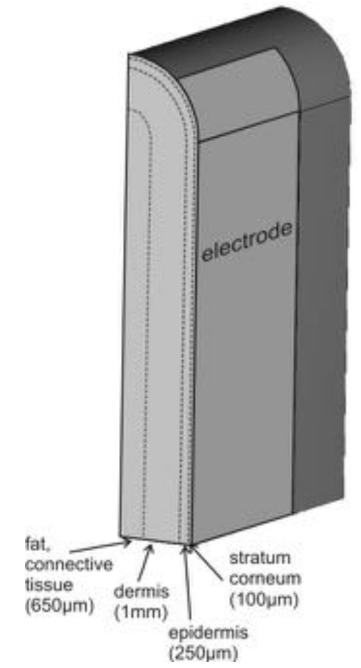

Figure 7: Schematics of a skinfold as described in a numerical model. Only one quarter of the skinfold is presented here.

Theoretical explanation of the process of electroporation offers useful insight into the understanding of the underlying biological processes and allows for predicting the outcome of the treatment [21]. Therefore, due effort needs to be invested into measurements of tissue electrical properties and their changes during electroporation.

Further, one of the concerns associated with electroporation could be the amount of resistive heating in the tissue. Excessive heating is unwanted not only to avoid skin burns and assure patient safety, but also to avoid damage to viable cells. Potential excess of the resistive heating during electroporation has been demonstrated [24], therefore thermal aspect in treatment planning and theoretical analysis of specific applications of electroporation-based treatments should be considered. In order to stay within the safety limit while achieving successful treatment, heating needs to estimated, by means of theoretical models, as a part of treatment planning [25].

REFERENCES

[1] D. Miklavčič, N. Pavšelj, FX Hart. Electric Properties of Tissues. Wiley Encyclopedia of Biomedical Engineering, John Wiley & Sons, New York, 2006.

[2] K.R. Foster and H.P. Schwan. Dielectric properties of tissues and biological materials: a critical review. *Critical Reviews in Biomedical Engineering* 17: 25-104, 1989.

[3] C. Gabriel, A. Peyman and E.H. Grant. Electrical conductivity of tissue at frequencies below 1 MHz. *Phys. Med. Biol.* 54(16): 4863-4878, 2009.

[4] Applied Bioelectricity, From Electrical Stimulation to Electropathology, J. Patrick Reilly, Springer-Verlag New York, 1998.

[5] Kyle C. Smith and James C. Weaver. Electrodiffusion of Molecules in Aqueous Media: A Robust, Discretized Description for Electroporation and Other Transport Phenomena. *IEEE Trans. Biomed. Eng.* 59(6), 1514-1522, 2012.

[6] S. Huclova, D. Erni and J. Frohlich. Modelling and validation of dielectric properties of human skin in the MHz region focusing on skin layer morphology and material composition. *J. Phys. D: Appl. Phys.* 45(2): 025301, 2012

[7] F.X. Hart. Bioimpedance in the clinic. *Zdravniski vestnik-Slovenian Medical Journal* 78(12): 782-790, 2009

[8] D. Cukjati, D. Batiuskaite, D. Miklavčič, L.M. Mir. Real time electroporation control for accurate and safe *in vivo* nonviral gene therapy. *Bioelectrochemistry* 70: 501-507, 2007.

[9] A. Ivorra and B. Rubinsky. *In vivo* electrical impedance measurements during and after electroporation of rat liver. *Bioelectrochemistry* 70: 287-295, 2007.

[10] M. Pavlin, D. Miklavčič. Effective conductivity of a suspension of permeabilized cells: A theoretical analysis. *Biophys. J.* 85: 719-729, 2003.

[11] M. Pavlin, M. Kanduser, M. Rebersek, G. Pucihar, F.X. Hart, R. Magjarevic and D. Miklavcic. Effect of cell electroporation on the conductivity of a cell suspension. *Biophys. J.* 88: 4378-4390, 2005.

[12] A. Ivorra, B. Al-Sakere B, B. Rubinsky and L.M. Mir. *In vivo* electrical conductivity measurements during and after tumor electroporation: conductivity changes reflect the treatment outcome. *Phys. Med. Biol.* 54(19):5949-5963, 2009.

[13] Y. Granot, A. Ivorra, E. Maor and B. Rubinsky. *In vivo* imaging of irreversible electroporation by means of electrical impedance tomography. *Phys. Med. Biol.* 54(16): 4927-4943, 2009.

[14] M. Essone Mezeme, G. Pucihar, M. Pavlin, C. Brosseau, D. Miklavčič. A numerical analysis of multicellular environment for modeling tissue electroporation. *Appl. Phys. Lett.* 100: 143701, 2012.

[15] M. Kranjc, F. Bajd, I. Serša, D. Miklavčič. Magnetic resonance electrical impedance tomography for measuring electrical conductivity during electroporation. *Physiol. Meas.* 35: 985-996, 2014.

[16] R.E. Neal, P.A. Garcia, J.L. Robertson, R.V. Davalos. Experimental Characterization and Numerical Modeling of Tissue Electrical Conductivity during Pulsed Electric Fields for Irreversible Electroporation Treatment Planning. *IEEE Trans. Biomed. Eng.* 59(4): 1076 – 1085, 2012

[17] N. Pavšelj, D. Miklavčič. Numerical modeling in electroporation-based biomedical applications. *Radiol. Oncol.* 42:159-168, 2008.

[18] N. Pavšelj, Z. Bregar, D. Cukjati, D. Batiuskaite, L.M. Mir and D. Miklavčič. The course of tissue permeabilization studied on a mathematical model of a subcutaneous tumor in small animals. *IEEE Trans. Biomed. Eng.* 52(8):1373-1381, 2005.

[19] N. Pavšelj and V. Préat. DNA electrotransfer into the skin using a combination of one high- and one low-voltage pulse. *Journal of Controlled Release* 106:407-415, 2005.

[20] N. Pavšelj, V. Préat, D. Miklavčič. A numerical model of skin electropermeabilization based on *in vivo* experiments. *Annals Biomed. Eng.* 35:2138-2144, 2007.

[21] D. Miklavčič, M. Snoj, A. Županič, B. Kos, M. Čemažar, M. Kropivnik, M. Bračko, T. Pečnik, E. Gadžijev, G. Serša. Towards treatment planning and treatment of deep-seated solid tumors by electrochemotherapy. Biomed. Eng. Online 9: 10, 2010.

[22] I. Edhemović, E.M. Gadžijev, E. Brecelj, D. Miklavčič, B. Kos, A. Županič, B. Mali, T. Jarm, D. Pavliha, M. Marčan, G. Gašljević, V. Gorjup, M. Mušič, T. Pečnik Vavpotič, M. Čemažar, M. Snoj, G. Serša. Electrochemotherapy: A new technological approach in treatment of metastases in the liver. *Technol. Cancer Res. Treat.* 10: 475-485, 2011.

[23] A. Županič, B. Kos, D. Miklavčič. Treatment planning of electroporation-based medical interventions: electrochemotherapy, gene electrotransfer and irreversible electroporation. *Phys. Med. Biol.* 57: 5425-5440, 2012.

[24] I. Lacković, R. Magjarević, D. Miklavčič. Three-dimensional finite-element analysis of joule heating in electrochemotherapy and *in vivo* gene electrotransfer. *IEEE T. Diel. El. Insul.* 15: 1338-1347, 2009

[25] N. Pavšelj, D. Miklavčič. Resistive heating and electropermeabilization of skin tissue during *in vivo* electroporation: A coupled nonlinear finite element model. *Int. J. Heat Mass Transfer* 54: 2294-2302, 2011

[26] A. Županič, D. Miklavčič. Tissue heating during tumor ablation with irreversible electroporation. *Elektroteh. Vestn.* 78: 42-47, 2011

[27] Robert E. Neal II , Paulo A. Garcia, John L. Robertson, Rafael V. Davalos, Experimental Characterization and Numerical Modeling of Tissue Electrical Conductivity during Pulsed Electric Fields for Irreversible Electroporation Treatment Planning *IEEE Trans. Biomed. Eng.* 59(4), 1076-1085, 2012.

[28] P.A. Garcia, R.V. Davalos, D. Miklavčič. A numerical investigation of the electric and thermal cell kill distributions in electroporation-based therapies in tissue. *PLOS One* 9(8): e103083, 2014

[29] Kos B, Voigt P, Miklavčič D, Moche M. Careful treatment planning enables safe ablation of liver tumors adjacent to major blood vessels by percutaneous irreversible electroporation (IRE). *Radiol. Oncol.* 49: 234-241, 2015.

ACKNOWLEDGEMENT

This work was supported by the Slovenian Research Agency and the European Commission and performed in the scope of LEA EBAM.

Damijan Miklavčič was born in Ljubljana, Slovenia, in 1963. He received a Masters and a Doctoral degree in Electrical Engineering from University of Ljubljana in 1991 and 1993, respectively. He is currently Professor and the Head of the Laboratory of Biocybernetics at the Faculty of Electrical Engineering, University of Ljubljana.

His research areas are biomedical engineering and study of the interaction of electromagnetic fields with biological systems. In the last years he has focused on the engineering aspects of electroporation as the basis of drug delivery into cells in tumor models *in vitro* and *in vivo*. His research includes biological experimentation, numerical modeling and hardware development for electrochemotherapy, irreversible electroporation and gene electrotransfer.

Nataša Pavšelj was born in Slovenia, in 1974. She received her B.Sc., M.Sc. and Ph.D. degrees from the University of Ljubljana in 1999, 2002 and 2006, respectively. Her main research interests lie in the field of electroporation, including finite element numerical modeling of electric field distribution in different biological tissue setups (subcutaneous tumors, skin fold) and comparison of the theoretical results with the experimental work. In recent years Nataša Pavšelj is interested in transdermal drug delivery by means of electroporation and modeling of mass transport, heat transfer and electric phenomena.

NOTES

Lipid Membranes Electroporation: Insights from Molecular Dynamics Simulations

Mounir Tarek
Theory, Simulations and Modeling
UMR 7565 Structure et Réactivité des Systèmes Moléculaires Complexes
CNRS-Nancy Université France

Abstract: We describe here the molecular dynamics simulation methods devised to perform *in silico* experiments of membranes subject to nanosecond, megavolt-per-meter pulsed electric fields and of membranes subject to charge imbalance, mimicking therefore the application of low voltage – long duration pulses. At the molecular level, the results show the two types of pulses produce similar effects: Provided the TM voltage these pulses create are higher than a certain threshold, hydrophilic pores stabilized by the membrane lipid head groups form within the nanosecond time scale across the lipid core. Similarly, when the pulses are switched off, the pores collapse (close) within similar time scales. It is shown that for similar TM voltages applied, both methods induce similar electric field distributions within the membrane core. The cascade of events following the application of the pulses, and taking place at the membrane, is a direct consequence of such an electric field distribution.

Electroporation disturbs transiently or permanently the integrity of cell membranes [1-3]. These membranes consist of an assembly of lipids, proteins and carbohydrates that self–organize into a thin barrier that separates the interior of cell compartments from the outside environment [4]. The main lipid constituents of natural membranes are phospholipids that arrange themselves into a two-layered sheet (a bilayer). Experimental evidence suggests that the effect of an applied external electric field to cells is to produce aqueous pores specifically in the lipid bilayer [5-9]. Information about the sequence of events describing the electroporation phenomenon can therefore be gathered from measurements of electrical currents through planar lipid bilayers along with characterization of molecular transport of molecules into (or out of) cells subjected to electric field pulses. It may be summarized as follows: The application of electrical pulses induces rearrangements of the membrane components (water and lipids) that ultimately lead to the formation of aqueous hydrophilic pores [5-10], whose presence increases substantially the ionic and molecular transport through the otherwise impermeable membranes [11].

In erythrocyte membranes, large pores could be observed using electron microscopy [12], but in general, the direct observation of the formation of nano-sized pores is not possible with conventional techniques. Furthermore, due to the complexity and heterogeneity of cell membranes, it is difficult to describe and characterize their electroporation in terms of atomically resolved processes. Atomistic simulations in general, and molecular dynamics (MD) simulations in particular, have proven to be effective for providing insights into both the structure and the dynamics of model lipid membrane systems in general [13-25]. Several MD simulations have recently been conducted in order to model the effect of electric field on membranes [26-30], providing perhaps the most complete molecular model of the electroporation process of lipid bilayers.

The effects of an electric field on a cell may be described considering the latter as a dielectric layer (cell surface membrane) embedded in conductive media (internal: cytoplasm and external: extracellular media). When relatively low-field pulses of microsecond or millisecond duration are applied to this cell (by placing for instance the cell between two electrodes and applying a constant voltage pulse) the resulting current causes accumulation of electrical charges at both sides of the cell membrane. The time required to charge the surface membrane is dependent upon the electrical parameters of the medium in which it is suspended. For a spherical cell it is estimated using equivalent network RC circuits in the 100 ns time scale [26, 31-34]. A charging time constant in the range of hundreds of nanoseconds was also obtained from derivations based on the Laplace equation (see e.g. [35] for the first-order analysis on a spherical vesicle; [36] for the second-order analysis; and [37] for the second-order analysis for two concentric spherical vesicles *i.e.* modeling an organelle).

If on the other hand, the pulse duration is short enough relative to the charging time constant of the resistive-capacitive network formed by the conductive intracellular and extracellular fluids and the cell membrane dielectric, which is the case for nanosecond pulses, then the electric field acts directly and mainly on the cell membrane.

Simulations allow ones to perform *in silico* experiments under both conditions, *i.e*. submitting the system either to nanosecond, megavolt-per-meter pulsed electric fields or to charge imbalance, mimicking therefore the application of low voltage – long duration pulses. In the following we will describe the results of such simulations, after a brief general introduction to MD simulations of membranes.

MD SIMULATIONS OF LIPID MEMBRANES

Molecular dynamics (MD) refers to a family of computational methods aimed at simulating macroscopic behaviour through the numerical integration of the classical equations of motion of a microscopic many-body system. Macroscopic properties are expressed as functions of particle coordinates and/or momenta, which are computed along a phase space trajectory generated by classical dynamics [38, 39] When performed under conditions corresponding to laboratory scenarios, MD simulations can provide a detailed view of the structure and dynamics of a macromolecular system. They can also be used to perform "computer experiments" that cannot be carried out in the laboratory, either because they do not represent a physical behaviour, or because the necessary controls cannot be achieved.

MD simulations require the choice of a potential energy function, *i.e*. terms by which the particles interact, usually referred to as a force field. Those most commonly used in chemistry and biophysics, *e.g*. GROMOS [40] CHARMM [41] and AMBER [42], are based on molecular mechanics and a classical treatment of particle-particle interactions that precludes bond dissociation and therefore the simulation of chemical reactions. Classical MD force fields consist of a summation of bonded forces associated with chemical bonds, bond angles, and bond dihedrals, and non-bonded forces associated with van der Waals forces and electrostatic interactions. The parameters associated with these terms are optimized to reproduce structural and conformational changes of macromolecular systems.

Conventional force fields only include point charges and pair-additive Coulomb potentials, which prevent them from describing realistic collective electrostatic effects, such as charge transfer, electronic excitations or electronic polarization, which is often considered as a major limitation of the classical force fields. Note that constant efforts are undertaken on the development of potential functions that explicitly treat electronic polarizability in empirical force fields [43-45] but none of these "polarizable" force fields is widely used in large-scale simulations for now, the main reasons for that being the dramatic increase of the computational time of simulation and additional complications with their parameterization. In this perspective, classical force fields provide an adequate description of the properties of membrane systems and allow semi-quantitative investigations of membrane electrostatics.

MD simulations use information (positions, velocities or momenta, and forces) at a given instant in time, t, to predict the positions and momenta at a later time, $t + \Delta t$, where Δt is the time step, of the order of a femtosecond, taken to be constant throughout the simulation. Numerical solutions to the equations of motion are thus obtained by iteration of this elementary step. Computer simulations are usually performed on a small number of molecules (few tens to few hundred thousand atoms), the system size being limited of course by the speed of execution of the programs, and the availability of computer power. In order to eliminate edge effects and to mimic a macroscopic system, simulations of condensed phase systems consider a small patch of molecules confined in a central simulation cell, and replicate the latter using periodic boundary conditions (PBCs) in the three directions of Cartesian space. For membranes for instance the simulated system would correspond to a small fragment of either a black film, a liposome or multilamellar oriented lipid stacks deposited on a substrate [46, 47].

Traditionally, phospholipids have served as models for investigating *in silico* the structural and dynamical properties of membranes. From both a theoretical and an experimental perspective, zwitterionic phosphatidylcholine (PC) lipid bilayers constitute the best characterized systems [48-51] (Fig. 1). More recent studies have considered a variety of alternative lipids, featuring different, possibly charged, head groups [52-56], and more recently mixed bilayer compositions [57-63]. Despite their simplicity, bilayers built from PC lipids represent remarkable test systems to probe the computation methodology and to gain additional insight into the physical properties of membranes [14, 17, 20, 64].

Up to recently, most of membrane models consisted of simulating fully hydrated pure phospholipid bilayers, without taking into account the effect of salt concentration (see sections below). For such systems, the average structure of the lipid water interface at the atomic-scale may be provided by the density distributions of different atom types along the bilayer normal (Fig. 1), which can be measured experimentally on multilamellar stacks by neutron and X-ray diffraction techniques [65], as well as calculated from MD simulations. These distributions highlight the composition and properties of the membrane that appears as a broad hydrophilic interface, with only a thin slab of pure hydrocarbon fluid in the middle (Fig. 1). They indicate clearly the roughness of the lipid headgroup area and how water density decays smoothly from the bulk value and penetrates deeply into the bilayer at a region delimiting the membrane/water interface.

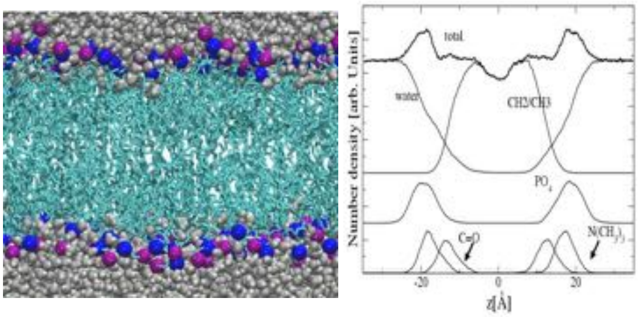

Figure 1: *Left:* configuration of a Palmitoyl-Oleyl-Phosphatidyl-Choline (POPC) hydrated bilayer system from a well equilibrated constant pressure MD simulation performed at 300K. Only the molecules in the simulation cell are shown. Water molecules (O gray; H white) and the Phosphate (blue) and Nitrogen (purple) atoms of the lipid head groups are depicted by their van der Waals radii, and the acyl chains (cyan) are represented as sticks. *Right:* Number density profiles (arbitrary units) along the bilayer normal, *z*, averaged over 2 ns of the MD trajectory. The total density, water and hydrocarbon chain contributions are indicated, along with those from the POPC headgroup moieties. The bilayer center is located at $z = 0$.

MODELING MEMBRANE ELECTROPORATION

The effects of an electric field on a cell may be described considering the latter as a dielectric layer (cell surface membrane) embedded in conductive media (internal: cytoplasm and external: extracellular media). When relatively low-field pulses of microsecond or millisecond duration are applied to this cell (by placing for instance the cell between two electrodes and applying a constant voltage pulse) the resulting current causes accumulation of electrical charges at both sides of the cell membrane. The time required to charge the surface membrane is dependent upon the electrical parameters of the medium in which it is suspended. For a spherical cell it is estimated in the 100ns time scale [26, 31-34]. If the pulse duration is short enough relative to the charging time constant of the resistive-capacitive network formed by the conductive intracellular and extracellular fluids and the cell membrane dielectric, then the electric field acts directly and mainly on the cell membrane.

Simulations allow ones to perform *in silico* experiments under both conditions, i.e. submitting the system either to Nanosecond, megavolt-per-meter pulsed electric fields or to charge imbalance, mimicking therefore the application of low voltage – long duration pulses. In the following we will describe the results of such simulations.

A- ELECTROPORATION INDUCED BY DIRRECT EFFECT OF AN ELECTRIC FIELD

In simulations, it is possible to apply "directly" a constant electric field $\vec{E}$ perpendicular to the membrane (lipid bilayers) plane. In practice, this is done by adding a force $\vec{F} = q_i \vec{E}$ to all the atoms bearing a charge q_i [66-70]. MD simulations adopting such an approach have been used to study membrane electroporation [26-30], lipid externalization [71], to activate voltage-gated K^+ channels [72] and to determine transport properties of ion channels [73-76].

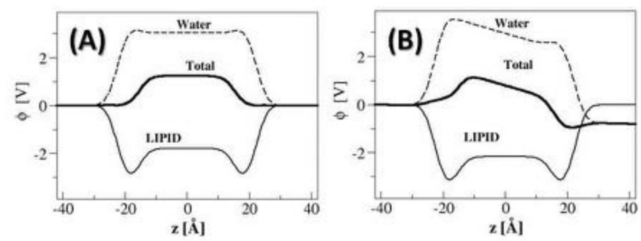

Figure 2: Electrostatic potential profiles $\phi(z)$along the membrane normal **z** of a POPC lipid bilayer (A) at rest and (B) subject to a transverse electric field $\vec{E}$. **z**=0 represents the centre of the lipid bilayer and the arrow the bilayer-water interfaces. Are shown the contribution from water, lipid and the total electrostatic profile. Note that the TM voltage $\boldsymbol{\Delta V}$ (potential difference between the upper and lower water baths) created under electric field (panel B) is mainly due to water dipoles reorientation.

The consequence of such perturbation stems from the properties of the membrane and from the simulations set-up conditions: Pure lipid membranes exhibit a heterogeneous atomic distributions across the bilayer to which are associated charges and molecular dipoles distributions. Phospholipid head-groups adopt in general a preferential orientation. For hydrated PC bilayers at temperatures above the gel to liquid crystal transition, the phosphatidyl-choline dipoles point on average 30 degrees away from the membrane normal [17, 77]. The organization of the phosphate (PO_4^-), choline ($N(CH_3)_3^+$) and the carbonyl (C=O) groups of the lipid head group give hence rise to a permanent dipole and the solvent (water) molecules bound to the lipid head group moieties tend to orient their dipoles to compensate the latter [78]. The electrostatic characteristics of the bilayer may be gathered from estimates of the electrostatic profile $\phi(z)$ that stems from the distribution of all the charges in the system. $\phi(z)$ is derived from MD simulations using Poisson's equation and expressed as the double integral of $\rho(z)$, the molecular charge density distributions:

$$\Delta\phi(z) = \phi(z) - \phi(0) = -\frac{1}{\epsilon_0}\iint_0^z \rho(z'')dz''dz' .$$

For lipid bilayers, most of which are modelled without consideration of a salt concentration, an applied electric field acts specifically and primarily on the interfacial water dipoles (small polarization of bulk water molecules). The reorientation of the lipid head groups appears not to be affected at very short time scales [28, 79], and not exceeding few degrees toward the field direction at longer time scale [29]. Hence, within a very short time scale - typically few picoseconds [28] –a transverse field $\vec{E}$ induces an overall TM potential $\Delta\boldsymbol{V}$ (*cf*. Fig 2). It is very important to note here that, because of the MD simulation setup (and the use of PBCs), $\vec{E}$ induces a voltage difference $\Delta\boldsymbol{V} \approx |\vec{E}|.L_Z$ over the whole system, where L_z is the size of the simulation box in the field direction. In the example shown in Fig 2, L_z is ~ 10 nm. The electric field (0.1 V.nm^{-1}) applied to the POPC bilayer induces $\Delta\boldsymbol{V}$ ~ 1V.

MD simulations of pure lipid bilayers have shown that the application of electric fields of high enough magnitude leads to membrane electroporation, with a rather common poration sequence: The electric field favours quite rapidly (within a few hunder picoseconds) formation of water defects and water wires deep into the hydrophobic core [27]. Ultimately water fingers forming at both sides of the membrane join up to form water channels (often termed pre-pores or hydrophobic pores) that span the membrane. Within nanoseconds, few lipid head-groups start to migrate from the membrane-water interface to the interior of the bilayer, stabilizing hydrophilic pores (~1 to 3 nm diameter). All MD studies reported pore expansion as the electric field was maintained. In contrast, it was shown in one instance [28] that a hydrophilic pore could reseal within few nanoseconds when the applied field was switched off. Membrane complete recovery, i.e. migration of the lipid head group forming the hydrophilic pore toward the lipid/water interface, being a much longer process, was not observed. More recently systematic studies of pore creation and annihilation life time as a function of field strength have shed more light onto the complex dynamics of pores in simple lipid bilayers [80]. Quite interstingly, addition of salt has been shown to modulate these characteristic time scales [81].

For typical MD system sizes (128 lipids; 6 nm x 6 nm membrane cross section), most of the simulations reported a single pore formation at high field strengths. For much larger systems, multiple pore formation with diameters ranging from few to 10 nm could be witnessed [27, 28]. Such pores are in principle wide enough to transport ions and small molecules. One attempt has so far been made to investigate such a molecular transport under electroporation [28]. In this simulation, partial transport of a 12 base pairs DNA strand across the membrane could be followed. The strand considered diffused toward the interior of the bilayer when a pore was created beneath it and formed a stable complex DNA/lipid in which the lipid head groups encapsulate the strand. The process provided support to the gene delivery model proposed by Golzio et al. [82] in which, an ‘‘anchoring step’’ connecting the plasmid to permeabilized cells membranes that takes place during DNA transfer assisted by electric pulses, and agrees with the last findings from the same group [83]. More recently, it was shown that even a single 10 ns electric pulses of high enough magnitude can enhance small siRNA transport through lipid membranes (Fig. 3) [84]

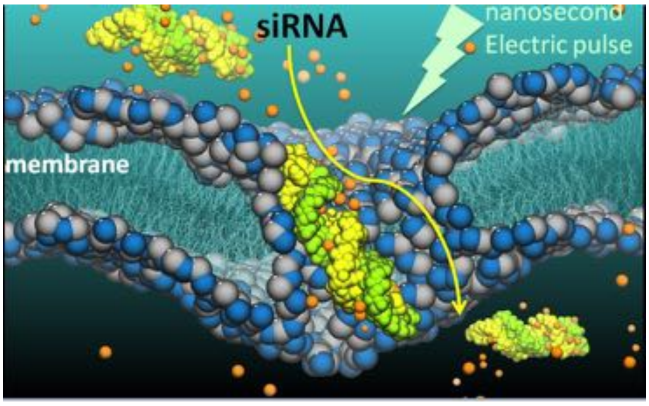

Figure 3: A single 10 ns high-voltage electric pulse can permeabilize lipid vesicles and allow the delivery of siRNA to the cytoplasm. Combining experiments and molecular dynamics simulations has allowed us to provide the detailed molecular mechanisms of such transport and to give practical guidance for the design of protocols aimed at using nanosecond-pulse siRNA electro-delivery in medical and biotechnological applications

The eletroporation process takes place much more rapidly under higher fields, without a major change in the pore formation characteristics. The lowest voltages reported to electroporate a PC lipid bilayer are ~ 2 V [29, 79]. Ziegler and Vernier [30] reported minimum poration external field strengths for 4 different PC lipids with different chain lengths and composition (number of unsaturations). The authors find a direct correlation between the minimum porating fields (ranging from 0.26 V.nm^{-1} to 0.38 V.nm^{-1}) and the membrane thickness (ranging from 2.92 nm to 3.92 nm). Note that estimates of electroporation thresholds from simulations should, in general be considered only as indicative since it is related to the time scale the pore formation may take. A field strength threshold is “assumed” to be reached when no membrane rupture is formed within the 100 ns time scale. Finally.

B- ELECTROPORATION INDUCED BY IONIC SALT CONCENTRATION GRADIENTS

Regardless of how low intensity millisecond electrical pulses are applied, the ultimate step is the charging of the membrane due to ions flow. The resulting ionic charge imbalance between both sides of the lipid bilayer is locally the main effect that induces the TM potential. In a classical set up of membrane simulations, due to the use of 3d PBCs, the TM voltage cannot be controlled by imposing a charge imbalance Q_S across the bilayer, even when ions are present in the electrolytes. Several MD simulations protocols that can overcome this limitation have been recently devised (Fig. 4):

The double bilayer setup : It was indeed shown that TM potential gradients can be generated by a charge imbalance across lipid bilayers by considering a MD unit cell consisting of three salt-water baths separated by two bilayers and 3d-PBCs [85] (cf. Fig. 4.A). Setting up a net charge imbalance between the two independent water baths at time t=0 induces a TM voltage $\Delta\boldsymbol{V}$ by explicit ion dynamics.

The single bilayer setup : Delemotte et al. [86] introduced a variant of this method where the double layer is not needed, avoiding therefore the over-cost of simulating a large system. The method consists in considering a unique bilayer surrounded by electrolyte baths, each of them terminated by an air/water interface [87]. The system is set-up as indicated in Fig. 4.B. First, a hydrated bilayer is equilibrated at a given salt concentration using 3d periodic boundary conditions. Air water interfaces are then created on both sides of the membrane, and further equilibration is undertaken at constant volume, maintaining therefore a separation between the upper and lower electrolytes. A charge imbalance Q_S between the two sides of the bilayer are generated by simply displacing at time t=0 an adequate number of ions from one side to the other. As far as the water slabs are thicker than 25-30 Å, the presence of air water interfaces has no incidence on the lipid bilayer properties and the membrane “feels” as if it is embedded in infinite baths whose characteristics are those of the modeled finite solutions.

Extension to Liposomes : The availability of large computer resources has extended the realm of simulations of membrane electroporation to study systems large enough to allow modelling of small liposomes. Fig. 4.C represents such a liposome constructed from a POPC bilayer and equilibrated in a 200 mM NaCl salt solution. The system contains over 1,400 lipid molecules forming a liposome of internal diameter of 8 nm. The system size (210 x 210 x 210 Å^3) was chosen large enough to avoid interaction between the central liposome and its replica, resulting

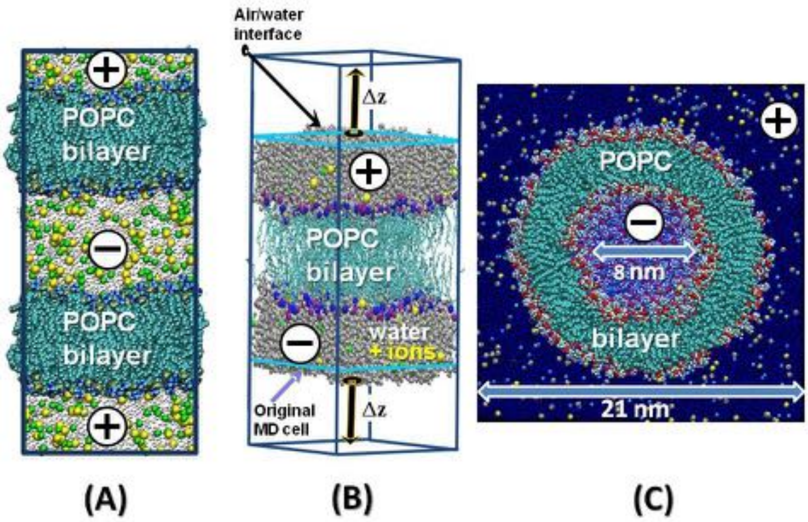

Figure 4: Molecular dynamics simulations set-ups of three systems using the charge imbalance method. (A) The double bilayer setup: two lipid bilayers are separated by electrolyte baths at 1M NaCl salt concentration. Note that due to the use of PBCs (drawn box) the upper and lower electrolytes are in contact. Q_S is imposed between the central water bath and the two others. (B) The single bilayer set-up: here one single bilayer is surrounded by water baths (maintained at 1M NaCl). The original MD cell represented the classical set-up and the large cell that allowing for the creation of water air interfaces. Q_S is imposed between the lower and upper bath. (C) The Liposome setup: A small spherical liposome is embedded in a 1M NaCl electrolyte. Q_S is imposed between the inner and outer water baths and 3d PBCs (drawn box) are used.

in an overall number of atoms ~ 890,000. In such a set-up a charge imbalance Q_s was imposed after the system equilibration between the inner and outer side of the liposome.

Fig. 5 reports the electrostatic potential profiles along the normal to the membrane generated from MD simulations a POPC bilayer in contact with 1M NaCl salt water baths at various charge imbalances Q_s, using the single bilayer method. For all simulations, the profiles computed at the initial stage show plateau values in the aqueous regions and, for increasing Q_s, an increasing potential difference between the two electrolytes indicative of a TM potential $\boldsymbol{\Delta V}$. Quite interestingly, the profiles show clearly that, in contrast to the electric field case where the TM voltage is mainly due to the water dipole reorientation (Fig. 2), most of the voltage drop in the charge imbalance method is due to the contribution from the ions. Indeed the sole collapse of the electrostatic potential due to the charge imbalance separation by the membrane lipid core accounts for the largest part of $\boldsymbol{\Delta V}$.

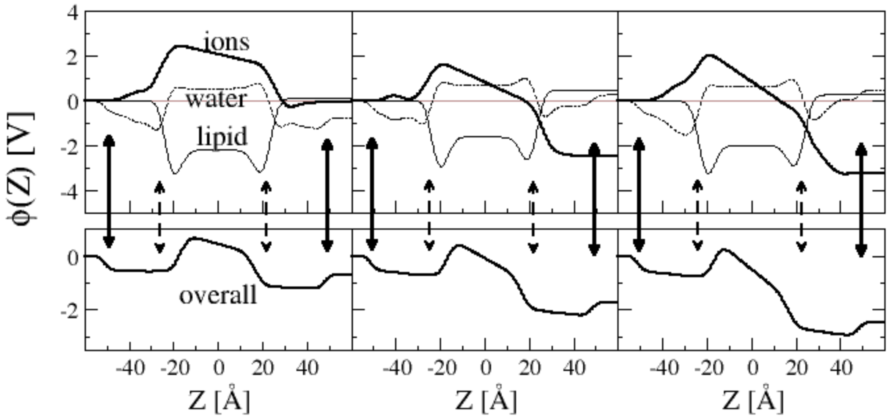

Figure 5: Components of the electrostatic potential profiles along the lipid bilayer normal Z of a POPC membrane estimated from at the initial stage of the MD simulations of the system at 1 M NaCl salt concentration using the single bilayer method. Z=0 represents here the center of the lipid bilayer, the broken arrow the location of the bilayer/water interfaces, and the solid arrows the locations of the air water interfaces. From left to right increasing amounts of net charge imbalance Q_s between the lower and upper electrolytes induce transmembrane voltages (that may be estimated from the difference between the electrostatic potentials of the two water bath) of increasing amplitudes. Are shown in the top panels the contributions from lipid, water and ions, and in the lower panels the total electrostatic potential. Note that the most of the transmembrane voltage is due to the contribution from ions.

Using the charge imbalance set-up, it was possible for the first time to directly demonstrate *in silico* that the simulated lipid bilayer behaves as a capacitor[86] (Fig 6). Simulations at various charge imbalances Q_s show a linear variation of $\boldsymbol{\Delta V}$ from which the capacitance can be estimated as $C = Q_s.\Delta V^{-1}$. The capacitance values extracted from simulations are expected to depend on the lipid composition (charged or not) and on the force field parameters used and as such constitutes a supplementary way of checking the accuracy of lipid force field parameters used in the simulation. Here, in the case of POPC bilayers embedded in a 1M solution of NaCl [86], the later amounts to 0.85 μF.cm^{-2} which is in reasonable agreement with the value usually assumed in the literature *e.g.* 1.0 μF.cm^{-2} [85, 88] and with recent measurements for planar POPC lipid bilayers in a 100 mM KCl solution (0.5 μF.cm^{-2}).

For large enough induced TM voltages, the three protocols lead to electroporation of the lipid bilayer. As in the case of the electric field method, for $\boldsymbol{\Delta V}$ above 1.5-2.5 Volts, the electroporation process starts with the formation of water fingers that protrude inside the hydrophobic core of the membrane. Within nanoseconds, water wires bridging between the two sides of the membrane under voltage stress appear.

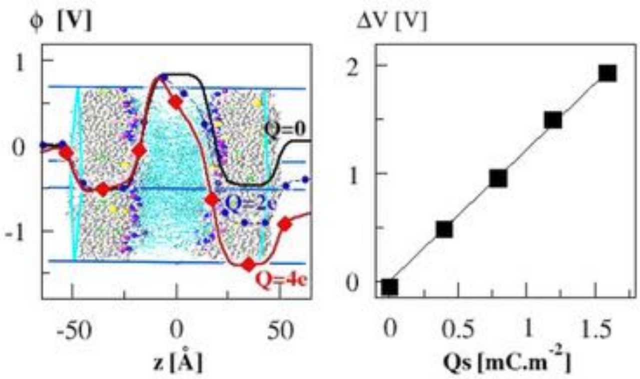

Figure 6: *Left:* Electrostatic potential across a POPC lipid bilayer for different net charge imbalances Qs between the upper and lower electrolytes from MD simulations considering the setup of Fig. 5. ϕ(z), is estimated as an in-plane average of the EP distributions (Eq. 1). As a reference it was set to zero in the lower electrolyte. *Right:* TM potential ΔV as a function of the charge imbalance Qs par unit area. The capacitance of the bilayer can be derived from the slope of the curve.

If the simulations are further expended, lipid head-groups migrate along one wire and form a hydrophilic connected pathway (Fig.7). Because salt solutions are explicitly considered in these simulations, ion conduction through the hydrophilic pores occurred following the electroporation of the lipid bilayers. Details about the ionic transport through the pores formed within the bilayer core upon electroporation could be gathered [89]. The MD simulations of the double bilayer system [90, 91], and the results presented here for the single bilayer set-up and for the liposome show that both cations and anions exchange through the pores between the two baths, with an overall flux of charges directed toward a decrease of the charge imbalance. Ions translocation through the pores from one bulk region to the other lasts from few tens to few hundreds picoseconds, and leads to a decrease of the charge imbalance and hence to the collapse of $\boldsymbol{\Delta V}$. Hence, for all systems, when the charge imbalance reached a level where the TM voltage was down to a couple of hundred mV, the hydrophilic pores "close" in the sense that no more ionic translocation occurs (Fig 7.F). The final topology of the pores toward the end of the simulations remain stable for time spans exceeding the 10 nanoseconds scale, showing as reported in previous simulations [28] that the complete recovery of the original bilayer structure requires a much longer time scale.

Note that in order to maintain $\boldsymbol{\Delta V}$ constant the modeler needs to maintain the initial charge imbalance by "injecting" charges (ions) in the electrolytes at a paste equivalent to the rate of ions translocation through the hydrophilic pore. This protocol is, in particular for the single bilayer setup, adequate for performing simulations under constant voltage (low voltage, ms duration) or constant current conditions, which is suitable for comparison to experiments undertaken under similar conditions [92].

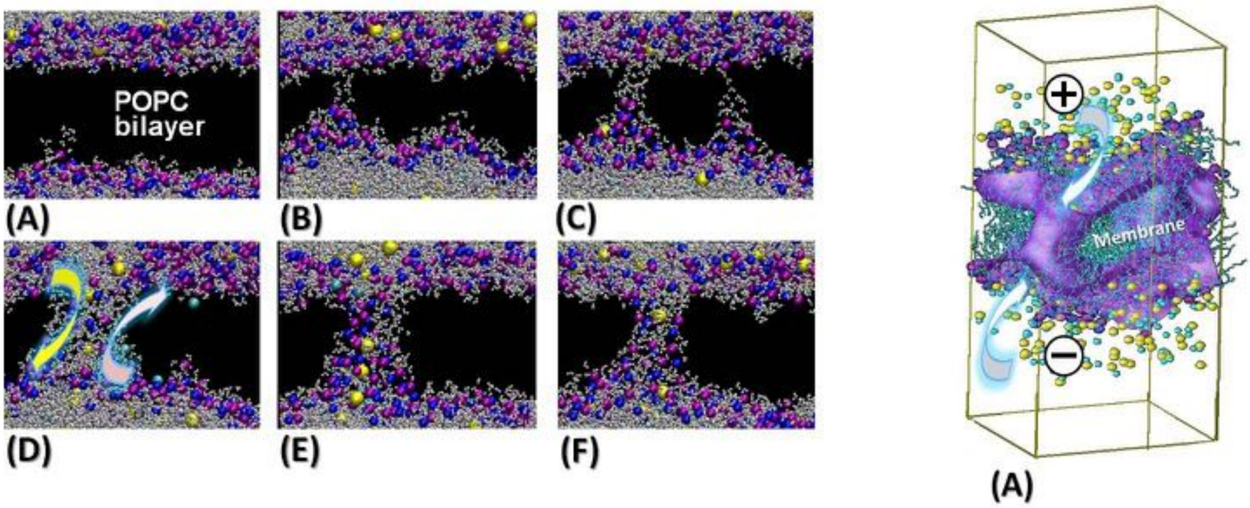

Figure 7: *Left* Sequence of events following the application of a TM voltage to a POPC lipid bilayer using the charge imbalance method (panels A to F). Note the migration of Na+ (yellow) and Cl- (cyan) ions through the formed hydrophilic pores that are lined with lipid phosphate (magenta) and nitrogen (blue) head group atoms. Panel F represents the state of a non conducting pore reached when the exchange of ions between the two baths lowered $\boldsymbol{Q_s}$ and therefore $\boldsymbol{\Delta V}$ to values ≈ 200 mV. *Right* Topology of the nanometer wide hydrophilic pores formed under high transmembrane $\boldsymbol{\Delta V}$ imposed by the charge imbalance method in the planar bilayer (A) and in the liposome (B). The arrows highlight the subsequent ionic flow through the pores.

DISCUSSION

In order to determine the detailed mechanism of the pore creation, it is helpful to probe the electric filed distribution across the bilayer, both at rest and under the effect of a TM voltage. Figure 8.A displays the electrostatic potential profiles for a lipid bilayer subject to increasing electric fields that generate TM potentials ranging from 0 V to ~ 3V. At 0 V, the lipid bilayer is at rest and the profiles reveal, in agreement with experiment [93], the existence of a positive potential difference between the membrane interior and the adjacent aqueous phases.

At rest, the voltage change across the lipid water interfaces gives rise locally to large electric fields (in the present case up to 1.5 $V.nm^{-1}$) oriented toward the bulk, while at the center of the bilayer, the local electric field is null (Fig. 8.B,C). When external electric fields of magnitudes respectively of 0.06 and 0.30 $V.nm^{-1}$ are applied, reorientation of the water molecules gives rise to TM potentials of respectively ~ 0.75 and 3 V. Figures 8.B and C reveal the incidence of such reorganization on the local electric field both at the interfaciale region and within the bilayer core. In particular one notes that the field in the membrane core has risen to a value ~ 1 V.nm^{-1} for the highest $\boldsymbol{\Delta V}$ imposed.

For the charge imbalance method, the overall picture is similar (Fig. 9.A and B), where again, the TM voltages created give rise to large electric fields within the membrane core, oriented perpendicular to the bilayer.

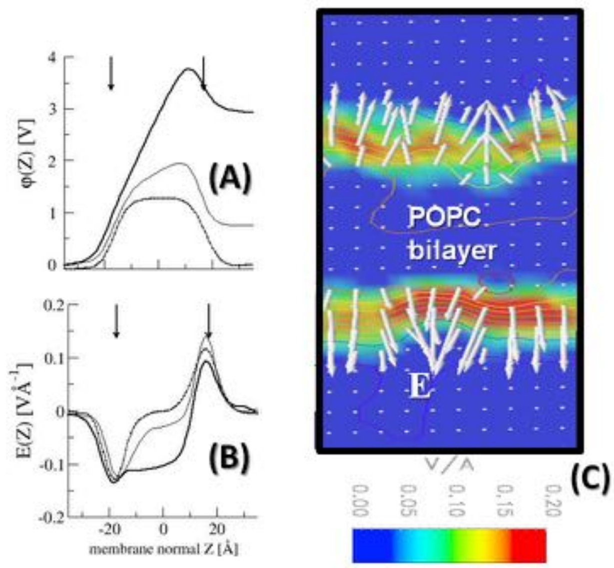

Figure 8: (A) Electrostatic potential profiles across a lipid bilayer subject to electric fields of 0.0 V.nm^{-1} (dotted line) 0.06 V.nm^{-1} (thin line) and 0.30 V.nm^{-1} (bold line). (B) Corresponding electric field profiles. (C) 2d (out of plane) map of the electric field distribution. The local electric field direction and strength are displayed as white arrows. Note that the larger fields are located at the lipid water interfaces and are oriented toward the solvent.

Qualitatively, in both methods, the cascade of events following the application of the TM voltage, and taking place at the membrane, is a direct consequence of such a field distribution. Indeed, water molecules initially restrained to the interfacial region, as they randomly percolate down within the membrane core, are subject to a high electric field, and are therefore inclined to orient their dipole along this local field. These molecules can easily hydrogen bond among themselves, which results in the creation of single water files. Such fingers protrude through the hydrophobic core from both sides of the membrane. Finally, these fingers meet up to form water channels (often termed pre-pores or hydrophobic pores) that span the membrane (Fig. 9.C). As the TM voltage is maintained, these water wires appear to be able to overcome the free energy barrier associated to the formation of a single file of water molecules spanning the bilayer (estimated to be ~ 108 kJ/mol in the absence of external electric field [94]). As the electrical stress is maintained, lipid head group migrate along the stable water wires and participate in the formation of larger "hydophilic pores", able to conduct ions and larger molecules as they expend.

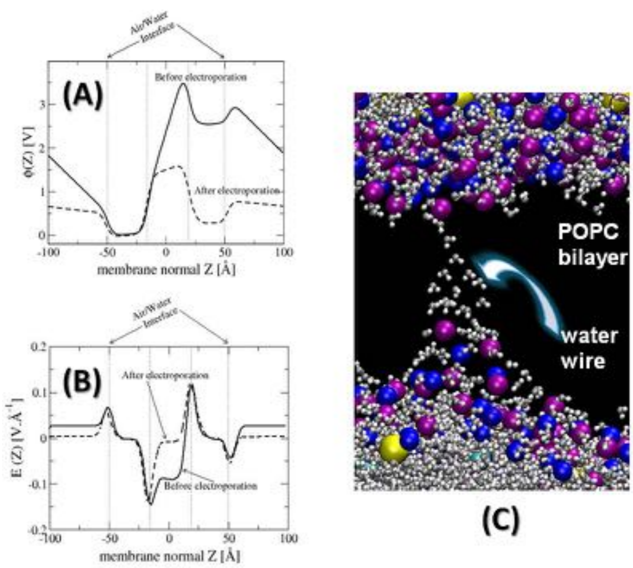

Figure 9: (A) Electrostatic potential profiles across a POPC lipid membrane subject to a charge imbalance (single bilayer set-up) before (solid line) and after (broken line) electroporation. (B) Corresponding electric field profiles. (C) Snapshot taken from the MD simulation of the lipid bilayer subject to a TM voltage taken at the early stage of the pore formation showing the configuration of water molecules represented as balls and sticks (oxygen: grey) and (hydrogen: white) forming a continuous wire through the hydrophobic core of the membrane.

CONCLUSION

Currently, computational approaches remain potentially the only techniques able to follow, at the atomic scale the local perturbation lipid membranes undergo when they are subject to external electric field. The results obtained so far are believed to capture the essence of the several aspects of the electroporation phenomena in bilayers' membranes, and could serve as an additional, complementary source of information to the current arsenal of experimental tools. At rest, *i.e.* before the membrane breakdown, many characteristics of the bilayer (hydrophobic core thickness, area per lipid, intrinsic dipole potential, capacitance …) are in satisfactory agreement with experiment, which indicate that the force fields and protocols used in MD simulations of lipid bilayers are rather well optimized. Despite their intrinsic differences, all MD simulations of lipid bilayers subject to high enough TM voltages, regardless of how the latter are generated, provide support to the stochastic pore formation theories in which, the stress imposed on the membrane is released thanks to formation of nanometer scale hydrophilic pores that span the lipid core.

Recently experimental and theoretical investigations of electroporation of small patches of planar lipid bilayers have been conducted by means of linearly rising current. The experiments were conducted on ~120-μm-diameter patches of planar phospholipid bilayers. The steadily increasing voltage across the bilayer imposed by linearly increasing current led to electroporation of the membrane for voltages above a few hundred millivolts. This method shows new molecular mechanisms of electroporation. We recorded small voltage drops preceding the breakdown of the bilayer due to irreversible electroporation. These voltage drops were often followed by a voltage re-rise within a fraction of a second. Modeling the observed phenomenon by equivalent electric circuits showed that these events relate to opening and closing of conducting pores through the bilayer. Molecular dynamics simulations performed under similar conditions indicate that each event is likely to correspond to the opening and closing of a single pore of about 5 nm in diameter, the conductance of which ranges in the 100-nS scale. This combined experimental and theoretical investigation provides a better quantitative characterization of the size, conductance and lifetime of pores created during lipid bilayer electroporation. Such a molecular insight should enable better control and tuning of electroporation parameters for a wide range of biomedical and biotechnological applications.

Much more effort is still needed in order to investigate the cascade of events involved in more complex events such as the transport of large molecules across the membranes. Recent success stories in this direction [84] show that the modellers need to seek much more combined studies with experimentalists in order to provide better understanding of such processes.

REFERENCES

[1] N. Eberhard, A. E. Sowers, and C. A. Jordan, *Electroporation and electrofusion in cell lbiology*, New York: Plenum Press, 1989.

[2] J. A. Nickoloff, *Animal cell electroporation and electrofusion protocols*, Totowa, NJ: Humana Press, 1995.

[3] S. Li, *Electroporation protocols: preclinical and clinical gene medecine*, Totowa, NJ.: Humana press, 2008.

[4] R. B. Gennis, *Biomembranes: molecular structure and function*, Heidelberg: Spring Verlag, 1989.

[5] I. G. Abidor, V. B. Arakelyan, L. V. Chernomordink *et al*., “Electrical breakdown of BLM: main experimental facts and their qualitative discussion.,” *Bioelectrochem. Bioenerg.*, 6, 37-52, 1979.

[6] R. Benz, F. Beckers, and U. Zimmerman, “Reversible electrical breakdown of lipid bilayer membranes - Charge-pulse relaxation study,” *J. Membr. Biol.* , 48, 181-204, 1979.

[7] J. C. Weaver, and Y. A. Chizmadzhev, “Theory of electroporation. A review,” *Bioelectrochem. Bioenerg.*, 41, 135-160, 1996.

[8] J. C. Weaver, “Electroporation of biological membranes from multicellular to nano scales,” *IEEE Trans. Dielectr. Electr. Insul.*, 10, 754-768, 2003.

[9] C. Chen, S.W. Smye, M.P. Robinson *et al*., “Membrane electroporation theories: a review,” *Med. Biol. Eng. Comput.*, 44, 5-14, 2006.

[10] G. Pucihar, T. Kotnik, B. Valic *et al*., “Numerical determination of transmembrane voltage induced on irregularly shaped cells,” *Annals Biomed. Eng.* , 34, 642-652, 2006.

[11] G. Pucihar, T. Kotnik, D. Miklavcic *et al*., “Kinetics of transmembrane transport of small molecules into electropermeabilized cells,” *Biophys. J.* , 95, 2837-2848, 2008.

[12] D. C. Chang, "Structure and dynamics of electric field-induced membrane pores as revealed by rapid-freezing electron microscopy," *Guide to Electroporation and Electrofusion*, pp. 9-27, Orlando, Florida: Academic Press, 1992.

[13] D. P. Tieleman, S. J. Marrink, and H. J. C. Berendsen, “A computer perspective of membranes: molecular dynamics studies of lipid bilayer systems.,” *Biochim. Biophys. Acta.*, 1331, 235-270, 1997.

[14] D. J. Tobias, K. Tu, and M. L. Klein, “Atomic-scale molecular dynamics simulations of lipid membranes,” *Curr. Opin. Colloid Int. Sci.*, 2, 15-26, 1997.

[15] L. R. Forrest, and M. S. P. Sansom, “Membrane simulations: bigger and better,” *Curr. Opin. Struct. Biol.*, 10, 174-181, 2000.

[16] S. E. Feller, “Molecular dynamics simulations of lipid bilayers,” *Curr. Opin. Coll In.*, 5, 217-223, 2000.

[17] D. J. Tobias, "Membrane simulations," *Computational Biochemistry and Biophysics*, A. D. M. J. O.H. Becker, B. Roux, M. Watanabe, ed., New York: Marcel Dekker, 2001.

[18] R. J. Mashl, H. L. Scott, S. Subramaniam *et al*., “Molecular simulation of dioleylphosphatidylcholine bilayers at differing levels of hydration,” *Biophys. J.*, 81, 3005-3015, 2001.

[19] L. Saiz, and M. L. Klein, “Computer simulation studies of model biological membranes,” *Acc. Chem. Res.*, 35, 482-489, 2002.

[20] C. Anézo, A. H. d. Vries, H. D. Höltje *et al*., “Methodological issues in lipid bilayer simulations,” *J. Phys. Chem. B*, 107, 9424-9433, 2003.

[21] M. L. Berkowitz, D. L. Bostick, and S. Pandit, “Aqueous solutions next to phospholipid membrane surfaces: Insights from simulations.,” *Chem. Rev.*, 106, no. 4, 1527-1539, 2006.

[22] E. Lindahl, and M. S. P. Sansom, “Membrane proteins: molecular dynamics simulations.,” *Curr. Opin. Struct. Biol.*, 18, 425-431, 2008.

[23] O. Edholm, "Time and length scales in lipid bilayer simulations," *Computationl Modeling of Membrane Bilayers*, Current Topics in Membranes S. E. Feller, ed., pp. 91-110 Elsevier, 2008.

[24] S. E. Feller, *Computationla Modeling of Membrane Bilayers*: Elsevier, 2008.

[25] S. J. Marrink, A. H. de Vries, and D. P. Tieleman, “Lipids on the move: Simulations of membrane pores, domains, stalks and curves,” *Biochim. Biophys. Acta. Biomembranes*, 1788, 149-168, 2009.

[26] Q. Hu, S. Viswanadham, R. P. Joshi *et al*., "Simulations of transient membrane behavior in cells subjected to a high-intensity ultrashort electric pulse," *Phys. Rev. E.,* 71, 031914, 2005.
[27] D. P. Tieleman, "The molecular basis of electroporation.," *BMC Biochemistry,* 5, 10, 2004.
[28] M. Tarek, "Membrane electroporation: A molecular dynamics simulation.," *Biophys J*., 88, 4045-4053, 2005.
[29] R. A. Bockmann, B. L. de Groot, S. Kakorin *et al*., "Kinetics, statistics, and energetics of lipid membrane electroporation studied by molecular dynamics simulations," *Biophys J,* 95, 1837-1850, 2008.
[30] M. J. Ziegler, and P. T. Vernier, "Interface water dynamics and porating electric fields for phospholipid bilayers," *J. Phys Chem. B,* 112, 13588-13596, 2008.
[31] S. J. Beebe, and K. H. Schoenbach, "Nanosecond pulsed electric fields: A new stimulus to activate intracellular signaling," *J. Biomed. Biotech*., 4, 297-300, 2005.
[32] Z. Vasilkoski, A. T. Esser, T. R. Gowrishankar *et al*., "Membrane electroporation: The absolute rate equation and nanosecond time scale pore creation," *Phys. Rev. E.,* 74, 021904, 2006.
[33] R. Sundararajan, "Nanosecond Electroporation: another look," *Mol. Biotech*., 41, 69-82, 2009.
[34] J. Deng, K. H. Schoenbach, E. S. Buescher *et al*., "The Effects of Intense Submicrosecond Electrical Pulses on Cells," *Biophys J,* 84, 2709-2714, 2003.
[35] H. Pauly, and H. P. Schwan, "Uber Die Impedanz Einer Suspension Von Kugelformigen Teilchen Mit Einer Schale - Ein Modell Fur Das Dielektrische Verhalten Von Zellsuspensionen Und Von Proteinlosungen," *Z Naturforsch B,* 14, no. 2, 125-131, 1959.
[36] T. Kotnik, D. Miklavcic, and T. Slivnik, "Time course of transmembrane voltage induced by time-varying electric fields - a method for theoretical analysis and its application " *Bioelectrochem. Bioenerg*., 45, no. 1, 3-16, Mar, 1998.
[37] T. Kotnik, and D. Miklavcic, "Theoretical evaluation of voltage inducement on internal membranes of biological cells exposed to electric fields," *Biophys J,* 90, no. 2, 480-491, Jan, 2006.
[38] M. P. Allen, and D. J. Tildesley, *Computer simulation of liquids*, Oxford: Clarendon Press, 1987.
[39] A. R. Leach, *Molecular modelling: principles and applications*, Second Edition ed.: Prentice Hall, 2001.
[40] L. D. Schuler, X. Daura, and W. F. van Gunsteren, "An improved GROMOS96 force field for aliphatic hydrocarbons in the condensed phase," *J. Comp. Chem,* 22, 1205-1218, 2001.
[41] A. D. MacKerell Jr., D. Bashford, M. Bellott *et al*., "All-atom empirical potential for molecular modeling and dynamics studies of proteins.," *J. Phys. Chem. B,* 102, 3586-3616, 1998.
[42] D. A. Case, D. A. Pearlman, J. W. Caldwell *et al*., *AMBER6*, San Francisco: University of California, 1999.
[43] P. E. M. Lopes, B. Roux, and A. D. MacKerell, "Molecular modeling and dynamics studies with explicit inclusion of electronic polarizability: theory and applications," *Theor. Chem. Acc*., 124, 11-28, 2009.
[44] A. Warshel, M. Kato, and A. V. Pisliakov, "Polarizable force fields: history, test cases, and prospects," *J. Chem. Theory Comput.* , 3, 2034–2045, 2007.
[45] T. A. Halgren, and W. Damm, "Polarizable force fields," *Curr. Opin. Struct. Biol*., 11, 236–242, 2001.
[46] E. Lindahl, and O. Edholm, "Mesoscopic undulations and thickness fluctuations in lipid bilayers from molecular dynamics simulations," *Biophys. J*., 79, 426-433, 2000.
[47] S. J. Marrink, and A. E. Mark, "Effect of undulations on surface tension in simulated bilayers.," *J. Phys. Chem. B,* 105, 6122-6127, 2001.
[48] S.W. Chiu, M. Clark, E. Jakobsson *et al*., "Optimization of hydrocarbon chain interaction parameters: Application to the simulation of fluid phase lipid bilayers," *J. Phys. Chem. B,* 103, 6323-6327, 1999.
[49] T. Rög, K. Murzyn, and M. Pasenkiewicz-Gierula, "The dynamics of water at the phospholipid bilayer: A molecular dynamics study," *Chem. Phys. Lett*., 352, 323-327, 2002.
[50] L. Saiz, and M. L. Klein, "Structural properties of a highly polyunsaturated lipid bilayer from molecular dynamics simulations," *Biophys. J*., 81, 204-216, 2001.
[51] S. E. Feller, K. Gawrisch, and A. D. MacKerell, "Polyunsaturated fatty acids in lipid bilayers: intrinsic and environmental contributions to their unique physical properties," *J. Am. Chem. Soc*., 124, 318-326, 2002.
[52] M. L. Berkowitz, and M. J. Raghavan, "Computer simulation of a water/membrane interface," *Langmuir,* 7, 1042-1044, 1991.
[53] K. V. Damodaran, and K. M. Merz, "A comparison of DMPC and DLPE-based lipid bilayers," *Biophys. J.,* 66, 1076--1087, 1994.
[54] J. J. L. Cascales, H. J. C. Berendsen, and J. G. d. l. Torre, "Molecular dynamics simulation of water between two charged layers of dipalmitoylphosphatidylserine," *J. Phys. Chem*., 100, 8621-8627, 1996.
[55] P. Mukhopadhyay, L. Monticelli, and D. P. Tieleman, "Molecular dynamics simulation of a palmitoyl-oleoyl phosphatidylserine bilayer with Na+ Counterions and NaCl," *Biophys. J*., 86, 1601-1609, 2004.
[56] S. W. Chiu, S. Vasudevan, E. Jakobsson *et al*., "Structure of sphingomyelin bilayers: A simulation study," *Biophys. J*., 85, 3624-3635, 2003.
[57] S. A. Pandit, D. Bostick, and M. L. Berkowitz, "Mixed Bilayer Containing Dipalmitoylphosphatidylcholine and Dipalmitoylphosphatidylserine: Lipid Complexation, Ion Binding, and Electrostatics," *Biophys J,* 85, 3120-3131, 2003.
[58] R. Y. Patel, and P. V. Balaji, " Characterization of symmetric and asymmetric lipid bilayers composed of varying concentrations of ganglioside GM1 and DPPC," *J. Phys Chem. B,* 112, 3346-3356, 2008.
[59] M. Dahlberg, and A. Maliniak, "Molecular dynamics simulations of cardiolipin bilayers," *J. Phys Chem. B,* 112, 11655-11663, 2008.
[60] A. A. Gurtovenko, and I. Vattulainen, "Effect of NaCl and KCl on phosphatidylcholine and phosphatidylethanolamine lipid membranes: Insight from atomic-scale simulations for understanding salt-induced effects in the plasma membrane " *J. Phys Chem. B,* 112, 1953-1962, 2008.
[61] R. Vacha, M. L. Berkowitz, and P. Jungwirth, "Molecular model of a cell plasma membrane with an asymmetric multicomponent composition: Water permeation and ion effects," *Biophys J,* 96, 4493-4501, 2009.
[62] T. Rog, H. Martinez-Seara, N. Munck *et al*., "Role of cardiolipins in the inner mitochondrial membrane: Insight

gained through atom-scale simulations," *J. Phys Chem. B*, 113, 3413-3422 2009.

[63] Z. Li, R. M. Venable, L. A. Rogers *et al*., "Molecular dynamics simulations of PIP2 and PIP3 in lipid bilayers: Determination of ring orientation, and the effects of surface roughness on a poisson-boltzmann description," *Biophys J*, 97, 155-163, 2009.

[64] C. Chipot, M. L. Klein, and M. Tarek, "Modeling lipid membranes.," *Handbook of Materials Modeling*, S. Yip, ed., pp. 929-958, Dordrecht, The Netherland: Springer, 2005.

[65] M. C. Wiener, and S. H. White, "Structure of fluid dioleylphosphatidylcholine bilayer determined by joint refinement of x--ray and neutron diffraction data. III. Complete structure," *Biophys. J.*, 61, 434-447, 1992.

[66] Q. Zhong, P. B. Moore, D. M. Newns *et al*., "Molecular dynamics study of the LS3 voltage-gated ion channel," *FEBS Lett*., 427, 267-270 1998.

[67] Y. Yang, D. Henderson, P. Crozier *et al*., "Permeation of ions through a model biological channel: effect of periodic boundary condition and cell size. ," *Molec. Phys*, 100, 3011-3019, 2002.

[68] D. P. Tieleman, J. H. C. Berendsen, and M. S. P. Sansom, "Voltage-dependent insertion of alamethicin at phospholipid/water and octane water interfaces.," *Biophys. J*., 80, 331-346, 2001.

[69] P. S. Crozier, D. Henderson, R. L. Rowley *et al*., "Model channel ion currents in NaCl extended simple point charge water solution with applied-field molecualr dynamics," *Biophys. J.*, 81, 3077-3089, 2001.

[70] B. Roux, "The membrane potential and its representation by a constant electric field in computer simulations," *Biophys J*, 95, 4205-4216, 2008.

[71] P. T. Vernier, M. J. Ziegler, Y. Sun *et al*., "Nanopore formation and phosphatidylserine externalization in a phospholipid Bilayer at high transmembrane potential," *J. Am. Chem. Soc.* , 128, 6288-6289, 2006.

[72] W. Treptow, B. Maigret, C. Chipot *et al*., "Coupled motions between pore and voltage-sensor domains: a model for *Shaker* B, a voltage-gated potassium channel.," *Biophys. J*., 87, 2365-2379, 2004.

[73] A. Aksimentiev, and K. Schulten, "Imaging α−hemolysin with molecular dynamics: ionic conductance, osmotic permeability, and the electrostatic potential map," *Biophys. J.*, 88, 3745-3761, 2005.

[74] F. Khalili-Araghi, E. Tajkhorshid, and K. Schulten, "Dynamics of K+ ion conduction through Kv1.2. ," *Biophys. J.*, 91, L72–L74, 2006.

[75] M. Sotomayor, V. Vasquez, E. Perozo *et al*., "Ion conduction through MscS as determined by electrophysiology and simulation," *Biophys. J.*, 92, 886-902, 2007.

[76] C. Chimerel, L. Movileanu, S. Pezeshki *et al*., "Transport at the nanoscale: temperature dependence of ion conductance," *Eur. Biophys. J. Biophy. Lett*., 38, 121-125, 2008.

[77] L. Saiz, and M. L. Klein, "Electrostatic interactions in a neutral model phospholipid bilayer by molecular dynamics simulations," *J. Chem. Phys*., 116, 3052-3057, 2002.

[78] K. Gawrisch, D. Ruston, J. Zimmerberg *et al*., "Membrane dipole potentials, hydration forces, and the ordering of water at membrane surfaces," *Biophys. J*., 61, 1213-1223, 1992.

[79] P. T. Vernier, and M. J. Ziegler, "Nanosecond field alignment of head group and water dipoles in electroporating phospholipid bilayers," *J. Phys Chem. B*, 111, 12993-12996, 2007.

[80] Z. A. Levine, and P. T. Vernier, "Life cycle of an electropore: Field dependent and field-indepedent steps in pore creation and annihilation," *J. Membr. Biol*., 236, 27-36, 2012.

[81] Z. A. Levine, and P. T. Vernier, "Calcium and phosphatidylserine inhibit lipid electropore formation and reduce pore lifetime," *J. Membr. Biol*., 2012.

[82] M. Golzio, J. Teissie, and M.-P. Rols, "Direct visualization at the single-cell level of electriclly mediated gene delivery," *Proc. Natl. Acad. Sci. U.S.A*., 99, 1292-1297, 2002.

[83] A. Paganin-Gioannia, E. Bellarda, J. M. Escoffrea *et al*., "Direct visualization at the single-cell level of siRNA electrotransfer into cancer cells," *Proc. Nat. Acad. Sci. U.S.A*., 108, 10443-10447, 2011.

[84] M. Breton, L. Delemotte, A. Silve *et al*., "Transport of siRNA through Lipid Membranes Driven by Nanosecond Electric Pulses: An Experimental and Computational Study.," *J. Amer. Chem. Soc*., 134, 13938–13941, 2012.

[85] J. N. Sachs, P. S. Crozier, and T. B. Woolf, "Atomistic simulations of biologically realistic transmembrane potential gradients," *J. Chem. Phys*., 121, 10847-10851, 2004.

[86] L. Delemotte, F. Dehez, W. Treptow *et al*., "Modeling membranes under a transmembrane potential.," *J. Phys Chem. B*, 112, 5547-5550, 2008.

[87] D. Bostick, and M. L. Berkowitz, "The implementation of slab geometry for membrane-channel molecular dynamics simulations," *Biophys J*, 85, 97-107, 2003.

[88] B. Roux, "Influence of the membrane potential on the free energy of an intrinsic protein," *Biophys. J.*, 73, 2980-2989, 1997.

[89] A. A. Gurtovenko, J. Jamshed Anwar, and I. Vattulainen, "Defect-mediated trafficking across cell membranes: Insights from in silico modeling," *Chem. Rev*., 110, 6077-6103, 2010.

[90] A. A. Gurtovenko, and I. Vattulainen, "Pore formation coupled to ion transport through lipid membranes as induced by transmembrane ionic charge imbalance: Atomistic molecular dynamics study," *J. Am. Chem. Soc*., 127, 17570-17571, 2005.

[91] S. K. Kandasamy, and R. G. Larson, "Cation and anion transport through hydrophilic pores in lipid bilayers," *J. Chem. Phys*., 125, 074901, 2006.

[92] Kutzner C, Grubmüller H, de Groot BL *et al*., "Computational electrophysiology: the molecular dynamics of ion channel permeation and selectivity in atomistic detail," *Biophys J*, 101, 809-817, 2011.

[93] Y. A. Liberman, and V. P. Topaly, "Permeability of biomolecular phospholipid membranes for fat-soluble ions," *Biophysics. USSR*, 14, 477, 1969.

[94] S. J. Marrink, F. Jähniga, and H. J. Berendsen, "Proton transport across transient single-file water pores in a lipid membrane studied by molecular dynamics simulations," *Biophys J*, 71, 632-647, 1996

ACKNOWLEDGEMENT
Simulations presented in this work benefited from access to the HPC resources of the Centre Informatique National de l'Enseignement Superieur (CINES) FRANCE. The authors would like to acknowledge very fruitful and insightful discussion with Damijan Miklavcic, Luis Mir and Thomas Vernier. Research conducted in the scope of the EBAM European Associated Laboratory (LEA). M.T acknowledges the support of the French Agence Nationale de la Recherche, under grant *(ANR-10_, BLAN-916-03-INTCELL)*.

Mounir Tarek born in Rabat-Morocco in 1964. He received a Ph.D. in Physics from the University of Paris in 1994. He is a senior research scientist (Directeur de Recherches) at the CNRS. He joined the CNRS after a four years tenure at the National Institute of Standards and Technology (Gaithersburg MD USA) following three years tenure at the University of Pennsylvania (Post-doc in M.L. Klein group). For the last few years, he worked on large-scale state-of-the-art molecular simulations of lipid membranes and TM proteins probing their structure and dynamics.

NOTES

In vitro Cell Electropermeabilization

Justin Teissié
IPBS UMR 5089 CNRS and Université de Toulouse, Toulouse, France

Abstract: Electropulsation is one of the most successful methods to introduce foreign molecules in living cells *in vitro*. This lecture describes the factors controlling electropermeabilization to small molecules (< 4 kDa). The description of *in vitro* events brings the attention of the reader on the processes occurring before, during and after electropulsation of cells. The role of the different electrical parameters (Field strength, pulse duration, delay between pulses) is delineated. The kinetic of the processes affecting the cell surface is described outlining that most of the exchange across the membrane takes place after the pulse during the so called resealing. Cell contribution to this critical step is tentatively explained.

INTRODUCTION

The application of electric field pulses to cells leads to the transient permeabilization of the plasma membrane (electropermeabilization). This phenomenon brings new properties to the cell membrane: it becomes permeabilized, fusogenic and exogenous membrane proteins can be inserted. It has been used to introduce a large variety of molecules into many different cells *in vitro* [1, 2].

The present lecture is reporting what is called "classical electropermeabilization". This meant that it is relevant of the effect of pulses lasting from µs to several ms, with a rising time of a few hundreds of ns. In this time domain, dielectric spectroscopy of a cell shows that the membrane can be considered as a non conductive insulator (indeed some active leaks may be present).

One of the limiting problems remains that very few is known on the physicochemical mechanisms supporting the reorganisation of the cell membrane. Electropermeabilization is not simply punching holes in a one lipid bilayer. The physiology of the cell is controlling many parameters. The associated destabilisation of the membrane unpermeability is a stress for the cells and may affect the cell viability.

This lecture explains the factors controlling electropermeabilization to small molecules (< 4 kDa). The events occurring before, during and after electropulsation of cells are described.

Preambule: what is a biological membrane?

The target of cell electropermeabilization is the cell membrane, more precisely the plasma membrane. In many textbooks, the description of a biological membrane is limited to a lipid bilayer. This is far from the biological complexity and should be used only for soft matter investigations. When the process is applied to a cell (and to a tissue), a more sophisticated description of the biological membrane organization is needed. It is a complex assembly between proteins and a mixture of lipids. It results from a network of weak forces resulting in a complex pattern of lateral pressure across the membrane. A lot of lateral and rotational movements of the membrane components on the sub-microsecond timescale is present. Spontaneous transverse movements are energy driven or result from membrane traffic related events (endocytosis, exocytosis). The distribution of lipids is not homogeneous as assumed in the fluid matrix model but localized specific accumulations are detected (rafts). This is due to the fact that a biological membrane is an active entity where a flow of components is continuously occurring (so called membrane traffic). Endocytosis and exocytosis are processes involved in the membrane organization. They are affected by stresses applied on the cell. This costs a lot of energy provided by the cell metabolism. Another consequence is the ionic gradient across the membrane resulting from the balance between active pumping and spontaneous leaks. A final aspect is that damages to the membrane are repaired not only by an intra-membraneous process (as for a viscoelastic material) but by a patching process mediated by cytosolic vesicles.

It is therefore very difficult to provide an accurate physical description of a biological membrane at the molecular level. Either oversimplifying approximations are used (using lipid vesicles, a soft matter approach) or a phenomenological description is provided with fitting to physical chemical equations (a life science approach). Both are valid as long as you keep aware of the limits in accuracy. The present lecture will be within the life science approach to give the suitable informations for Clinical and well as biotechnological applications.

A- A biophysical description and a biological validation

A-1 The external field induces membrane potential difference modulation

An external electric field modulates the membrane potential difference as a cell can be considered as a spherical capacitor [3]. The transmembrane potential difference (TMP) induced by the electric field after a (capacitive) charging time, $\Delta\Psi_i$ is a complex function $g(\lambda)$ of the specific conductivities of the membrane (λ_m), the pulsing buffer (λo) and the cytoplasm (λ_i), the membrane thickness, the cell size (r) and packing. Thus,

$$\Delta\Psi_i = f \cdot g(\lambda) \cdot r \cdot E \cdot \cos\theta \qquad (1)$$

in which θ designates the angle between the direction of the normal to the membrane at the considered point on the cell surface and the field direction, E the field intensity, r the radius of the cell and f, a shape factor (a cell being a spheroid). Therefore, $\Delta\Psi_i$ is not uniform on the cell surface. It is maximum at the positions of the cell facing the electrodes. These physical predictions were checked experimentally by videomicroscopy by using potential difference sensitive fluorescent probes [4-6]. This is valid with dilute cell suspensions. In dense systems, self shielding in the cell population affects the local field distribution and reduces the local (effective) field distribution [7]. Stronger field intensities are needed to get the same induced potential. Another factor affecting the induced potential differences is the shape or the cell and their relative orientation to the field lines. When the resulting transmembrane potential difference ΔΨ (i.e. the sum between the resting value of cell membrane ΔΨo and the electroinduced value ΔΨi) reaches locally 250 mV, that part of the membrane becomes permeable for small charged molecules [3, 8].

One more parameter is that as the plasma membrane must be considered as a capacitor, there is a membrane charging time that may affect the magnitude of the TMP when the pulse duration is short or in poorly conducting pulsing buffers.

A-2 Parameters affecting electropermeabilization

A-2-1 Electric field parameters

Permeabilization is controlled by the field strength. Field intensity larger than a critical value ($E_{p,r}$) must be applied to the cell suspension. From Eq. (1), permeabilization is first obtained for θ close to 0 or π. $E_{p,r}$ is such that:

$$\Delta\Psi_{i,perm} = f \cdot g(\lambda) \cdot r \cdot E_{p,r} \qquad (2)$$

Permeabilization is therefore a local process on the cell surface. The extend of the permeabilized surface of a spherical cell, Aperm, is given by:

$$A_{perm} = A_{tot} \frac{\left(1 - \frac{E_{p,r}}{E}\right)}{2} \qquad (3)$$

where A_{tot} is the cell surface and E is the applied field intensity. Increasing the field strength will increase the part of the cell surface, which is brought to the electropermeabilized state.

These theoretical predictions are experimentally directly supported on cell suspension by measuring the leakage of metabolites (ATP) [9] or at the single cell level by digitised fluorescence microscopy [10, 11]. The permeabilized part of the cell surface is a linear function of the reciprocal of the field intensity. Permeabilization, due to structural alterations of the membrane, remained restricted to a cap on the cell surface. In other words, the cell obeys the physical predictions! The area affected by the electric field depends also on the shape (spheroid) and on the orientation of the cell with the electric field lines [12]. Changing the field orientation between the different pulses increases the fraction of the cell surface which is permeabilized.

Experimental results obtained either by monitoring conductance changes on cell suspension [13] or by fluorescence observation at the single cell level microscopy [10, 11] shows that the density of the local alterations is strongly controlled by the pulse duration. An increase of the number of pulses first leads to an increase of local permeabilization level.

The field strength controls the geometry of the part of the cell which is permeabilized. This is straightforward for spherical cells (and validitated by fluorescence microscopy) but more complicated with other cell shapes. Within this cap, the density of defects is uniform and under the control of the pulse(s) duration.

A-2-2 Cell size

The induced potential is dependent on the size of the cell (Eq (1)). The percentage of electropermeabilized cells in a population, where size heterogeneity is present, increases with an increase in the field strength. The relative part of the cell surface which is permeabilized is larger on a larger cell at a given field strength [13]. Large cells are sensitive to lower field strengths than small one. Plated cells are permeabilized with Ep value lower than when in suspension. Furthermore large cells in a population appear to be more fragile. An irreversible permeabilization of a subpopulation is observed when low field pulses (but larger than Ep) are applied. Another characteristic is that the 'loading' time is under the control of the cell size [14].

A-3 Forces acting on the membrane

The external electrical field pulse generates a net transient mechanical force which tends to stretch the spherical membrane [15]. This force appears due to

Maxwell stresses existing in the spherical dielectric shell which cause deformation. The total radial force acts on the membrane during the transient process and tends to stretch the microorganism. It can even lead to rupture of the membrane resulting in the death of the microorganism [16]. But as the cellular elasticity is based upon the actin cytoskeleton, this stretching would affect the internal cell organization

B- Structural Investigations

B-1 P31 NMR investigations of the polar head region of phospholids

NMR of the phosphorus atom in the phosphatidylcholine headgroup was strongly affected when lipid multilayers were submitted to electric field pulses. It is concluded that the conformation of the headgroup was greatly affected while no influence on the structure and dynamics of the hydrocarbon chains could be detected [17]. On electropermeabilized CHO cells, a new anisotropic peak with respect to control cells was observed on 31 P NMR spectroscopic analysis of the phospholipid components [18]. A reorganization of the polar head group region leading to a weakening of the hydration layer may account for these observations. This was also thought to explain the electric field induced long lived fusogenicity of these cells..

B-2 Structural approaches with advanced technologies

Atomic Force Microscopy (AFM) has been extensively used to image live biological samples at the nanoscale cells in absence of any staining or cell preparation. [19]. AFM, in the imaging modes, can probe cells morphological modifications induced by EP. In the force spectroscopy mode, it is possible to follow the nanomechanical properties of a cell and to probe the mechanical modifications induced by EP. transient rippling of membrane surface were observed as consequences of electropermeabilization and a decrease in membrane elasticity by 40% was measured on living CHO cells [20]. An inner effect affected the entire cell surface that may be related to cytoskeleton destabilization.

Due to the nonlinear and coherent nature of second harmonic generation (SHG) microscopy, 3D radiation patterns from stained neuronal membranes were sensitive to the spatial distribution of scatterers in the illuminated patch, and in particular to membrane defect formation formation. higher scatterers (membrane alterations) densities, lasting < 5 milliseconds, were observed at membrane patches perpendicular to the field whereas lower density was observed at partly tangent locations [21, 22]. Higher pore densities were detected at the anodic pole compared to cathodic pole.

C-Practical aspects of electropermeabilization

C-1 Sieving of electropermeabilization

Electropermeabilization allows a post-pulse free-like diffusion of small molecules (up to 4 kDa) whatever their chemical nature. Polar compounds cross easily the membrane. But the most important feature is that this reversible membrane organisation is nevertheless long-lived in cells. Diffusion is observed during the seconds and minutes following the ms pulse. Most of the exchange took place after the pulse [10, 11]. Resealing of the membrane defects and of the induced permeabilization is a first order multistep process, which appears to be controlled by protein and organelles reorganisation. But as for other macroscopic damage to a plasma membrane, electropermeabilization has been shown to cause internal vesicles (lysosomes) to undergo exocytosis to repair membrane damage, a calcium mediated process called lysosomal exocytosis. Membrane resealing is thus a cellular process.

C-2 Associated transmembrane exchange

Molecular transfer of small molecules (< 4 kDa) across the permeabilized area is mostly driven by the concentration gradient across the membrane. Electrophoretic forces during the pulse may contribute [10]. Free diffusion of low weight polar molecules after the pulse can be described by using the Fick equation on its electropermeabilized part [9]. This gives the following expression for a given molecule S and a cell with a radius r:

$$\phi(S,t) = 2\pi r^2 \cdot P_S \cdot \Delta S \cdot X(N,T)\left(1-\tfrac{E_{p,r}}{E}\right)\exp(-k\cdot(N,T)\cdot t) \quad (4)$$

where Φ(S, t) is the flow at time t after the N pulses of duration T (the delay between the pulses being short compared to t), P_s is the permeability coefficient of S across the permeabilized membrane and ΔS is the concentration difference of S across the membrane. X is reporting the density of conducting defects in the field affected cap on the cell surface. Ep depends on r (size). The delay between pulses is clearly playing a role in the definition of X but this remains to be investigated in details. For a given cell, the resealing time (reciprocal of k) is a function of the pulse duration but not of the field intensity as checked by digitised videomicroscopy [9]. A strong control by the temperature is observed. The cytoskeletal integrity should be preserved [24]. Resealing of cell membranes is a complex process which is controlled by the ATP level. Starved cells are fragile. An open question is to know if it is a self-resealing or other components of the cell are involved. Organelle fusion may be involved as in the case of other membrane repair occurring with after laser induced damage.

C-3 Cellular responses

Reactive oxygen species (ROS) are generated at the permeabilized loci, depending on the electric field parameters [25]. These ROS can affect the viability. This is a major drawback for the transfer of sensitive species (nucleic acids). Adding antioxydants is a safe approach [26].
When a cell is permeabilized, an osmotic swelling may result, leading to an entrance of water into the cell. This increase of cell volume is under the control of the pulse duration and of course of the osmotic stress [27].

There is a loss of the bilayer membrane asymmetry of the phospholipids on erythrocytes[28].

When cells are submitted to short lived electric field pulses, a leakage of metabolites from the cytoplasm is observed which may bring a loss in viability. This can occur just after the pulse (short term death) or on a much longer period when cells have resealed (long term death) [23].

CONCLUSION

All experimental observations on cell electropermeabilization are in conflict with a naive model where it is proposed to result from holes punched in a lipid bilayer (see [29] as a recent review). Structural changes in the membrane organization supporting permeabilization remains poorly characterized. New informations appear provided by coarse grained computer-based simulations. Nevertheless it is possible by a careful cell dependent selection of the pulsing parameters to introduce any kind of polar molecules in a mammalian cell while preserving its viability. The processes supporting the transfer are very different for different molecules. Transfer is electrophoretically mediated during the pulse and is mostly present after the pulse driven by diffusion for small charged molecules (drugs) [30, 9]. SiRNA are only transferred by the electrophoretic drag present during the pulse [31]. DNA plasmids are accumulated in spots on the electropermeabilized cell surface during the pulse and slowly translocated in the cytoplasm along the microtubules by a metabolic process [32, 33]

ACKNOWLEDGEMENT

Supports from the CNRS and the region Midi Pyrénées must be acknowledged.
This state of the art in Electropermeabilization is mostly due to the collective work of scientists and students in my former group of "Cell Biophysics" in Toulouse. *Research conducted in the scope of the EBAM European Associated Laboratory (LEA) and in the framework of COST Action TD1104,*

REFERENCES

[1] Potter, H., *Application of electroporation in recombinant DNA technology, in Methods in Enzymology,* vol. 217, I. Academic Press, Editor. 1993.

[2] Orlowski, S. and L.M. Mir, *Cell electropermeabilization: a new tool for biochemical and pharmacological studies*. Biochim Biophys Acta, 1993. 1154(1): 51-63.

[3] Teissié, J. and M.P. Rols, *An experimental evaluation of the critical potential difference inducing cell membrane electropermeabilization*. Biophys J, 1993. 65(1): 409-13.

[4] Gross, D., L.M. Loew, and W.W. Webb, *Optical imaging of cell membrane potential changes induced by applied electric fields*. Biophys J, 1986. 50: 339-48.

[5] Lojewska, Z., et al., *Analysis of the effect of medium and membrane conductance on the amplitude and kinetics of membrane potentials induced by externally applied electric fields*. Biophys J, 1989. 56(1): 121-8.

[6] Hibino, M., et al., *Membrane conductance of an electroporated cell analyzed by submicrosecond imaging of transmembrane potential*. Biophys J, 1991. 59(1): 209-20.

[7] Pucihar, G., et al., *Electropermeabilization of dense cell suspensions*. Biophys J. 2007 36(3): 173-185

[8] Teissié, J. and T.Y. Tsong, *Electric field induced transient pores in phospholipid bilayer vesicles*. Biochemistry, 1981. 20(6): 1548-54.

[9] Rols, M.P. and J. Teissie, *Electropermeabilization of mammalian cells. Quantitative analysis of the phenomenon*. Biophys J, 1990. 58(5): 1089-98.

[10] Gabriel, B. and J. Teissie, *Direct observation in the millisecond time range of fluorescent molecule asymmetrical interaction with the electropermeabilized cell membrane*. Biophys J, 1997. 73(5): 2630-7.

[11] Gabriel, B. and J. Teissie, *Time courses of mammalian cell electropermeabilization observed by millisecond imaging of membrane property changes during the pulse*. Biophys J, 1999. 76(4): 2158-65.

[12] Valič B, Golzio M, Pavlin M, Schatz A, Faurie C, Gabriel B, Teissié J, Rols MP, Miklavčič D. *Effect of electric field induced transmembrane potential on spheroidal cells: theory and experiment*. Eur. Biophys. J. **32**: 519-528, 2003

[13] Kinosita, K., Jr. and T.Y. Tsong, V*oltage-induced conductance in human erythrocyte membranes*. Biochim Biophys Acta, 1979. 554(2): 479-97.

[14] Sixou, S. and J. Teissie, *Specific electropermeabilization of leucocytes in a blood sample and application to large volumes of cells*. Biochim Biophys Acta, 1990. 1028(2): 154-60.

[15] Winterhalter M and Helfrich W *Deformation of spherical vesicles by electric fields* J. Colloid Interface Sci. 1988. 122 583–6

[16] Harbich W. and Helfrich W *Alignment and opening of giant lecithin vesicles by electric fields* Z Naturforsch 1991 34a, , 133-1335.

[17] Stulen G. *Electric field effects on lipid membrane structure*. Biochim Biophys Acta. 1981 ; 640(3):621-7

[18] Lopez A, Rols MP, Teissie J.*31P NMR analysis of membrane phospholipid organization in viable, reversibly*

electropermeabilized Chinese hamster ovary cells. Biochemistry. 1988 ;27(4):1222-8

[19] Pillet F, Chopinet L, Formosa C, Dague E Atomic Force Microscopy and pharmacology: From microbiology to cancerology Biochimica et Biophysica Acta 1840 (2014) 1028–1050

[20] Chopinet L, Roduit C, Rols MP, Dague E Destabilization induced by e*lectroper*meabilization analyzed by atomic force microscopy Biochimica et Biophysica Acta 2013 1828 2223–2229

[21] Zalvidea D, Claverol-Tintur´e E Second Harmonic Generation for time-resolved monitoring of membrane pore dynamics subserving electroporation of neurons BIOMEDICAL OPTICS EXPRESS 2011 / Vol. 2, No. 2 / 305-314

[22] Moen, EK. Ibey, BL. Beier HT Detecting Subtle Plasma Membrane Perturbation in Living Cells Using Second Harmonic Generation Imaging Biophysical Journal 2014 106 L37–L40

[23] Gabriel, B. and J. Teissie, *Control by electrical parameters of short- and long-term cell death resulting from electropermeabilization of Chinese hamster ovary cells*. Biochim Biophys Acta, 1995. 1266(2): 171-8.

[24] Teissié, J. and M.P. Rols, *Manipulation of cell cytoskeleton affects the lifetime of cell membrane electropermeabilization*. Ann N Y Acad Sci, 1994. 720: 98-110.

[25] Gabriel, B. and J. Teissie, *Generation of reactive-oxygen species induced by electropermeabilization of Chinese hamster ovary cells and their consequence on cell viability*. Eur J Biochem, 1994. 223(1): 25-33.

[26] Markelc B, Tevz G, Cemazar M, Kranjc S, Lavrencak J, Zegura B, Teissie J, Sersa G. *Muscle gene electrotransfer is increased by the antioxidant tempol in mice*. Gene Ther. 2011. doi: 10.1038

[27] Golzio, M., et al., *Control by osmotic pressure of voltage-induced permeabilization and gene transfer in mammalian cells*. Biophys J, 1998. 74(6): 3015-22.

[28] Haest, C.W., D. Kamp, and B. Deuticke, *Transbilayer reorientation of phospholipid probes in the human erythrocyte membrane*. *Lessons from studies on electroporated and resealed cells*. Biochim Biophys Acta, 1997. 1325(1): 17-33.

[29] Teissie J, Golzio M, Rols MP Mechanisms of cell membrane electropermeabilization: a minireview of our present (lack of ?) knowledge.Biochim Biophys Acta, 2005 .1724(3): 270-80

[30] Pucihar G, Kotnik T, Miklavcic D, Teissié J. *Kinetics of transmembrane transport of small molecules into electropermeabilized cells* Biophys J. 2008; **95**(6) :2837-48

[31] Paganin-Gioanni A, Bellard E, Escoffre JM, Rols MP, Teissié J, Golzio M. *Direct visualization at the single-cell level of siRNA electrotransfer into cancer cells*.Proc Natl Acad Sci U S A. 2011;**108**(26): 10443-7.

[32] Wolf H, Rols MP, Boldt E, Neumann E, Teissié J.*Control by pulse parameters of electric field-mediated gene transfer in mammalian cells*. Biophys J. 1994;**66**(2):524-31.

[33] Golzio M, Teissie J, Rols MP.*Direct visualization at the single-cell level of electrically mediated gene delivery*.Proc Natl Acad Sci U S A. 2002; **99**(3): 1292-7.

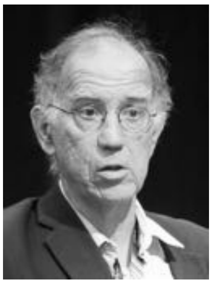

Teissié Justin was born 24 March 1947 in Poitiers, France. Got a degree in Physics at the Ecole superieure de Physique et de Chimie Industrielles de Paris (ESPCI) in 1970. Got a PhD in Macromolecular Chemistry on a project on fluorescence detection of action potential under the supervision of Prof. Monnerie (ESPCI) and Changeux (Institut Pasteur) in 1973. Got a DSC in Biophysics on a project on fluorescence characterisation of Langmuir Blodgett films in Toulouse in 1979. Was a Post Doc at the Medical School of the John Hopkins University in Baltimore in 1979-81. Present position: Directeur de recherches au CNRS emeritus. Author of more than 200 papers.

NOTES

NOTES

Nanoelectropulses: Theory and Practice

P. Thomas Vernier

Frank Reidy Research Center for Bioelectrics, Old Dominion University, Norfolk, VA, USA

INTRODUCTION

To utilize the diverse *effects* of electric fields on biological systems we must understand the ***causes***. In particular, we want to know the details of the ***interactions*** between electric fields and biomolecular structures. By looking at very short time scales (nanoseconds) and at single events (non-repetitive stimuli), we reduce the number of larger-scale disturbances and concentrate on reversible perturbations. The analysis is primarily in the time domain, but pulse spectral content may be important.

Of course, some important *effects* may be a consequence of irreversible processes driven by longer electric field exposures (microseconds, milliseconds). Short-pulse studies can help to dissect these processes.

Although modeling is of necessity a significant component of nanosecond bioelectrics investigations, experimental observations are fundamental, and to conduct experiments in nanosecond bioelectrics, one must be able to generate and accurately monitor the appropriate electrical stimuli, a non-trivial engineering challenge. We will discuss cause and effect here from both **scientific and engineering perspectives**, using data from experiments and simulations. It is commonplace in electrical engineering, and increasingly so in biology, to attack a problem with a combination of modeling and experimental tools. In nanosecond bioelectrics, observations (in vitro and in vivo) give rise to models (molecular and continuum), which drive experiments, which adjust and calibrate the models, which feed back again to empirical validation. This feedback loop focuses investigations of a very large parameter space on the critical ranges of values for the key variables.

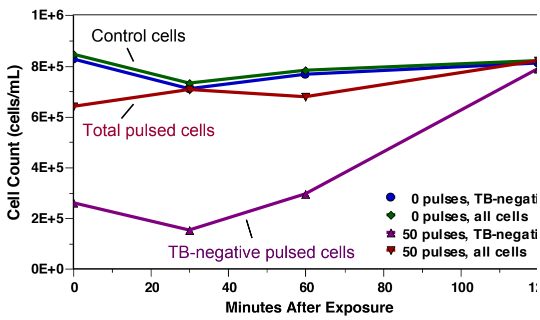

Figure 1. Nanoelectropulsed Jurkat T lymphoblasts recover over 2 hrs from initial Trypan blue permeabilization after exposure to 50, 20 ns, 4 MV/m pulses at 20 Hz.

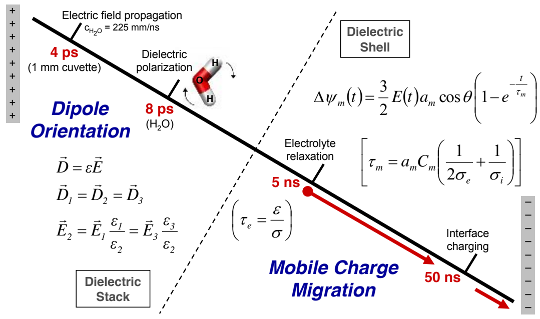

Figure 2. Timeline representing the sequence of events following electrical polarization of a biological tissue or aqueous suspension of cells. The sub-nanosecond regime can be modeled by the dielectric properties of the system. For longer times the distribution of fields and potentials is dominated by the migration of charged species.

NANOSECOND BIOELECTRICS

From longstanding theory that models the cell as a dielectric shell [1–4] came the notion that nanosecond-scale electric pulses could "bypass" the cell membrane, depositing most of their energy inside the cell instead of in the plasma membrane, the primary target of longer pulses. This idea was investigated experimentally beginning in the late 1990s [5–6]. Even though one early report indicated that the electric field-driven conductive breakdown of membranes can occur in as little as 10 ns [7], *and* a more careful theoretical analysis demonstrated that pulses with field amplitudes greater than about 1 MV/m will produce porating transmembrane potentials within about 2 ns [8], *and* a well-grounded model predicted "poration everywhere" in the nanosecond pulse regime [9], procedures used to detect electroporation of the plasma membrane (and the loss of membrane integrity in general) produced negative results for pulses with durations less than the charging time constant of a small cell in typical media (< 50 ns).

In addition to highlighting the limitations of traditional experimental methods for observing membrane permeabilization, this apparent discrepancy between model and observation points also to inadequacies in the dielectric shell model itself, at time scales below the membrane (cell) charging time. Higher-frequency effects associated with the dielectric properties of high-permittivity aqueous media and low-permittivity biological membranes [10–13] have not received much attention until recently. For the electropermeabilizing conditions that are most commonly studied (μs, kV/m pulses) these effects are secondary and minor, but for nanosecond pulses they cannot be ignored.

Several lines of experimental evidence indicate that nanosecond electric pulses cause changes in the integrity and organization of the cell membrane.

Trypan blue permeabilization. While remaining PI-negative, the cell volume of Jurkat T lymphoblasts exposed to a series of 50, 20 ns, 4 MV/m pulses increases, and they become visibly permeable to Trypan blue (TB) (Figure 1). With increasing time after pulse exposure, these weakly TB-positive cells become again impermeable to TB. Similar observations have recently been reported for B16 murine melanoma cells exposed to sub-nanosecond (800 ps) pulses at very high fields [14].

Nanosecond porating transmembrane potentials. Fluorescence imaging with a membrane potential-sensitive dye shows that porating transmembrane potentials are generated during nanoelectropulse exposure [15].

Nanoelectropulse-induced PS externalization. Loss of asymmetry in membrane phospholipid distribution resulting from phosphatidylserine (PS) externalization occurs immediately after nanoelectropulse exposure [16], consistent with membrane reorganization driven directly by nanosecond-duration electric fields and a mechanism in which nanometer-diameter pores provide a low-energy path for electrophoretically facilitated diffusion of PS from the cytoplasmic leaflet of the plasma membrane to the external face of the cell [8].

Simulations link PS externalization and nanoporation. In molecular dynamics (MD) simulations of electroporation, hydrophilic pores appear within a few nanoseconds [17], and PS migrates electrophoretically along the pore walls to the anode-facing side of the membrane [18–19], in silico replication of experimental observations in living cells [20].

Nanoelectropermeabilization. The first direct evidence for nanoelectropermeabilization was obtained by monitoring influx of YO-PRO-1 (YP) [21], a more sensitive indicator of membrane permeabilization than propidium (Pr) [22]. Additional direct evidence comes from patch clamp experiments, which reveal long-lasting increases in membrane conductance following exposure to 60 ns pulses [23–25].

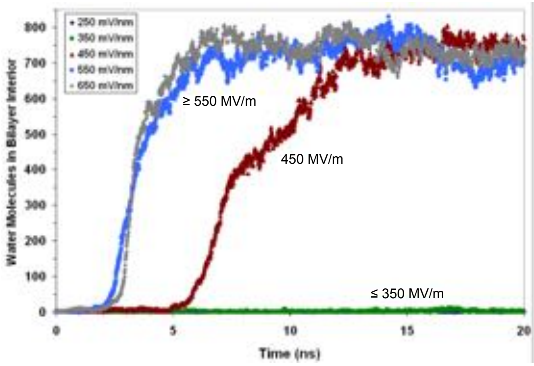

Figure 3. Electric field-driven intrusion of water into a simulated lipid bilayer.

Nanosecond activation of electrically excitable cells. Electrically excitable cells provide a highly responsive environment for nanoelectropulse biology. Adrenal chromaffin cells [26] and cardiomyocytes [27] react strongly to a single 4 ns pulse, and muscle fiber has been shown to respond to a 1 ns stimulus [28].

Nanosecond bioelectrics and the dielectric stack model. Figure 2 depicts a time line of events in an aqueous suspension of living cells and electrolytes between two electrodes after an electric pulse is applied. Water dipoles re-orient within about 8 ps The field also alters the electro-diffusive equilibrium among charged species and their hydrating water, with a time constant that ranges from 0.5 to 7 ns, depending on the properties of the media. Pulses shorter than the electrolyte relaxation time do not generate (unless the field is very high) enough interfacial charge to produce porating transmembrane potentials. The dielectric shell model in this regime can be replaced with a simpler, dielectric stack model, in which the local electric field depends only on the external (applied) electric field and the dielectric permittivity of each component of the system.

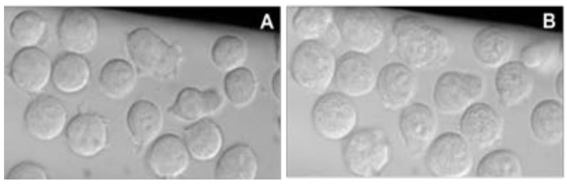

Figure 4. Differential interference contrast (DIC) images of Jurkat T lymphoblasts before (A) and 30 s after (B) exposure to 5 ns, 10 MV/m electric pulses (30 pulses delivered at 1 kHz). Note pulse-induced swelling, blebbing, and intracellular granulation and vesicle expansion, results of the osmotic imbalance caused by electropermeabilization of the cell membrane.

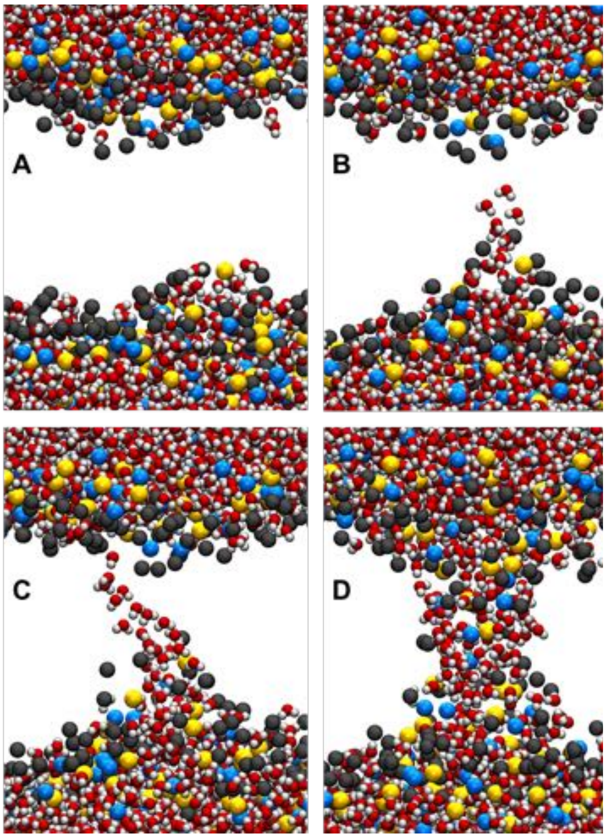

Figure 5. Electropore creation sequence. (A) Molecular dynamics representation of a POPC lipid bilayer system. Small red and white spheres at the top and bottom of the panel are water oxygen and hydrogen atoms. Gold and blue spheres are head group phosphorus and nitrogen, respectively, and large gray spheres are phospholipid acyl oxygens. For clarity, atoms of the hydrocarbon chains in the interior of the bilayer are not shown. In the presence of a porating electric field, a water intrusion appears (B), and extends across the bilayer (C). Head groups follow the water to form a hydrophilic pore (D). The pore formation sequence, from the initiation of the water bridge to the formation of the head-group-lined pore takes less than 5 ns.

Nanoelectropermeabilization and continuum models. MD simulations at present provide the only available molecular-scale windows on electropore formation in lipid bilayers. Current models perform reasonably well, but simulations of electroporation still contain many assumptions and simplifications. To validate these models we look for intersections between all-atom molecular assemblies, continuum representations of cell suspensions and tissues, and experimental observations of cells and whole organisms. For example, a leading continuum model assumes an exponential relation between the transmembrane potential and several indices of electropore formation [29]. The MD results in Figure 3, showing water intrusion into the membrane interior as a function of applied electric field, qualitatively demonstrate this same non-linear relation between field and poration. The challenge is to achieve a quantitative congruency of the coefficients.

NANOSECOND EXPERIMENTS AND MODELS

Experiments and molecular models of membrane permeabilization. Figure 4 shows a simple and direct response of cells to nanoelectropulse exposure — swelling [25,30,31]. Electropermeabilization of the cell membrane results in an osmotic imbalance that is countered by water influx into the cell and an increase in cell volume. This phenomenon, initiated by electrophysical interactions with basic cell constituents — ions, water, and phospholipids — on a much shorter time scale (a few nanoseconds) than usually considered by electrophysiologists and cell biologists, provides a simple, direct, and well-defined connection between simulations and experimental systems. By correlating observed kinetics of permeabilization and swelling with rates of pore formation and ion and water transport obtained from molecular simulations and continuum representations, we are improving the accuracy and applicability of the models.

Molecular dynamics and macroscale (continuum) models. Figure 5 shows the main steps in the electric field-driven formation of a nanopore in a typical MD simulation of a porating phospholipid bilayer, part of a larger scheme for the step-by-step development (and dissolution) of the electrically conductive defects that contribute at least in part to what we call a permeabilized membrane [32]. These molecular simulations permit us to conduct virtual experiments across a wide parameter space currently inaccessible in practice to direct observation. Although we cannot yet align the detailed energetics and kinetics that can be extracted from MD simulations with laboratory results, it is possible to compare MD data with the predictions of the macroscale models used to describe electroporation.

Figure 6 shows how pore initiation time (time between application of porating electric field and the appearance of a membrane-spanning water column (Fig. 5C)) varies with the magnitude of the electric field in MD simulations [32]. The value of the electric field in the membrane interior, extracted from simulations by integrating the charge density across the system, is used as a normalizing quantity.

This membrane internal field results from the interaction of the applied external field with the interface water and head group dipoles, and it corresponds to the large dipole potential found in the membrane interior even in the absence of an applied field [33]. The nonlinear decrease in pore initiation time with increased electric field may be interpreted as a lowering of the activation energy

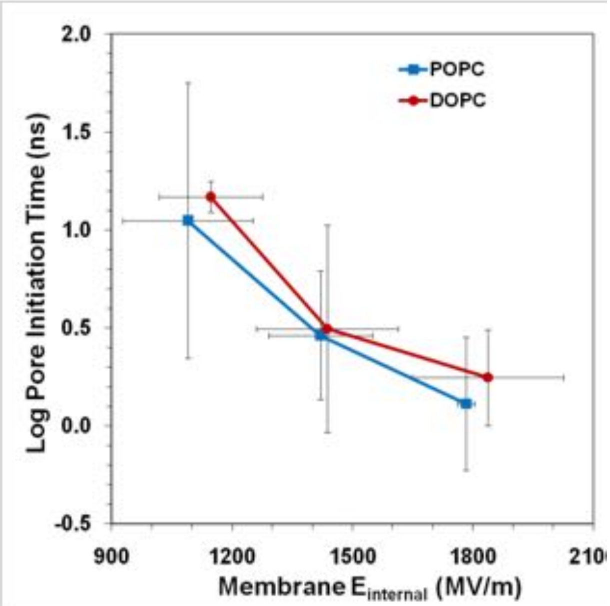

Figure 6. Electropore initiation time is a nonlinear function of the magnitude of the porating electric field. Pore initiation time (time required to form the water bridge shown in Fig. 1C) is exponentially dependent on the applied electric field, expressed here as the electric field observed in the lipid bilayer interior in molecular dynamics simulations. Error bars are standard error of the mean from at least three independent simulations. Data are from Tables 4 and 5 of [32].

for the formation of the pore-initiating structures described above. We can use simulation results like those in Fig. 6 to reconcile molecular dynamics representations with continuum models, and ultimately both of these to experiment. For example, the relation between electric field and pore creation rate is described in the Krassowska-Weaver stochastic pore model in the following expression,

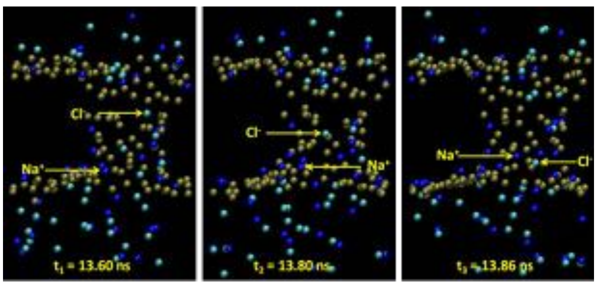

Figure 7. Sodium and chloride ions migrating through a lipid nanopore in the presence of an external electric field.

$$K_{pore} = Ae^{-E(r,V_m)/k_BT}, \quad (1)$$

where K_{pore} is the pore creation rate, A is a rate constant, $E(r,V_m)$ is the energy of a pore with radius r at transmembrane potential V_m, and k_B, and T are the Boltzmann constant and the absolute temperature [29,34–36]. One of our objectives is to reconcile the pore creation rate in (1) with our simulated pore initiation times, reconciling the two models.

As the availability of computing power increases, we also expect to validate the stochastic pore model expression for pore density,

$$\frac{dN}{dt} = \alpha e^{\beta\left(\Delta\psi_m^2\right)}\left(1-\frac{N}{N_{eq}}\right), \quad (2)$$

where N and N_{eq} are pores per unit area, instantaneous and equilibrium values, α and β are empirical electroporation model parameters, and $\Delta\psi_m$ is the transmembrane potential.

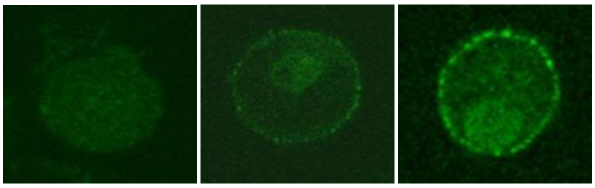

Figure 8. Immunocytochemical labeling of dopamine-β-hydroxylase (DβH) using an anti-DβH antibody coupled with a fluorescently-tagged 2° antibody. DβH is externalized by exocytotic fusion of vesicles with plasma membrane. Left panel, control. Center panel, 2 min after treatment with the pharmacological stimulant DMPP. Right panel, 2 min after a single, 5 ns, 5 MV/m pulse.

Computing power is needed not only to enable simulations of larger systems. The large variability in pore initiation time indicated by the error bars in Fig. 6 means that independent simulations of each condition must be repeated many times to ensure valid results. (A surprising number of conclusions in the existing literature have been published on the basis of single simulations.)

Because of the complexity of all of the structures, systems, and processes which comprise the permeabilized membrane of a living cell (the electropermeome), a comprehensive analytical understanding of permeabilization (pore?) lifetime remains a major challenge for both models and experimental approaches.

Better models can contribute also to our understanding of practical problems in bioelectrics. For example, despite years of study, controversy remains regarding the effects, or lack of effects, of exposures to low levels of radio-frequency (RF) electromagnetic fields [37,38]. Part of the reason for failure to establish certainty on this issue arises from the difficulty of conducting experiments with a sufficient number of variables and a sufficient number of samples to generate reliable data sets. With accurate simulation tools, honed by reconciliation with experiment, we can explore the large variable and statistical space in which suspected biophysical effects might occur, narrowing the range of experimental targets and focusing on systems in which effects are most likely and in which mechanisms will be clear.

Experiments and molecular models of ion conductance. The earliest identified and most direct indicators of electric field-driven membrane permeabilization are changes in electrical properties, including an increase in ion conductance [39,40]. Data from careful experimental work can be interpreted as measured values corresponding to the conductance of a single pore [41–44]. By combining continuum models of electroporation with this experimental data and with established values for ion electrophoretic mobilities and affinities between ions and phospholipids, we can draw conclusions about pore geometry and areal density. But the inaccessibility (so far) of membrane electropores to direct observation and manipulation of their physical structure prevents us from definitively bridging the gap between model and experiment.

A recently developed method for stabilizing electropores in molecular dynamics simulations of phospholipid bilayers [45] allows extraction of ion conductance from these model systems and thus provides a new and independent connection between models and experiments, in this case from the atomically detailed models of lipid electropores constructed with molecular dynamics. Figure 7 shows one of these stabilized pores with electric field-driven ions passing through it.

Although the magnitude of the conductance measured in these simulations is highly dependent on the accuracy of the ion and water models and their interactions with the phospholipid bilayer interface (and there is much room for improvement in this area), initial results are consistent with expectations from both continuum models and experimental observations.

NANOSECOND EXCITATION

Nanoelectrostimulation of neurosecretory and neuromuscular cells. Applications of pulsed electric fields in the clinic, particularly in electrochemotherapy and gene electrotransfer, are well known and described in detail in other parts of this course. We note here a potential biomedical application specifically of nanosecond electric pulses, the activation and modulation of the activity of neurosecretory and neuromuscular processes, an area which remains relatively unexplored. The sensitivity of electrically excitable cells to nanoelectropulses raises the possibility that very low energy (nanosecond, megavolt-per-meter pulses are high power, but low total energy because of their brief duration) devices for cardiac regulation (implanted pacemakers and defibrillators), remote muscle activation (spinal nerve damage), and neurosecretory modulation (pain management) can be constructed with nanoelectropulse technology. Figure 8 demonstrates functional activation of an adrenal chromaffin cell after a single 5 ns, 5 MV/m pulse [46,47].

ACKNOWLEDGMENT

Collaborative insights from Francesca Apollonio, Delia Arnaud-Cormos, Gale Craviso, Rumiana Dimova, M. Laura Fernández, Wolfgang Frey, Julie Gehl, Martin Gundersen, Volker Knecht, Malgorzata Kotulska, Philippe Leveque, Micaela Liberti, Carmela Marino, Caterina Merla, Damijan Miklavčič, Lluis Mir, Andrei Pakhomov, Uwe Pliquett, Ramon Reigada, Marcelo Risk, Marie-Pierrre Rols, Maria Rosaria Scarfi, Aude Silve, Mounir, Tarek, Justin Teissié, Peter Tieleman, Mayya Tokman, and Jim Weaver (and very important to me but too many to name members of their research groups), and modeling and experimental expertise from Maura Casciola, Federica Castellani, Ming-Chak Ho, Zachary Levine, Paolo Marracino, Stefania Romeo, Esin Sözer, and Yu-Hsuan Wu contributed to this work. Computing resources were provided by the USC Center for High Performance Computing and Communications (http://www.usc.edu/hpcc/) and High-Performance Computing facilities at Old Dominion University. Additional important support comes from the U.S. Air Force Office of Scientific Research.

REFERENCES

[1] Sher, L. D., E. Kresch, and H. P. Schwan. 1970. On the possibility of nonthermal biological effects of pulsed electromagnetic radiation. Biophys. J. 10:970-979.

[2] Drago, G. P., M. Marchesi, and S. Ridella. 1984. The frequency dependence of an analytical model of an electrically stimulated biological structure. Bioelectromagnetics 5:47-62.

[3] Plonsey, R., and K. W. Altman. 1988. Electrical stimulation of excitable cells - a model approach. Proceedings of the IEEE 76:1122-1129.

[4] Schoenbach, K. H., R. P. Joshi, J. F. Kolb, N. Y. Chen, M. Stacey, P. F. Blackmore, E. S. Buescher, and S. J. Beebe. 2004. Ultrashort electrical pulses open a new gateway into biological cells. Proceedings of the IEEE 92:1122-1137.

[5] Hofmann, F., H. Ohnimus, C. Scheller, W. Strupp, U. Zimmermann, and C. Jassoy. 1999. Electric field pulses can induce apoptosis. J. Membr. Biol. 169:103-109.
[6] Schoenbach, K. H., S. J. Beebe, and E. S. Buescher. 2001. Intracellular effect of ultrashort electrical pulses. Bioelectromagnetics 22:440-448.
[7] Benz, R., and U. Zimmermann. 1980. Pulse-length dependence of the electrical breakdown in lipid bilayer membranes. Biochim. Biophys. Acta 597:637-642.
[8] Vernier, P. T., Y. Sun, L. Marcu, C. M. Craft, and M. A. Gundersen. 2004. Nanoelectropulse-induced phosphatidylserine translocation. Biophys. J. 86:4040-4048.
[9] Gowrishankar, T. R., and J. C. Weaver. 2006. Electrical behavior and pore accumulation in a multicellular model for conventional and supra-electroporation. Biochem. Biophys. Res. Commun. 349:643-653.
[10] Grosse, C., and H. P. Schwan. 1992. Cellular membrane potentials induced by alternating fields. Biophys. J. 63:1632-1642.
[11] Gowrishankar, T. R., and J. C. Weaver. 2003. An approach to electrical modeling of single and multiple cells. Proc. Natl. Acad. Sci. U. S. A. 100:3203-3208.
[12] Kotnik, T., and D. Miklavcic. 2000. Second-order model of membrane electric field induced by alternating external electric fields. IEEE Trans. Biomed. Eng. 47:1074-1081.
[13] Timoshkin, I. V., S. J. MacGregor, R. A. Fouracre, B. H. Crichton, and J. G. Anderson. 2006. Transient electrical field across cellular membranes: pulsed electric field treatment of microbial cells. Journal of Physics D-Applied Physics 39:596-603.
[14] Schoenbach, K. H., S. Xiao, R. P. Joshi, J. T. Camp, T. Heeren, J. F. Kolb, and S. J. Beebe. 2008. The effect of intense subnanosecond electrical pulses on biological cells. IEEE Trans. Plasma Sci. 36:414-422.
[15] Frey, W., J. A. White, R. O. Price, P. F. Blackmore, R. P. Joshi, R. Nuccitelli, S. J. Beebe, K. H. Schoenbach, and J. F. Kolb. 2006. Plasma membrane voltage changes during nanosecond pulsed electric field exposure. Biophys. J. 90:3608-3615.
[16] Vernier, P. T., Y. Sun, L. Marcu, C. M. Craft, and M. A. Gundersen. 2004. Nanosecond pulsed electric fields perturb membrane phospholipids in T lymphoblasts. FEBS Lett. 572:103-108.
[17] Tieleman, D. P. 2004. The molecular basis of electroporation. BMC Biochem 5:10.
[18] Hu, Q., R. P. Joshi, and K. H. Schoenbach. 2005. Simulations of nanopore formation and phosphatidylserine externalization in lipid membranes subjected to a high-intensity, ultrashort electric pulse. Phys Rev E Stat Nonlin Soft Matter Phys 72:031902.
[19] Vernier, P. T., M. J. Ziegler, Y. Sun, W. V. Chang, M. A. Gundersen, and D. P. Tieleman. 2006. Nanopore formation and phosphatidylserine externalization in a phospholipid bilayer at high transmembrane potential. J. Am. Chem. Soc. 128:6288-6289.
[20] Vernier, P. T., M. J. Ziegler, Y. Sun, M. A. Gundersen, and D. P. Tieleman. 2006. Nanopore-facilitated, voltage-driven phosphatidylserine translocation in lipid bilayers - in cells and in silico. Physical Biology 3:233-247.
[21] Vernier, P. T., Y. Sun, and M. A. Gundersen. 2006. Nanoelectropulse-driven membrane perturbation and small molecule permeabilization. BMC Cell Biol. 7:37.
[22] Idziorek, T., J. Estaquier, F. De Bels, and J. C. Ameisen. 1995. YOPRO-1 permits cytofluorometric analysis of programmed cell death (apoptosis) without interfering with cell viability. J. Immunol. Methods 185:249-258.
[23] Pakhomov, A. G., J. F. Kolb, J. A. White, R. P. Joshi, S. Xiao, and K. H. Schoenbach. 2007. Long-lasting plasma membrane permeabilization in mammalian cells by nanosecond pulsed electric field (nsPEF). Bioelectromagnetics 28:655-663.
[24] Pakhomov, A. G., R. Shevin, J. A. White, J. F. Kolb, O. N. Pakhomova, R. P. Joshi, and K. H. Schoenbach. 2007. Membrane permeabilization and cell damage by ultrashort electric field shocks. Arch. Biochem. Biophys. 465:109-118.
[25] Pakhomov, A. G., A. M. Bowman, B. L. Ibey, F. M. Andre, O. N. Pakhomova, and K. H. Schoenbach. 2009. Lipid nanopores can form a stable, ion channel-like conduction pathway in cell membrane. Biochem. Biophys. Res. Commun. 385:181-186.
[26] Vernier, P. T., Y. Sun, M. T. Chen, M. A. Gundersen, and G. L. Craviso. 2008. Nanosecond electric pulse-induced calcium entry into chromaffin cells. Bioelectrochemistry 73:1-4.
[27] Wang, S., J. Chen, M. T. Chen, P. T. Vernier, M. A. Gundersen, and M. Valderrabano. 2009. Cardiac myocyte excitation by ultrashort high-field pulses. Biophys. J. 96:1640-1648.
[28] Rogers, W. R., J. H. Merritt, J. A. Comeaux, C. T. Kuhnel, D. F. Moreland, D. G. Teltschik, J. H. Lucas, and M. R. Murphy. 2004. Strength-duration curve for an electrically excitable tissue extended down to near 1 nanosecond. IEEE Trans. Plasma Sci. 32:1587-1599.
[29] DeBruin, K. A., and W. Krassowska. 1998. Electroporation and shock-induced transmembrane potential in a cardiac fiber during defibrillation strength shocks. Ann. Biomed. Eng. 26:584-596.
[30] F. M. Andre, M. A. Rassokhin, A. M. Bowman, and A. G. Pakhomov, "Gadolinium blocks membrane permeabilization induced by nanosecond electric pulses and reduces cell death," *Bioelectrochemistry*, vol. 79, pp. 95-100, Aug 2010.
[31] O. M. Nesin, O. N. Pakhomova, S. Xiao, and A. G. Pakhomov, "Manipulation of cell volume and membrane pore comparison following single cell permeabilization with 60- and 600-ns electric pulses," *Biochim Biophys Acta*, vol. 1808, pp. 792-801, Dec 20 2010.
[32] Z. A. Levine and P. T. Vernier, "Life cycle of an electropore: field-dependent and field-independent steps in pore creation and annihilation," *J Membr Biol*, vol. 236, pp. 27-36, Jul 2010.
[33] R. J. Clarke, "The dipole potential of phospholipid membranes and methods for its detection," *Adv Colloid Interface Sci*, vol. 89-90, pp. 263-81, Jan 29 2001.
[34] I. P. Sugar and E. Neumann, "Stochastic model for electric field-induced membrane pores. Electroporation," *Biophys Chem*, vol. 19, pp. 211-25, May 1984.
[35] S. A. Freeman, M. A. Wang, and J. C. Weaver, "Theory of electroporation of planar bilayer membranes: predictions of the aqueous area, change in capacitance, and pore-pore separation," *Biophys J*, vol. 67, pp. 42-56, Jul 1994.
[36] R. W. Glaser, S. L. Leikin, L. V. Chernomordik, V. F. Pastushenko, and A. I. Sokirko, "Reversible electrical breakdown of lipid bilayers: formation and evolution of

pores," *Biochim Biophys Acta*, vol. 940, pp. 275-87, May 24 1988.
[37] J. M. S. McQuade, J. H. Merritt, S. A. Miller, T. Scholin, M. C. Cook, A. Salazar, O. B. Rahimi, M. R. Murphy, and P. A. Mason, "Radiofrequency-radiation exposure does not induce detectable leakage of albumin across the blood-brain barrier," *Radiation Research*, vol. 171, pp. 615-621, May 2009.
[38] N. D. Volkow, D. Tomasi, G. J. Wang, P. Vaska, J. S. Fowler, F. Telang, D. Alexoff, J. Logan, and C. Wong, "Effects of cell phone radiofrequency signal exposure on brain glucose metabolism," *JAMA*, vol. 305, pp. 808-13, Feb 23 2011.
[39] Stämpfli, R., and M. Willi. 1957. Membrane potential of a Ranvier node measured after electrical destruction of its membrane. *Experientia* 13:297-298.
[40] Coster, H. G. L. 1965. A quantitative analysis of the voltage-current relationships of fixed charge membranes and the associated property of "punch-through". *Biophys. J.* 5:669-686.
[41] Chernomordik, L. V., S. I. Sukharev, S. V. Popov, V. F. Pastushenko, A. V. Sokirko, I. G. Abidor, and Y. A. Chizmadzhev. 1987. The electrical breakdown of cell and lipid membranes: the similarity of phenomenologies. *Biochim. Biophys. Acta* 902:360-373.
[42] Kalinowski, S., G. Ibron, K. Bryl, and Z. Figaszewski. 1998. Chronopotentiometric studies of electroporation of bilayer lipid membranes. *Biochim. Biophys. Acta* 1369:204-212.
[43] Melikov, K. C., V. A. Frolov, A. Shcherbakov, A. V. Samsonov, Y. A. Chizmadzhev, and L. V. Chernomordik. 2001. Voltage-induced nonconductive pre-pores and metastable single pores in unmodified planar lipid bilayer. *Biophys. J.* 80:1829-1836.
[44] Koronkiewicz, S., S. Kalinowski, and K. Bryl. 2002. Programmable chronopotentiometry as a tool for the study of electroporation and resealing of pores in bilayer lipid membranes. *Biochim. Biophys. Acta* 1561:222-229.
[45] Fernandez, M. L., M. Risk, R. Reigada, and P. T. Vernier. 2012. Size-controlled nanopores in lipid membranes with stabilizing electric fields. *Biochem. Biophys. Res. Commun.* 423:325-330.
[46] G. L. Craviso, P. Chatterjee, G. Maalouf, A. Cerjanic, J. Yoon, I. Chatterjee, and P. T. Vernier, "Nanosecond electric pulse-induced increase in intracellular calcium in adrenal chromaffin cells triggers calcium-dependent catecholamine release," *Ieee Transactions on Dielectrics and Electrical Insulation*, vol. 16, pp. 1294-1301, Oct 2009.
[47] G. L. Craviso, S. Choe, P. Chatterjee, I. Chatterjee, and P. T. Vernier, "Nanosecond electric pulses: a novel stimulus for triggering Ca^{2+} influx into chromaffin cells via voltage-gated Ca^{2+} channels," *Cell Mol Neurobiol*, vol. 30, pp. 1259-65, Nov 2010.

NOTES

P. Thomas Vernier is Research Professor at the Frank Reidy Research Center for Bioelectrics at Old Dominion University and Adjunct Research Professor in the Ming Hsieh Department of Electrical Engineering at the University of Southern California. His research and industrial experience includes ultraviolet microscopy analysis of S-adenosylmethionine metabolism in the yeast *Rhodotorula glutinis*, molecular biology of the temperature-sensitive host restriction of bacterial viruses in *Pseudomonas aeruginosa*, low-level environmental gas monitoring, wide-band instrumentation data recording, and semiconductor device modeling and physical and electrical characterization. He currently concentrates on the effects of nanosecond, megavolt-per-meter electric fields on biological systems, combining experimental observations with molecular dynamics simulations, and on the integration of cellular and biomolecular sensors, carbon nanotubes, and quantum dots with commercial integrated electronic circuit fabrication processes.

Vernier received his Ph.D. in Electrical Engineering from the University of Southern California in 2004, and is a member of the American Chemical Society, American Society for Microbiology, Bioelectrochemical Society, Bioelectromagnetics Society, Biophysical Society, and Institute of Electrical and Electronics Engineers.

NOTES

Electrochemotherapy in clinical practice: Lessons from development and implementation - and future perspectives

Julie Gehl

Center for Experimental Drug and Gene Electrotransfer, Department of Oncology, Herlev and Gentofte Hospital, University of Copenhagen, Denmark.

Abstract: In just two decades electrochemotherapy has developed from an experimental treatment to standard therapy. This paper describes this development and also goes into the details of how a new technology can become implemented, to benefit patients. Electrochemotherapy is a technology that involves the use of electric pulses and chemotherapy. Thus the development of this technology has required specialists in biology, engineering and medicine to pull together, in order to achieve this accomplishment. This paper describes the development of equipment, as well as standard operating procedures, for treatment with electrochemotherapy. This chapter also deals with sharing knowledge about the use of the technology, and ensuring access for patients.

DEVELOPMENT OF ELECTROCHEMOTHERAPY

Initial studies on the organization of the cell membrane, and on deformation of this membrane by electric forces, were performed through the particularly the 1960s and 70s. In 1977 rupture of erythrocytes was described in a Nature paper [1], and another highly influential paper was Neumanns study from 1982 [2], demonstrating DNA electrotransfer which is now one of the most frequently used laboratory methods in molecular biology.

A very active field in cancer therapy in the 1970s and 80s was resistance to drug therapy, and there was great optimism that understanding resistance to therapy could ultimately lead to a cure for cancer. Different important cellular resistance systems were discovered, e.g. the multidrug transporter p-glycoprotein, that enables cancer cells to export chemotherapy [3]. In this landscape electroporation was a new technology that allowed circumvention of membrane based resistance by simply plowing a channel through cell membrane, allowing non-permeant drugs inside.

A number of studies were published about enhancement of cytotoxicity by electroporation [4,5] in vitro, and also in vivo [6], principally from Lluis Mir's group at Institut Gustave-Roussy. It was also here that, in a remarkable short time-frame, the first clinical study was reported, preliminary results in French in 1991, and the final publication in 1993 [7]. A few years later [8], the first studies from the US came out, as well as studies from Slovenia [9], and Denmark [10].

Out of a wish to create electroporation equipment for clinical use, which would be able to perform both gene therapy and electrochemotherapy, which could be adapted by the user to accommodate developments, and which was a useful instrument for the treating physician, i.e. by showing precise recordings of voltage and current along with the treatment, the Cliniporator consortium was formed. This European consortium developed and tested the Cliniporator [11,12].

A subsequent European consortium, named ESOPE (European Standard Operating Procedures for Electrochemotherapy) set out to get the Cliniporator approved for clinical use, to produce electrodes for it, to test the system in a clinical protocol, as well as to make concluding standard operating procedures.

Four groups went into the clinical study of which three had previous experience with electrochemotherapy. And the methods used differed between those three centers.

In France, a hexagonal electrode was used, with 7.9 mm between electrodes and a firing sequence allowing each of seven electrodes to be pairwise activated 8 times, a total of 96 pulses delivered at high frequency, with a voltage of 1.3 kV/cm (voltage to electrode distance ratio). Patients were sedated, bleomycin was given iv, and the procedure took place in an operating theatre [7].

In the Slovenian studies, patients were treated with cisplatin intratumorally, and with plate electrodes using 1.3 kV/cm, anesthesia not described. Pulses were administered as two trains of each four pulses [9].

In Denmark we used intratumoral bleomycin, a linear array electrode of two opposing rows of needles activated against each other using 1.2 kV/cm, 8 pulses at 1 Hz. Local anesthesia with lidocaine was used [10].

In other words, there was agreement about the overall purpose, but three different approaches. The ESOPE study [13] brought these three approaches together, and on the technical side, the three different electrodes were manufactured, and the final conclusion of the different methods and electrodes were defined in collaboration.

The standard operating procedures [14] are very detailed, allowing a newcomer to the field to immediately implement the procedure. Thus it is described how to administer the drug and pulses, how to make treatment decisions, and how to evaluate response and perform follow-up.

The standard operating procedures, together with the availability of certified equipment, marked a dramatic change in the use of electrochemotherapy. Thus when the standard operating procedures were published in 2006 only few European centers were active, and after the publication of the procedures the number of centers quickly rose and is today over 140. It would be estimated that this number will continue to grow, and also that the generators now being placed in various institutions will be increasingly used also for new indications.

IMPLEMENTATION

In an ideal world, new developments in cancer therapy become immediately available to patients. But experience shows that from the development of the technology, and the emergence of the first results, there is still quite a road to be traveled in order for the individual patient to be able to be referred, if the treatment is relevant to the particular case. First of all, equipment must be present at the individual institution, along with knowledgeable surgeons and oncologists trained to provide the treatment. The logistical set up must be in place, and this includes availability of time in the operating rooms and competent nursing support. Patients need to know that the treatment is an option. As electrochemotherapy is an option for patients suffering from different types of cancer, it requires continuous work to address specialists in the different fields. Information available on the internet can be an important resource for patients, as well as professionals.

Various countries have different approval mechanisms for new treatments, and endorsement can be a time-consuming affair. The most renowned national agency is the National Institute of Health and Care Excellence (NICE) in the UK, which has a rigorous scrutinization of new technologies and where central documents are freely available. NICE has guidances for electrochemotherapy for cutaneous metastases, and primary skin cancers respectively [15,16]. These national recommendations, as well as the integration of electrochemotherapy into specific guidelines (see e.g. [17]) are very important for the improving accessibility to treatment.

RESEARCH

A very important point is that the standard operating procedures were a very important foundation – but must be followed up with more detailed experience and further developments. Several groups have published further studies on electrochemotherapy, broadening the knowledge base and answering specific questions of clinical importance [18-26].

Furthermore, electrochemotherapy is now being developed for a number of new indications, including mucosal head and neck cancer, gastro-intestinal cancers, lung cancer (primary and secondary), gynecological cancers, sarcoma, bone metastases, as well as brain metastases. For each of these indications standard operating procedures will need to be developed, in order to allow dissemination of the treatment.

REFERENCES

[1] Kinosita K, Tsong TY. Formation and resealing of pores of controlled sizes in human erythrocyte membrane. Nature 1977;268:438-41.

[2] Neumann E, Schaefer-Ridder M, Wang Y, Hofschneider PH. Gene transfer into mouse lyoma cells by electroporation in high electric fields. EMBO J 1982;1(7):841-45.

[3] Skovsgaard T, Nissen NI. Membrane transport of anthracyclines. Pharmacol Ther 1982;18(3):293-311.

[4] Okino M, Mohri H. Effects of a high-voltage electrical impulse and an anticancer drug on in vivo growing tumors. JpnJCancer Res 1987;78(0910-5050 SB - M SB - X):1319-21.

[5] Orlowski S, Belehradek Jr J, Paoletti C, Mir LM. Transient electropermeabilization of cells in culture. Increase of the cytotoxicity of anticancer drugs. Biochemical Pharmacology 1988;37(24):4727-33.

[6] Mir LM, Orlowski S, Belehradek J, Jr., Paoletti C. Electrochemotherapy potentiation of antitumour effect of bleomycin by local electric pulses. Eur J Cancer 1991;27(1):68-72.

[7] Belehradek M, Domenge C, Luboinski B, Orlowski S, Belehradek Jr J, Mir LM. Electrochemotherapy, a new antitumor treatment. First clinical phase I-II trial. Cancer 1993;72(12):3694-700.

[8] Heller R. Treatment of cutaneous nodules using electrochemotherapy. [Review] [32 refs]. Journal of the Florida Medical Association 1995;82(2):147-50.

[9] Sersa G, Stabuc B, Cemazar M, Jancar B, Miklavcic D, Rudolf Z. Electrochemotherapy with cisplatin: Potentiation of local cisplatin antitumor effectiveness by application of electric pulses in cancer patients. European Journal of Cancer 1998;34(8):1213-18.

[10] Gehl J, Geertsen PF. Efficient palliation of haemorrhaging malignant melanoma skin metastases by electrochemotherapy. Melanoma Res 2000;10(6):585-9.

[11] Andre FM, Gehl J, Sersa G, Preat V, Hojman P, Eriksen J, et al. Efficiency of High- and Low-Voltage Pulse Combinations for Gene Electrotransfer in Muscle, Liver, Tumor, and Skin. Human Gene Therapy 2008;19(11):1261-71.

[12] Hojman P, Gissel H, Andre F, Cournil-Henrionnet C, Eriksen J, Gehl J, et al. Physiological effect of high and low voltage pulse combinations for gene electrotransfer in muscle. HumGene Ther 2008(1557-7422 (Electronic)).
[13] Marty M, Sersa G, Garbay JR, Gehl J, Collins CG, Snoj M, et al. Electrochemotherapy - An easy, highly effective and safe treatment of cutaneous and subcutaneous metastases: Results of ESOPE (European Standard Operating Procedures of Electrochemotherapy) study. Ejc Supplements 2006;4(11):3-13.
[14] Mir LM, Gehl J, Sersa G, Collins CG, Garbay JR, Billard V, et al. Standard operating procedures of the electrochemotherapy: Instructions for the use of bleomycin or cisplatin administered either systemically or locally and electric pulses delivered by the CliniporatorTM by means of invasive or non-invasive electrodes. European Journal of Cancer Supplements 2006;4(11):14-25.
[15] National Institute for H, Care E. Electrochemotherapy for metastases in the skin from tumours of non-skin origin and melanoma. http://publicationsniceorguk/electrochemotherapy-for-metastases-in-the-skin-from-tumours-of-non-skin-origin-and-melanoma-ipg446 2013.
[16] (NICE) NIfHaCE. Electrochemotherapy for primary basal cell carcinoma and primary squamous cell carcinoma. www.nice.org.uk2014.
[17] Stratigos A, Garbe C, Lebbe C, Malvehy J, Del Marmol V, Pehamberger H, et al. Diagnosis and treatment of invasive squamous cell carcinoma of the skin: European consensus-based interdisciplinary guideline. Eur J Cancer 2015;51(14):1989-2007.
[18] Matthiessen LW, Chalmers RL, Sainsbury DC, Veeramani S, Kessell G, Humphreys AC, et al. Management of cutaneous metastases using electrochemotherapy. Acta Oncol 2011;50:621-29.
[19] Matthiessen LW, Johannesen HH, Hendel HW, Moss T, Kamby C, Gehl J. Electrochemotherapy for large cutaneous recurrence of breast cancer: A phase II clinical trial. Acta Oncologica 2012;51(6):713-21.
[20] Campana LG, Valpione S, Falci C, Mocellin S, Basso M, Corti L, et al. The activity and safety of electrochemotherapy in persistent chest wall recurrence from breast cancer after mastectomy: a phase-II study. Breast Cancer ResTreat 2012;134:1169-78.
[21] Campana LG, Bianchi G, Mocellin S, Valpione S, Campanacci L, Brunello A, et al. Electrochemotherapy treatment of locally advanced and metastatic soft tissue sarcomas: results of a non-comparative phase II study. World JSurg 2014;38:813-22.
[22] Campana LG, Mali B, Sersa G, Valpione S, Giorgi CA, Strojan P, et al. Electrochemotherapy in non-melanoma head and neck cancers: a retrospective analysis of the treated cases. BrJOral MaxillofacSurg 2014.
[23] Curatolo P, Mancini M, Clerico R, Ruggiero A, Frascione P, Di Marco P, et al. Remission of extensive merkel cell carcinoma after electrochemotherapy. Arch Dermatol 2009;145(4):494-5.
[24] Curatolo P, Quaglino P, Marenco F, Mancini M, Nardo T, Mortera C, et al. Electrochemotherapy in the treatment of Kaposi sarcoma cutaneous lesions: a two-center prospective phase II trial. Ann Surg Oncol 2012;19(1):192-8.
[25] Quaglino P, Mortera C, Osella-Abate S, Barberis M, Illengo M, Rissone M, et al. Electrochemotherapy with intravenous bleomycin in the local treatment of skin melanoma metastases. AnnSurgOncol 2008;15:2215-22.
[26] Quaglino P, Matthiessen LW, Curatolo P, Muir T, Bertino G, Kunte C, et al. Predicting patients at risk for pain associated with electrochemotherapy. Acta Oncol 2015;54(3):298-306.

Julie Gehl heads the Center for Experimental drug and gene Electrotransfer at Department of Oncology, Herlev Hospital at the University of Copenhagen. The center undertakes both preclinical and clinical investigations of the use of electrotransfer in drug and gene delivery. Julie Gehl is an MD, and specialist in Oncology. Dr. Gehl has an extensive publication record, is an experienced principal investigator and has guided numerous ph.d. students and students.

NOTES

NOTES

Gene electrotransfer *in vitro*: a 30 years old story

Marie-Pierre Rols

Institut de Pharmacologie et de Biologie Structurale, Toulouse, France

Abstract: Cell membranes can be transiently permeabilized under application of electric pulses. This process, called electropermeabilization or electroporation, allows hydrophilic molecules, such as anticancer drugs and DNA, to enter into cells and tissues. Electroporation is nowadays used in clinics to treat cancers. Vaccination and gene therapy are other fields of application of DNA electrotransfer. Open questions exist about the behavior of the membranes both while the field is on (µs to ms time range) and after its application (from seconds to several minutes and hours). Also, there is a lack of understanding on how molecules are transported in complex environments, such as those found in tissues. As our objectives are to give a complete molecular description of the mechanisms, our strategy is to use different complementary systems with increasing complexities (model membranes, cells in 2D and 3D culture, spheroids and tissues in living mice) and different microscopy tools to analyze the processes. Single cell imaging experiments revealed that the uptake of molecules (nucleic acids, antitumor drugs) takes place in well-defined membrane regions and depends on their chemical and physical properties (size, charge). If small molecules can freely cross the electropermeabilised membrane and have a free access to the cytoplasm, heavier molecules, such as plasmid DNA, face physical barriers (plasma membrane, cytoplasm crowding, nuclear envelope) which reduce transfection efficiency and engender a complex mechanism of transfer. Gene electrotransfer requires that the DNA is present during the application of the electric field pulses and involves different steps, occurring over relatively large time scales. As will be presented, these steps include the initial interaction with the electropermeabilised membrane, the crossing of the membrane, the transport within the cell and finally gene expression.

INTRODUCTION

The use of electroporation to deliver therapeutic molecules including drugs, proteins and nucleic acids in a wide range cells and tissues has been developed over the last decade (1-5). This strategy is nowadays used in clinics to treat cancers. Vaccination and oncology gene therapy are also major fields of application of DNA electrotransfer (6, 7). Translation of preclinical studies into clinical trials in human and veterinary oncology has started (8-10). The first phase I dose escalation trial of plasmid interleukin electroporation has been carried out in patients with metastatic melanoma and has shown encouraging results (11). The method has also been successfully used for the treatment of dogs and horses (8, 12). But the safe and efficient use of this physical method for clinical purposes requires the knowledge of the mechanisms underlying the electropermeabilization phenomena. Despite the fact that the pioneering work on plasmid DNA electrotransfer in cells was initiated 33 years ago (13), many of the mechanisms underlying DNA electrotransfer remain to be elucidated (14, 15). Even if *in vitro* electrotransfer is efficient in almost all cell lines, *in vivo* gene delivery and expression in tumors are usually not. It is still mandatory, for increasing gene transfer and expression, to increase our knowledge of the process. Our strategy consists on using different imaging tools, to directly visualize the processes, and different experimental models with increasing complexities.

MEMBRANE ELECTROPERMEABIZATION

The use of video microscopy allows visualization of the permeabilization phenomenon at the single cell level. Propidium iodide uptake in the cytoplasm is a fast process that can be detected seconds after the application of electric pulses. Exchange across the permeabilized membrane is not homogeneous on the whole cell membrane. It occurs at the sides of the cells facing the electrodes in an asymmetrical way where it is more pronounced at the anode-facing side of the cells than at the cathode (Figure 1), i.e. in the hyperpolarized area than in the depolarized area, which is in agreement with theoretical considerations.

Electropermeabilization can be described as a 3-step process in respect with electric field: (i) before electropulsation, the plasma membrane acts as a physical barrier that prevents the free exchange of hydrophilic molecules between the cell cytoplasm and external medium; (ii) during electropulsation, the transmembrane potential increases which induces the formation of transient permeable structures facing the electrodes and allows the exchange of molecules; (iii) after electropulsation, membrane resealing occurs.

A direct transfer into the cell cytoplasm of the negatively charged small molecules such as siRNA is observed on the side facing the cathode. When added after electropulsation, siRNA do not penetrate the cells. Therefore, electric field acts on both the permeabilization of the membrane and on the electrophoretic drag of the charged molecules from the bulk into the cytoplasm. The mechanism involved is clearly specific for the physico-chemical properties of the electrotransferred molecule (16).

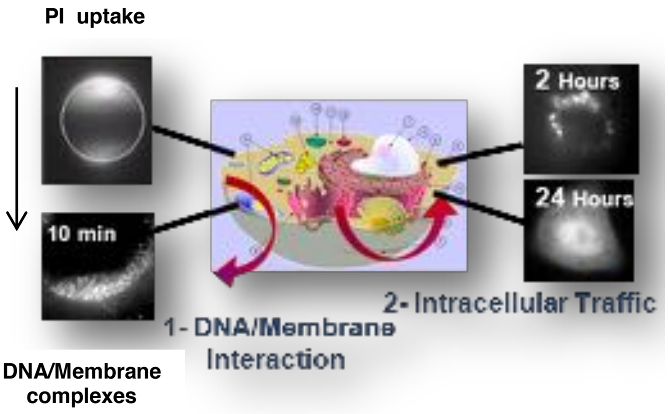

Figure 1: **Molecule electrotransfer mechanisms.** Left: During electric pulses application: Plasma membrane is electropermeabilized facing the 2 electrodes (PI uptake). DNA aggregates are formed. This interaction takes place only on the membrane facing the cathode. Right: About 2 h after electric pulses application, DNA molecules are present around the nucleus. Finally, eGFP expression is detected for hours. The arrow indicates the direction of the electric field.

Progress in the knowledge of the involved mechanisms is still a biophysical challenge. One of our challenges was to detect and visualize at the single-cell level the incidence of phospholipid scrambling and changes in membrane order (17, 18). The pulses induced the formation of long-lived permeant structures and resulted in a rapid phospholipid flip/flop within less than 1s and were exclusively restricted to the regions of the permeabilized membrane. Our results could support the existence of direct interactions between the movement of membrane zwitterionic phospholipids and the electric field. We also performed experiments on lateral mobility of proteins and showed that electropermeabilization affects the lateral mobility of Rae-1, a GPi anchored protein. Our results suggest that 10-20 % of the membrane surface is occupied by defects or pores and that these structures propagate rapidly over the cell surface.

We also took advantage of atomic force microscopy to directly visualize the consequences of electropermeabilization and to locally measure the membrane elasticity. We visualized transient rippling of membrane surface and measured a decrease in membrane elasticity. Our results obtained both on fixed and living CHO cells give evidence of an inner effect affecting the entire cell surface that may be related to cytoskeleton destabilization. Thus, AFM appears as a useful tool to investigate basic process of electroporation on living cells in absence of any staining (19, 20).

MECHANISMS OF ELECTROTRANSFER OF DNA MOLECULES INTO CELLS

Single-cell microscopy and fluorescent plasmids can be used to monitor the different steps of electrotransfection (16, 21). DNA molecules, which are negatively charged, migrate electrophoretically when submitted to the electric field. Under electric fields which are too small to permeabilize the membrane, the DNA simply flows around the membrane in the direction of the anode. Beyond a critical field value, above which cell permeabilization occurs, the DNA interacts with the plasma membrane.

1) DNA/Membrane interaction

This interaction only occurs at the pole of the cell opposite the cathode and this demonstrates the importance of electrophoretic forces in the initial phase of the DNA/membrane interaction. When the DNA-membrane interaction occurs, one observes the formation of "*microdomains*" whose dimensions lie between 0.1 and 0.5 µm (Figure 1). Also seen are clusters or aggregates of DNA which grow during the application of the field. However once the field is cut the growth of these clusters stops. DNA electrotransfer can be described as a multi-step-process: the negatively charged DNA migrates electrophoretically towards the plasma membrane on the cathode side where it accumulates.

This interaction, which is observed for several minutes, lasts much longer than the duration of the electric field pulse. Translocation of the plasmid from the plasma membrane to the cytoplasm and its subsequent passage towards the nuclear envelope take place with a kinetics ranging from minutes to hours (22). When plasmid has reached the nuclei, gene expression can take place and this can be detected up to several days in the case of dividing cells or weeks in some tissues such as muscles.

The dynamics of this process has been poorly understood because direct observations have been limited to time scales that exceed several seconds. We studied experimentally the transport of two types of molecules into cells (plasmid DNA and propidium iodide) which are relevant for gene therapy and chemotherapy with a temporal resolution of 2 ms allowing the visualization of the DNA/membrane interaction process during pulse application (23). DNA molecules interact with the membrane during the application of the pulse. At the beginning of the pulse application plasmid complexes or aggregates appear at sites on the cell membrane. The formation of plasmid complexes at fixed sites suggests that membrane domains may be responsible for DNA uptake and their lack of mobility could be due to their interaction with the actin cytoskeleton. Data reported evidences for the involvement of cytoskeleton (Figure

2). Actin indeed polymerizes around the DNA/membrane complexes (24-26).

We also investigated the dependence of DNA/membrane interaction and gene expression on electric pulse polarity, repetition frequency and duration. Both are affected by reversing the polarity and by increasing the repetition frequency or the duration of pulses (27, 28). The results revealed the existence of 2 classes of DNA/membrane interaction: (i) a metastable DNA/membrane complex from which DNA can leave and return to external medium and (ii) a stable DNA/membrane complex, where DNA cannot be removed, even by applying electric pulses of reversed polarity. Only DNA belonging to the second class leads to effective gene expression (27).

2) Intracellular traffic of plasmid DNA.

Even if the first stage of gene electrotransfection, i.e. migration of plasmid DNA towards the electropermeabilised plasma membrane and its interaction with it, becomes understood we are not totally able to give guidelines to improve gene electrotransfer. Successful expression of the plasmid depends on its subsequent migration into the cell. Therefore, the intracellular diffusional properties of plasmid DNA, as well as its metabolic instability and nuclear translocation, represent other cell limiting factors that must be taken into account (29). The cytoplasm is composed of a network of microfilament and microtubule systems, along with a variety of subcellular organelles present in the cytosol. The mesh-like structure of the cytoskeleton, the presence of organelles and the high protein concentration means that there is substantial molecular crowding in the cytoplasm which hinders the diffusion of plasmid DNA. These apparently contradictory results might be reconciled by the possibility of a disassembly of the cytoskeleton network that may occur during electropermeabilisation, and is compatible with the idea that the cytoplasm constitutes an important diffusional barrier to gene transfer. In the conditions induced during electropermeabilisation, the time a plasmid DNA takes to reach the nuclei is significantly longer than the time needed for a small molecule. Therefore, plasmid DNA present in the cytosol after being electrotransferred can be lost before reaching the nucleus, for example because of cell division. Finally, after the cytoskeleton, the nuclear envelope represents the last, but by no means the least important, obstacle for the expression of the plasmid DNA. The relatively large size of plasmid DNA (2-10 MDa) makes it unlikely that the nuclear entry occurs by passive diffusion. We recently showed how electrotransferred DNA is transported in the cytoplasm towards the nucleus (26). For this purpose, we have performed single particle tracking (SPT) experiments of individual DNA aggregates in living cells (25). We analyzed the modes of DNA aggregates motion in CHO cells. We showed fast active transport of the DNA aggregates over long distances. Tracking experiments in cells treated with different drugs affecting both the actin and the tubulin networks clearly demonstrate that this transport is related to the cellular microtubule network.

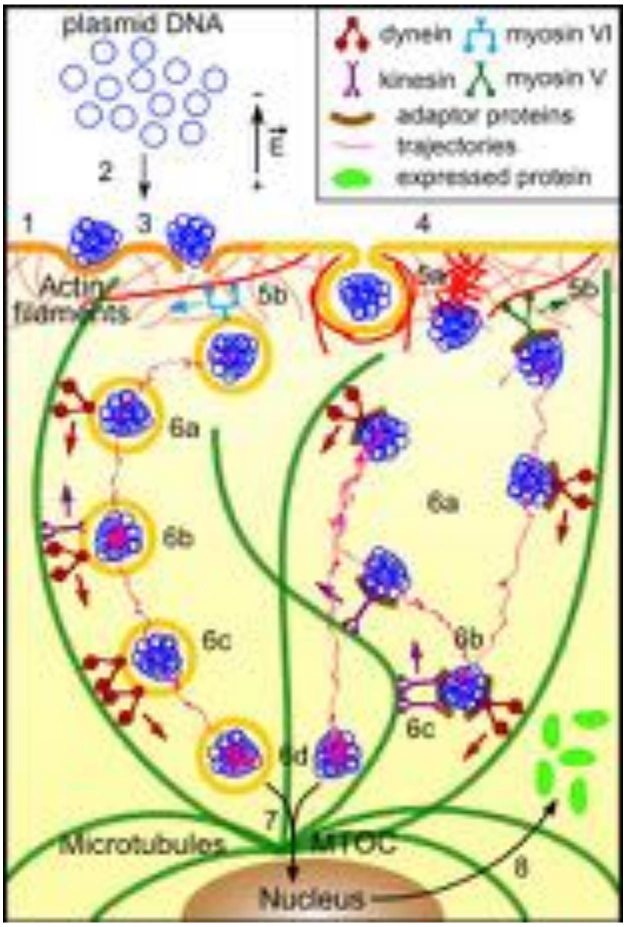

Figure 2: DNA electrotransfer as a multistep process. During the application of the electric field: (1) the plasma membrane is permeabilized (orange), (2) the DNA is electrophoretically pushed on the membrane side facing the cathode therefore (3) DNA/membrane interactions occur. DNA aggregates are inserted into the membrane and remain there for tens of minutes. After the application of the electric field and resealing of the membrane (yellow), (4) the DNA is internalized via endocytosis (DNA in vesicles). Free DNA is perhaps also internalized through electropores. For gene expression to occur (5-6), DNA has to cross the cytoplasm toward the nucleus. Our study suggests (5) actin related motion that can be in the form of (5a) actin polymerization that pushes the DNA, free or in vesicles (actin rocketing) and/or (5b) transport via the myosins (in both directions). We observe (6) microtubules related motion which can mean (6a) transport via kinesin and dynein, (6b) DNA interaction with oppositely directed motors and with (6c) several motors of the same type (6d). Once being in the perinuclear region (in vesicles and perhaps also free, 7), DNA has to cross the nuclear envelope, after endosomal escape in case of DNA in vesicles. Finally, DNA is expressed in proteins found in the cytoplasm (8). From ref (26).

3) New developments.

As mentioned above, the dense latticework of the cytoskeleton impedes free diffusion of DNA in the intracellular medium. Electrotransferred plasmid DNA, containing specific sequences could then use the microtubule network and its associated motor proteins to move through the cytoplasm to nucleus (30). Clear limits of efficient gene expression using electric pulses are therefore due to the passage of DNA molecules through the plasma membrane and to the cytoplasmic crowding and transfer through the nuclear envelope. A key challenge for electro-mediated gene therapy is to pinpoint the rate limiting steps in this complex process and to find strategies to overcome these obstacles. One of the possible strategies to enhance DNA uptake into cells is to use short (10-300 ns) but high pulse (up to 300 kV/cm) induce effects that primarily affect intracellular structures and functions. As the pulse duration is decreased, below the plasma membrane charging time constant, plasma membrane effects decrease and intracellular effects predominate (31, 32). An idea, to improve transfection success, is thus to perform classical membrane permeabilisation allowing plasmid DNA electrotransfer to the cell cytoplasm, and then after, when DNA has reached the nuclear envelope, to specifically permeabilise the nuclei using these short strong nanopulses. Thus, when used in conjunction with classical electropermeabilisation, nanopulses gave hope to increase gene expression. However, data showed that nsEPs have no major contribution to gene electrotransfer in CHO cells and no effect on constitutive GFP expression in HCT-116 cells (33). Another idea was to combine electric pulses and ultrasound assisted with gas microbubbles. Cells were first electroporated with plasmid DNA and then sonoporated. Twenty-four hours later, cells that received electrosonoporation demonstrated a four-fold increase in transfection level and a six-fold increase in transfection efficiency compared with cells having undergone electroporation alone (34). Although electroporation induced the formation of DNA aggregates into the cell membrane, sonoporation induced its direct propulsion into the cytoplasm. Sonoporation can therefore improve the transfer of electro-induced DNA aggregates by allowing its free and rapid entrance into the cells. These results demonstrated that *in vitro* gene transfer by electrosonoporation could provide a new potent method for gene transfer.

LIPID VESICLES AND SPHEROIDS AS CONVENIENT (NEW) APPROACHES TO STUDY GENE ELECTROTRANSFER

New lines of research are necessary to characterize the membranes domains observed during electrotransfer. For that purpose, we used giant unilamellar vesicles to study the effect of permeabilizing electric fields in simple membrane models. GUVs (Giant Unilamellar Vesicles) represent a convenient way to study membrane properties such as lipid bilayer composition and membrane tension. They offer the possibility to study and visualize membrane processes due to their cell like size in absence of any constraint due to cell cytoskeleton. Experiments showed a decrease in vesicle radius which is interpreted as being due to lipid loss during the permeabilization process (Figure 3).

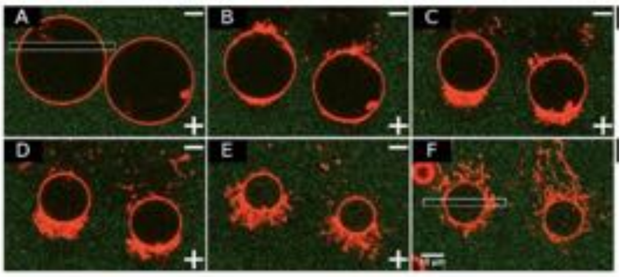

Figure 3: **Microcopic observations of GUVs submitted to electric pulses in the presence of pDNA.** From (35)

Three mechanisms responsible for lipid loss were directly observed and will be presented: pore formation, vesicle formation and tubule formation, which may be involved in molecules uptake (36). We also gave evidence that GUVs are a good model to study the mechanisms of electrofusion, with a direct interest to their use as vehicles to deliver molecules (37). However, a direct transfer of DNA into the GUVs took place during application of the electric pulses (35). That gives clear evidence that “lipid bubble” is not a cell and a tissue is not a simple assembly of single cells. Therefore, in the last past few years, we decided to use an *ex vivo* model, namely tumor multicellular tumor spheroids, for the understanding of the DNA electrotransfer process in tissues.

Upon growth, spheroids display a gradient of proliferating cells. These proliferating cells are located in the outer cell-layers and the quiescent cells are located more centrally. This cell heterogeneity is similar to that found in avascular microregions of tumors. We used confocal microscopy to visualize the repartition of permeabilized cells in spheroids submitted to electric pulses. Electrotransfer of bleomycin and cisplatin confirmed the relevance of the model in the case of electrochemotherapy and doxorubicin showed its potential to screen new antitumor drug candidates for ECT. Confocal microscopy was used to visualize the topological distribution of permeabilized cells in 3D spheroids. Our results revealed that cells were efficiently permeabilized, whatever their localization in the spheroid, even those in the core. The combination of antitumor drugs and electric pulses led to changes in spheroid macroscopic morphology and cell cohesion, to tumor spheroid growth arrest and finally to its complete dislocation, mimicking previously observed *in vivo* situations. Taken together, these results indicate that the spheroid model is relevant for the study and optimization of electromediated drug delivery protocols (38). Small molecules can be efficiently transferred into cells, including the ones present inside the spheroids, gene expression is limited to the external layers of cells (39). Taken together, these results, in agreement with the ones obtained by the group of R. Heller (40), indicate that the spheroid model is more relevant to an *in vivo* situation than cells cultured as monolayers (41, 42).

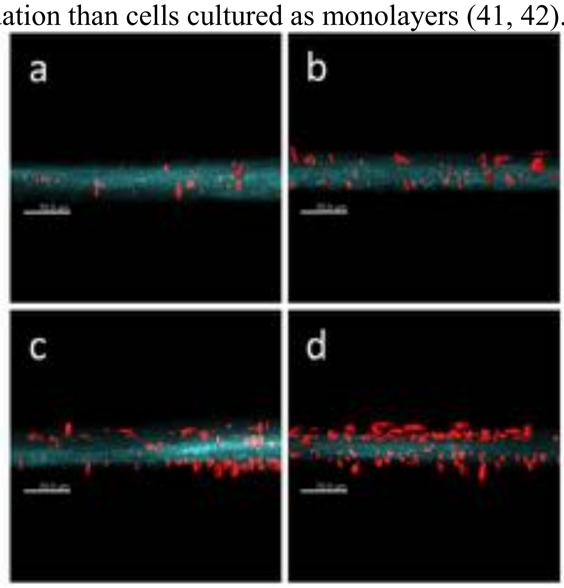

Figure 4: 3D dermal tissue electropermeabilization. Reconstructed human dermal tissue was electropermeabilized in the presence of propidium iodide (red) with 8 pulses of 5 ms duration at 1 Hz. Electric field intensity was 0 V/cm (a), 200 V/cm (b), 300 V/cm (c), 400 V/cm (d) and observed under a fluorescent biphoton microscope. Collagens are blue. From (43).

In order to assess the effects of ECM composition and organization, as well as intercellular junctions and communication, in normal tissue response to electric pulses, we are now developing an innovative three-dimensional (3D) reconstructed human connective tissue model (43). 3D human dermal tissue is reconstructed *in vitro* by a tissue engineering approach. This human cell model present multiple layers of primary dermal fibroblasts embedded in a native, collagen-rich ECM and can be a useful tool to study skin DNA electrotransfer mechanisms. We just showed that the cells within this standardized 3D tissue can be efficiently electropermeabilized by milliseconds electric pulses (Figure 4).

We believe that a better comprehension of gene electrotransfer in such a model tissue would help improve electrogene therapy approaches such as the systemic delivery of therapeutic proteins and DNA vaccination.

CONCLUSIONS

Classical theories of electropermeabilization present some limits to give a full description of the transport of molecules through membranes. Certain effects of the electric field parameters on membrane permeabilization, and the associated transport of molecules, are well established but a great deal of what happens at the molecular level remains speculative. Molecular dynamics simulations are giving interesting new insight into the process (32, 44). Electroinduced destabilisation of the membrane includes both lateral and transverse redistribution of lipids and proteins, leading to mechanical and electrical modifications which are not yet fully understood. One may suggest that such modifications can be involved in the subsequent transport of molecules interacting with them such as the DNA molecules. Experimental verification of the basic mechanisms leading to the electropermeabilization and other changes in the membrane, cells and tissues remain a priority given the importance of these phenomena for processes in cell biology and in medical applications.

REFERENCES

[1] Gothelf, A., L. M. Mir, and J. Gehl. 2003. Electrochemotherapy: results of cancer treatment using enhanced delivery of bleomycin by electroporation. Cancer Treat Rev 29:371-387.
[2] Rols, M. P. 2010. Gene transfer by electrical fields. Curr Gene Ther 10:255.
[3] Andre, F. M., and L. M. Mir. 2010. Nucleic acids electrotransfer in vivo: mechanisms and practical aspects. Curr Gene Ther 10:267-280.
[4] Mir, L. M. 2008. Application of electroporation gene therapy: past, current, and future. Methods Mol Biol 423:3-17.
[5] Yarmush, M. L., A. Golberg, G. Sersa, T. Kotnik, and D. Miklavcic. 2014. Electroporation-based technologies for medicine: principles, applications, and challenges. Annual review of biomedical engineering 16:295-320.
[6] Vandermeulen, G., E. Staes, M. L. Vanderhaeghen, M. F. Bureau, D. Scherman, and V. Preat. 2007. Optimisation of intradermal DNA electrotransfer for immunisation. J Control Release 124:81-87.
[7] Chiarella, P., V. M. Fazio, and E. Signori. 2010. Application of electroporation in DNA vaccination protocols. Curr Gene Ther 10:281-286.

[8] Cemazar, M., T. Jarm, and G. Sersa. 2010. Cancer electrogene therapy with interleukin-12. Curr Gene Ther 10:300-311.
[9] Heller, L. C., and R. Heller. 2010. Electroporation gene therapy preclinical and clinical trials for melanoma. Curr Gene Ther 10:312-317.
[10] Escoffre, J. M., and M. P. Rols. 2012. Electrochemotherapy: Progress and Prospects. Curr Pharm Des.
[11] Daud, A. I., R. C. DeConti, S. Andrews, P. Urbas, A. I. Riker, V. K. Sondak, P. N. Munster, D. M. Sullivan, K. E. Ugen, J. L. Messina, and R. Heller. 2008. Phase I trial of interleukin-12 plasmid electroporation in patients with metastatic melanoma. J Clin Oncol 26:5896-5903.
[12] Tamzali, Y., L. Borde, M. P. Rols, M. Golzio, F. Lyazrhi, and J. Teissie. 2011. Successful treatment of equine sarcoids with cisplatin electrochemotherapy: A retrospective study of 48 cases. Equine veterinary journal.
[13] Neumann, E., M. Schaefer-Ridder, Y. Wang, and P. H. Hofschneider. 1982. Gene transfer into mouse lyoma cells by electroporation in high electric fields. Embo J 1:841-845.
[14] Escoffre, J. M., T. Portet, L. Wasungu, J. Teissie, D. Dean, and M. P. Rols. 2009. What is (Still not) Known of the Mechanism by Which Electroporation Mediates Gene Transfer and Expression in Cells and Tissues. Mol Biotechnol 41:286-295.
[15] Cemazar, M., M. Golzio, G. Sersa, M. P. Rols, and J. Teissie. 2006. Electrically-assisted nucleic acids delivery to tissues in vivo: where do we stand? Curr Pharm Des 12:3817-3825.
[16] Paganin-Gioanni, A., E. Bellard, J. M. Escoffre, M. P. Rols, J. Teissie, and M. Golzio. 2011. Direct visualization at the single-cell level of siRNA electrotransfer into cancer cells. Proc Natl Acad Sci U S A 108:10443-10447.
[17] Escoffre, J. M., M. Hubert, J. Teissie, M. P. Rols, and C. Favard. 2014. Evidence for electro-induced membrane defects assessed by lateral mobility measurement of a GPi anchored protein. Eur Biophys J.
[18] Escoffre, J. M., E. Bellard, C. Faurie, S. C. Sebai, M. Golzio, J. Teissie, and M. P. Rols. 2014. Membrane disorder and phospholipid scrambling in electropermeabilized and viable cells. Biochim Biophys Acta 1838:1701-1709.
[19] Chopinet, L., C. Roduit, M. P. Rols, and E. Dague. 2013. Destabilization induced by electropermeabilization analyzed by atomic force microscopy. Biochim Biophys Acta 1828:2223-2229.
[20] Chopinet, L., C. Formosa, M. P. Rols, R. E. Duval, and E. Dague. 2013. Imaging living cells surface and quantifying its properties at high resolution using AFM in QI (TM) mode. Micron 48:26-33.
[21] Golzio, M., J. Teissie, and M. P. Rols. 2002. Direct visualization at the single-cell level of electrically mediated gene delivery. Proc Natl Acad Sci U S A 99:1292-1297.
[22] Faurie, C., M. Rebersek, M. Golzio, M. Kanduser, J. M. Escoffre, M. Pavlin, J. Teissie, D. Miklavcic, and M. P. Rols. 2010. Electro-mediated gene transfer and expression are controlled by the life-time of DNA/membrane complex formation. J Gene Med 12:117-125.
[23] Escoffre, J. M., T. Portet, C. Favard, J. Teissie, D. S. Dean, and M. P. Rols. 2011. Electromediated formation of DNA complexes with cell membranes and its consequences for gene delivery. Biochim Biophys Acta 1808:1538-1543.
[24] Rosazza, C., J. M. Escoffre, A. Zumbusch, and M. P. Rols. 2011. The actin cytoskeleton has an active role in the electrotransfer of plasmid DNA in mammalian cells. Mol Ther 19:913-921.
[25] Rosazza, C., E. Phez, J. M. Escoffre, L. Cezanne, A. Zumbusch, and M. P. Rols. 2011. Cholesterol implications in plasmid DNA electrotransfer: Evidence for the involvement of endocytotic pathways. Int J Pharm.
[26] Rosazza, C., A. Buntz, T. Riess, D. Woll, A. Zumbusch, and M. P. Rols. 2013. Intracellular tracking of single plasmid DNA-particles after delivery by electroporation. Mol Ther.
[27] Faurie, C., M. Rebersek, M. Golzio, M. Kanduser, J. M. Escoffre, M. Pavlin, J. Teissie, D. Miklavcic, and M. P. Rols. 2010. Electro-mediated gene transfer and expression are controlled by the life-time of DNA/membrane complex formation. Journal of Gene Medicine 12:117-125.
[28] Haberl, S., M. Kanduser, K. Flisar, D. Hodzic, V. B. Bregar, D. Miklavcic, J. M. Escoffre, M. P. Rols, and M. Pavlin. 2013. Effect of different parameters used for in vitro gene electrotransfer on gene expression efficiency, cell viability and visualization of plasmid DNA at the membrane level. J Gene Med 15:169-181.
[29] Lechardeur, D., and G. L. Lukacs. 2006. Nucleocytoplasmic Transport of Plasmid DNA: A Perilous Journey from the Cytoplasm to the Nucleus. Hum Gene Ther 17:882-889.
[30] Vaughan, E. E., and D. A. Dean. 2006. Intracellular trafficking of plasmids during transfection is mediated by microtubules. Mol Ther 13:422-428.
[31] Beebe, S. J., J. White, P. F. Blackmore, Y. Deng, K. Somers, and K. H. Schoenbach. 2003. Diverse effects of nanosecond pulsed electric fields on cells and tissues. DNA Cell Biol 22:785-796.
[32] Vernier, P. T., Y. Sun, and M. A. Gundersen. 2006. Nanoelectropulse-driven membrane perturbation and small molecule permeabilization. BMC Cell Biol 7:37.
[33] Chopinet, L., T. Batista-Napotnik, A. Montigny, M. Rebersek, J. Teissie, M. P. Rols, and D. Miklavcic. 2013. Nanosecond Electric Pulse Effects on Gene Expression. J Membr Biol.
[34] Escoffre, J. M., K. Kaddur, M. P. Rols, and A. Bouakaz. 2010. In vitro gene transfer by electrosonoporation. Ultrasound Med Biol 36:1746-1755.
[35] Portet, T., C. Favard, J. Teissie, D. Dean, and M. P. Rols. 2011. Insights into the mechanisms of electromediated gene delivery and application to the loading of giant vesicles with negatively charged macromolecules. Soft Matter 7:3872-3881.
[36] Portet, T., F. Camps i Febrer, J. M. Escoffre, C. Favard, M. P. Rols, and D. S. Dean. 2009. Visualization of membrane loss during the shrinkage of giant vesicles under electropulsation. Biophys J 96:4109-4121.
[37] Mauroy, C., P. Castagnos, M. C. Blache, J. Teissie, I. Rico-Lattes, M. P. Rols, and M. Blanzat. 2012. Interaction between GUVs and catanionic nanocontainers: new insight into spontaneous membrane fusion. Chem Commun (Camb) 48:6648-6650.
[38] Gibot, L., L. Wasungu, J. Teissie, and M. P. Rols. 2013. Antitumor drug delivery in multicellular spheroids by electropermeabilization. J Control Release 167:138-147.
[39] Wasungu, L., J. M. Escoffre, A. Valette, J. Teissie, and M. P. Rols. 2009. A 3D in vitro spheroid model as a way to study the mechanisms of electroporation. Int J Pharm 379:278-284.

[40] Marrero, B., and R. Heller. 2012. The use of an in vitro 3D melanoma model to predict in vivo plasmid transfection using electroporation. Biomaterials.
[41] Chopinet, L., L. Wasungu, and M. P. Rols. 2011. First explanations for differences in electrotransfection efficiency in vitro and in vivo using spheroid model. Int J Pharm.
[42] Gibot, L., and M. P. Rols. 2013. Progress and Prospects: The Use of 3D Spheroid Model as a Relevant Way to Study and Optimize DNA Electrotransfer. Current Gene Therapy 13:175-181.
[43] Madi, M., M. P. Rols, and L. Gibot. 2015. Efficient In Vitro Electropermeabilization of Reconstructed Human Dermal Tissue. J Membr Biol.
[44] Polak, A., D. Bonhenry, F. Dehez, P. Kramar, D. Miklavcic, and M. Tarek. 2013. On the electroporation thresholds of lipid bilayers: molecular dynamics simulation investigations. J Membr Biol 246:843-850.

ACKNOWLEDGEMENT

This research was performed in the scope of the EBAM European Associated Laboratory (LEA) and is a result of networking efforts within COST TD1104. We were supported by the Centre National de la Recherche Scientifique (CNRS), the Agence Nationale de la Recherche (ANR), Projet PIERGEN ANR-12-ASTR-0039, the Direction Générale de l'Armement (DGA), and the Midi-Pyrénées Région. This state of the art in the electrotransfer of DNA is mostly due to the works of the PhD students and post-docs I have/had the pleasure to supervise and/or work with: Muriel Golzio, Cécile Faurie, Emilie Phez, Jean-Michel Escoffre, Thomas Portet, Chloé Mauroy, Louise Chopinet, Elisabeth Bellard, Christelle Rosazza, Amar Tamra, Moinecha Madi, Luc Wasungu, Flavien Pillet and Laure Gibot and Nathalie Joncker.

Marie-Pierre Rols was born in Decazeville, the "gueules noires" city of the Duc Decazes, France, in 1962. She received a Masters in Biochemistry, a Ph.D. in Cell Biophysics and the Habilitation à Diriger les Recherches from the Paul Sabatier University of Toulouse in 1984, 1989 and 1995, respectively. She is currently Director of Research at the IPBS-CNRS laboratory in Toulouse, group leader of the Cellular Biophysics team and head of the Biophysical and Structural Biology Department. She is secretary of the French Society for Nanomedecine. Her research interests lie in the fields of membrane electropermeabilization in cells and tissues, mainly on the mechanism of nucleic acids electrotransfer. Marie-Pierre Rols is the author of 100 articles in peer-reviewed journals. In 1993 she received the Galvani Prize of the Bioelectrochemical Society, in 2006 a joined prize of the Midi-Pyrénées Région.

NOTES

NOTES

Drug and gene delivery in the skin by electroporation

Véronique Préat
Université catholique de Louvain, Bruxelles, Belgium

STRUCTURE OF THE SKIN

Skin is composed of three primary layers: the epidermis, which provides waterproofing and serves as a barrier to infection; the dermis, which serves as a location for the appendages of skin; and the hypodermis (subcutaneous adipose layer).

The epidermis consists of stratified squamous epithelium. The epidermis contains no blood vessels, and cells in the deepest layers are nourished by diffusion from blood capillaries extending to the upper layers of the dermis. The main type of cells which make up the epidermis are keratinocytes, with melanocytes and Langerhans cells also present. The main barrier to drug permeation is the stratum corneum, the outermost layer of the skin made of corneocytes embedded in a multiple lipid bilayers.

The dermis is the layer of skin beneath the epidermis that consists of connective tissue and cushions the body from stress and strain. The dermis is tightly connected to the epidermis by a basement membrane. It also contains many nerve endings that provide the sense of touch and heat. It contains the hair follicles, sweat glands, sebaceous glands, apocrine glands, lymphatic vessels and blood vessels. The blood vessels in the dermis provide nourishment and waste removal to its own cells as well as the Stratum basale of the epidermis. The dermis is structurally divided into two areas: a superficial area adjacent to the epidermis, called the papillary region, and a deep thicker area known as the reticular region.

TRANSDERMAL AND TOPICAL DRUG DELIVERY

The easy accessibility and the large area of the skin make it a potential route of administration. Despite these potential advantages for the delivery of drugs across or into the skin, a significant physical barrier impedes the transfer of large molecules. First, transdermal transport of molecules is limited by the low permeability of the stratum corneum, the outermost layer of the skin. Only potent lipophilic low molecular weight (<500) drugs can be delivered by passive diffusion at therapeutic rates. Hence, the transdermal penetration of hydrophilic and/or high molecular-weight molecules, including DNA, requires the use of methods to enhance skin permeability and/or to provide a driving force acting on the permeant. Both chemical (e.g. penetration enhancer) and physical (e.g. iontophoresis, electroporation, or sonophoresis) methods have been used.

TRANSDERMAL DRUG DELIVERY BY ELECTROPORATION

It has been demonstrated that application of high voltage pulses permeabilizes the stratum corneum and enhances drug transport. Electroporation of skin was shown to enhance and expedite transport across and/or into skin for many different compounds. Within a few minutes of high-voltage pulsing, molecular transport across skin increased by several orders of magnitude.

In vitro, the transport of several conventional drugs (e.g., fentanyl, β blockers, peptides (e.g., LHRH or calcitonine) was shown to be enhanced. Few in vivo studies confirm the increased transport and rapid onset of action.

The parameters affecting the efficacy of transport have been extensively studied. The electrical parameters (voltage, number and duration of the pulses), the formulation parameters (ionic strength…) allow the control of drug delivery.

The mechanism of drug transport is mainly electrophoretic movement and diffusion through newly created aqueous pathways in the stratum corneum created by the "electroporation" of the lipid bilayers.

The alterations in skin induced by high-voltage pulsing are relatively minor (decrease in skin resistance, hydration, lipid organisation) and reversible. However, light sensation and muscle contraction that can be reduced by developing better electrode design, have been observed.

TOPICAL DRUG DELIVERY BY ELECTROPORATION

Besides the permeabilization of the stratum corneum and the subsequent corneum and the subsequent increased skin permeability, electroporation also enhances the permeability of the viable cells of the skin and the subcutaneous tissue. Hence, it is an efficient method to deliver molecules into the skin when these molecules are applied topically or more efficiently for macromolecules including DNA when they are injected intradermally.

As the skin is an immunocompetent organ, DNA delivery in the skin by electroporation seems particularly attractive for DNA vaccination.

SKIN GENE DELIVERY

The skin represents an attractive site for the delivery of nucleic acids-based drugs for the treatment of topical or systemic diseases and immunisation. It is the most accessible organ and can easily be monitored and removed if problems occur. It is the largest organ of the body (15% of total adult body weight) and delivery to large target area could be feasible. However attempts at therapeutic cutaneous gene delivery have been hindered by several factors. Usually, except for viral vectors, gene expression is transient and typically disappears with 1 to 2 weeks due to the continuous renewal of the epidermis. Moreover, DNA penetration is limited by the barrier properties of the skin, rendering topical application rather inefficient.

The potential use of DNA-based drugs to the skin could be: (i) gene replacement by introducing a defective or missing gene, for the treatment of genodermatosis (ii) gene therapeutic by delivering a gene expressing protein with a specific pharmacological effect, or suicidal gene, (iii) wound healing, (iv) immunotherapy with DNA encoding cytokines and (v) DNA vaccine. The gene encoding the protein of interest can be inserted in a plasmid that carries this gene under the control of an appropriate eukaryotic promoter (e.g., the CMV promoter in most cases). Alternatively, it can be inserted in viral vectors.

Effective gene therapy requires that a gene encoding a therapeutic protein must be administered and delivered to target cells, migrate to the cell nucleus and be expressed to a gene product. DNA delivery is limited by: (i) DNA degradation by tissues or blood nucleases, (ii) low diffusion at the site of administration, (iii) poor targeting to cells, (iv) inability to cross membrane, (v) low cellular uptake and (vi) intracellular trafficking to the nucleus.

Epidermal gene transfer has been achieved with ex vivo approaches. Genes of interest have been introduced, mainly with viral vectors, in keratinocytes or fibroblasts and then grafted on nude mice or patients. Permanent expression can be achieved. In vivo approaches, which are more patient-friendly, less invasive, less time consuming and less expensive, are more attractive and will gradually replace the ex vivo gene transfer protocols.

The methods developed for gene transfer into the skin are based on the methods developed for gene transfection in vitro and in other tissues in vivo as well as methods developed to enhance transdermal drug delivery. They include (i) topical delivery, (ii) intradermal injection, (iii) mechanical methods, (iv) physical methods and (v) biological methods.

Topical application of naked plasmid DNA to the skin is particularly attractive to provide a simple approach to deliver genes to large areas of skin. However, the low permeability of the skin to high molecular weight hydrophilic molecules limits the use of this approach. Gene expression after topical delivery of an aqueous solution of DNA on intact skin has been reported to induce gene expression but the expression is very low. Hence, topical DNA delivery into the skin can only be achieved if the barrier function of the stratum corneum is altered. The selection of appropriate vector or method to promote the penetration of DNA through and/or into the skin has been shown to be paramount.

One of the simplest ways of gene delivery is injecting naked DNA encoding the therapeutic protein. In 1990, Wolff et al. observed an expression during several months after injection of naked DNA into the muscle. Expression following the direct injection of naked plasmid DNA has been then established for skin. The epidermis and the dermis can take up and transiently express plasmid DNA following direct injection into animal skin. However, the expression remains low and physical and/or mechanical methods have been developed to enhance gene expression.

ELECTROPORATION IN SKIN GENE DELIVERY

Electrotransfer has been widely used to introduce DNA into various types of cells in vitro and is one of the most efficient non-viral methods to enhance gene transfer in various tissues in vivo. Electrotransfer involves plasmid injection in the target tissue and application of short high voltage electric pulses by electrodes. The intensity and the duration of pulses and the more appropriate type of electrodes must be evaluated for each tissue. It is generally accepted that the electric field plays a double role in DNA transfection: it transiently disturbs membranes and increases cells permeability and promotes electrophoresis of negatively charged DNA.

Electrotransfer may be used to increase transgene expression 10 to 1000-fold more than the injection of naked DNA into the skin. Local delivery combined with electrotransfer could result in a significant increase of serum concentrations of a specific protein. Neither long-term inflammation nor necroses are generally observed.

After direct intradermal injection of plasmid, the transfected cells are typically restricted to the epidermis and dermis. However, when high voltage pulse are applied after this intradermal injection, other cells, including adipocytes, fibroblasts and numerous dendritic-like cells within the dermis and subdermal layers were transfected. After topical application of plasmid on tape stripped rat skin followed by electrotransfer, GFP expression was also reported but was very low and restricted to the epidermis.

Duration of expression after electrotransfer depends on the targeted tissue. In contrast to the skeletal muscle where expression lasts for several months, gene expression is limited to only of few weeks into the skin. For example, after intradermal electrotransfer of plasmid coding erythropoietin, the expression persisted for 7 weeks at the DNA injection site, and hematocrit levels were increased for 11 weeks. With reporter gene, shorter expressions were reported, probably due to an immune response.

Several authors tried to increase the effectiveness of the electrotransfer into the skin. By co-injecting a nuclease inhibitor with DNA, transfection expression was significantly increased. The use of a particulate adjuvant (gold particles) enhanced the effectiveness of DNA vaccination by electrotransfer. For the skin, combination of one high-voltage pulse and one low-voltage pulse delivered by plate electrodes has been proven to be efficient and well tolerated. The design of electrodes and injection method can also be optimised.

Electrotransfer has no detrimental effect on wound healing. A single injection of a plasmid coding keratinocyte growth factor coupled with electrotransfer improved and accelerated wound closure in a wound-healing diabetic mouse model.

Vaccination is another interesting application of electrotransfer into the skin. Intradermal electrotransfer enhanced DNA vaccine delivery to skin and both humoral and cellular immune responses have been induced. Hence, it could be developed as a potential alternative for DNA vaccine delivery without inducing any irreversible change.

Electrotransfer of DNA encoding either IL-2, IL-12 or an antiangiogenic compound for the treatment of melanoma is currently tested in clinical trials.

REFERENCES

References on skin structure

[1] http://en.wikipedia.org/wiki/Skin

[2] References on transdermal and topical drug delivery

[3] Schuetz YB, Naik A, Guy RH, Kalia YN. Emerging strategies for the transdermal delivery of peptide and protein drugs. Expert Opin Drug Deliv. 2005):533-48.

[4] Nanda A, Nanda S, Ghilzai NM. Current developments using emerging transdermal technologies in physical enhancement methods. Curr Drug Deliv. 2006 3:233-42.

[5] Hadgraft J, Lane ME. Skin permeation: the years of enlightenment. Int J Pharm. 2005 305:2-12

[6] Prausnitz MR, Langer R. Transdermal drug delivery. Nat Biotechnol. 2008 Nov;26(11):1261-8. Review.

References on transdermal drug delivery by electroporation

[7] Denet A.R., Vanbever R. and Préat V., Transdermal drug delivery by electroporation, Advanced drug delivery reviews, 2004;56:659-74. Review.

[8] Jadoul A., Bouwstra J., and Préat V., Effects of iontophoresis and electroporation on the stratum corneum – Review of the biophysical studies, Advanced drug delivery reviews, 35, 1999, 89-105

[9] Prausnitz M.R., A practical assessment of transdermal drug delivery by skin elecroporation, Advanced drug delivery reviews, 35, 1999, 61-76

[10] Vanbever R. and Préat V., In vivo efficacy and safety of skin electroporation, Advanced drug delivery reviews, 35, 1999, 77-88

[11] Wong TW, Chen TY, Huang CC, Tsai JC, Hui SW. Painless skin electoporation as a novel way for insulin delivery. Diabetes Technol Ther; 2011. 13(9): 929-35.

[12] Charoo NA, Rahman Z, Repka MA, Murthy SN, Electroporation : an avenue for transdermal drug delivery. Curr. Drug Deliv. 2010; 7(2): 125-36. Review

References on skin gene delivery

[13] Hengge UR. Gene therapy progress and prospects: the skin--easily accessible, but still far away. Gene Ther 2006; 13(22):1555-1563.

[14] Branski LK, Pereira CT, Herndon DN et al. Gene therapy in wound healing: present status and future directions. Gene Ther 2007; 14(1):1-10.

References on electroporation on skin gene delivery

[15] Gothelf A, Gehl J. Gene electrotransfer to skin; review of existing literature and clinical perspectives. Curr Gene Ther. 2010 Aug;10(4):287-99. Review

[16] Byrnes CK, Malone RW, Akhter N et al. Electroporation enhances transfection efficiency in murine cutaneous wounds. Wound Repair Regen 2004; 12(4):397-403.

[17] Drabick JJ, Glasspool-Malone J, King A et al. Cutaneous transfection and immune responses to intradermal nucleic acid vaccination are significantly enhanced by in vivo electropermeabilization. Mol Ther 2001; 3(2):249-255.

[18] André FM, Gehl J, Sersa G, Préat V, Hojman P, Eriksen J, Golzio M, Cemazar M, Pavselj N, Rols MP, Miklavcic D, Neumann E, Teissié J, Mir LM. Efficiency of high- and low-voltage pulse combinations for gene electrotransfer in muscle, liver, tumor, and skin. Hum Gene Ther. 2008 Nov;19(11):1261-71

[19] Dujardin N, Staes E, Kalia Y et al. In vivo assessment of skin electroporation using square wave pulses. J Control Release 2002; 79(1-3):219-227.

[20] Dujardin N, Van Der Smissen P., Preat V. Topical gene transfer into rat skin using electroporation. Pharm Res 2001; 18(1):61-66.

[21] Glasspool-Malone J, Somiari S, Drabick JJ et al. Efficient nonviral cutaneous transfection. Mol Ther 2000; 2(2):140-146.

[22] Heller LC, Jaroszeski MJ, Coppola D et al. Optimization of cutaneous electrically mediated plasmid DNA delivery using novel electrode. Gene Ther 2007; 14(3):275-280.

[23] Heller R, Schultz J, Lucas ML et al. Intradermal delivery of interleukin-12 plasmid DNA by in vivo electroporation. DNA Cell Biol 2001; 20(1):21-26.
[24] Pavselj N, Préat V. DNA electrotransfer into the skin using a combination of one high- and one low-voltage pulse. J Control Release 2005; 106(3):407-415.
[25] Zhang L, Widera G, Rabussay D. Enhancement of the effectiveness of electroporation-augmented cutaneous DNA vaccination by a particulate adjuvant. Bioelectrochemistry 2004; 63(1-2):369-373.
[26] Vandermeulen G, Staes E, Vanderhaeghen ML, Bureau MF, Scherman D, Préat V. Optimisation of intradermal DNA electrotransfer for immunisation. J Control Release. 2007 Dec 4;124(1-2):81-7.
[27] Pavselj N, Préat V, Miklavcic D. A numerical model of skin electropermeabilization based on in vivo experiments. Ann Biomed Eng. 2007 Dec;35(12):2138-44.

NOTES

Electroporation in Electrochemotherapy of Tumors

Maja Čemažar
Institute of Oncology Ljubljana, Slovenia

Abstract: Electrochemotherapy consists of chemotherapy followed by local application of electric pulses to the tumor to increase drug delivery into cells in tumors. Drug uptake can be increased by electroporation only for drugs having impeded transport through the plasma membrane. Among many drugs which have been tested so far, only cisplatin and bleomycin have found their way from preclinical testing to clinical trials. *In vitro* studies demonstrated a several-fold increase of their cytotoxicity by electroporation of cells. *In vivo*, electroporation of tumors after local or systemic administration of either of the drugs *i.e*. electrochemotherapy, proved to be an effective antitumor treatment. Electrochemotherapy studies using either bleomycin or cisplatin in several tumor models elaborated treatment parameters for effective local tumor control. In veterinary medicine, electrochemotherapy proved to be effective in primary tumors in cats, dogs and horses. In clinical studies, electrochemotherapy was performed on accessible tumor nodules of different malignancies in progressive disease. All clinical studies provided evidence that electrochemotherapy is an effective treatment for local tumor control in patients with different types of cancer. The perspectives of electrochemotherapy are also in combination with other established treatment modalities, like irradiation, and new approaches, like gene therapy. Since application of electric pulses to the tumors induces transient reduction of tumor perfusion and oxygenation, it can be exploited in several other treatment combinations such as with bioreductive drugs and hyperthermia.

INTRODUCTION

Treatments for cancer may be divided into different categories based on their goals and mode of action. Very often, the different types of treatment are used in combination, either simultaneously or sequentially. In general, cancer treatment includes three major treatment modalities: surgery and radiation, which are local treatment modalities and chemotherapy, which is a systemic treatment modality.

Chemotherapy, a systemic treatment modality for cancer, is effective for drugs which readily cross the plasma membrane and are cytotoxic once they reach their intracellular targets. However, among the chemotherapeutic drugs which are very cytotoxic, there is some having hampered transport through the plasma membrane. These drugs are good candidates for electrochemotherapy. Electrochemotherapy is a local treatment combining chemotherapy and application of electric pulses to the tumor. In electrochemotherapy, the optimal anti-tumor effectiveness is achieved when electric pulses are given at the time of the highest extracellular concentration of the hydrophilic chemotherapeutic drug, thereby increasing its transport through the plasma membrane towards the intracellular targets [1-4].

PRECLINICAL DATA

In vitro studies

Electroporation proved to be effective in facilitating transport of different molecules across the plasma membrane for different biochemical and pharmacological studies. However, when using chemotherapeutic drugs, this facilitated transport increases intracellular drug accumulation with the aim to increase their cytotoxicity. Since electroporation can facilitate drug transport through the cell membrane only for molecules which are poorly permeant or non-permeant, suitable candidates for electrochemotherapy are limited to those drugs that are hydrophilic and/or lack a transport system in the membrane. Several chemotherapeutic drugs were tested *in vitro* for potential application in combination with electroporation of cells. Among the tested drugs, only two were identified as potential candidates for electrochemotherapy of cancer patients. The first is bleomycin, which is hydrophilic and has very restricted transport through the cell membrane, but its cytotoxicity can be potentiated up to several 1000 times by electroporation of cells. A few hundred internalized molecules of bleomycin are sufficient to kill the cell. The second is cisplatin, whose transport through the cell membrane is also hampered. Early studies suggested that cisplatin is transported through the plasma membrane mainly by passive diffusion, while recent studies have demonstrated that transporters controlling intracellular copper homeostasis are significantly involved in influx (Ctr1) and efflux (ATP7A and ATP7B) of the cisplatin [5]. Electroporation of the plasma membrane enables greater flux and accumulation of the drug in the cells, which results in an increase of cisplatin cytotoxicity by up to 80-fold [1-4]. This promising preclinical data obtained *in vitro* on a number of different cell lines has paved the way for testing these two drugs in electrochemotherapy *in vivo* on different tumor models.

In vivo studies

Bleomycin and cisplatin were tested in an electrochemotherapy protocol in animal models *in vivo* (Fig 1). Extensive studies in different animal models with different types of tumors, either transplantable or spontaneous, were performed. The antitumor effectiveness of electrochemotherapy was demonstrated on tumors in mice, rats, hamsters, cats, dogs, horses and rabbits. Tumors treated by electrochemotherapy were either subcutaneous or located in muscle, brain or liver, being sarcomas, carcinomas, gliomas or malignant melanoma [1-4,6,7].

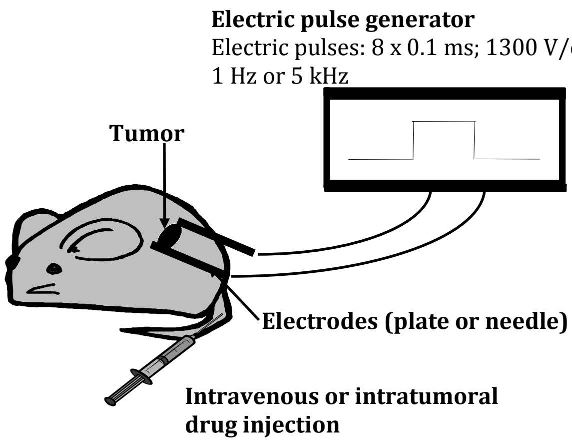

Figure 1: Protocol of electrochemotherapy of experimental tumors presented schematically. The drug is injected either intravenously or intratumorally at doses which do not usually exert an antitumor effect. After an interval which allows sufficient drug accumulation in the tumors, electric pulses are applied to the tumor either by plate or needle electrodes. The electrodes are placed in such a way that the whole tumor is encompassed between the electrodes, providing good electric field distribution in the tumors for optimal electroporation of cells in the tumors.

In these studies, different factors controlling antitumor effectiveness were determined:

- ❖ The drugs can be given by different *routes of administration*, they can be injected either intravenously or intratumorally. The prerequisite is that, at the time of application of electric pulses to the tumor, a sufficient amount of drug is present in the tumor. Therefore, after intravenous drug administration into small laboratory animals (for example 4 mg/kg of cisplatin or 0.5 mg/kg bleomycin), only a few minutes interval is needed to reach the maximal drug concentration in the tumors. After intratumoral administration, this interval is even shorter and the application of electric pulses has to follow the administration of the drug as soon as possible (within a minute) [1-4].
- ❖ Good antitumor effectiveness may be achieved by good tissue electroporation. Electroporation of the plasma membrane is obtained if the cell is exposed to a sufficiently high electric field. This depends on the *electric field distribution in the tissue* which is controlled by the electrode geometry and tissue composition. The electric field distribution in the tissue and cell electroporation can be improved by rotating the electric field. Surface tumours can be effectively treated by plate electrodes, whereas appropriate electric field distribution in the deeper parts of the tumour is assured by using needle electrodes [8-10].

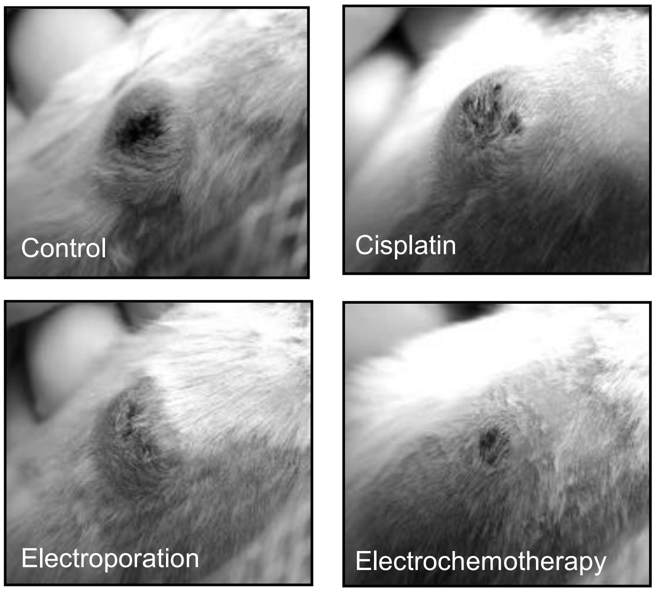

Figure 2: Example of good antitumor effectiveness in SA-1 tumors after electrochemotherapy with cisplatin. Cisplatin was given intravenously (4 mg/kg), 3 min thereafter 8 electric pulses were applied to the tumor with plate electrodes. Electric pulses were applied in two directions; 4 pulses in one and the other 4 in the perpendicular direction. Eight days after the treatment good antitumor effectiveness of electrochemotherapy with cisplatin is evident, compared to the single treatments with cisplatin or electric pulses.

- ❖ The antitumor effectiveness depends on the *amplitude, number, frequency and duration of the electric pulses applied*. Several studies in which parallel plate electrodes were used for surface tumors showed that amplitude over distance ratio above 1000 V/cm is needed for tumor electroporation, and that above 1500 V/cm, irreversible changes in the normal tissues adjacent to the tumor occur. So, the window for effective and safe electrochemotherapy is between 1000-1500 V/cm. In most studies, the amplitude over distance ratio of 1300 V/cm induced good antitumor effectiveness without sub-optimal electroporation of the tissue or damage to the tissue due to irreversible cell permeabilisation [8]. For other types of electrodes, the electric field distribution and thus, also the necessary amplitude of electric pulses, need to be determined by numerical calculations. *Repetition frequencies of the pulses* for electrochemotherapy are either 1 Hz or 5 kHz with equal effect if the concentration of drug present in the tumor is high enough. The minimal number of pulses used is 4; most studies use 8 electric pulses of 100 μs [1,4,9,11-13].

All the experiments conducted *in vivo* in animals provided sufficient data to demonstrate that electrochemotherapy with either bleomycin or cisplatin is effective in the treatment of solid tumors, using drug concentrations which have no or minimal antitumor effect without application of electric pulses. A single treatment by electrochemotherapy already induces partial or complete regression of tumors, whereas treatment with bleomycin or cisplatin alone or application of electric pulses alone has no or minimal antitumor effect (Figure 2).

Mechanisms of action

The principal mechanism of electrochemotherapy is *electroporation* of cells in the tumors, which increases the drug effectiveness by enabling the drug to reach the intracellular target. This was demonstrated in studies which measured the intratumoral drug accumulation and the amount of drug bound to DNA. Basically, the amounts of bleomycin and cisplatin in the electroporated tumours were up to 2-4 fold higher than in those without application of electric pulses [1-4]. Recently, besides already described apoptosis and necrosis after electrochemotherapy, an immunogenic cell death was demonstrated following electrochemotherapy with bleomycin [14].

Besides membrane electroporation, which facilitates drug transport and its accumulation in the cell, other mechanisms that are involved in the antitumor effectiveness of electrochemotherapy were described. The application of electric pulses to tissues induces a transient, but reversible *reduction of blood flow* [14,16]. Restoration of the blood flow in normal tissue is much faster than that in tumors [17,18]. The vascular lock in the tumor induces *drug entrapment* in the tissue, providing more time for the drug to act.

The cytotoxic effect of electrochemotherapy is not limited only to tumor cells in the tumors. Electrochemotherapy also acts on stromal cells, including endothelial cells in the lining of tumor blood vessels, which undergo cell death [18]. Consequently, by vascular-disrupting action of electrochemotherapy, a cascade of tumor cell death occurs due to long-lasting hypoxia in the affected vessels. This represents yet another mechanism involved in the antitumor effectiveness of electrochemotherapy, i.e. a *vascular-disrupting effect* [19-21]. This vascular-disrupting action of electrochemotherapy is important in clinical situations where haemorrhagic tumor nodules need to be treated [22].

A difference in the antitumor effectiveness of electrochemotherapy was observed between immunocompetent and immunodeficient experimental animals, indicating on involvement of the *immune response* in antitumor effectiveness [23]. Due to massive tumor antigen shedding in organisms after electrochemotherapy, systemic immunity can be induced and also up-regulated by additional treatment with biological response modifiers like IL-2, GM-CSF and TNF-α [23-27].

To sum up, the electrochemotherapy protocol was optimized in preclinical studies *in vitro* and *in vivo*, and basic mechanisms were elucidated. In addition to the electroporation of cells, vascular lock leading to drug entrapment in tumors, a vascular- disrupting effect and involvement of the immune response were also demonstrated. Based on all this data, electrochemotherapy with bleomycin and cisplatin was promptly evaluated in clinical trials and is now in routine use in human and veterinary oncology.

PERSPECTIVES

Knowledge about the mechanisms involved in the antitumor effectiveness of electrochemotherapy opened new possibilities for the application of electric pulses or electrochemotherapy in the treatment of cancer.

The chemotherapeutic drugs which increase effectiveness of radiation therapy are radiosensitizing drugs. These include bleomycin and cisplatin. Recently, some new drugs and chemicals were used in combination with electric pulses in preclinical studies, such as Mitomycin C, Ruthenium compounds, Doxorubicin and Calcium. The results of the studies in mice shown positive effects [7,28-32]. Since drug delivery induced by electroporation is site-specific, it could be used for tumor-specific delivery of radiosensitizing drugs. By increased radiosensitizing drug delivery into tumors and not in the surrounding normal tissue, the therapeutic index of tumor irradiation is increased. In our studies, we combined electrochemotherapy with bleomycin or cisplatin with radiotherapy and demonstrated a good potentiation of the sarcoma tumor radiation response: 1.9-fold for electrochemotherapy with bleomycin and 1.6- fold for electrochemotherapy with cisplatin [33,34]. The radiosensitizing effect of electrochemotherapy with cisplatin was also demonstrated in breast cancer and with bleomycin in a fractionated radiation regime which makes this treatment potentially available also in the clinic [35,36].

The application of electric pulses was shown to modulate tumor blood flow. Both reduced blood flow and lowered partial oxygen pressure (pO_2) in the tumors are consequences of the applied electric pulses [37]. The reduced pO_2 can activate bioreductive drugs to exhibit a cytotoxic effect on hypoxic cells [38]. In well- oxygenated cells, the drug remains inactive. On the other hand, tumor hypoxia induced by application of electric pulses can improve therapeutic conditions for the use of hyperthermia since tumor cells are more sensitive to heat in sub-optimal physiological conditions [39].

Electrochemotherapy is an effective cytoreductive treatment; however, its curative effect depends on the permeabilisation of possibly all cells in the tumour. Since permeabilisation of every single cell in the tumour is virtually impossible, electrochemotherapy could be combined with other cytoreductive treatments that should have a local or systemic component. One recent approach was to combined electrochemotherapy with cold plasma, another local ablative therapy. The effect of combination was superior to that of single treatments [40]. A more systemic action can be achieved by a combination of electrochemotherapy with electrotransfer of different therapeutic genes acting either locally or sistemically, such as p53, IL-2; GM-CSF or IL-12. The results of the studies demonstrate positive results, further supporting this concept [41-44].

Finally, electrochemotherapy with cisplatin or bleomycin is also successfully used in veterinary medicine. It was used to treat different tumors, such as mammary adenocarcinoma, fibrosarcoma, cutaneous mast cell tumor, hemangioma, hemangiosarcoma, perianal tumors, neurofibroma and sarcoids in dogs, cats, hamsters, rabbits and horses. Recent reports demonstrated successful treatment of different neoplasms in companion animals and sarcoids in horses either of electrochemotherapy alone or in combination with other treatment, mainly surgery [45-54]. Hopefully, electrochemotherapy will be broadly used in veterinary medicine for the treatment of different malignancies, both in primary and metastatic disease.

In conclusion, electroporation in electrochemotherapy has already been very well exploited; however, there are new biomedical applications of electroporation in cancer treatment that still need testing and development.

REFERENCES

[1] Sersa G. Electrochemotherapy: animal work review. In. Jaroszeski MJ, Heller R, Gilbert R, editors. *Electrochemotherapy, electrogenetherapy, and transdermal drug delivery. Electrically mediated delivery of molecules to cells*. Totowa, New Jersey: Humana Press, 2000. p. 119-36.

[2] Mir LM. Therapeutic perspectives of in vivo cell electropermeabilization. *Bioelectrochem* 2001; 53: 1-10.

[3] Gehl J. Electroporation: theory and methods, perspectives for drug delivery, gene therapy and research. *Acta Physiol Scan* 2003; 177: 437-47.

[4] Mir LM. Bases and rationale of the electrochemotherapy. *EJC Suppl* 2006; 4: 38-44.

[5] Howell SB, Safaei R, Larson CA, Sailor MJ. Sopper transporters and the cellular pharmacology of the Platinum-containing cancer drugs. *Mol Pharmacol* 2010; 77:887-94.

[6] Agerholm-larsen B, Iversen HK, Ibsen P, Moller JM, Mahmood F, Jansen KS, Gehl J. Preclinical validation of electrochemotherapy as an effective treatment for brain tumors. *Cancer Res* 2011; 71:3753-62.

[7] Vásquez JL, Ibsen P, Lindberg H, Gehl J. In vitro and in vivo experiments on electrochemotherapy for bladder cancer. *J Urol*. 2015;193: 1009-15.

[8] Miklavcic D, Beravs K, Semrov D, Cemazar M, Demsar F, Sersa G. The importance of electric field distribution for effective in vivo electroporation of tissues. *Biophys J* 1998; 74: 2152-8.

[9] Miklavcic D, Corovic S, Pucihar G, Pavselj N. Importance of tumor coverage by sufficiently high local electric field for effective electrochemotherapy. *EJC Suppl* 2006; 4: 45-51.

[10] Corovic S, Al Hakere B, Haddad V, Miklavcic D, Mir LM. Importance of the contact surface between electrodes and treated tissue in electrochemotherapy. *Tech Cancer Res Treat* 2008; 7: 292—99.

[11] Sersa G, Miklavcic D, Cemazar M, Rudolf Z, Pucihar G, Snoj M. Electrochemotherapy in treatment of tumours. *Eur J Surg Oncol* 2008; 34: 232-40.

[12] Miklavcic D, Pucihar G, Pavlovec M, Ribaric S, Mali M, Macek-Lebar A, Petkovsek M, Nastran J, Kranjc S, Cemazar M, Sersa G. The effect of high frequency electric pulses on muscle contractions and antitumor efficiency in vivo for a potential use in clinical electrochemotherapy. *Bioelectrochemistry* 2005; 65: 121-8.

[13] Sersa G, Kranjc S, Cemazar M, Scancar J, Krzan M, Neumann E. Comparison of antitumor effectiveness of electrochemotherapy using different electric pulse repetition frequencies. *J membrane biology* 2010; 236: 155-162.

[14] Calvet CY, Famin D, André FM, Mir LM. Electrochemotherapy with bleomycin induces hallmarks of immunogenic cell death in murine colon cancer cells. Oncoimmunology. 2014 Apr 15;3:e28131. eCollection 2014.

[15] Sersa G, Cemazar M, Parkins CS, Chaplin DJ. Tumour blood flow changes induced by application of electric pulses. *Eur J Cancer* 1999; **35:** 672-7.

[16] Bellard E, Markelc B, Pelofy S, Le Guerroué F, Sersa G, Teissié J, Cemazar M, Golzio M. Intravital microscopy at the single vessel level brings new insights of vascular modification mechanisms induced by electropermeabilization. *J Control Release* 2012; 163: 396-403.

[17] Gehl J, Skovsgaard T and Mir LM. Vascular reactions to in vivo electroporation: characterization and consequences for drug and gene delivery. *Biochim Biophys Acta* 2002; 1569: 51-8.

[18] Cemazar M, Parkins CS, Holder AL, Chaplin DJ, Tozer GM and Sersa G. Electroporation of human microvascular endothelial cells: evidence for anti-vascular mechanism of electrochemotherapy. *Br J Cancer* 2001; 84: 556-70

[19] Jarm T, Cemazar M, Miklavcic D, Sersa G. Antivascular effects of electrochemotherapy: implications in treatment of bleeding metastases. *Exp Rev Anticancer Ther* 2010; 10: 729-746.

[20] Sersa G, Jarm T, Kotnik T, Coer A, Podkrajsek M, Sentjurc M, Miklavcic D, Kadivec M, Kranjc S, Secerov A, Cemazar M. Vascular disrupting action of electroporation and electrochemotherapy with bleomycin in murine sarcoma. *Brit J Cancer*, 2008, 98: 388-98

[21] Markelc B, Bellard E, Sersa G, Pelofy S, Teissie J, Coer A, Golzio M, Cemazar. In vivo molecular imaging and histological analysis of changes induced by electric pulses used for plasmid DNA electrotransfer to the skin: a study in a dorsal window chamber in mice. *J Membrane Biol* 2012; 245: 545-554.

[22] Gehl J, Geertsen PF. Palliation of haemorrhaging and ulcerated cutaneous tumours using electrochemotherapy. EJC Suppl 2006; 4: 35-37.

[23] Sersa G, Miklavcic D, Cemazar M, Belehradek JJr, Jarm T, Mir LM. Electrochemotherapy with CDDP on LPB sarcoma: comparison of the anti-tumor effectiveness in immunocompetent and immunodeficient mice. *Bioelectroch Bioener* 1997; 43: 279-283.

[24] Sersa G, Cemazar M, Menart V, Gaberc-Porekar V, Miklavčič D. Antitumor effectiveness of electrochemotherapy is increased by TNF-α on SA-1 tumors in mice. *Cancer Letters* 1997; 116: 85-92.

[25] Mir LM, Roth C, Orlowski S, Quintin-Colona F, Fradelizi D, Belahradek J, Kourilsky P. Systemic antitumor effects of electrochemotherapy combined with histoincompatible cells secreting interleukin 2. *J Immunother* 1995; **17:** 30-8.

[26] Heller L, Pottinger C, Jaroszeski MJ, Gilbert R, Heller R. In vivo electroporation of plasmids encoding GM-CSF or interleukin-2 into existing B16 melanoma combined with electrochemotherapy inducing long-term antitumour immunity. *Melanoma Res* 2000; 10: 577-83.

[27] Cemazar M, Todorovic V, Scancar, J Lampreht U, Stimac M, Kamensek U, Kranjc S, Coer A, Sersa G. Adjuvant INF-a therapy to electrochemotherapy with intravenous cisplatin in murine sarcoma exerts synergistic antitumor effectiveness *Radiol Oncol* 2015; 49:32-40

[28] Vásquez JL, Gehl J, Hermann GG. Electroporation enhances mitomycin C cytotoxicity on T24 bladder cancer cell line: a potential improvement of intravesical chemotherapy in bladder cancer. *Bioelectrochemistry* 2012; **88:**127-33.

[29] Hudej R, Miklavcic D, Cemazar M, Todorovic V, Sersa G, Bergamo A, Sava G, Martincic A, Scancar J, Keppler BK, Turel I. Modulation of Activity of Known Cytotoxic Ruthenium(III) Compound (KP418) with Hampered Transmembrane Transport in Electrochemotherapy In Vitro and In Vivo. *J Membr Biol* 2014 Jun 24. [Epub ahead of print].

[30] Frandsen SK, Gissel H, Hojman P, Tramm T, Eriksen J, Gehl J. Direct therapeutic applications of calcium electroporation to effectively induce tumor necrosis. *Cancer Res* 2012 15; **72:**1336-41.

[31] Kulbacka J, Daczewska M, Dubińska-Magiera M, Choromańska A, Rembiałkowska N, Surowiak P, Kulbacki M, Kotulska M, Saczko J. Doxorubicin delivery enhanced by electroporation to gastrointestinal adenocarcinoma cells with P-gp overexpression. *Bioelectrochemistry* 2014;100:96-104.

[32] Frandsen SK, Gissel H, Hojman P, Eriksen J, Gehl J. Calcium electroporation in three cell lines: a comparison of bleomycin and calcium, calcium compounds, and pulsing conditions. *Biochim Biophys Acta* 2014;1840:1204-8.

[33] Sersa G, Kranjc S, Cemazar M. Improvement of combined modality therapy with cisplatin and radiation using electroporation of tumors. *Int J Radiat Oncol Biol Phys* 2000; 46: 1037-41.

[34] Kranjc S, Grosel A, Cemazar M, Sentjurc M, Sersa G. Improvement of combined modality therapy with bleomycin and radiation using electroporation of LPB sarcoma cells and tumors in mice. *BMC Cancer* 2005; 5: 115.

[35] Raeisi E, Aghamiri SM, Bandi A, Rahmatpour N, Firoozabadi SM, Kafi-Abad SA, Mir LM. The antitumor efficiency of combined alectrochemotherapy and a single dose irradiation on a breast cancer tumor model. *Radiol Oncol* 2012; 46: 226-32.

[36] Kranjc S, Tevz G, Kamensek U, Vidic S, Cemazar M, Sersa G. Radiosensitizing effect of electrochemotherapy in a fractionated radiation regime in radiosensitive murine sarcoma and radioresistant adenocarcinoma tumor model. *Radiat Biol* 2009 172:677-85.

[37] Sersa G, Krzic M, Sentjurc M, Ivanusa T, Beravs K, Kotnik V, Coer A, Swartz HM, Cemazar M. Reduced blood flow and oxygenation in SA-1 tumours after electrochemotherapy with cisplatin. *Br J Cancer* 2002; 87:1047-54.

[38] Cemazar M, Parkins CS, Holder AL, Kranjc S, Chaplin DJ and Sersa G. Cytotoxicity of bioreductive drug tirapazamine is increased by application of electric pulses in SA-1 tumours in mice. *Anticancer Res* 2001; 21: 1151-1156.

[39] Karner KB, Lesnicar H, Cemazar M, Sersa G. Antitumour effectiveness of hyperthermia is potentiated by local application of electric pulses to LPB tumours in mice. *Anticancer Res* 2004; 24: 2343-8.

[40] Daeschlein G1, Scholz S, Lutze S, Arnold A, von Podewils S, Kiefer T, Tueting T, Hardt O, Haase H, Grisk O, Langner S, Ritter C, von Woedtke T, Jünger M. Comparison between cold plasma, electrochemotherapy and combined therapy in a melanoma mouse model. Exp Dermatol. 2013 Sep;22(9):582-6. doi: 10.1111/exd.12201.

[41] Heller L, Pottinger C, Jaroszeski MJ, Gilbert R, Heller R. In vivo electroporation of plasmid encoding GM-CSF or interleukin-2 into existing B16 melanomas combined with electrochemotherapy induces long-term antitumour immunity. *Melanoma Res* 2000; 10: 577-83.

[42] Matsubara H, Maeda T, Gunji Y, Koide Y, Asano T, Ochiai T, Sakiyama S, Tagawa M. Combinatory anti-tumor effects of electroporation-mediated chemotherapy and wild-type p53 gene transfer to human esophageal cancer cells. *Int J Oncol* 2001; 18: 825-9.

[43] Grosel A, Sersa G, Kranjc S, Cemazar M. Electrogene therapy with p53 of murine sarcomas alone or combined with electrochemotherapy using cisplatin. *DNA Cell Biol* 2006; 25:674-83.

[44] Sedlar A, Dolinsek T, Markelc B, Prosen L, Kranjc S, Bosnjak M, Blagus T, Cemazar M, Sersa G. Potentiation of

electrochemotherapy by intramuscular IL-12 gene electrotransfer in murine sarcoma and carcinoma with different immunogenicity. *Radiol Oncol* 2012, 4: 302-11.

[45] Mir LM, Devauchelle P, Quintin_Colonna F, Delisle F, Dolinger S, Fradelizi D, Belehradek JrJ, Orlowski S. First clinical trial of cat soft-tissue carcomas treatment by electrochemotherapy. *Br J Cancer* 1997; 76: 1617-22.

[46] Tozon N, Sersa G, Cemazar M. Electrochemotherapy: Potentiation of local antitumour effectiveness of cisplatin in dogs and cats. *Anticancer Res* 2001; 21: 2483-6.

[47] Cemazar M, Tamzali Y, Sersa G, Tozon N, Mir LM, Miklavcic D, Lowe R, Teissie T. Electrochemotherapy in veterinary oncology. *J Vet Int Med* 2008; 22: 826-31.

[48] Kodre V, Cemazar M, Pecar J, Sersa G, Cőr A, Tozon N. Electrochemotherapy compared to surgery for treatment of canine mast cell tumours. *Anticancer Res* 2009; 23: 55-62.

[49] Pavlin D, Cemazar M, Cör A, Sersa G, Pogacnik A, Tozon N. Electrogene therapy with interleukin-12 in canine mast cell tumors. *Radiol Oncol* 2011; 45: 30-9.

[50] Tamzali Y, Borde L, Rols MP, Golzio M, Lyazrhi F, Teissie J. Succesful treatment of equine sarcoids with cisplatin electrochemotherapy: A retrospective study of 48 cases. *Equine Vet J* 2012; 44: 214-40.

[51] Spugnini Ep, Fanciulli M, Citro G, Baldi A. Preclinical models of electrochemotherapy: the role of veterinary patients. *Future Oncol* 2012; 8:829-37.

[52] Spugnini EP, Renaud SM, Buglioni S, Carocci F, Dragonetti E, Murace R, Cardelli P, Vincenzi B, Baldi A, Citro G. Electrochemotherapy with cisplatin enhances local control after surgical ablation of fibrosarcoma in cats: an approach to imporve the therapeutic index of highly toxic chemotherapy drugs. *J Transl Med* 2011; 9:152.

[53] Tozon N, Pavlin D, Sersa G, Dolinsek T, Cemazar M. Electrochemotherapy with intravenous bleomycin injection: an observational study in superficial squamous cell carcinoma in cats. *J Feline Med Surg* 2014; **16:** 291–9.

[54] Brunner CH, Dutra G, Silva CB, Silveira LM, Martins Mde F. Electrochemotherapy for the treatment of fibropapillomas in Chelonia mydas. *Zoo Wildl Med* 2014;45:213-8.

ACKNOWLEDGEMENT

This research was funded by research grants from Slovenian Research Agency and was conducted in the scope of the EBAM European Associated Laboratory (LEA) and COST Action TD1104.

Maja Čemažar received her PhD in basic medical sciences from the Medical Faculty, University of Ljubljana in 1998. She was a postdoctoral fellow and researcher at Gray Cancer Institute, UK from 1999 to 2001. She was an associate researcher at the Institute of Pharmacology and Structural Biology in Toulouse, France in 2004. Currently, she works at the Department of Experimental Oncology, Institute of Oncology Ljubljana and teaches at the Faculty of Health Sciences, University of Primorska, Slovenia. Her main research interests are in the field of gene electrotransfer employing plasmid DNA encoding different immunomodulatory and antiangiogenic therapeutic genes. In 2006 she received the Award of the Republic of Slovenia for important achievements in scientific research and development in the field of experimental oncology.

She is the author of more than 150 articles in peer-reviewed journals.

NOTES

Clinical electrochemotherapy

Gregor Serša
Institute of Oncology Ljubljana, Slovenia

Abstract: Electrochemotherapy consists of administration of the chemotherapeutic drug followed by application of electric pulses to the tumor, in order to facilitate the drug uptake into the cells. Only two chemotherapeutics are currently used in electrochemotherapy, bleomycin and cisplatin, which both have hampered transport through the plasma membrane without electroporation of tumors. Based on extensive preclinical studies, elaborating on parameters for effective tumor treatment and elucidating the mechanisms of this therapy, electrochemotherapy is now in clinical use. It is in standard treatment of melanoma cutaneous metastases in Europe. However it is effective also for cutaneous metastases of other tumor types, like basal and squamous cell tumors of head and neck. Currently the technology is being developed also for treatment of bigger, deep seated tumors. With new electrodes and new electric pulse generators, clinical trials are on-going for treatment of liver metastases and primary tumors, of pancreas, bone metastases and soft tissue sarcomas, as well as brain metastases, tumors in in esophagus or in rectum.

INTRODUCTION

Electrochemotherapy protocols were optimized in preclinical studies *in vitro* and *in vivo*, and basic mechanisms elucidated, such as electroporation of cells, tumor drug entrapment (vascular lock), vascular-disrupting effect and involvement of the immune response. Based on all this data, electrochemotherapy with bleomycin and cisplatin was promptly evaluated in clinical trials. Recent reviews elaborate on its technology and biomedical applications in medical practice [1,2].

CLINICAL STUDIES

The results of several clinical studies have confirmed the preclinical data: high antitumor effectiveness of electrochemotherapy with bleomycin and cisplatin on cutaneous and subcutaneous tumor nodules with different histology was demonstrated.

The first clinical study was published in 1991 on head and neck tumor nodules [3], which was thereafter followed by several others [4-42]. These clinical studies demonstrated the antitumor effectiveness of electrochemotherapy using either bleomycin or cisplatin, given intravenously or intratumorally. Successful treatment of cutaneous and subcutaneous tumor nodules by electrochemotherapy was reported also from the Sydney Melanoma Unit as well as several Italian cancer centers [41-64]. In addition to single or multiple cutaneous or subcutaneous melanoma nodules, a response was demonstrated in breast and head and neck cancer nodules, as well as Kaposi's sarcoma, hypernephroma, chondrosarcoma and basal cell carcinoma. However, these clinical studies were performed with slightly variable treatment protocols, different electrodes and different electric pulse generators. Thus, there was a need for a prospective multi-institutional study, which was conducted by a consortium of four cancer centres gathered in the ESOPE project funded under the European Commission's 5th Framework Programme. In this study, the treatment response after electro-chemotherapy according to tumor type, drug used, route of administration and type of electrodes, was tested [42]. The results of this study can be summarized as follows:

- An objective response rate of 85% (73.7% complete response rate) was achieved for electrochemotherapy-treated tumor nodules, regardless of tumor histology and drug or route of administration used (Figure 1).
- At 150 days after treatment, the local tumor control rate for electrochemotherapy was 88% with bleomycin given intravenously, 73% with bleomycin given intratumorally and 75% with cisplatin given intratumorally, demonstrating that all three approaches were equally effective in local tumor control.
- Side effects of electrochemotherapy were minor and tolerable (muscle contractions and pain sensation).

In all clinical studies reported before the ESOPE study and in the ESOPE study, 288 patients were treated: 782 tumor nodules were treated by electrochemotherapy with bleomycin and 398 tumor nodules were treated by electrochemotherapy with cisplatin. The results of the ESOPE study confirmed previously reported results on the effectiveness of electrochemotherapy and Standard Operating

Procedures (SOP) for electrochemotherapy were prepared [43].

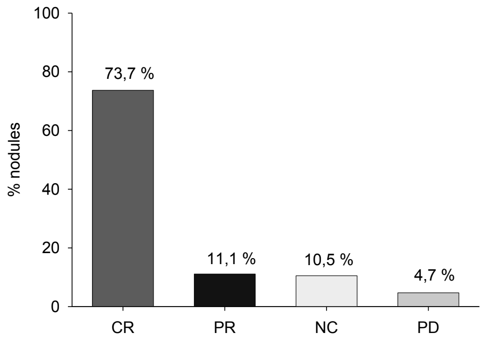

Figure 1: Treatment response of tumor nodules treated by electrochemotherapy in the ESOPE project. CR: complete response; PR: partial response; NC: no change; PD: progressive disease.

The ESOPE study set the stage for introduction of electrochemotherapy in Europe. After the encouraging results of the ESOPE study, several cancer centers have started to use electrochemotherapy and reported the results of their studies. Collectively, the results were again similar as reported in the ESOPE study. However some advances in the treatment were reported. Predominantly it was reported that tumors bigger than 3 cm in diameter can be successfully treated by electrochemotherapy in successive electro-chemotherapy sessions [59,60]. In general, electrochemotherapy provides a benefit to patients especially in quality of life [60], because electrochemotherapy is nowadays used predominantly in palliative intent [59,60].

CLINICAL USE AND TREATMENT PROCEDURES FOR ELECTROCHEMOTHERAPY

Based on all these reports, electrochemotherapy has been recognized as a treatment option for disseminated cutaneous disease in melanoma, and accepted in many national and also international guidelines for treatment of melanoma [65].

Treatment advantages and clinical use for electrochemotherapy can be summarized as follows:

- Effective in treatment of tumors of different histology in the cutaneous or subcutaneous tissue.
- Palliative treatment with improvement of patient's quality of life.
- Treatment of choice for tumors refractory to conventional treatments.
- Cytoreductive treatment before surgical resection in an organ sparing effect.
- Treatment of bleeding metastases.

The treatment procedure is as follows: based on SOP, tumor nodules can be treated by electrochemotherapy with injection of bleomycin intravenously or intratumorally and by electrochemotherapy with cisplatin given intratumorally. The choice of the chemotherapeutic drug in not based on tumor histology, but depends on the number and size of the nodules. After drug injection, the tumor nodules are exposed to electric pulses. The interval between intravenous drug injection and application of electric pulses is 8-28 min, and after intratumoral injection, as soon as possible. Different sets of electrodes are available for application; plate electrodes for smaller tumor nodules and needle electrodes for the treatment of larger (3 cm) and thicker tumor nodules. The treatment can be performed in a single session or can be repeated in case of newly emerging nodules or on those nodules which relapsed in some regions which were not treated well in the first treatment [42,43,59,60].

Electrochemotherapy does not induce side effects due to chemotherapeutic drugs since the drug dosage is very low. However, the application of electric pulses to the tumors induces contraction of the underlying muscles. For electroporation, square wave electric pulses with amplitude over distance ratio of 1000-1300 V/cm, duration of 100 μs, frequency 1 Hz or 5 kHz are used. These muscle contractions are painful, but the pain dissipates immediately after electric pulse application. Nevertheless, in SOP, the procedures for alleviating pain by local anaesthesia or by general anaesthesia in case of treating multiple nodules, are also described [43].

The treatment after a single electrochemotherapy session in most cases results in complete tumor eradication. When necessary, treatment can be repeated at 4-8 week intervals with equal antitumor effectiveness. The treatment has a good cosmetic effect without scarring of the treated tissue

In summary, electrochemotherapy has been recognized as a valid treatment approach; over 140 cancer centers have started to use it and have reported positive results. So far the effectiveness of the therapy is on case based evidence and further controlled and randomized studies are needed for the translation of this technology into broader and standard clinical practice. For further acceptance of electrochemotherapy in medical community, the first important step has been made, since electrochemotherapy for treatment of melanoma skin metastases and for treatment of primary basal cell and primary squamous cell carcinoma was recently listed in NICE guidelines.

Recently all published studies up to 2012 on electro-chemotherapy in treatment of superficial nodules were reviewed in systematic review and meta-analysis [66]. Data analysis confirmed that electrochemotherapy had a significantly ($p<0.001$) higher effectiveness (by more than 50%) than bleomycin or cisplatin alone, where only 8% of the tumors were in CR. After a single electro-chemotherapy, the treatment can be repeated with similar effectiveness. The overall effectiveness of electrochemotherapy was 84.1% objective responses (OR), from these 59.4% complete responses (CR). Another recent review and a clinical study suggested that SOP may need refinement; since the currently used SOP for electrochemotherapy may not be suitable for tumors bigger than 3 cm in diameter, but such tumors are suitable for the multiple consecutive electrochemotherapy sessions [67].

NEW CLINICAL APPLICATIONS OF ELECTROCHEMOTHERAPY

Based on clinical experience that electrochemotherapy can be effectively used in treatment of cancer with different histology, when appropriately executed, the treatment could be used also for treatment of deep seated tumors. Prerequisite for that is further development of the technology in order to reach and effectively treat the tumors located either in the muscle, liver, bone, esophagus, rectum, brain or other internal organs.

The first steps in technological development have already been made. For example, there is already the first report in treatment of melanoma metastasis in the muscle, 2 cm under the skin. With long needle electrodes and new electric pulses generator Cliniporator Vitae™ it was possible to treat this deep seated metastasis 2 x 1.4 cm in diameter [68].

Further development of such electrodes enabled treatment of liver metastases (Figure 2). At the Institute of Oncology Ljubljana, Slovenia a clinical trial was launched, where liver metastases of colorectal tumors are treated and effectiveness evaluated at the two stage operation (NCT01264952). So far 16 patients were enrolled. No immediate or late side-effects of electrochemotherapy were observed [69,70]. The delivery of electric pulses during open surgery was synchronized with ECG in order to avoid possible arrhythmias. Specific treatment plan is prepared for the treatment, in order to predict the exact location of the electrodes for sufficient coverage of the tumors with the electric field in the tumor and in the safety margins of the tumor [72]. In this prospective pilot study 29 metastases in 16 patients were treated in 16 electrochemotherapy sessions. Radiological evaluation of all the treated metastases showed 85% complete responses and 15% partial responses. In a group of 7 patients that underwent a second operation at 6-12 weeks after the first one, during which electrochemotherapy was performed, the histology of resected metastases treated by electrochemotherapy showed less viable tissue ($P=0.001$) compared to non-treated ones [70].

Furthermore, a recent report has demonstrated feasibility and safety of electrochemotherapy in treatment of locally advanced pancreatic tumors [72].

Figure 2: Electrochemotherapy of liver metastasis. Electrodes were inserted into the tumor and around the tumor in healthy liver tissue and connected to electric pulse generator. Electric pulses were delivered between the pairs of electrodes according to the treatment plan.

Similar technology is being used in treatment of bone metastases or soft tissue sarcoma. The tumors are similarly as in treatment of liver metastases punctured by long needle electrodes, so that electrodes are placed around and in the tumor. The clinical trials are still ongoing but according to the preliminary report at the Second Users meeting of Electro-chemotherapy in Bologna, Italy (2013) the technology is feasible, safe and effective. Recent report.

Another approach that is in development is the use of endoluminal electrodes for the treatment of tumors in esophagus or in rectum. The first reports demonstrate that the technology is available, and was tested also in dogs. The translation of this technology into the human clinics is underway; the clinical trial for the treatment of unresectable colon tumors is ongoing [73].

In several studies also breast chest wall breast cancer recurrences were treated. A review of these data has demonstrated that the treatment of such metastases is equally effective as other tumors [74]. The feasibility and effectiveness was elaborated also in recent clinical studies by Campana et al. [75,76]. Recently also a study from Herlev Cancer Center has demonstrated that even big chest wall breast cancer recurrences can be treated successfully by electrochemotherapy [77].

The last but not least also electrodes for treatment of brain tumors are developed [78,79]. They will enable treatment of brain tumors, minimally invasively. The clinical trial is was launched.

CONCLUSION

Electrochemotherapy is one of the biomedical applications of electroporation. Its development has reached clinical application and is an example of successful translational medicine. However its development is not finished yet; new technical developments will certainly enable further clinical uses and eventually clinical benefit for the patients. Another application of electroporation is still awaiting such translation, gene therapy based on gene electrotransfer. In relation to this, first clinical results are encouraging, but standard clinical use is still far away.

REFERENCES

[1] Yarmush ML, Goldberg A, Sersa G, Kotnik T, Miklavcic D. Electroporation-based technologies for medicine: principles, applications, and challenges. *Ann Rev Biomed Eng* 2014; **16:** 295-320.

[2] Miklavcic D, Mali B, Kos B, Heller R, Sersa G. Electrochemotherapy: from the drawing board into medical practice. *BioMedical OnLine* 2014; **13:** 29.

[3] Mir LM, Belehradek M, Domenge C, Orlowski S, Poddevin B, Belehradek J Jr, Schwaab G, Luboinski B, Paoletti C. Electrochemotherapy, a new antitumor treatment: first clinical trial. *C R Acad Sci III* 1991; **313:** 613-8.

[4] Belehradek M, Domenge C, Luboinski B, Orlowski S, Belehradek J Jr, Mir LM. Electrochemotherapy, a new antitumour treatment. First clinical phase I-II trial. *Cancer* 1993; **72:** 3694-700.

[5] Rudolf Z, Stabuc B, Cemazar M, Miklavcic D, Vodovnik L, Sersa G. Electrochemotherapy with bleomycin: The first clinical experience in malignant melanoma patients. *Radiol Oncol* 1995; **29:** 229-35.

[6] Heller R, Treatment of cutaneous nodules using electrochemotherapy. *J. Florida M.A*. 1995; **82**: 147-150.

[7] Glass LF, Fenske NA, Jaroszeski M, Perrott R, Harvey DT, Reintgen DS, Heller R. Bleomycin-mediated electrochemotherapy of basal cell carcinoma. *J Am Acad Dermatol* 1996; **34:** 82-6.

[8] Glass LF, Pepine ML, Fenske NA, Jaroszeski M, Reintgen DS, Heller R. Bleomycin-mediated electrochemotherapy of metastatic melanoma. *Arch Dermatol* 1996; **132:** 1353-7.

[9] Heller R, Jaroszeski MJ, Glass LF, Messina JL, Rapaport DP, DeConti RC, Fenske NA, Gilbert RA, Mir LM, Reintgen DS. Phase I/II trail for the treatment of cutaneous and subcutaneous tumors using electrochemotherapy. *Cancer* 1996; **77:** 964-71.

[10] Reintgen DS, Jaroszeski MJ, Heller R. Electrochemotherapy, a novel approach to cancer. *The Skin Cancer Foundation Journal* 1996; **14:** 17-19.

[11] Domenge C, Orlowski S, Luboinski B, De Baere T, Belehradek J-Jr, Mir LM. Antitumor electrochemotherapy. New advances in the clinical protocol. *Cancer* 1996; **77:** 956-63.

[12] Glass LF, Jaroszeski M, Gilbert R, Reintgen DS, Heller R. Intralesional bleomycin-mediated electrochemotherapy in 20 patients with basal cell carcinoma. *J Am Acad Dermatol* 1997; **37:** 596-9.

[13] Heller R, Gilbert R et al. Electrochemotherapy: an emerging drug delivery method for the treatment of cancer. *Adv Drug Deliv Rev*. 1997; **26**: 185-197.

[14] Mir LM, Glass LF, Sersa G, Teissie J, Domenge C, Miklavcic D, Jaroszeski M-J, Orlowski S, Reintgen DS, Rudolf Z, Belehradek M, Gilbert R, Rols M-P, Belehradek JJr, Bachaud JM, DeConti R, Stabuc B, Cemazar M, Coninx P, Heller R. Effective treatment of cutaneous and subcutaneous malignant tumours by electrochemotherapy. *Brit J Cancer* 1998; **77:** 2336-42.

[15] Heller R, Jaroszeski MJ, Reintgen DS, Puleo CA, DeConti RC, Gilbert RA, Glass LF. Treatment of cutaneous and subcutaneous tumors with electrochemotherapy using intralesional bleomycin. *Cancer* 1998; **83:** 148-57.

[16] Panje WR, Hier MP, Garman GR, Harrel E, Goldman A, Bloch I. Electroporation therapy of head and neck cancer. *Am Otol Rhinol Laryngol* 1998; **107:** 779-85.

[17] Kubota Y, Mir LM, Nakada T, Sasagawa I, Suzuki H, Aoyama N. Successful treatment of metastatic skin lesions with electrochemotherapy. *J Urol* 1998; **160:** 1426.

[18] Sersa G, Stabuc B, Cemazar M, Jancar B, Miklavcic D, Rudolf Z. Electrochemotherapy with cisplatin: potentiation of local cisplatin antitumour effectiveness by application of electric pulses in cancer patients. *Eur J Cancer* 1998; **34:** 1213-8.

[19] Sersa G, Cemazar M, Rudolf Z, Fras AP. Adenocarcinoma skin metastases treated by electrochemotherapy with cisplatin combined with radiation. *Radiol Oncol* 1999; **33:** 291-6.

[20] Mir LM, Orlowski S. Mechanisms of electrochemotherapy. *Adv Drug Deliv Rev*. 1999; **35**: 107-118.

[21] Heller R, Gilbert R, et al. Clinical applications of electrochemotherapy. *Adv Drug Deliv Rev*. 1999; **35**: 119-129.

[22] Hofmann GA, Dev SB, et al. Electroporation therapy: a new approach for the treatment of head and neck cancer. *IEEE Trans Biomed Eng* 1999; **46**: 752-759.

[23] Gehl J, Geertsen P. Efficient palliation of hemorrhaging malignant melanoma skin metastases by electrochemotherapy. *Melanoma Res* 2000; **10:** 585-9.

[24] Rebersek M, Cufer T, Rudolf Z, Sersa G. Electrochemotherapy with cisplatin of breast cancer tumor nodules in a male patient. *Radiol Oncol* 2000; **34:** 357-61.

[25] Sersa G, Cufer T, Cemazar M, Rebersek M, Zvonimir R. Electrochemotherapy with bleomycin in the treatment of hypernephroma metastasis: case report and literature review. *Tumori* 2000; **86:**163-5.

[26] Rols MP, Bachaud JM, Giraud P, Chevreau C, Roche H, Teissie J. Electrochemotherapy of cutaneous metastases in malignant melanoma. *Melanoma Res* 2000; **10:** 468-74.

[27] Sersa G, Stabuc B, Cemazar M, Miklavcic D, Rudolf Z. Electrochemotherapy with cisplatin: the systemic antitumour

effectiveness of cisplatin can be potentiated locally by aplication of electric pulses in the treatment of malignant melanoma skin metastases. *Melanoma Res* 2000; **10:** 381-5.

[28] Sersa G, Stabuc B, Cemazar M, Miklavcic D, Rudolf Z. Electrochemotherapy with cisplatin: clinical experience in malignant melanoma patients. *Clin Cancer Res* 2000; **6:** 863-7.

[29] Rodriguez-Cuevas S, Barroso- Bravo S, Almanza- Estrada J, Cristobal- Martinez L, Gonzales-Rodriguez E. Electrochemotherapy in primary and metastatic skin tumors: Phase II trial using intralesional bleomycin. *Arch Med Res* 2001; **32:** 273-6.

[30] Allegretti JP, Panje WR. Electroporation therapy for head and neck cancer including carotid arthery involvement. *Laryngoscope* 2001; **111:** 52-6.

[31] Burian M, Formanek M, Regele H. Electroporation therapy in head and neck cancer. *Acta Otolaryngol* 2003; **123:** 264-8.

[32] Sersa G, Cemazar M, Rudolf Z. Electrochemotherapy: advantages and drawbacks in treatment of cancer patients. *Cancer Therapy* 2003; **1:** 133–42.

[33] Shimizu T, Nikaido T, Gomyo H, Yoshimura Y, Horiuchi A, Isobe K, Ebara S, Takaoka K. Electrochemotherapy for digital chondrosarcoma. *J Ortop Sci* 2003; **8:** 248-51.

[34] Gothelf A, Mir LM, Gehl J. Electrochemotherapy: results of cancer treatment using enhanced delivery of bleomycin by electroporation. *Cancer Treat Rew* 2003; **29:** 371–87.

[35] Gehl J. Electroporation: theory and methods, perspectives for drug delivery, gene therapy and research. *Acta Physiol Scand* 2003; **177:** 437-447.

[36] Byrne CM, Thompson JF, Johnston H, Hersey P, Quinn MJ, Hughes M, McCarthy WH. Treatment of metastatic melanoma using electroporation therapy with bleomycin (electrochemotherapy). *Melanoma Res* 2004; **15:** 45-51.

[37] Rebersek M, Cufer T, et al. Electrochemotherapy with cisplatin of cutaneous tumor lesions in breast cancer. *Anticancer Drugs* 2004; 15: 593-597.

[38] Snoj M, Rudolf Z, Cemazar M, Jancar B, Sersa G. Successful sphincter-saving treatment of anorectal malignant melanoma with electrochemotherapy, local excision and adjuvant brachytherapy. *Anti-Cancer Drugs* 2005; **16:** 345–8.

[39] Kubota Y, Tomita Y, Tsukigi M, Kurachi H, Motoyama T, Mir LM. A case of perineal malignant melanoma successfully treated with electrochemotherapy. *Melanoma Res* 2005; **15:** 133-4.

[40] Bloom DC, Goldfarb PM. The role of intratumour therapy with electroporation and bleomycin in the management of advanced squamous cell carcinoma of the head and neck. *Eur J Surg Oncol* 2005; **31**: 1029-35.

[41] Sersa G. The state-of-the-art of electrochemotherapy before the ESOPE study: advantages and clinical uses. *Eur J Cancer Suppl* 2006; **4:** 52–9.

[42] Marty M, Sersa G, Garbay JR, Gehl J, Collins CG, Snoj M, et al. Electrochemotherapy – An easy, highly effective and safe treatment of cutaneous and subcutaneous metastases: Results of ESOPE (European Standard Operating Procedures of Electrochemotherapy) study. *EJC Supp*l 2006; **4**: 3-13.

[43] Mir LM, Gehl J, Sersa G, Collins CG, Garbay JR, Billard V, et al. Standard operating procedures of the electrochemotherapy: Instructions for the use of bleomycin or cisplatin administered either systemically or locally and electric pulses delivered by Cliniporator ™ by means of invasive or non-invasive electrodes. *EJC Supp*l 2006; **4**: 14-25.

[44] Snoj M, Rudolf Z, et al. Long lasting complete response in melanoma treated by electrochemotherapy. *EJC Supp*l 2006; **4**: 26-28.

[45] Garbay JR, Billard V, et al. Successful repetitive treatments by electrochemotherapy of multiple unrespectable Kaposi sarcoma nodules. *EJC Supp*l 2006; **4**: 29-31.

[46] Whelan MC, Larkin JO et al. Effective treatment of an extensive recurrent breast cancer which was refractory to multimodal therapy by multiple applications of electrochemotherapy. *EJC Supp*l 2006; **4**: 32-34.

[47] Gehl J and Geertsen PF, Palliation of haemorrhaging and ulcerated cutaneous tumours using electrochemotherapy. *EJC Supp*l 2006; **4**: 35-37.

[48] Mir LM, Bases and rationale of the electrochemotherapy. *EJC Supp*l 2006; **4**: 38-44.

[49] Miklavcic D, Corovic S, et al. Importance of tumour coverage by sufficiently high localelectric field for effective electrochemotherapy. *EJC Supp*l 2006; **4**: 45-51.

[50] Byrne CM and Thompson JF, Role of electrochemotherapy in the treatment of metastatic melanoma and other metastatic and primary skin tumors. *Expert Rev. Anticancer Ther* 2006; **6**: 671-678.

[51] Sersa G, Čemažar M et al. Electrochemotherapy of tumours. *Radiol Oncol* 2006; **40**: 163-174.

[52] Tijink BM, De Bree M, et al. How we do it: Chemo-electroporation in the head and neck for otherwise untreatable patients. *Clin Otolaryngol*. 2006; **31**: 447-51.

[53] Larkin JO, Collins CG, et al. Electrochemotherapy: aspects of preclinical development and early clinical experience. *Ann Surg* 2007; **245**: 469-479.

[54] Sersa G, Miklavcic D, Cemazar M, Rudolf Z, Pucihar G, Snoj M. Electrochemotherapy in treatment of tumours. *Eur J Surg Oncol* 2008; **34:** 232-40.

[55] Testori A, Soteldo J, et al. The treatment of cutaneous and subcutaneous lesions with electrochemotherapy with bleomycin. *European Dermatology* 2008; **3**: 2-3.

[56] Colombo GL, Di Matteo S, et al. Cost-effectiveness analysis of electrochemotherapy with the CliniporatorTM vs other methods for the control and treatment of cutaneous and subcutaneous tumors. *Ther Clin Risk Manag* 2008; **4**: 541-48.

[57] Sadadcharam MD, Soden M, et al. Electrochemotherapy: an emerging cancer treatment. *Int. J. Hyperthermia* 2008; **24**: 263-73.

[58] Gehl J (2008). Electroporation for drug and gene delivery in the clinic: doctors go electric. In: S. Li ed. *Methods in Molecular Biology Vol.423*: Humana Press, 351-359.

[59] Campana LG, Mocellin S, et al. Bleomycin-based electrochemotherapy: clinical outcome from a single institution's experience with 52 patients. *Ann Surg Oncol* 2008; **16**: 191-9.

[60] Quaglino P, Mortera C, et al. Electrochemotherapy with intravenous bleomycin in the local treatment of skin melanoma metastases. *Ann Surg Oncol* 2008; **15**: 2215-22.

[61] Curatolo P, Mancini M, et al. Successful treatment of penile Kaposi's sarcoma with electrochemotherapy. *Dermatol Surg* 2008; **34**: 1-5.

[62] Fantini F, Gualdi G, et al. Metastatic basal cell carcinoma with squamous differentiation: report of a case with response of cutaneous metastases to electrochemotherapy. *Arch Dermatol* 2008; **144**: 1186-1188.

[63] Guida M, Porcelli G, et al. Locoregional therapy. *Eur J Cancer Supp*l 2008; **6**: 132-133.

[64] Snoj M, Čemažar M, et al. Limb sparing treatment of bleeding melanoma recurrence by electrochemotherapy. *Tumori* 2009; **95**: 398-402.

[65] Testori A, Rutkowski P, Marsden J, Bastholt L, Chiarion-Sileni V, Hauschild A, Eggermont AM, Surgery and radiotherapy in the treatment of cutaneous melanoma, *Ann Oncol* 2009; **20 Suppl 6**: 22-9.

[66] Mali B, Jarm T, Snoj M, Sersa G, Miklavcic D. Antitumor effectiveness of electrochemotherapy: a systematic review and meta-analysis. *Eur J Surg Oncol* 2013; **39:** 4-16.

[67] Mali B, Miklavcic D, Campana L, Cemazar M, Sersa G, Snoj M, Jarm T. Tumor size and effectiveness of electro-chemotherapy. *Radiol Oncol* 2013; **47:** 32-41.

[68] Miklavcic D, Snoj M, Zupanic A, Kos B, Cemazar M, Kropivnik M, Bracko M, Pecnik T, Gadzijev E, Sersa G. Towards treatment planning and treatment of deep-seated solid tumors by electrochemotherapy, *Biomed Eng Online* 2010; **9:** 10.

[69] Edhemovic I, Gadzijev EM, Brecelj E, Miklavcic D, Kos B, Zupanic A, Mali B, Jarm T, Pavliha D, Marcan M, Gasljevic G, Gorjup V, Music M, Pecnik Vavpotic T, Cemazar M, Snoj M, Sersa G. Electrochemotherapy: a new technological approach in treatment of metastases in the liver. *Tecnol Cancer Res Treat* 2011; **10;** 475-85.

[70] Edhemovic I, Brecelj E, Gasljevic G, Marolt Music M, Gorjup V, et al. Intraoperative electrochemotherapy of colon liver metastases. *J Surg Oncol* 2014; **110:** 320-327.

[71] Kos B, Zupanic A, Kotnik T, Snoj M, Sersa G, Miklavcic D. Robustness of treatment planning for electrochemotherapy of deep-seated tumors. *J Membr Biol* 2010; **236:** 147-53.

[72] Granata V, Fusco R, Piccirilo M, Palaia R, Lastoria S, Petrillo A, Izzo F. Feasibility and safety of intraoperative electrochemotherapy in locally advanced pancreatic tumor: a preliminary report. *Int J Surg* 2015; **18:** 230-6.

[73] Soden DM, Larkin JO, Collins CG, Tangney M, Aarons S, Piggott J, Morrissey A, Dunne C, O'Sullivan GC. Successful application of targeted electrochemotherapy using novel flexible electrodes and low dose bleomycin to solid tumours. *Cancer Lett* 2006; **232:** 300-10.

[74] Sersa G, Cufer T, Paulin Kosir S, Cemazar M, Snoj M. Electrochemotherapy of chest wall breast cancer recurrence. *Cancer Treatm Rew* 2011; **38:** 379-86.

[75] Campana LG, Valpione S, Falci C, Mocellini S, Basso M, Corti L, Balestrieri N, Marchet A, Rossi SR. The activity and safety of electrochemotherapy in persistent chest wall recurrence from breast cancer after mastectomy: a phase-II study. *Breast Cancer Res Treat* 2012; **134:**1169-78.

[76] Campana LG, Mali B, Sersa G, Valpione S, Giorgi CA, Strojan P, Miklavcic D, Rosi CR. Electrochemotherapy in non-melanoma head and neck cancers: a retrospective analysis in the treated cases. *Br J Oral Maxillofac Surg* 2014; **52:** 957-64.

[77] Matthiesen LW, Johannesen HH, Hendel HW, Moss T, Kamby C, Gehl J. Electrochemotherapy for large cutaneous recurrences of breast cancer: A phase II clinical study. *Acta Oncol* 2012; **51:** 713-21.

[78] Mahmood F, Gehl J. Optimizing clinical performance and geometrical robustness of a new electrode device for intracranial tumor electroporation. *Bioelectrochemistry* 2011; **81:** 10-6.

[79] Agerholm-Larsen B, Iversen HK, Ibsen P, Moller JM, Mahmood F, Jensen KS, Gehl J. Preclinical validation of electrochemotherapy as an effective treatment for brain tumors. *Cancer Res* 2011; **71(11):** 3753-62.

ACKNOWLEDGEMENT
This research was funded by a research grant from the Research Agency of the Republic of Slovenia and was conducted in the scope of the EBAM European Associated Laboratory (LEA) and resulted from the networking efforts of the COST Action TD1104 (www.electroporation.net).

Gregor Sersa, graduated from the Biotechnical Faculty at the University of Ljubljana in 1978, where he is currently a professor of molecular biology. He is employed at the Institute of Oncology in Ljubljana as Head of the Department of Experimental Oncology. His specific field of interest is the effect of electric field on tumor cells and tumors as drug and gene delivery system in different therapeutic approaches. Besides experimental work, he is actively involved in the education of undergraduate and postgraduate students at the University of Ljubljana.

NOTES

Transport of small molecules and nucleic acids *in vivo* during and after cell electropulsation

Lluis M Mir[1,2]

[1]*Vectorology and Anticancer Therapies, UMR 8203, CNRS, Univ. Paris-Sud, Université Paris-Saclay, Gustave-Roussy, 114,Rue Edouard Vaillant, F-94805 Villejuif Cédex, France* [2]*European Associated Laboratory (LEA) on the pulsed Electric fields in Biology And Medicine (LEA EBAM).*

In vivo tissues electropulsation allows for the transport of drugs inside the cells, as illustrated by the transport of cytotoxic drugs (bleomycin or cisplatin) to cancer cells in tumors treatment by electrochemotherapy. Macromolecules can also be transported in vivo inside the cells thanks to the delivery of electric pulses to the appropriate tissues.

In vivo there are however large differences in the transport of small molecules and large macromolecules (like coding DNAs or RNAs) after tissues electropulsation. One major difference is the bioavailability of these two classes of molecules, impacting even before the delivery of the electric pulses. Indeed, small molecules can be injected systemically, they can distribute in the whole body. Therefore they will easily reach the extracellular fluids of the target tissues and therefore, after the pulses delivery, they will enter the electropermeabilized cells. Biological effects will then be observed if these molecules are pharmacologically active at concentrations compatible with the dose injected systemically and further diluted in the body.

Cell electropermeabilization is of interest only for those molecules for which the cell membrane is an impassable barrier. We termed "nonpermeant molecules" (reference 1) all those molecules. All the nucleic acids, short or long, are nonpermeant. One characteristic of the nonpermeant molecules, shared by the small molecules and nucleic acids, is their hydrophilicity. However, for the small hydrophilic molecules, the hydrophilicity that restricts their crossing of the cell membrane is not sufficient: to be nonpermeant, the small molecules must not be recognized and internalized by a transporter, channel, or receptor system. Reversible cell electropermeabilization allows the uptake of these nonpermeant small molecules into living cells. Of course, reversible cell electropermeabilization will also allow the penetration of "permeant" molecules, but the delivery of the pulses will show no interest in this case. Indeed, because the electropermeabilized state lasts only a few minutes in the best of the cases, the transport during this period will be low compared to (or can even be masked by) the transport of these molecules across the "non-electropermeabilized" membrane. Indeed, in vivo it is not possible to rapidly and efficiently "wash" the tissues: the presence of the molecules in the vicinity of the cells and the uptake of permeant molecules will last much more time than the duration of the permeabilized state (of course depending on the pharmacodynamics of these molecules).

One characteristic that differentiates the small molecules transport from the large macromolecules internalization is the mechanism of membrane crossing. For small molecules, crossing is mainly driven by diffusion through the electropermeabilized membrane. A small contribution due electrophoretic transport during the pulse cannot be excluded if the molecule is charged. Therefore, for the small molecules, the key element is to achieve a good level of cell permeabilization and short pulses are sufficient and appropriate (100 µs pulses). Following the classical diffusion rules (Fick's law), the smaller the molecule the faster the crossing of the membrane and the larger the transport across the membrane even though in vivo, no quantitative study supports directly this assertion. Therefore, large macromolecules have an extremely restricted access to the cell inside by diffusion across the electropermeabilized membrane, like in vitro (experimental data exists that reports, in vitro, the relationship between the molecular weight of the molecules and their uptake by a given strain of cells electropermeabilized under identical experimental conditions [1]).

Concerning the transport of large molecules, the most developed use is the transfer of plasmids. Plasmids, like the other nucleic acids short or long, are heavily charged macromolecules, with one net charge every 300 Daltons of molecular weight. Therefore nucleic acids are easily pulled/pushed by electric forces. Several protocols are used for nucleic acids electrotransfer in vivo. They depend on the tissue (muscle, skin – as presented by Pr V. Preat in this course -, liver, tumors, etc.). If short and limited expression is sought, short pulses (100 µs) can be used. However, in terms of plasmids transfer and level and duration of expression of the electrotransferred genes, the most efficient protocols use pulses of long duration: between 5 to 50 ms duration if only identical pulses of intermediate voltage (150 to 300 V/cm, on the average – [2,3]), or even 100 to 400 ms duration of low voltage (80 – 100 V/cm) if one or several of these pulses are delivered after one short (100 µs) electropermeabilizing pulse – [4,5]). The use of these combinations of pulses has revealed large differences between the tissues [6,7]. The differences between the tissues are due to physiological as well as histological differences between the main cell type of these tissues. One very important difference is the structure of the extracellular matrix of the cells, that is also one of the main differences between the in vitro and in vivo states of the cells, and that may impose the use of these electrophoretic long pulses to facilitate its crossing by large macromolecules like the plasmids.

REFERENCES

[1] Silve and L. M. Mir, Cell electropermeabilisation and small molecules cellular uptake: the electrochemotherapy concept, In "Electroporation in Science and Medicine", Stephen Kee, Edward Lee and Julie Gehl Eds, Springer, New York, 2010, pp 69-82.

[2] M.P. Rols, C. Delteil, M. Golzio, P. Dumond, S. Cros, and J. Teissie, In vivo electrically mediated protein and gene transfer in murine melanoma, Nat. Biotechnol. 16, 168–171, 1998.

[3] L.M. Mir, M.F. Bureau, J. Gehl, R. Rangara, D. Rouy, J.-M. Caillaud, P. Delaere, D. Branellec, B. Schwartz and D. Scherman, High efficiency gene transfer into skeletal muscle mediated by electric pulses, Proceedings of the National Academy of Sciences PNAS USA, 96, 4262-4267, 1999.

[4] S. Šatkauskas, M. F. Bureau, M. Puc, A. Mahfoudi, D. Scherman, D. Miklavcic and L. M. Mir, Mechanisms of in vivo DNA electrotransfer: respective contributions of cell electropermeabilization and DNA electrophoresis, Molecular Therapy, 5, 133-140, 2002.

[5] S. Šatkauskas, F. André, M. F. Bureau, D. Scherman, D. Miklavčič and L. M. Mir, The electrophoretic component of the electric pulses determines the efficacy of in vivo DNA electrotransfer, Human Gene Therapy, 16, 1194-1201, 2005.

[6] F.M. André, J. Gehl, G. Sersa, V. Préat, P. Hojman, J. Eriksen, M. Golzio, M. Cemazar, N. Pavselj, M-P. Rols, D. Miklavcic, J. Teissié, and L.M. Mir, High efficacy of high and low voltage pulse combinations for gene electrotransfer in muscle, liver, tumor and skin, Human Gene Therapy, 19, 1261-1271, 2008.

[7] F.M. André and L.M. Mir, Nucleic acids electrotransfer in vivo: Mechanisms and Practical aspects, Current Gene Therapy 4, 267-280, 2010.Liu MA. DNA vaccines: an historical perspective and view to the future. Immunol Rev. 2011;239(1):62-84. Review

Lluis M. Mir was born in Barcelona, Spain, in 1954. He received a Masters in Biochemistry in 1976 from Ecole Normale Supérieure, Paris, and a Doctorate (D.Sc.) in Cell Biology in 1983. In 1978 he entered CNRS as Attaché de Recherches in the Laboratory of Basic Pharmacology and Toxicology, Toulouse. In 1983 he was promoted to Chargé de Recherches at CNRS, and in 1985 he moved to the Laboratory of Molecular Oncology CNRS-Institute Gustave-Roussy and Univ. Paris Sud, Villejuif). In 1989 he moved to the Laboratory of Molecular Pharmacology (Villejuif), and in 2002 to the Laboratory of Vectorology and Gene Transfer (Villejuif). In 1999, he was promoted to Directeur de Recherches at CNRS.

Lluis M. Mir was one of the pioneers of the research of electropermea-bilization (electroporation) and the applications of this technique for antitumor electrochemotherapy and DNA electrotransfer. He is the author of 193 articles in peer-reviewed journals, 21 chapters in books, and over 500 presentations at national and international meetings, invited lectures at international meetings and seminars. He received the Award for the medical applications of electricity of the Institut Electricité Santé in 1994, the Annual Award of Cancerology of the Ligue contre le Cancer (committee Val-de-Marne) in 1996, and Award of the Research of Rhône-Poulenc-Rorer in 1998 and the medal of the CNFRS under the auspices of the Sciences Academy in 2012. He is an Honorary Senator of the University of Ljubljana (2004). He is also fellow of the American Institute of Biological and Medical Engineering. He has been visiting professor of the Universities of Berkeley (USA), Bielefeld (Germany) and Jerusalem (Israel). He is the director of the laboratory of Vectorology (UMR 8203 of CNRS, Universiy Paris-Sud and Institut Gustave-Roussy), and he is also the founder and co-director of the European Associated Laboratory on Electroporation in Biology and Medicine of the CNRS, the Universities of Ljubljana, Primorska, Toulouse and Limoges, the Institute of Oncology Ljubljana and the Institut Gustave-Roussy

NOTES

Development of devices and electrodes

Damijan Miklavčič, Matej Reberšek
University of Ljubljana, Faculty of Electrical Engineering, Ljubljana, Slovenia

Abstract: Since first reports on electroporation, numerous electroporation based biotechnological and biomedical applications have emerged. The necessary pulse generators are characterized by the shape of the pulses and their characteristics: pulse amplitude and duration. In addition, the electrodes are the important "connection" between the cells/tissue and pulse generator. The geometry of the electrodes together with the cell/tissue sample properties determine the necessary output power and energy that the electroporators need to provide. The choice of electroporator – the pulse generator depends on biotechnological and biomedical application but is inherently linked also to the electrodes choice.

INTRODUCTION

Since first reports on electroporation (both irreversible and reversible), a number of applications has been developed and list of applications which are based on electroporation is still increasing. First pulse generators have been simple in construction and have provided an exponentially decaying pulse of up to several thousands of volts. Also the electrodes were very simple in their design – usually parallel plate electrodes with couple of millimeters distance between them was used, and cells in suspension were placed in-between [1]. Later, new pulse generators were developed which were/are able to provide almost every shape of pulse, and also electrodes which can be bought are extremely diverse [2]–[5]. It is important to note that most often nowadays devices that generate rectangular pulses are being used.

The amplitude of pulses and their duration depend strongly on biotechnological/biomedical application. For electrochemotherapy most often a number of 1000 V pulses of 100 µs duration are needed. For effective gene transfer longer pulses 5-20 ms pulses but of lower amplitude, or a combination of short high- and longer low-voltage pulses are used. For other applications like tissue ablation by means of irreversible electroporation, or liquid-food or water sterilization, thousands of volts pulses are needed. In addition to the pulse amplitude and duration, an important parameter to be taken into account is also the power and energy that need to be provided by the generator.

The energy that needs to be provided is governed by the voltage, current and pulse duration and/or number of pulses. The current if the voltage is set is governed by the load, and this is determined by the geometry of the load, and the load is determined by geometry of the tissue/cell sample and its electrical conductivity. The geometry of the tissue to be exposed to electric pulses are predominantly determined by the shape of the electrodes, the distance between them, depth of electrode penetration/immersion into the sample. Tissue/cell suspension electrical conductivity depends on tissue type or cell sample properties and can be considerably increased while tissue/cells are being exposed to electrical pulses of sufficient amplitude.

Based on the above considerations not a single pulse generator will fit all applications and all needs of a researcher [6]. One can either seek for a specialized pulse generator which will only provide the pulses for this specific biotechnological or biomedical application, or for a general purpose pulse generator which will allow to generate "almost" all what researcher may find interesting in his/her research. Irrespective of the choice, it has to be linked also to the electrodes choice [7]–[9].

THERAPEUTIC AND TECHNOLOGICAL APPLICATIONS OF ELECTROPORATION

Nowadays electroporation is widely used in various biological, medical, and biotechnological applications [10]–[13]. Tissue ablation relying on irreversible electroporation is less than a decade old, but its efficacy is promising especially in treating non-malignant tissue, in the field of water treatment where efficacy of chemical treatment is enhanced with electroporation, in food preservation where electroporation has proven, in some cases, to be as effective as pasteurization [14]. In contrast, applications based on reversible electroporation are currently more widespread and established in different experimental and/or practical protocols. Probably the most important of them is the introduction of definite amount of small or large molecules to cytoplasm through the plasma membrane. Furthermore, slight variation of electric field parameters results in an application where molecules can be directly inserted into the plasma membrane or cells can be effectively fused.

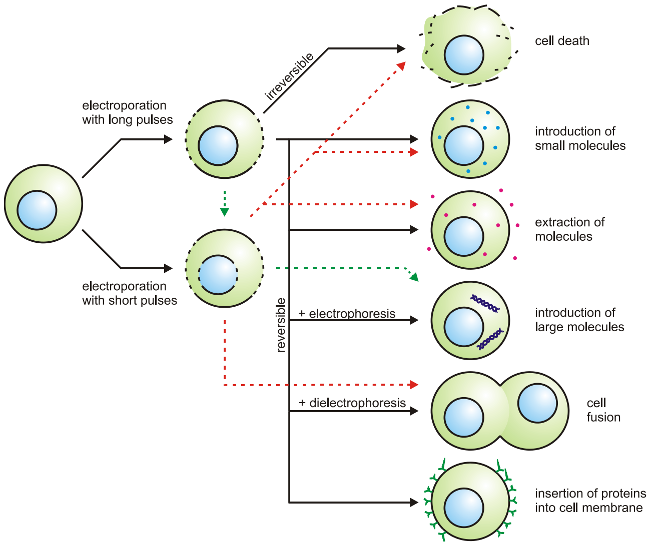

Figure 1: Exposure of a cell to an electric field may result either in permeabilization of cell membrane or its destruction. In this process the electric field parameters play a major role. If these parameters are within certain range, the permeabilization is reversible; therefore it can be used in applications such as introduction of small or large molecules into the cytoplasm, insertion of proteins into cell membrane or cell fusion.

ELECTROCHEMOTHERAPY

The most representative application of delivery of small molecules through electroporated membrane is electrochemotherapy. It was demonstrated in several preclinical and clinical studies, both on humans and animals, that electrochemotherapy can be used as treatment of choice in local cancer treatment [15], [16]. Most often a number of short rectangular 100 µs long pulses with amplitudes up to 1000 V, are applied. Number of pulses that are usualy delivered is 8. These can be delivered at pulse repetition frequency of 1 Hz or 5 kHz [17]. New technological developments were made available for in treating deep seated tumours, where 3000 V, 50 A and 100 µs pulses are being delivered [18]. Recent advances in treating liver metastasis, bone metastasis and soft tissue sarcoma have been reported [19], [20].

TISSUE ABLATION BY NON-THERMAL IREVERSIBLE ELECTROPORATION

The ablation of undesirable tissue through the use of irreversible electroporation has recently been suggested as a minimally invasive method for tumor removal but could also be used in cardiac tissue ablation instead of RF heating tissue ablation or other tissue ablation techniques [11], [21]. Smilarly as in electrochemotherapy pulses of 50 or 100 µs with amplitudes up to 3000 V are used. The number of pulses delivered to the target tissue is however considerably higher. If in electrochemotherapy 8 pulses are delivered, here 96 pulses are used. Pulse repetition frequency needs to be low 1 or 4 Hz in order to avoid excessive heating [22].

GENE ELECTROTRANSFER

Exogenous genetic material can be delivered to cells by using non-viral methods such as electropermeabilization. Electrotransfection can be achieved using: exponentially decaying pulses; square wave pulses with superimposed RF signals; or only long square wave pulses up 20 ms and with amplitudes ranging from 200 to 400 V [23]. Although no consensus can be reached, it can however be stated that longer pulses are generally used in gene transfection than in electrochemotherapy. Furthermore, two distinct roles of electric pulses were described. In experiments where several short high voltage pulses (e.g. 8 × 100 µs of 1000 V) were followed by long low voltage pulses (e.g. 1 × 100 ms of 80 V) [24]. It was demonstrated that short high voltage pulses are permeabilizing the membrane while the longer lower voltage pulses have an electrophoretic effect on DNA itself facilitating interaction of plasmid with the membrane [25]. Skin can be an excellent target for gene transfer protocols due to its accessibility [26].

ELECTROFUSION

So far we have presented applications of electroporation that are used to introduce different molecules either to the cytosol or to the cell plasma membrane. But electroporation of cell plasma membrane can also result in fusion of cells. This process has been termed electrofusion. First reports of *in vitro* electrofusion of cells date back into 1980s. In the reports it has been shown that fusion between two cells can proceed only if the cells are in contact prior or immediately after electroporation. The contact between the cells can be achieved either by dielectrophoretic connection of neighboring cells, which is followed by electroporation or by centrifugation of cell suspension after exposure to electric field. In both cases cells must be reversibly permeabilized, otherwise they lose viability and there is no electrofusion [27]. Electrofusion in *in vitro* environment is possible due to high possibility of cell movement while cells in tissues are more or less fixed, nevertheless *in vivo* electrofusion has been observed in B16 melanoma tumors as well as cells to tissue fusion. Electrofusion of cells of different sizes can be achieved by nanosecond pulsed electric fields [28].

ELECTROEXTRACTION

Electroporation can be used to extract substances (e.g. juice, sugar, pigments, lipid and proteins) from biological tissue or cells (e.g. fruits, sugar beets, microalgae, wine and yeast). Electroextraction can be more energy and extraction efficient, and faster than classical extraction methods (pressure, thermal denaturation and fermentation) [29]–[33].

ELECTRO- PASTEURIZATION AND STERILIZATION

Irreversible electroporation can be used in applications where permanent destruction of microorganisms is required, i.e. food processing and water treatment [34]. Still, using irreversible electroporation in these applications means that substance under treatment is exposed to a limited electric field since it is desirable that changes in treated substance do not occur (e.g. change of food flavor) and that no by-products emerge due to electric field exposure (e.g. by-products caused by electrolysis). This is one of the reasons why short (in comparison to medical applications) in the range of 1-3 µs are used. Especially industrial scale batch or flowthrough exposure systems may require huge power generators with amplitudes up to 40 kV and peak currents up to 500 A. Although batch and flow-through processes are both found on industrial scale, flow-through is preferred. Such mode of operation requires constant operation requiring higher output power of pulse generators [12], [35].

ELECTRIC FIELD DISTRIBUTION *IN VIVO*

In most applications of tissue permeabilization it is required to expose the volume of tissue to E intensities between the two "thresholds" i.e. to choose in advance a suitable electrode configuration and pulse parameters for the effective tissue electroporation [36]. Therefore electric field distribution in tissue has to be estimated before the treatment, which can be achieved by combining results of rapid tests or *in situ* monitoring [37] with models of electric field distribution [38]–[42]. However, modeling of electric field distribution in tissue is demanding due to heterogeneous tissue properties and usually complex geometry. Analytical models can be employed only for simple geometries. Usually they are developed for 2D problems and tissue with homogenous electrical properties. Therefore in most cases numerical modeling techniques are still more acceptable as they can be used for modeling 3D geometries and complex tissue properties. For that purpose mostly finite element method and finite difference method are applied. Both numerical methods have been successfully applied and validated by comparison of computed and measured electric field distribution. Furthermore, advanced numerical models were build, which take into consideration also tissue conductivity increase due to tissue or cell electroporation. These advanced models describe E distribution as a function of conductivity σ(E). In this way models represent electroporation tissue conductivity changes according to distribution of electric field intensities [43].

ELECTRODES FOR IN VITRO AND IN VIVO APPLICATIONS

Effectiveness of electroporation in *in vitro*, *in vivo* or clinical environment depends on the distribution of electric field inside the treated sample. Namely, the most important parameter governing cell membrane permeabilization is local electric field [36]. To achieve this we have to use an appropriate set of electrodes and an electroporation device – electroporator that generates required voltage or current signals. Although both parts of the mentioned equipment are important and necessary for effective electroporation, electroporator has a substantially more important role since it has to be able to deliver the required signal to its output loaded by impedance of the sample between electrodes.

Nowadays there are numerous types of electrodes that can be used for electroporation in any of the existing applications [44]–[47]. According to the geometry, electrodes can be classified into several groups, i.e. parallel plate electrodes, needle arrays, wire electrodes, tweezers electrodes, coaxial electrodes, etc (Fig. 2). Each group comprises several types of electrodes that can be further divided according to the applications, dimensions, electrode material etc. In any case selection of electrode type plays an important role in characterization of the load that is connected to the output of the electroporator. During the design of the electroporator load characterization represents the starting point and greatest engineering problem, because electrical characteristics of substance between electrodes (e.g. cell suspension, tissue, etc.) vary from experiment to experiment and even during the course of experiment. In general the load between electrodes has both a resistive and a capacitive component. The value of each component is defined by geometry and material of electrodes and by electrical and chemical properties of the treated sample. In *in vitro* conditions these parameters that influence the impedance of the load can be well controlled since size and geometry of sample are known especially if cuvettes are used. Furthermore, by using specially prepared cell media, electrical and chemical properties are defined or can be measured. On the other hand, in *in vivo* conditions, size and geometry can still be controlled to a certain extent but electrical and chemical properties can only be estimated, especially if needle electrodes are used that penetrate through different tissues. However, even if we manage to reliably define these properties during the development of the device, it is practically impossible to predict changes in the electrical and chemical properties of the sample due to exposure to high-voltage electric pulses [48]. Besides electropermeabilization of cell membranes which increases electrical conductivity of the sample, electric pulses also cause side effects like Joule heating and electrolytic contamination of the sample, which further leads to increased sample conductivity [49].

ELECTRIC PULSES

For better understanding and critical reading of various reports on electroporation phenomenon and electroporation based applications, complete disclosure of pulse parameters needs to be given. Electric pulses are never “square” or “rectangular”, but they are characterized by their rise time, duration/width, fall time, pulse repetition frequency. Rise time and fall time are determined as time needed to rise from 10% to 90% of the amplitude, drop from 90% to 10% of amplitude, respectively. Pulse width is most often defined as time between 50% amplitude on the rise and 50% amplitude on the fall. Pulse repetition frequency is the inverse of the sum of pulse width and pause between two consecutive pulses. These may seem trivial when discussing pulses of 11 ms, but become an issue when discussing ns or even ps pulses [50], [51]. The cell membrane damage and uptake of ions is significantly reduced when using bipolar ns pulses instead of monopolar [52]. Shapes other than “rectangular” have been investigated with respect to electroporation efficiency [53]. It was suggested exposure of cells to pulse amplitudes above given critical amplitude and duration of exposure to this above critical value seem to be determining level of membrane electroporation irrespective of pulse shape. Exponentially decaying pulses are difficult to be considered as such but were predominantly used in 80s for gene electrotransfer. Their shape was convenient as the first peak part of the pulses acts as the permeabilizing part, and the tail of the pulse acts as electrophoretic part pushing DNA as towards and potentially through the cell membrane [24].

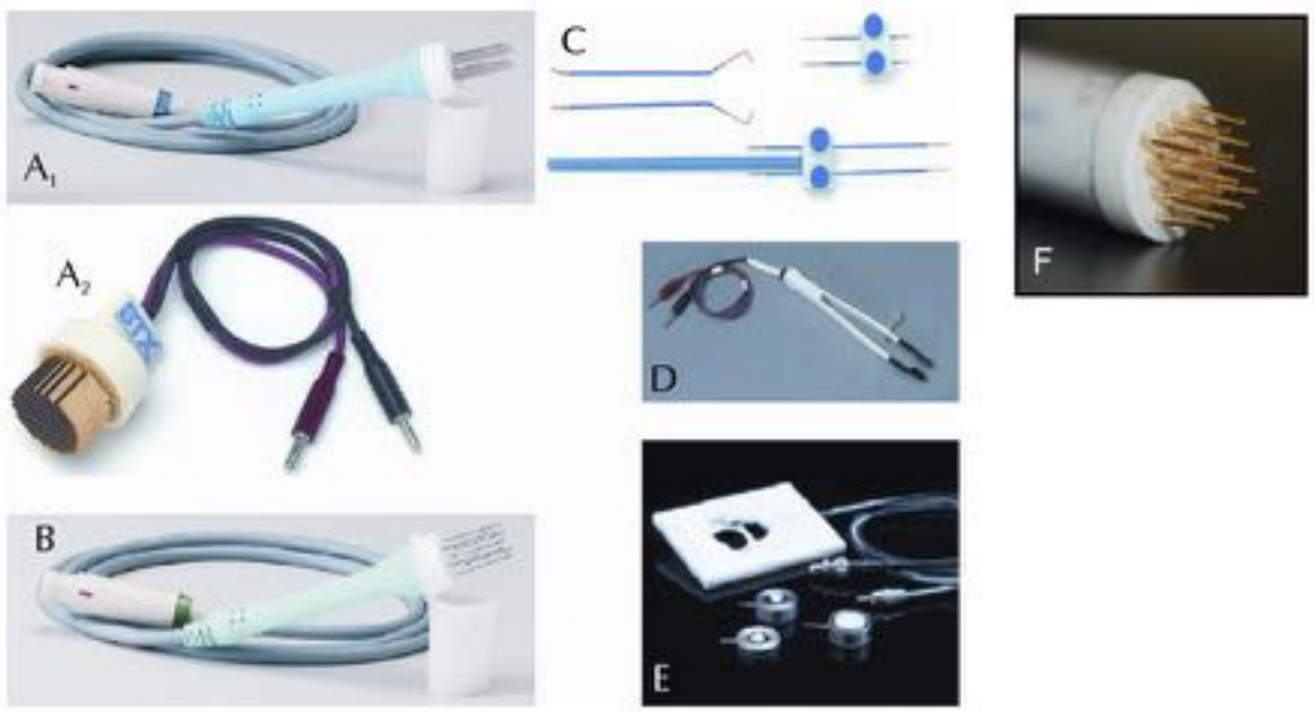

Figure 2: Examples of commercially available electrode for electropermeabilization. Electrodes belong to the following group: A_1 and A_2 –parallel plate electrodes, B – needle arrays, C – wire electrodes, D – tweezers electrodes, E – coaxial electrodes and F – multiple electrodes array. Electrodes A_1 and B are produced by IGEA, Italy and are used for clinical applications of electrochemotherapy and electrotransfection. Electrodes A_2, C and E are used for different in vitro applications and are produced by: E – Cyto Pulse Sciences, U.S.A.; A_2, C and also D that are used for in vivo applications, are produced by BTX Hardware division, U.S.A, F are used for skin gene electrotransfer [26].

ELECTROPORATORS – THE NECESSARY PULSE GENERATORS

Electroporator is an electronic device that generates signals, usually square wave or exponentially decaying pulses, required for electroporation [54]. Parameters of the signal delivered to electrodes with the treated sample vary from application to application. Therefore, in investigating of electroporation phenomenon and development of electroporation based technologies and tretaments it is important that electroporator is able to deliver signals with the widest possible range of electrical parameters if used in research. If however used for a specific application only, e.g. clinical treatment such as electrochemotherapy, pulse generator has to provide exactly required pulse parameters in a reliable manner. Moreover, electroporator must be safe and easy to operate and should offer some possibilities of functional improvements. Clinical electroporators used in electrochemotherapy of deep-seated tumors or in non-thermal tissue ablation are also equipped with ECG synchronization algorithms which minimasizes possible influence of electric pulse delivery on heart function [55].

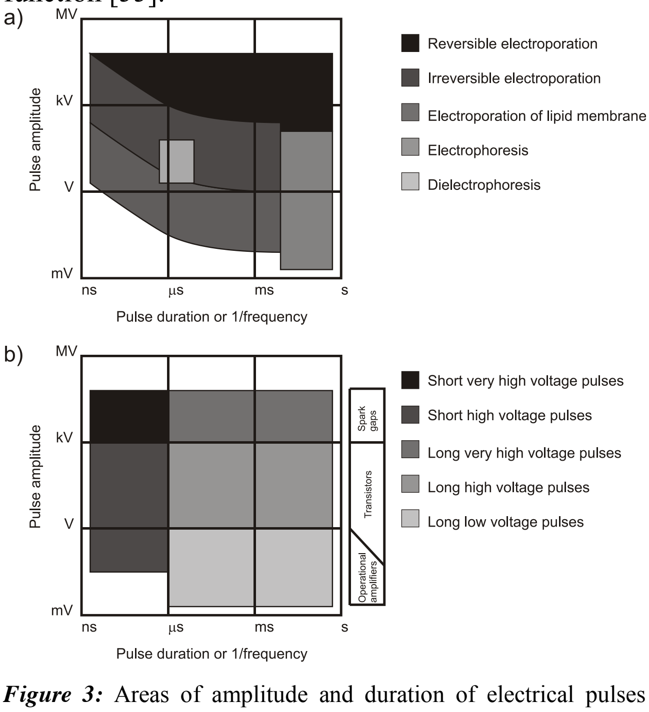

Figure 3: Areas of amplitude and duration of electrical pulses which are used in the research of electroporation and related effects (a). Five different areas of electroporation pulse generation (b). To amplify or to generate very-high-voltage electroporation pulses (over a few kV) spark gaps and similar elements are used, for high-voltage (a few V to a few kV) transistors and for low-voltage operational amplifiers are used. Nanosecond (short) pulses are generated with different techniques than pulses longer than 1 µs. Originally published in Advanced electroporation techniques in biology and medicine by Reberšek and Miklavčič 2010 [3].

In principle, electroporators can be divided in several groups depending on biological applications, but from the electrical point of view only two types of electroporators exist: devices with voltage output (output is voltage signal U(t)) and devices with current output (output is current signal I(t)). Both types of devices have their advantages and disadvantages, but one point definitely speaks in favor of devices with voltage output. For example, if we perform *in vitro* experiments with parallel plate electrodes with plate sides substantially larger than the distance between them, the electric field strength E that is applied to the sample can be approximated by the voltage-to-distance ratio U/d, where d is the electrode distance and U the amplitude of applied signal obtained from an electroporator with voltage output. On the other hand, if an electroporator with current output is used, the same approximation could be used only if additional measurement of voltage difference between electrodes is performed or if the impedance Z of the sample is known, measured or approximated and voltage difference between electrodes is estimated using Ohm's law $U = I \cdot Z$. Nevertheless, there are several commercially available electroporator that fulfill different ranges of parameters and can be used in different applications. A list of commercially available electrodes and electroporators has been presented in 2004 by Puc and colleagues [56] and updated in 2010 [3] in a manuscripts that describe techniques of signal generation required for cell/tissue electropermeabilization.

To be sure the applied pulses are adequate we have to measure the applied voltage and current during the pulse delivery.

In nanosecond applications rise time of the pulse is sometimes shorter than the electrical length (the time in which an electrical signal travels through the line) between the source and the load. In this case, the impedance of the load and the transmission line has to match the impedance of the generator, so that there are no strong pulse reflections and consequently pulse prolongations.

Based on the studies reported in the literature it is very difficult to extract a general advice how to design experiments or treatments with electroporation. In principle we can say that pulse amplitude (voltage-to-distance ratio) should typically be in the range from 200 V/cm up to 2000 V/cm. Pulse durations should be in the range of hundreds of microseconds for smaller molecules and from several milliseconds up to several tens of milliseconds for macromolecules such as plasmid DNA (in the latter case, due to the very long pulse duration, optimal pulse amplitude can even be lower than 100 V/cm). If there is any possibility to obtain the equipment that generates bipolar pulses or have a possibility to change electric field orientation in the sample, these types of pulses/electroporators should be used because bipolar pulses yield a lower poration threshold, higher uptake, reduce electrolyte wear and electrolytic contamination of the sample, and an unaffected viability compared to unipolar pulses of the same amplitude and duration. Better permeabilisation or gene transfection efficiency and survival can also be obtained by changing field orientation in the sample using special commutation circuits that commute electroporation pulses between the electrodes [44], [46], [57].

This general overview of electrical parameters should however only be considered as a starting point for a design of experiments or treatments. Optimal values of parameters namely also strongly depend on the cell type used, on the molecule to be introduced, and on specific experimental conditions. The pulse characteristics determined as optimal or at least efficient and the tissue/sample will than determine the architecture of the pulse generator, whether it will be a Marx generator, Blumlein, or... [6].

CONCLUSIONS

Electroporation has been studied extensively until now, and a number of applications has been developed. Electrochemotherapy has been demonstrated as an effective local treatment of solid tumors and is the most mature therapeutic application right now. Electroporation for gene transfection however has been long used in *in vitro* situation. With a hold on viral vectors electroporation represents a viable non-viral alternative also for *in vivo* gene transfection. Clinical applications and expansion of electrochemotherapy and tissue ablation have been hindered by the lack of adequate electroporators and their certification in Europe (CE Medical Device) and limited approval by FDA in USA [54]. Cliniporator (IGEA, s.r.l. Carpi, Italy) was certified in EU (CE mark) as a medical device and is offered on the market along with standard operating procedures for electrochemotherapy of cutaneous and subcutaneous tumors. NanoKnife (AngioDynamics, Queensbury, USA) was certified in EU and approved by the FDA for surgical ablation of soft tissue, including cardiac and smooth muscle. Some electroporators are now available under the license for clinical evaluation purpuses: Cellectra, Elgen, Medpulser, Cliniporator VITAE, BetaTech, DermaVax, EasyVax, Ellisphere, TriGrid [4].

Development of new applications warrants further development of pulse generators and electrodes. Based on the above considerations however, a single pulse generator will not fit all applications and all needs of researchers. One can either seek for a specialized pulse generator which will only provide the pulses for his/her specific biotechnological or biomedical application, or for a general purpose pulse generator which will allow to generate “almost” all what researcher may find interesting/necessary in his/her research. Irrespective of the choice, this has to be linked also to the electrodes choice and tissue/sample conductivity.

REFERENCES

[1] M. Reberšek, D. Miklavčič, C. Bertacchini, and M. Sack, “Cell membrane electroporation-Part 3: the equipment,” *Electr. Insul. Mag. IEEE*, vol. 30, no. 3, pp. 8–18, 2014.

[2] K. Flisar, M. Puc, T. Kotnik, and D. Miklavcic, “Cell membrane electropermeabilization with arbitrary pulse waveforms,” *IEEE Eng. Med. Biol. Mag. Q. Mag. Eng. Med. Biol. Soc.*, vol. 22, no. 1, pp. 77–81, Feb. 2003.

[3] M. Reberšek and D. Miklavčič, “Concepts of Electroporation Pulse Generation and Overview of Electric Pulse Generators for Cell and Tissue Electroporation,” in *Advanced Electroporation Techniques in Biology and Medicine*, A. G. Pakhomov, D. Miklavčič, and M. S. Markov, Eds. Boca Raton: CRC Press, 2010, pp. 323–339.

[4] L. G. Staal and R. Gilbert, “Generators and Applicators: Equipment for Electroporation,” in *Clinical Aspects of Electroporation*, S. T. Kee, J. Gehl, and E. W. Lee, Eds. New York: Springer, 2011, pp. 45–65.

[5] G. A. Hofmann, “Instrumentation and electrodes for in vivo electroporation,” in *Electrochemotherapy, Electrogenetherapy, and Transdermal Drug Delivery*, M. J. Jaroszeski, R. Heller, and R. Gilbert, Eds. Totowa: Humana Press, 2000, pp. 37–61.

[6] M. Reberšek and D. Miklavčič, “Advantages and Disadvantages of Different Concepts of Electroporation Pulse Generation,” *Automatika*, vol. 52, no. 1, pp. 12–19, Mar. 2011.

[7] M. Reberšek, C. Faurie, M. Kandušer, S. Čorović, J. Teissié, M.-P. Rols, and D. Miklavčič, “Electroporator with automatic change of electric field direction improves gene electrotransfer in-vitro,” *Biomed. Eng. Online*, vol. 6, p. 25, 2007.

[8] P. Kramar, D. Miklavcic, and A. M. Lebar, “A system for the determination of planar lipid bilayer breakdown voltage and its applications,” *NanoBioscience IEEE Trans. On*, vol. 8, no. 2, pp. 132–138, 2009.

[9] J. M. Sanders, A. Kuthi, Yu-Hsuan Wu, P. T. Vernier, and M. A. Gundersen, “A linear, single-stage, nanosecond pulse generator for delivering intense electric fields to biological loads,” *IEEE Trans. Dielectr. Electr. Insul.*, vol. 16, no. 4, pp. 1048–1054, Aug. 2009.

[10] S. Haberl, J. Teissié, W. Frey, and D. Miklavčič, “Cell Membrane Electroporation – Part 2: The Applications,” *IEEE Electr. Insul. Mag.*, vol. 29, no. 1, pp. 19–27, Feb. 2013.

[11] C. Jiang, R. V. Davalos, and J. C. Bischof, “A Review of Basic to Clinical Studies of Irreversible Electroporation Therapy,” *IEEE Trans. Biomed. Eng.*, vol. 62, no. 1, pp. 4–20, Jan. 2015.

[12] S. Mahnič-Kalamiza, E. Vorobiev, and D. Miklavčič, "Electroporation in Food Processing and Biorefinery," *J. Membr. Biol.*, vol. 247, no. 12, pp. 1279–1304, Dec. 2014.

[13] M. L. Yarmush, A. Golberg, G. Serša, T. Kotnik, and D. Miklavčič, "Electroporation-Based Technologies for Medicine: Principles, Applications, and Challenges," *Annu. Rev. Biomed. Eng.*, vol. 16, no. 1, pp. 295–320, Jul. 2014.

[14] M. Morales-de la Peña, P. Elez-Martínez, and O. Martín-Belloso, "Food Preservation by Pulsed Electric Fields: An Engineering Perspective," *Food Eng. Rev.*, vol. 3, no. 2, pp. 94–107, Mar. 2011.

[15] D. Miklavčič, B. Mali, B. Kos, R. Heller, and G. Serša, "Electrochemotherapy: from the drawing board into medical practice," *Biomed. Eng. Online*, vol. 13, no. 1, p. 29, 2014.

[16] D. E. Spratt, E. A. Gordon Spratt, S. Wu, A. DeRosa, N. Y. Lee, M. E. Lacouture, and C. A. Barker, "Efficacy of Skin-Directed Therapy for Cutaneous Metastases From Advanced Cancer: A Meta-Analysis," *J. Clin. Oncol.*, vol. 32, no. 28, pp. 3144–3155, Oct. 2014.

[17] B. Mali, T. Jarm, M. Snoj, G. Sersa, and D. Miklavcic, "Antitumor effectiveness of electrochemotherapy: A systematic review and meta-analysis," *Eur. J. Surg. Oncol. EJSO*, vol. 39, no. 1, pp. 4–16, Jan. 2013.

[18] C. Bertacchini, P. M. Margotti, E. Bergamini, A. Lodi, M. Ronchetti, and R. Cadossi, "Design of an irreversible electroporation system for clinical use," *Technol. Cancer Res. Treat.*, vol. 6, no. 4, pp. 313–320, Aug. 2007.

[19] D. Miklavčič, G. Serša, E. Brecelj, J. Gehl, D. Soden, G. Bianchi, P. Ruggieri, C. R. Rossi, L. G. Campana, and T. Jarm, "Electrochemotherapy: technological advancements for efficient electroporation-based treatment of internal tumors," *Med. Biol. Eng. Comput.*, vol. 50, no. 12, pp. 1213–1225, Dec. 2012.

[20] I. Edhemovic, E. Brecelj, G. Gasljevic, M. Marolt Music, V. Gorjup, B. Mali, T. Jarm, B. Kos, D. Pavliha, B. Grcar Kuzmanov, M. Cemazar, M. Snoj, D. Miklavcic, E. M. Gadzijev, and G. Sersa, "Intraoperative electrochemotherapy of colorectal liver metastases: Electrochemotherapy of Liver Metastases," *J. Surg. Oncol.*, vol. 110, no. 3, pp. 320–327, Sep. 2014.

[21] J. Lavee, G. Onik, P. Mikus, and B. Rubinsky, "A novel nonthermal energy source for surgical epicardial atrial ablation: irreversible electroporation," *Heart Surg. Forum*, vol. 10, no. 2, pp. E162–167, 2007.

[22] R. E. Neal, P. A. Garcia, J. L. Robertson, and R. V. Davalos, "Experimental Characterization and Numerical Modeling of Tissue Electrical Conductivity during Pulsed Electric Fields for Irreversible Electroporation Treatment Planning," *IEEE Trans. Biomed. Eng.*, vol. 59, no. 4, pp. 1076–1085, Apr. 2012.

[23] A. Gothelf and J. Gehl, "What you always needed to know about electroporation based DNA vaccines," *Hum. Vaccines Immunother.*, vol. 8, no. 11, pp. 1694–1702, Nov. 2012.

[24] S. Satkauskas, M. F. Bureau, M. Puc, A. Mahfoudi, D. Scherman, D. Miklavcic, and L. M. Mir, "Mechanisms of in vivo DNA electrotransfer: respective contributions of cell electropermeabilization and DNA electrophoresis," *Mol. Ther. J. Am. Soc. Gene Ther.*, vol. 5, no. 2, pp. 133–140, Feb. 2002.

[25] M. Kandušer, D. Miklavčič, and M. Pavlin, "Mechanisms involved in gene electrotransfer using high- and low-voltage pulses — An in vitro study," *Bioelectrochemistry*, vol. 74, no. 2, pp. 265–271, Feb. 2009.

[26] R. Heller, Y. Cruz, L. C. Heller, R. A. Gilbert, and M. J. Jaroszeski, "Electrically mediated delivery of plasmid DNA to the skin, using a multielectrode array," *Hum. Gene Ther.*, vol. 21, no. 3, pp. 357–362, Mar. 2010.

[27] M. Usaj, K. Flisar, D. Miklavcic, and M. Kanduser, "Electrofusion of B16-F1 and CHO cells: The comparison of the pulse first and contact first protocols," *Bioelectrochemistry*, vol. 89, pp. 34–41, Feb. 2013.

[28] L. Rems, M. Ušaj, M. Kandušer, M. Reberšek, D. Miklavčič, and G. Pucihar, "Cell electrofusion using nanosecond electric pulses," *Sci. Rep.*, vol. 3, Nov. 2013.

[29] M. Zakhartsev, C. Momeu, and V. Ganeva, "High-Throughput Liberation of Water-Soluble Yeast Content by Irreversible Electropermeation (HT-irEP)," *J. Biomol. Screen.*, vol. 12, no. 2, pp. 267–275, Jan. 2007.

[30] M. Sack, C. Eing, T. Berghofe, L. Buth, R. Stangle, W. Frey, and H. Bluhm, "Electroporation-Assisted Dewatering as an Alternative Method for Drying Plants," *IEEE Trans. Plasma Sci.*, vol. 36, no. 5, pp. 2577–2585, Oct. 2008.

[31] M. Sack, J. Sigler, S. Frenzel, C. Eing, J. Arnold, T. Michelberger, W. Frey, F. Attmann, L. Stukenbrock, and G. Müller, "Research on Industrial-Scale Electroporation Devices Fostering the Extraction of Substances from Biological Tissue," *Food Eng. Rev.*, vol. 2, pp. 147–156, Mar. 2010.

[32] E. Puértolas, G. Saldaña, S. Condón, I. Álvarez, and J. Raso, "Evolution of polyphenolic compounds in red wine from Cabernet Sauvignon grapes processed by pulsed electric fields during aging in bottle," *Food Chem.*, vol. 119, no. 3, pp. 1063–1070, Apr. 2010.

[33] S. Haberl, M. Jarc, A. Štrancar, M. Peterka, D. Hodžić, and D. Miklavčič, "Comparison of Alkaline Lysis with Electroextraction and Optimization of Electric Pulses to Extract Plasmid DNA from Escherichia coli," *J. Membr. Biol.*, Jul. 2013.

[34] J. R. Beveridge, S. J. MacGregor, L. Marsili, J. G. Anderson, N. J. Rowan, and O. Farish, "Comparison of the effectiveness of biphase and monophase rectangular pulses for the inactivation of micro-organisms using pulsed electric fields," *IEEE Trans. Plasma Sci.*, vol. 30, no. 4, pp. 1525–1531, Aug. 2002.

[35] S. Toepfl, "Pulsed electric field food processing industrial equipment design and commercial applications," *Stewart Postharvest Rev.*, vol. 8, no. 2, pp. 1–7, 2012.

[36] T. Kotnik, P. Kramar, G. Pucihar, D. Miklavcic, and M. Tarek, "Cell membrane electroporation- Part 1: The phenomenon," *IEEE Electr. Insul. Mag.*, vol. 28, no. 5, pp. 14–23, Oct. 2012.

[37] M. Kranjc, B. Markelc, F. Bajd, M. Čemažar, I. Serša, T. Blagus, and D. Miklavčič, "In Situ Monitoring of Electric Field Distribution in Mouse Tumor during Electroporation," *Radiology*, vol. 274, no. 1, pp. 115–123, Jan. 2015.

[38] D. Miklavcic, K. Beravs, D. Semrov, M. Cemazar, F. Demsar, and G. Sersa, "The importance of electric field distribution for effective in vivo electroporation of tissues.," *Biophys. J.*, vol. 74, no. 5, pp. 2152–2158, May 1998.

[39] N. Pavselj, Z. Bregar, D. Cukjati, D. Batiuskaite, L. M. Mir, and D. Miklavcic, "The Course of Tissue Permeabilization Studied on a Mathematical Model of a Subcutaneous Tumor in Small Animals," *IEEE Trans. Biomed. Eng.*, vol. 52, no. 8, pp. 1373–1381, Aug. 2005.

[40] D. Sel, D. Cukjati, D. Batiuskaite, T. Slivnik, L. M. Mir, and D. Miklavcic, "Sequential Finite Element Model of Tissue

Electropermeabilization," *IEEE Trans. Biomed. Eng.*, vol. 52, no. 5, pp. 816–827, May 2005.
[41] D. Miklavcic, S. Corovic, G. Pucihar, and N. Pavselj, "Importance of tumour coverage by sufficiently high local electric field for effective electrochemotherapy," *Eur. J. Cancer Suppl.*, vol. 4, no. 11, pp. 45–51, Nov. 2006.
[42] D. Miklavcic, M. Snoj, A. Zupanic, B. Kos, M. Cemazar, M. Kropivnik, M. Bracko, T. Pecnik, E. Gadzijev, and G. Sersa, "Towards treatment planning and treatment of deep-seated solid tumors by electrochemotherapy," *Biomed Eng Online*, vol. 9, no. 10, pp. 1–12, 2010.
[43] S. Corovic, I. Lackovic, P. Sustaric, T. Sustar, T. Rodic, and D. Miklavcic, "Modeling of electric field distribution in tissues during electroporation," *Biomed. Eng. Online*, vol. 12, no. 1, p. 16, 2013.
[44] R. A. Gilbert, M. J. Jaroszeski, and R. Heller, "Novel electrode designs for electrochemotherapy," *Biochim. Biophys. Acta*, vol. 1334, no. 1, pp. 9–14, Feb. 1997.
[45] S. Mazères, D. Sel, M. Golzio, G. Pucihar, Y. Tamzali, D. Miklavcic, and J. Teissié, "Non invasive contact electrodes for in vivo localized cutaneous electropulsation and associated drug and nucleic acid delivery," *J. Control. Release Off. J. Control. Release Soc.*, vol. 134, no. 2, pp. 125–131, Mar. 2009.
[46] M. Reberšek, S. Čorović, G. Serša, and D. Miklavčič, "Electrode commutation sequence for honeycomb arrangement of electrodes in electrochemotherapy and corresponding electric field distribution," *Bioelectrochemistry*, vol. 74, no. 1, pp. 26–31, Nov. 2008.
[47] J. Čemažar, D. Miklavčič, and T. Kotnik, "Microfluidic devices for manipulation, modification and characterization of biological cells in electric fields - a review," *Inf. MIDEM*, vol. 43, no. 3, pp. 143–161, Sep. 2013.
[48] M. Pavlin, M. Kandušer, M. Reberšek, G. Pucihar, F. X. Hart, R. Magjarević, and D. Miklavčič, "Effect of Cell Electroporation on the Conductivity of a Cell Suspension," *Biophys. J.*, vol. 88, no. 6, pp. 4378–4390, Jun. 2005.
[49] I. Lackovic, R. Magjarevic, and D. Miklavcic, "Three-dimensional finite-element analysis of joule heating in electrochemotherapy and in vivo gene electrotransfer," *Dielectr. Electr. Insul. IEEE Trans. On*, vol. 16, no. 5, pp. 1338–1347, 2009.
[50] O. N. Pakhomova, B. W. Gregory, V. A. Khorokhorina, A. M. Bowman, S. Xiao, and A. G. Pakhomov, "Electroporation-Induced Electrosensitization," *PLoS ONE*, vol. 6, no. 2, p. e17100, Feb. 2011.
[51] K. Mitsutake, A. Satoh, S. Mine, K. Abe, S. Katsuki, and H. Akiyama, "Effect of pulsing sequence of nanosecond pulsed electric fields on viability of HeLa S3 cells," *Dielectr. Electr. Insul. IEEE Trans. On*, vol. 19, no. 1, pp. 337–342, 2012.
[52] B. L. Ibey, J. C. Ullery, O. N. Pakhomova, C. C. Roth, I. Semenov, H. T. Beier, M. Tarango, S. Xiao, K. H. Schoenbach, and A. G. Pakhomov, "Bipolar nanosecond electric pulses are less efficient at electropermeabilization and killing cells than monopolar pulses," *Biochem. Biophys. Res. Commun.*, vol. 443, no. 2, pp. 568–573, Jan. 2014.
[53] T. Kotnik, D. Miklavčič, and L. M. Mir, "Cell membrane electropermeabilization by symmetrical bipolar rectangular pulses: Part II. Reduced electrolytic contamination," *Bioelectrochemistry*, vol. 54, no. 1, pp. 91–95, Aug. 2001.
[54] M. Reberšek, C. Bertacchini, M. Sack, and D. Miklavčič, "Cell Membrane Electroporation – Part 3: The Equipment," *IEEE Electr. Insul. Mag.*, In press.
[55] B. Mali, V. Gorjup, I. Edhemovic, E. Brecelj, M. Cemazar, G. Sersa, B. Strazisar, D. Miklavcic, and T. Jarm, "Electrochemotherapy of colorectal liver metastases-an observational study of its effects on the electrocardiogram," *Biomed. Eng. Online*, vol. 14, no. Suppl 3, p. S5, 2015.
[56] M. Puc, S. Čorović, K. Flisar, M. Petkovšek, J. Nastran, and D. Miklavčič, "Techniques of signal generation required for electropermeabilization: Survey of electropermeabilization devices," *Bioelectrochemistry*, vol. 64, no. 2, pp. 113–124, Sep. 2004.
[57] M. Reberšek, M. Kandušer, and D. Miklavčič, "Pipette tip with integrated electrodes for gene electrotransfer of cells in suspension: a feasibility study in CHO cells," *Radiol. Oncol.*, vol. 45, no. 3, pp. 204–208, 2011.

ACKNOWLEDGEMENT
This research was in part supported by Slovenian Research Agency, and by Framework Programs of European Commission through various grants. Research was conducted in the scope of the EBAM European Associated Laboratory (LEA)

Damijan Miklavčič was born in Ljubljana, Slovenia, in 1963. He received a Masters and a Doctoral degree in Electrical Engineering from University of Ljubljana in 1991 and 1993, respectively. He is currently Professor and the Head of the Laboratory of Biocybernetics at the Faculty of Electrical Engineering, University of Ljubljana..

His research areas are biomedical engineering and study of the interaction of electromagnetic fields with biological systems. In the last years he has focused on the engineering aspects of electroporation as the basis of drug delivery into cells in tumor models *in vitro* and *in vivo*. His research includes biological experimentation, numerical modeling and hardware development for electrochemotherapy, irreversible electroporation and gene electrotransfer.

Matej Reberšek, was born in Ljubljana, Slovenia, in 1979. He received the Ph.D. degree in electrical engineering from the University of Ljubljana, Slovenia.
He is a Research Associate in the Laboratory of Biocybernetics, at the Faculty of Electrical Engineering, University of Ljubljana. His main research interests are in the field of electroporation, especially design of.
electroporation devices and investigation of biological responses to nanosecond electrical pulses

NOTES

NOTES

Tumor stroma reactions to electrochemotherapy and its therapeutic implications

Gregor Serša
Institute of Oncology Ljubljana, Slovenia

Abstract: Electroporation is a platform technology for drug and gene delivery. However, application of electric pulses induces also several stromal effects in the tumors or normal tissues. One of them are vascular effects of electroporation that have profound effect on the accompanying drug or gene delivery. Furthermore, in electrochemotherapy even more pronounced effect on tumor vasculature is observed that significantly contributes to the overall antitumor effectiveness. So far no proof of concept has been evidenced in treatment of human tumors, except in the treatment of liver metastases, where such vascular changes have been evidenced. Besides the vascular effects of electrochemotherapy, the immunologic cell death of tumor cells was observed. However, this effect is not sufficient to have loco-regional antitumor effectiveness, but does contribute to the complete eradication of the treated tumors. In order to boost this effect, adjuvant immunotherapy using gene electrotransfer can boost the immune response and contribute to the loco-regional antitumor effectiveness or even have the effect on distant metastases (abscopal effect). To explore this idea, we have proposed and tested the concept of electrochemotherapy as *in situ* vaccination that can be boosted with peritumoral IL-12 immunogen electrotransfer.

INTRODUCTION

Electroporation is used as drug and gene delivery method. New evidence demonstrates that electroporation itself as well as electrochemotherapy have effect also on stromal cells, i.e. endothelial and immune response that contribute significantly to overall antitumor effectiveness of the either of therapies. This knowledge is now being explored and is being sought for the possible exploitation also in the combined treatment of electrochemotherapy and gene electrotransfer of plasmids encoding various therapeutic molecules.

VASCULAR EFFECTS

Electroporation

It all started with the observation that tumors become whitish, pale, after the application of electric pulses. This stimulated the initial preclinical studies that were exploring vascular effects of electroporation on a physiological level. Obtained results demonstrated that the application of electric pulses of different amplitude, duration, frequencies and their number, induced local and transient reduction of the perfusion in the exposed tissue [1], where the effect was more pronounced in tumors, than in the normal tissues [1, 2]. The difference in the responsiveness was attributed to the specificity of the tumor vasculature that is chaotic, and less developed than the normal vasculature.

These first studies stimulated more mechanistically oriented studies from which we developed a model of how electric pulses affect the vessels. The model postulated that vascular permeability is induced due to the rounding of endothelial cells (Figure 1). Consequently, the interstitial fluid pressure is increased, resulting in the compression of small blood vessels. This effect is reversible due to the recovery of the endothelial cells lining tumor blood vessels after 12 to 24 h [3].

The model was based on the findings in preclinical studies, which demonstrated that the application of electric pulses to the tissue immediately induced a transient reduction of blood flow for up to 80%, which was then restored [1]. This effect was observed in the area exposed to electric pulses, tumors or muscle, whereas it had no effect on distant tissues. Furthermore, the effect was reproducible on the same tumors, when electric pulses were applied 24 h after the application of the first set of pulses [1]. The changes in tumor perfusion were demonstrated to correlate with changes in tumor oxygenation, as measured by electron paramagnetic resonance (EPR) technique [4].

Later on, *in vitro* study evaluated the effect of electric pulses on cytoskeleton of the endothelial cells and on a model of endothelial cells lining. It was demonstrated that electric pulses profoundly disrupt actin and microtubule cytoskeletal network and induce loss of cell-to-cell junctions leading to rounding of endothelial cells and consequently the leakiness of the endothelium [5].

The disruption of the microvascular structures in the tumors and abrogation of the blood flow was confirmed also by histological analysis of tumors, i.e.

swollen endothelial cells were observed and stacked erythrocytes within the vessels [6]. However, the question, to what extent can the endothelial cells be affected by the applied electric field, remained. This was addressed by a mathematical model, which demonstrated that endothelial cells, lining of the vessels can be affected by the electric field and that they may be exposed to up to 40% higher electric field than the surrounding tumor cells [6].

The latest *in vivo* real time experiments on the normal and tumor vasculature in the dorsal window chamber model confirmed all the findings from before and added some new data. These real time experiments using fluorescently labelled dextrans of different sizes demonstrated the differential response of tumor and normal vessel to the application of electric pulses. Both types of vessels became leaky after application of electric pulses within 2 minutes. Vascular lock occurred immediately in both types of vessels. The restoration of blood flow occurred in both types of vessels within 10 minutes after application of electric pulses, however, i.e. blood flow in normal vessels was completely restored in 1 hour, while in tumor vessels even after 24 h the restoration was not completed in all vessels [7, 8].

Electrochemotherapy

Parallel to studies that investigated the effects of electric pulses on tumor vasculature were the studies investigating the effects of electrochemotherapy. The rationale behind was, that if the endothelial cells in the tumors exposed to electric pulses are permeabilized, than the drug molecules which are in the blood vessels, would enter the endothelial cells as well and should affect the vasculature in the tumors. Furthermore, if these endothelial cells would undergo apoptotic or necrotic cell death, the permeability of small vessels within the tumors can be affected, and blood flow in such blood vessels should be abrogated permanently, leading to the vascular disrupting effect. This vascular disrupting effect is well known, and is observed with some tubulin binding agents, like combretastatins, and was described after irreversible electroporation as well [5, 9, 10].

The model postulated that in addition to the vascular effects of electric pulses, the presence of the drug induces endothelial cell death that leads to abrogation of tumor blood flow and consequently to vascular disrupting effect of electrochemotherapy (Figure 1) [3].

Vascular effects of electrochemotherapy with bleomycin and cisplatin were investigated, and demonstrated to lead to the almost complete abrogation of tumor perfusion [4, 6, 9]. This was demonstrated at the level of the blood flow measurements, and tumor oxygenation. The effect was confirmed also by ultrasonography of tumors and staining of hypoxic areas in the tumors [6, 11]. Therefore, these *in vivo* studies indirectly demonstrated that electrochemo-therapy damages the tumor vasculature, which accounts for the vascular disrupting effect of electrochemotherapy, as it was proposed. The study *in vitro* also demonstrated that endothelial cells are susceptible to bleomycin and cisplatin, in the same or even higher degree as tumor cells [12] and that electrochemotherapy had also significant effect on cytoskeletal structures, which faster occurred after electrochemotherapy (within 10 min) than after electroporation alone [8]. Furthermore, the histological analysis of tumors has confirmed the findings, demonstrating the apoptotic endothelial cell death and disruption of the microcirculation of the tumors [6].

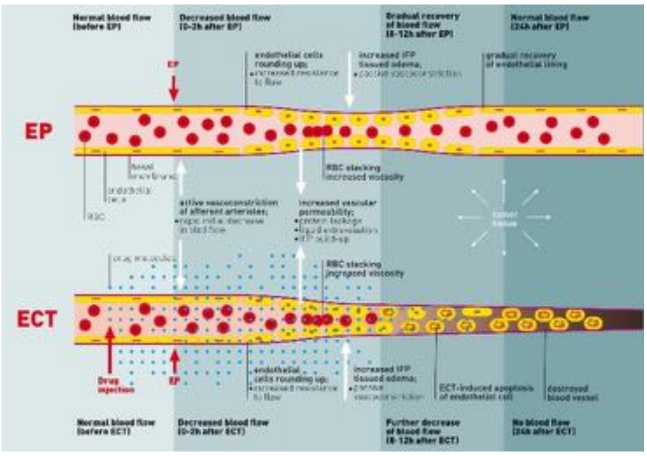

Figure 1: Model of the vascular effects in tumors of electroporation and electrochemotherapy that lead to vascular disrupting effect. With permission from Expert Review of Anticancer Therapy [3].

The latest intravital microscopy experiments have confirmed the findings *in vitro* and furthermore demonstrated that changes in tumor blood vessels occurred faster after electrochemotherapy than after electroporation alone. In contrast to our proposed model, indicating that endothelial cells start to die 8 hours after the treatment, these new data showed that the death of tumor endothelial cells starts within the first hour [8].

The striking finding of our study, however, was a differential susceptibility between the tumor vasculature and the surrounding normal vasculature [8]. The normal vasculature was not affected by electrochemotherapy, which could be attributed to the difference in the mitotic rate of the normal and tumor endothelial cells: i.e. due to the higher rate of division the tumor endothelial cells, should be more susceptible, similarly as the tumor vs. normal cells [14].

Clinical observations and implications

Due to the vascular disrupting effectiveness of electrochemotherapy, this therapy is now well established for the treatment of bleeding cutaneous metastases [15, 16]. Several published clinical cases describe effective and immediate abrogation of bleeding in such metastases, which gives electrochemotherapy an advantage over other established ablative techniques [9]. Furthermore, the vascular disrupting effect, which leads to a cascade of cell death in neighboring tumor cells, may substantially contribute to the overall effectiveness of electrochemotherapy. How much is the contribution of this indirect effect in addition to the direct effect on tumor cells is still not known and needs to be established. Certainly it varies according to the perfusion level or the vascularization of the tumors, therefore it will be difficult to determine the contribution of the vascular disrupting effectiveness of electrochemotherapy.

In contrast to irreversible electroporation, the effects of electrochemotherapy on the bigger vessels were not evaluated. Irreversible electroporation showed similar, vascular disrupting effects on microvasculature, as electrochemotherapy, although on bigger, well-structured vessels with strong muscular (media) layer, the scaffold of the vessels remained intact, whereas the endothelial cell lining was only transiently damaged [10]. Similar effects are also expected for electrochemotherapy. Namely, in the clinical study where colorectal liver metastases were treated with electrochemotherapy, 13 were afterward surgically removed and evaluated histologically, a significant reduction of viable tissue was observed. The typical response two months after electrochemotherapy was infarct-like necrosis of the tumor tissue and the surrounding tumor parenchyma, with the encapsulation of the treated tissue (fibrous pseudocapsule on the border between the normal liver tissue and the electrochemotherapy treated area). In some of the tumor samples, bigger vessels were not affected [17, 18].

However, 14 metastases that were located in the close vicinity of the major blood vessels of the liver were treated with electrochemotherapy only, since they were not amenable for surgical resection or radiofrequency ablation due to their location. Nevertheless, very good antitumor effectiveness was observed, with 71% of complete responses, and no side effects recorded [17, 18].

IMMUNE RESPONSE

It is known that malignant tumors are able to grow and spread because of their ability to escape the immune system surveillance. In fact, there is a process called “cancer immunoediting” that recognizes the existence of a fine interaction between the immune system and tumors, indicating the dual role the immunity plays in cancer [19]. Namely, the immune system not only protects the host against tumor growth, but can promote cancer development by selection of tumor variants with reduced immunogenicity [20]. One promising approach to treat cancer is so called active immunotherapy, aiming to induce an endogenous tumor specific immune response in the host. Immunotherapy strategies can include cancer vaccines based on plasmid DNA vectors used to deliver tumor antigens and/or immunomodulatory molecules to stimulate the immune system or oligonucleotides acting on immunosuppressor genes. Current data also support the idea that it is possible to strengthen the anti-cancer immune response by eliminating or inhibiting the immunosuppressive regulatory T cells (Treg) and by blocking the immune checkpoints [21, 22].

Based on the assumption that local treatments can elicit immune response, which can be boosted by gene electrotransfer of immunomodulatory molecules, we need to develop strategies to combine local tumor treatments, such as electrochemotherapy with gene electrotransfer that will be tailored to specific tumor, tissue, and specific mode of action of the therapeutic molecule. We also proposed a strategy, where electrochemotherapy treated tumor could be used as a live vaccine in conjunction with gene electrotransfer to tumors (intratumorally or peritumorally) boosting local immune response to tumor together with “abscopal effect” on distant metastases.

Electroporation

Electrochemotherapy induces apoptotic and necrotic cell death in tumors, and extensive necrotic areas in the tumors are observed after a few days [23]. This leads to tumor antigen shedding in the tumor surrounding. Several lines of evidence support this notion. Recently, properties of immunogenic cell death after electrochemotherapy were demonstrated in a murine tumor model [24].

Firstly, some of the preclinical studies demonstrated infiltration of immune cells into the tumors, indicating an inflammatory reaction [25]. This reaction is due also to the liberation of the cell metabolites that are shed from cells that underwent necrotic cell death, and elicits adaptive immune response [24]. Besides preclinical studies [26], also electrochemotherapy of human melanoma induced maturation of dendritic cells (DC) and their subsequent migration into draining lymph nodes [27]. Furthermore, the release of ATP after electroporation of cells serves also as attractant for DC and their precursors and favors their maturation into antigen presenting cells [24].

Secondly, for complete regression of the tumors after electrochemotherapy we need to eradicate (kill) all the tumor initiating (stem) cells. However, due to the technical limits, as well as tissue properties, we cannot effectively cover whole tumor with the sufficient electric field to permeabilize all cells within the tumor, or the drug is not available for the cells' uptake. Thus, we have to presume that the immune response is responsible for the eradication of all the remaining tumor cells, which is supported by the results of the study, where we demonstrated that after electrochemotherapy complete responses of the tumors were obtained in immunocompetent mice, whereas in T cell deficient nude mice were not obtained [26, 28, 29]. Such observations are common also after radiotherapy [30]. Another line of evidence comes from the studies where adjuvant treatment using different cytokines, like IL-2 and TNF-α were combined with electrochemotherapy resulting in increased antitumor effectiveness [25, 28, 31].

Thirdly, one of the first studies of electrochemotherapy in immunocompetent mice has indicated on the induction of the systemic immune response after electrochemotherapy of tumors. Monocytes isolated from venous blood of electrochemotherapy treated mice, showed increased ability to elicit oxidative burst by production of toxic oxygen species 7 days after treatment. Besides activation of monocytes, which are involved in non-specific tumor destruction and activation of other components of the immune system, also adaptive immune arm was activated, demonstrated by activation of T lymphocytes. However, this activation may not be sufficient for abscopal effect on distant metastases [32]. On the other hand, none of the *in vitro* and *in vivo* studies in mice or clinical studies have demonstrated that electrochemotherapy promotes metastatic process in the organism [32, 33]. However, it was shown that electrochemotherapy can induce immunogenic cell death demonstrated by exposure of calreticulin, liberation of ATP and the release of high mobility group box 1 protein from CT26 colon carcinoma cells *in vitro*. Such electrochemotherapy treated cells, when injected into syngeneic mice also protected the animals against tumor challenge demonstrating vaccination effect [24]. Hence, electrochemotherapy may represent an interesting approach to treat solid tumors while preventing recurrence and metastases.

Fourthly, the effect of electrochemotherapy depends also on the immunogenicity of the treated tumors; more immunogenic tumors respond better and with a higher cure rate [34, 35]. In line with these observations, we can also speculate that although electroporation is an effective technology for drug delivery, based mainly on physicoelectrical properties, the response rate of the tumors at least to some degree, depends also on the tumor type, having in mind also intrinsic sensitivity (resistance) to the chemotherapeutic drug [25, 35, 36]. Some lines of evidence for that exists also for human studies since slight variations in tumor responsiveness was observed in meta-analysis performed on clinical studies on electrochemotherapy published so far [37]. Furthermore, a clinical study on electrochemotherapy of melanoma in patients has demonstrated tumor infiltrating lymphocytes following treatment, but there was no correlation between their number or distribution and the local response or visceral spread. Whereas, FoxP3 as a master control gene of regulatory T cells (Treg) was upregulated in tumors that had faster dissemination into the visceral organs [38].

Electrotransfer of immunomodulatory genes adds a systemic component to electrochemotherapy

Gene electrotransfer is another electroporation based application, where plasmid DNA (pDNA) or siRNA molecules can be delivered to various tissues, including tumors [39, 40].

Gene electrotransfer is considered to be an effective tool in eliciting antigen-specific immune response in small and large animal models, being responsible for the generation of an inflammatory environment with immune cell infiltration [41]. The migration of these cells seems to be essential to initiate an adequate immune response to the DNA vaccine, proving that this technique is effective in the stimulation of humoral and cellular immunity [42].

Depending on the immunogenicity of the tumors and the immune status of the organism, *in vivo* gene electrotransfer of pDNAs coding for immunomodulatory molecules such as cytokines, chemokines, adjuvant sequences, siRNA, and/or administration of DNA vaccines carrying tumor specific or tumor associated antigens (TAA) can be used alone or in combination with chemotherapeutics for treatment of tumors [43]. Several therapeutic genes were examined, IL-12, VEGF, PDGF-α, etc. [44-46], but no detailed study of the immune response locally or systemically was conducted. All these studies report that gene electrotransfer is effective in activating the antitumor effectiveness. The therapeutic gene can be administered either intratumorally or peritumorally for predominantly local effectiveness, or into the muscle to induce systemic shedding of the therapeutic molecule. Some studies using IL-2 or IL-12 demonstrated also the antitumor effectiveness on distant untreated tumors, and long term memory of the immune system to tumor cells [25, 47]. As a single treatment, the intratumoral administration of cytokine gene electrotransfer seems the most appropriate way to obtain good therapeutic effect. One of the most studied cytokine is IL-12, with several preclinical studies in different tumor types demonstrating its effectiveness, which was proved also in clinical treatment of melanoma patients [44]. Daud et al. have demonstrated that treatment of a few melanoma nodules in the patient can elicit, in certain patients, slow, but an efficient immune response of the organism, that results in regression of the treated, and also non treated nodules, as well as prolonged survival without progression of the disease [48].

Some studies have also explored the combination of local therapies with the gene electrotransfer of immunomodulatory genes. The combinations with either radiotherapy or electrochemotherapy were explored. The strategy was similar, radiosensitization or chemosensitization by immunoadjuvant therapy that boosted the immune response of the organism against tumor [49-51]. A good potentiation of the radiation response and electrochemotherapy was noted, but the underlying immunomodulatory mechanisms were not explored. The knowledge of the mechanisms underlying the elicited immune response by local therapy, such as electrochemotherapy, would lead into the proper scheduling of suitable combination therapies for elicitation of systemic immune response. Thus, appropriate dosage of the pDNA encoding immunomodulatory molecules and the scheduling of it needs to be determined [52]. Additionally, suitable biomarkers that would predict the treatment response are needed. Currently, it seems that several consecutive immunogene therapies are necessary. Indeed, in preclinical studies, it was shown that at least three consecutive immunogene electrotransfers should be performed, one prior to electrochemotherapy and two consecutive ones thereafter [34]. Skin gene electrotransfer is very appealing, since the skin is a tissue with vast amounts of immune cells capable of eliciting an efficient vaccination and boosting effect. Some studies have already shown that dendritic cell (DC) activation in the treatment of melanoma may be an exciting approach [38].

We have proposed a model, a combination of electrochemotherapy with immunostimulating peritumoral IL-12 electrotransfer, as a proof of principle, that electrochemotherapy can be used as *in situ* vaccination boosted with immunogene electrotransfer (Figure 2) [54].

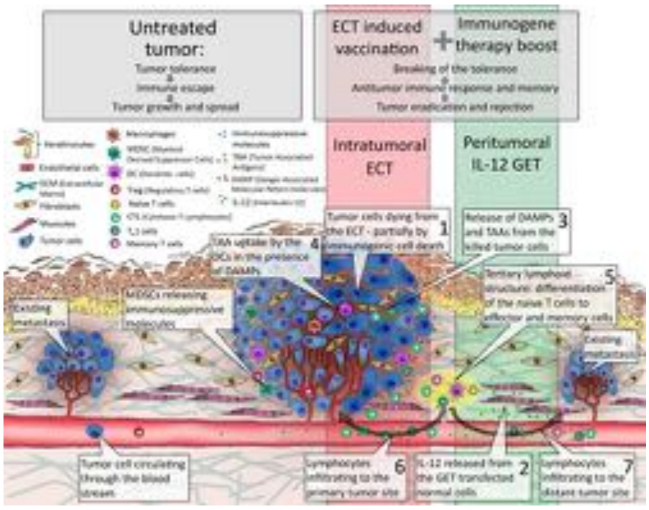

Figure 2: Proposed model for electrochemotherapy of tumors as in situ vaccination boosted by immunogene electrotransfer. With permission from Cancer Immunology, Immunotherapy [54].

In the untreated tumor (Figure 2, left) immunosuppressive microenvironment with suppressive immune cells like Tregs and myeloid-derived suppressor cells (MDSC) lead to tumor tolerance, tumor cells escape the immune system and can replicate uncontrollably and spread through the body to form distant secondary tumors. The electrochemotherapy induced vaccination boosted with IL-12 immunogene therapy (Figure 2, right) leads to the breaking of the tolerance to otherwise weekly immunogenic intrinsic tumor antigens that result in an anti-tumor immune response and memory responsible for regression of the treated tumor and untreated distant metastases. Namely, electrochemotherapy induced tumor cell deaths (Figure 2, speech balloon 1) combined with IL-12 released into the bloodstream from the transfected cells in the peritumoral region (Figure 2, speech balloon 2) create a pro-inflammatory microenvironment that leads to recruitment of circulating immune cells. Tumor cells die, at least in part, by immunogenic form of cell death characterized by the shedding of TAA and danger-associated molecular pattern molecules (DAMP) (Figure 2, speech balloon 3) from the dying cells. Released TAA are captured by DC (Figure 2, speech balloon 4) that migrate to local lymph node-like structures called tertiary lymphoid structures (TLS) [53] or to the draining lymph nodes (Figure 2, speech balloon 5) where they initiate adaptive anti-tumor immune response by priming the naive T cell to become effector and memory T cells. Tumors specific lymphocytes, like cytotoxic T lymphocytes and Th1 cells, are then released from the lymphoid structures via circulation and can infiltrate the primary tumor site (Figure 2, speech balloon 6) and distant metastases (Figure 2, speech balloon 7) where they exert their immunological actions.

Furthermore, an exciting therapeutic approach to further provide a systemic effectiveness and to enhance the local anti-tumor response of electrochemotherapy could be the immune checkpoint blockade or/and inhibiting Tregs.

CONCLUSION

Electrochemotherapy is an efficient local ablative treatment, which is currently employed in numerous oncology centers throughout Europe. However, it is a local treatment, which would need a systemic component that would boost the immune response of electrochemotherapy itself. Therefore, gene electrotransfer of immunomodulatory molecules in the peritumoral skin could add this systemic component, by enhancing locoregional and/or systemic response. Hence, we propose a strategy, where electrochemotherapy treated tumor could be used as a live vaccine in conjunction with gene electrotransfer to tumors.

ACKNOWLEDGEMENTS

This research was funded by a research grant from the Research Agency of the Republic of Slovenia and was conducted in the scope of the EBAM European Associated Laboratory (LEA) and resulted from the networking efforts of the COST Action TD1104 (www.electroporation.net)..

REFERENCES

[1] Sersa G, Cemazar M, Parkins CS et al. (1999) Tumour blood flow changes induced by application of electric pulses. Eur J Cancer 35: 672-677.

[2] Gehl J, Skovsgaard T, Mir LM (2002) Vascular reactions to in vivo electroporation: characterization and consequences for drug and gene delivery. Biochim Biophys Acta 1569: 51-58.

[3] Jarm T, Cemazar M, Miklavcic D et al. (2010) Antivascular effects of electrochemotherapy: implications in treatment of bleeding metastases. Expert Rev Anticanc 10: 729-746.

[4] Sersa G, Krzic M, Sentjurc M et al. (2002) Reduced blood flow and oxygenation in SA-1 tumours after electrochemotherapy with cisplatin. Brit J Cancer 87: 1047-1054.

[5] Kanthou C, Kranjc S, Sersa G et al. (2006) The endothelial cyto-skeleton as a target of electroporation-based therapies. Mol Cancer Ther 5: 3145-3152.

[6] Sersa G, Jarm T, Kotnik T et al. (2008) Vascular disrupting action of electroporation and electrochemotherapy with bleomy-cin in murine sarcoma. Brit J Cancer 98: 388-398.

[7] Bellard E, Markelc B, Pelofy S et al. (2012) Intravital microscopy at the single vessel level brings new insights of vascular modifi-cation mechanisms induced by electropermeabilization. J Con-trol Release 163: 396-403.

[8] Markelc B, Sersa G, Cemazar M (2013) Differential mechanisms associated with vascular disrupting action of electrochemother-apy: intravital microscopy on the level of single normal and tu-mor blood vessels. PLoS One 8: e59557.

[9] Sersa G, Miklavcic D, Cemazar M et al. (2008) Electrochemo-therapy in treatment of tumours. Eur J Surg Oncol 34: 232-240.

[10] Jiang C, Davalos RV, Bischof JC (2015) A review of basic to clinical studies of irreversible electroporation therapy. IEEE T Bio-Med Eng 62: 4-20.

[11] Cor A, Cemazar M, Plazar N et al. (2009) Comparison between hypoxic markers pimonidazole and glucose transporter 1 (Glut-1) in murine fibrosarcoma tumours after electrochemotherapy. Radiol Oncol 43: 195-202.

[12] Cemazar M, Parkins CS, Holder AL et al. (2001) Electroporation of human microvascular endothelial cells: evidence for an anti-vascular mechanism of electrochemotherapy. Brit J Cancer 84: 565-570.

[13] Meulenberg CJ, Todorovic V, Cemazar M (2012) Differential cellular effects of electroporation and electrochemotherapy in monolayers of human microvascular endothelial cells. PLoS One 7: e52713.

[14] Folkman J (2003) Angiogenesis and apoptosis. Semin Cancer Biol 13: 159-167.

[15] Gehl J, Geertsen PF (2006) Palliation of haemorrhaging and ulcerated cutaneous tumours using electrochemotherapy. Ejc Suppl 4: 35-37.

[16] Snoj M, Cemazar M, Srnovrsnik T et al. (2009) Limb sparing treatment of bleeding melanoma recurrence by electrochemo-therapy. Tumori 95: 398-402.

[17] Edhemovic I, Brecelj E, Gasljevic G et al. (2014) Intraoperative electrochemotherapy of colorectal liver metastases. J Surg Oncol 110: 320-327.

[18] Edhemovic I, Gadzijev EM, Brecelj E et al. (2011) Elec-trochemotherapy: a new technological approach in treatment of metastases in the liver. Technol Cancer Res T 10: 475-485

[19] Dunn GP, Old LJ, Schreiber RD (2004) The immunobiology of cancer immunosurveillance and immunoediting. Immunity. 21: 137-48.

[20] Zou WP (2005) Immunosuppressive networks in the tumour environment and their therapeutic relevance. Nat Rev Cancer. 5: 263-74.

[21] Bruserud O, Ersvaer E, Olsnes A, Gjertsen BT (2008) Anticancer immunotherapy in combination with proapoptotic therapy. Curr Cancer Drug Tar. 8: 666-75.

[22] Whelan MC, Casey G, MacConmara M, Lederer JA, Soden D, Collins JK, Tangney M, O'Sullivan GC (2010) Effective immunotherapy of weakly immunogenic solid tumours using a combined immunogene therapy and regulatory T-cell inactivation. Cancer Gene Ther. 17: 501-11.

[23] Cemazar M, Miklavcic D, Scancar J, Dolzan V, Golouh R, Sersa G (1999) Increased platinum accumulation in SA-1 tumour cells after in vivo electrochemotherapy with cisplatin. Br J Cancer. 79: 1386-91.

[24] Calvet CY, Famin D, Andre FM, Mir LM (2014) Electrochemotherapy with bleomycin induces hallmarks of immunogenic cell death in murine colon cancer cells. Oncoimmunology. 3: e28131.

[25] Mir LM, Roth C, Orlowski S, Quintin-Colonna F, Fradelizi D, Belehradek J, Jr., Kourilsky P (1995) Systemic antitumor effects of electrochemotherapy combined with histoincompatible cells secreting interleukin-2. J Immunother Emphasis Tumor Immunol. 17: 30-8.

[26] Miklavcic D, Semrov D, Mekid H, Mir LM (2000) A validated model of in vivo electric field distribution in tissues for electrochemotherapy and for DNA electrotransfer for gene therapy. Biochim Biophys Acta. 1523: 73-83.

[27] Gerlini G, Sestini S, Di Gennaro P, Urso C, Pimpinelli N, Borgognoni L (2013) Dendritic cells recruitment in melanoma metastasis treated by electrochemotherapy. Clin Exp Metastasis. 30(1): 37-45.

[28] Sersa G, Cemazar M, Menart V, Gaberc-Porekar V, Miklavcic D (1997) Anti-tumor effectiveness of electrochemotherapy with bleomycin is increased by TNF-alpha on SA-1 tumors in mice. Cancer Lett. 116: 85-92.

[29] Sersa G, Miklavcic D, Cemazar M, Belehradek J, Jarm T, Mir LM (1997) Electrochemotherapy with CDDP on LPB sarcoma: comparison of the anti-tumor effectiveness in immunocompetent and immunodeficient mice. Bioelectrochem Bioenerg. 43: 279-83.

[30] Frey B, Rubner Y, Wunderlich R, Weiss EM, Pockley AG, Fietkau R, Gaipl US (2012) Induction of abscopal anti-tumor immunity and immunogenic tumor cell death by ionizing irradiation - implications for cancer therapies. Curr Med Chem. 19: 1751-64.

[31] Cemazar M, Todorovic V, Scancar J, Lampreht U, Stimac M, Kamensek U, Kranjc S, Coer A, Sersa G (2015) Adjuvant TNF-α therapy to electrochemotherapy with intravenous cisplatin in murine sarcoma exerts synergistic antitumor effectiveness. Radiol oncol. 49(1): 32-40.

[32] Sersa G, Kotnik V, Cemazar M, Miklavcic D, Kotnik A (1996) Electrochemotherapy with bleomycin in SA-1 tumor-bearing mice--natural resistance and immune responsiveness. Anticancer Drugs. 7: 785-91.

[33] Todorovic V, Sersa G, Mlakar V, Glavac D, Flisar K, Cemazar M (2011) Metastatic potential of melanoma cells is not affected by electrochemotherapy. Melanoma Res. 21: 196-205.

[34] Sedlar A, Dolinsek T, Markelc B, Prosen L, Kranjc S, Bosnjak M, Blagus T, Cemazar M, Sersa G (2012) Potentiation of electrochemotherapy by intramuscular IL-12 gene electrotransfer in murine sarcoma and carcinoma with different immunogenicity. Radiol Oncol. 46: 302-11.

[35] Sersa G, Cemazar M, Miklavcic D, Mir LM (1994) Electrochemotherapy - variable antitumor effect on different tumor-models. Bioelectrochem Bioenerg. 35: 23-7.

[36] Cemazar M, Miklavcic D, Sersa G (1998) Intrinsic sensitivity of tumor cells to bleomycin as an indicator of tumor response to electrochemotherapy. Jpn J Cancer Res. 89: 328-33.

[37] Mali B, Jarm T, Snoj M, Sersa G, Miklavcic D (2013) Antitumor effectiveness of electrochemotherapy: a systematic review and meta-analysis. Eur J Surg Oncol. 39: 4-16.

[38] Quaglino P, Osella-Abate S, Marenco F, Nardo T, Gado C, Novelli M, Savoia P, Bernengo MG (2011) FoxP3 expression on melanoma cells is related to early visceral spreading in melanoma patients treated by electrochemotherapy. Pigment Cell Melanoma Res. 24: 734-6.

[39] Stevenson FK, Ottensmeier CH, Rice J (2010) DNA vaccines against cancer come of age. Curr Opin Immunol. 22: 264-70.

[40] Sioud M (2015) RNA interference: mechanisms, technical challenges, and therapeutic opportunities. Methods Mol Biol. 1218: 1-15.

[41] Scheerlinck JP, Karlis J, Tjelle TE, Presidente PJ, Mathiesen I, Newton SE (2004) In vivo electroporation improves immune responses to DNA vaccination in sheep. Vaccine. 22: 1820-5.

[42] Chiarella P, Massi E, De Robertis M, Sibilio A, Parrella P, Fazio VM, Signori E (2008) Electroporation of skeletal muscle induces danger signal release and antigen-presenting cell recruitment independently of DNA vaccine administration. Expert Opin Biol Ther. 8: 1645-57.

[43] Cemazar M, Sersa G (2007) Electrotransfer of therapeutic molecules into tissues. Curr Opin Mol Ther. 9: 554-62.

[44] Heller LC, Heller R (2010) Electroporation gene therapy preclinical and clinical trials for melanoma. Curr Gene Ther. 10: 312-7.

[45] Cemazar M, Jarm T, Sersa G (2010) Cancer electrogene therapy with interleukin-12. Curr Gene Ther. 10: 300-11.

[46] Glikin GC, Finocchiaro LM (2014) Clinical trials of immunogene therapy for spontaneous tumors in companion animals. ScientificWorldJournal. 2014: 718520.

[47] Pavlin D, Cemazar M, Kamensek U, Tozon N, Pogacnik A, Sersa G. (2009) Local and systemic antitumor effect of intratumoral and peritumoral IL-12 electrogene therapy on murine sarcoma. Cancer Biol Ther. 8(22): 2114-22.

[48] Daud AI, DeConti RC, Andrews S et al. (2008) Phase I trial of interleukin-12 plasmid electroporation in patients with metastatic melanoma. J Clin Oncol. 26: 5896-903.

[49] Ramirez LH, Orlowski S, An D et al. (1998) Electrochemotherapy on liver tumours in rabbits. Br J Cancer. 77: 2104-11.

[50] Sedlar A, Kranjc S, Dolinsek T, Cemazar M, Coer A, Sersa G (2013) Radiosensitizing effect of intratumoral interleukin-12 gene electrotransfer in murine sarcoma. BMC cancer. 13: 38.

[51] Tevz G, Kranjc S, Cemazar M, Kamensek U, Coer A, Krzan M, Vidic S, Pavlin D, Sersa G (2009) Controlled systemic release of interleukin-12 after gene electrotransfer to muscle for cancer gene therapy alone or in combination with ionizing radiation in murine sarcomas. J Gene Med. 11: 1125-37.

[52] Shirley SA, Lundberg CG, Li F, Burcus N, Heller R. (2015) Controlled gene delivery can enhance therapeutic outcome for cancer immune therapy for melanoma. Curr Gene Ther. 15(1): 32-43.

[53] Goc J, Fridman WH, Sautes-Fridman C, Dieu-Nosjean MC (2013) Characteristics of tertiary lymphoid structures in primary cancers. Oncoimmunology. 2: e26836.

[54] Sersa G, Teissie J, Cemazar M, Signori E, Kamensek U, Marshall G, Miklavcic D (2015) Electrochemotherapy of tumors as in situ vaccination boosted by immunogene electrotransfer. Cancer Immunol Immunother. Epub ahead of print.

Gregor Sersa, graduated from the Biotechnical Faculty at the University of Ljubljana in 1978, where he is currently a professor of molecular biology. He is employed at the Institute of Oncology in Ljubljana as Head of the Department of Experimental Oncology. His specific field of interest is the effect of electric field on tumor cells and tumors as drug and gene delivery system in different therapeutic approaches. Besides experimental work, he is actively involved in the education of undergraduate and postgraduate students at the University of Ljubljana.

NOTES

INVITED LECTURERS

Pulsed electric field application in food processing – Equipment design and matrix properties

Henry Jaeger
University of Natural Resources and Life Sciences (BOKU), Vienna, Austria

Abstract: When exposed to high electric field pulses cell membranes develop pores which may be permanent or temporary, depending on the intensity and treatment conditions. Pore formation increases membrane permeability which results in the loss of cell content or intrusion of surrounding media. Low intensity treatment has the potential to induce stress reactions in plant cells resulting in the promotion of a defense mechanism by increased production of secondary metabolites. An irreversible perforation of the cell membrane reduces its barrier effect permanently and causes cell death. Applied to fruit and vegetable cells mass transfer processes like pressing, extraction or drying are more effective, in the case of meat brining and pickling mass transport and microdiffusion could be enhanced. The loss of cell vitality caused by electroporation is furthermore a capable tool for the inactivation of microorganisms used for a non-thermal pasteurization of liquid food.

CELL DISINTEGRATION

Solid-liquid extraction, pressing or drying of food matrixes is strongly dependant on diffusion and mass transfer through the cells and tissue and is characterized by the disintegration of the material. To achieve high disintegration of solid tissue, thermal, mechanical, chemical or enzymatic methods are commonly used.

PEF technology can be applied as a method for cell disintegration. The occurring increase in membrane permeabilization positively affects the mass transfer rate and therefore diffusion of intracellular components in extracellular liquid is increased and extraction processes are improved, drying processes are accelerated and an increase of juice yield during pressing of PEF pre-treated fruit mashes can be obtained [1]. Increased microdiffusion into the cells can be used to enhance processes like meat brining or pickling as well as for the infusion of cryoprotectants to improve the quality of frozen-thawed products.

A comparison of juice yields of apple and carrot juice after PEF processing compared to control samples are presented in [2]. A juice yield increase was found depending on treatment conditions and performance of subsequent processing steps such as grinding or following processing steps such as pressing. In addition, the implementation of enzymes on pectin rich material effects depolymerization of pectin structure, whereas PEF treated cell material can be further utilized for pectin extraction. In addition to the higher juice yield obtained after PEF treatment, evaluation of selected quality criteria showed that application of high intensity electric field pulses on mash resulted in a higher release of bioactive compounds in juice than from samples processed in a conventional way [2,3,4].

Guderjan et al. [5] reported about facilitated oil extraction and a higher antioxidant capacity after the implementation of PEF on rapeseeds. Besides higher oil yield additional progress is shown in higher content of nutritional ingredients.

Extractability of intracellular pigments facilitated with high intensity electric field treatment showed to be a very efficient process for winning of these valuable components with beneficial antioxidant properties. PEF-induced cell permeabilisation and release of intracellular pigments (anthocyanins) from wine grapes was studied by Tedjo et al. [6]. They showed threefold increase of total anthocyanin content after applying electric field strength of 3 kV/cm and 50 pulses.

PEF enhanced permeability of potato tissue which resulted in improved mass transfer during air dehydration and therefore shorter drying time was demonstrated by Rastogi et al. [7]. Process duration for dehydration processes after PEF treatment can be reduced by up to 40 % and rehydration ability could be increased substantially [8].

A PEF-pretreatment can be utilized to improve uptake of salt and nitrite in fish and meat products. During production of cooked ham pickling brine is injected to induce nitrite, salt and spices and to improve yield after cooking. Injection is followed by a tumbling to improve brine distribution and to achieve mechanical disintegration. The impact of PEF on mass transport and microdiffusion of brine was investigated by Toepfl [9]. The drip loss after cooking of ham was observed to be reduced from 22% to 13% when processing PEF-treated (2 kV/cm and 10 kJ/kg) meat.

Application of PEF provides a good potential to replace conventional cell disintegration techniques and as continuous application of short treatment duration makes an attractive candidate as a novel non-thermal unit operation. PEF enhances mass transfer rates by electroporation of plant cell membranes improving tissue softness and influencing the textural properties. Subsequent processes such as drying, juice or oil recovery, extraction or infusion can be conducted at increased process yields in comparison to the processing of untreated raw materials or at lower energy and time consumption compared with enzymatic maceration or thermal cell disintegration.

NON-THERMAL PASTEURIZATION

According to several studies, the quality of a PEF pasteurised food product is closer to that of the fresh product than to that of the heat-pasteurised product and the safety of the fresh product is enhanced by the inactivation of vegetative pathogenic microorganisms.

The first commercial PEF application was installed in 2005 in the U.S. for fruit juice preservation. Clearance of FDA was already available since 1996, indicating the techniques potential for safe and gentle preservation. However, to make further use of this promising technology and to advance its industrial implementation, several aspects need to be taken into account in order to guarantee a satisfying process performance [10,11,12].

Effective inactivation for most of the spoilage and pathogenic microorganisms has been shown and colony count reductions depending on treatment intensity, product properties and type of microorganism in the range of 4-6 log-cycles are comparable to traditional thermal pasteurisation [13].

Most of the studies conducted in the past showed that PEF is only effective against vegetative microorganisms, yeasts and molds as well as mold ascospores but ineffective against bacterial endospores and viruses. Recent investigation indicated an increase of the inactivation of *B. subtilis* endospores when thermal treatment (75-115 °C) was combined with PEF application (15 kV/cm, 60-120 kJ/kg) [15]. The factors which affect microbial inactivation during PEF treatment are process factors such as electric field intensity, pulse width and shape, treatment time and temperature, microbial factors such as type, shape, size, concentration and growth stage of microorganism and media factors such as pH, antimicrobials and ionic compounds, electrical conductivity and medium ionic strength.

The microbial inactivation by PEF depends on characteristics such as type, shape, growth phase, and inoculation amount of microorganisms.

The cells in the logarithmic growth phase are more sensitive to inactivation by PEF. Inactivation by PEF is therefore higher in the logarithmic growth phase than in the stationary phase.

Microbial inactivation by PEF also depends on the characteristics of the microorganism-containing medium or food. Factors such as the electrical resistance, pH, water activity, viscosity, presence of solid particles, bubbles or oil droplets have an impact on the PEF effectiveness [15].

In order to obtain a maximum of food safety, a direct transfer of cells from the vital to the lethal fraction during the microbial inactivation is favorable. However, since the impact on food quality characteristics limits the applicable treatment intensities, a limited number of dead cells may result. Membrane damage and inactivation of microorganisms due to PEF was firstly considered as an all-or-nothing event, but a differentiated approach is required even if the critical parameters for the electrical breakdown of cell membranes are exceeded. Membrane damage and sublethal injury was found to be repairable under certain conditions and the extent to which cells repair their injuries was reported to depend on the treatment intensity, the microorganism and the treatment medium pH. On the one hand, sublethally injured cell fractions are a risk from a food quality and safety point of view since these cells may recover and regain their initial vitality. On the other hand, sublethally injured fractions have a potential for subsequent complete inactivation by the application of additional hurdles such as suboptimal storage conditions or the application of other inactivation methods such as the application of antimicrobials or other food preservation technologies.

The microbial inactivation rates differ considerably between inactivation in simple media and inactivation in a complex matrix [16]. This was partly attributed to the protective effect of some food compounds such as xanthan, proteins or fat. Other studies did not reveal differences in the microbial inactivation conducted in buffer or complex media, or did not detect the occurrence of sublethally injured cells after PEF treatment of complex food systems. However, inactivation kinetics obtained from PEF treatment in buffer systems have only limited comparability with real food products. In addition, model microorganisms used in most of the studies and the way of sample preparation differ significantly from the native state of the microbial population present in the real food system. The diverse and heterogeneous microbial flora present in real foods is not comparable to inoculated microorganisms in most cases due to strong variability of microbial species and physiological state of microorganisms. The consideration of microbial growth state, adaptation to the treatment media as well as the existence of inhomogeneous microbial populations with less sensitive subpopulations seem to be the most challenging aspects when transferring inactivation results to real products and industrial implementation. Assured food safety and stability, along with a desired level of microbial inactivation requires accurately defined treatment intensity followed by a predictable microbial inactivation. The transfer of inactivation results from model systems to real foods and the determination of appropriate PEF treatment parameters require the consideration of existing particularities. The impact of food constituents on PEF effectiveness is not fully elucidated. Some authors report a protective effect of xanthan, proteins or fat. Other studies did not reveal differences in the microbial inactivation conducted in buffer or complex media. Investigation of the inactivation of *E. coli* in ovalbumin solution, fish egg suspension, dairy cream and in phosphate buffer did not show a protective effect of emulsified lipids, soluble proteins or conductive food particulate. However, inactivation of *Enterobacter sakazakii* in peptone water and infant formula milk by PEF at 40 kV/cm for 300 µs was found to cause 2,7 log-cycles and 1,2 log-cycles reductions respectively showing an impact of the complex composition of infant formula milk in comparison to peptone water. When considering PEF effectiveness as a function of the treatment media, the critical field strength and treatment time required was found to be dependent not only on cell geometry but also on the properties of the media.

In addition to the protective effect of food constituents, food matrix properties such as electrical conductivity, heat capacity and viscosity have to be considered. These parameters affect the power requirements necessary the generation of a desired electric field level as well as the power consumption during operation. Viscosity will determine the flow behaviour and residence time distribution in the treatment chamber resulting in treatment time variations and subsequently also in a non-uniform temperature increase with the occurrence of hot spots.

TECHNICAL ASPECTS

The treatment chamber is the key component of the PEF system for the direct application of the electric field in contact with the treatment media. Its design should consider the uniformity of the electric field distribution in combination with the flow characteristics in continuous applications as well as the extent of the temperature increase [17].

Various treatment chamber designs such as parallel plates, coaxial cylinders or co-linear configurations have been used for PEF processing and some modifications of these basic designs have been proposed. [18].

An adequate shape of the electrodes and the insulator is a prerequisite for an optimal electric field distribution and will reduce dielectric breakdown effects of the food, since local high electric field strength levels can be avoided e.g., by providing a round-edged insulator geometry. Dielectric breakdowns of the food are undesired since they cause arcing, which leads to the destruction of the food, damage on the electrode and insulator surface, as well as an explosion of the treatment chamber due to the pressure increase. Electric field homogeneity and the avoidance of low field intensities are not only desirable from the microbial inactivation point of view, but also from the fact that energy dissipation and power consumption will take place in low field regions without contributing to the microbial inactivation.

In addition to considerations of the distribution of the electric field strength and flow velocity, hygienic aspects need to be taken into account for the design and operation of a PEF unit. One of the main aspects related to chamber design is the insulator shape and its impact on the flow and electric field distribution [19]. The insulator and its specific design have a considerable impact on the process performance as they affect the electric field strength distribution and therefore the microbial inactivation. The velocity profile in the treatment chamber (laminar, transitional or turbulent) determines the residence time distribution and therefore the total treatment time of the product. Since the fluid velocity differs depending on the location in the treatment chamber, longer treatment times will occur near the wall of the treatment chamber due to lower flow velocity and shorter treatment times occur in the center of the treatment chamber where the higher flow of velocity is. Examples for modifications as insulator gap/diameter for co-linear treatment chambers can be found in literature, where it is stated that a gap increase will provide smaller electric field strength, but also will provide a more homogeneous distribution.

The alteration of the electric field distribution by modifying the insulator geometry can be used to improve the microbial inactivation results. However, this depends strongly on other processing conditions, such as the number of pulses, media conductivity and velocity profile, that have to be considered during the microbial inactivation process. Due to the high inhomogeneities presented in a continuous treatment system, PEF processing should be characterized in terms of the electric field strength, treatment time and specific energy input [20]. An average value from the previously mentioned parameters with their respective standard deviation as well as occurring maximum and minimum values should be described in detail for the process. The lowest value of electric field strength, treatment time and energy input will be the limiting factors for food safety reasons and the maximum value for the resulting product temperature should be considered with regard to product quality. The modification of a co-linear treatment chamber by inserting static mixing devices provides a possibility to improve electric field strength distribution, aiming to increase the average value and reduce the standard deviation. This will result in an increased microbial inactivation. The insertion of static mixing devices also provides a more homogeneous velocity profile (thus a more homogeneous treatment time as well) and a more homogeneous temperature distribution, which aims at a higher retention of heat sensitive compounds [21].

REFERENCES

[1] Jaeger, H.; Balasa, A.; Knorr, D. Food Industry Applications for Pulsed Electric Fields. In: Electrotechnologies for Extraction from Food Plants and Biomaterials, Series: Food Engineering Series, Vorobiev, Eugene; Lebovka, Nikolai (Eds.), VIII, Hardcover, ISBN: 978-0-387- 79373-3; 2008, 181-216.

[2] Jaeger, H; Schulz, M; Lu, P; Knorr, D. (2012): Adjustment of milling, mash electroporation and pressing for the development of a PEF assisted juice production in industrial scale. Innov Food Sci Emerg, 14: 46-60.

[3] Knorr, D.; Geulen, M.; Grahl, T.; Sitzmann, W. Food application of high electric field pulses. Trends in Food Science and Technology, 1994, 5, 71-75.

[4] Schilling, S., Alber, T., Toepfl, S., Neidhart, S., Knorr, D., Schieber, A., Carle, R. Effects of pulsed electric field treatment of apple mash on juice yield and quality attributes of apple juices.Innovative Food Science & Emerging Technologies, 2007, 8, 127-134.

[5] Guderjan, M.; Elez-Martínez, P.; Knorr, D. Application of pulsed electric fields at oil yield and content of functional food ingredients at the production of rapeseed oil. Innov. Food Sci. Emerg.Technol., 2007, 8, 55-68. (4) Eshtiaghi, M. N.; Knorr, D. Method for treating sugar beet. International Patent. 1999, Patent No. WO 99/6434.

[6] Tedjo, W.; Eshtiaghi, M. N.; Knorr, D. Einsatz nicht thermischer Verfahren zur Zell-Permeabilisierung von Weintrauben und Gewinnung von Inhaltsstoffen. Flüssiges Obst, 2002, 9, 578-583.

[7] Rastogi, N. K.; Eshtiaghi, M. N.; Knorr, D. Accelerated mass transfer during osmotic dehydration of high intensity electrical field pulse pretreated carrots.Journal of Food Science, 1999, 64(6), 1020-1023. (5) Raso, J. and V. Heinz, Eds. Pulsed electric fields technology for the food industry. Food Engineering Series. Heidelberg, Springer Verlag. 2006.

[8] Taiwo, K. A.; Angersbach, A.; Knorr, D. Influence of high intensity electric field pulses and osmotic dehydration on the rehydration characteristics of apple slices at different temperatures. Journal of Food Engineering, 2002, 52, 185-192. (6) Toepfl, S.; Heinz, V.; Knorr, D. Overview of Pulsed Electric Field Processing for Food. Emerging Technologies for Food Processing, D.-W. Sun, ed., Elsevier, Oxford. 2005.

[9] Toepfl, S. Pulsed Electric Fields (PEF) for Permeabilization of Cell Membranes in Food- and Bioprocessing - Applications, Process and Equipment Design and Cost Analysis, PhD, University of Technology, Berlin. 2006.

[10] Knorr D, Froehling A, Jaeger H, Reineke K, Schlueter O, Schoessler K. 2011. Emerging Technologies in Food Processing. Annual Review of Food Science and Technology 2: 203-35

[11] Lelieveld HLM, Notermans S, de Haan SWH, eds. 2007. Food preservation by pulsed electric fields. Abington, UK: Woodhead Publishing

[12] Raso J, Heinz V. 2007. Pulsed electric fields technology for the food industry. New York: Springer

[13] Barbosa-Cánovas GV, Góngora-Nieto MM, Pothakamury UR, Swanson BG. 1999. Preservation of foods with pulsed electric fields. San Diego: Academic Press

[14] Siemer C, Kiessling M, Toepfl S. 2011. Inaktivierung bakterieller Endosporen durch kombinierte Anwendung gepulster elektrischer Felder und thermischer Energie.

[15] Barsotti, L., Merle, P., & Cheftel, J. 1999. Food processing by pulsed electric fields:1. Physical effects. Food Reviews International 15(2): 163 – 180.

[16] Jaeger, H; Schulz, A; Karapetkov, N; Knorr, D. (2009): Protective effect of milk constituents and sublethal injuries limiting process effectiveness during PEF inactivation of Lb. rhamnosus. Int J Food Microbiol 134(1-2): 154-161.

[17] Knoerzer K, Juliano P, Roupas P, Versteeg C, eds. 2011. Innovative Food Processing Technologies: Advances in Multiphysics Simulation. Oxford: Wiley-Blackwell

[18] Huang K, Wang J. 2009. Designs of pulsed electric fields treatment chambers for liquid foods pasteurization process: A review. Journal of Food Engineering 95: 227-39

[19] Gerlach D, Alleborn N, Baars A, Delgado A, Moritz J, Knorr D. 2008. Numerical simulations of pulsed electric fields for food preservation: A review. Innovative Food Science & Emerging Technologies 9: 408-17

[20] Knorr D, Engel K-H, Vogel R, Kochte-Clemens B, Eisenbrand G. 2008. Statement on the Treatment of Food using a Pulsed Electric Field. Molecular Nutrition & Food Research 52: 1539-42

[21] Jaeger, H; Meneses, N; Knorr, D. (2009): Impact of PEF treatment inhomogeneity such as electric field distribution, flow characteristics and temperature effects on the inactivation of E. coli and milk alkaline phosphatase. Innov Food Sci Emerg 10(4): 470-480.

Henry Jaeger is Professor of Food Technology at the University of Natural Resources and Life Sciences (BOKU) in Vienna and visiting lecturer at Technische Universität Berlin. He moved back to academia from an industry position in Research and Development at Nestlé where he worked on process development in the field of preservation technologies. Before, he was researcher in the Department of Food Biotechnology and Food Process Engineering at Technische Universität Berlin where he also obtained his PhD and an Engineering Degree (Dipl.-Ing.) in Food Technology in 2006. His research field covers the application of alternative food processing technologies for gentle food preservation as well as the targeted modification of food structures.

NOTES

NOTES

Multiphoton imaging and optogenetic tools to assess bioelectric effects *in vivo*

Rodney P. O'Connor

XLIM Research Institute, UMR CNRS 7252, University of Limoges, France

Abstract: Fluorescence imaging techniques are an essential tool for the study of pulsed electric field effects on cell physiology and electroporation and related effects. Fluorescence live cell imaging uses synthetic fluorescent indicators that have several issues which limit experiments *in vivo* to short periods; however, there have been significant recent advances in the engineering of fluorescent protein sensors that can overcome these shortcomings. A number of new genetically encoded fluorescent proteins are now available that rival the sensitivity of synthetic fluorophores and that allow the imaging *in vivo* in intact tissues. A review of some of these molecular fluorescent sensors will be presented with specific focus on those tools that might interest researchers in bioelectrics research. A further discussion on multiphoton microscopy will describe this type of nonlinear fluorescence imaging that makes use of these new fluorescent sensors *in vivo* with significant potential applications in tissue and animal models of cancer. In general, the goal is to introduce these tools and techniques that have been developed in the neuroscience community and to discuss how these approaches might be leveraged by researchers working in bioelectrics research with interest in investigating electroporation and related therapeutics for cancer.

APPLICATION OF FLUORESCENCE IMAGING IN BIOELECTRICS RESEARCH

Fluorescence microscopy is an indispensable technique that has been widely used to study cell physiology, pulsed electric field effects and electroporation over the last 30 years of bioelectrics research. The strength of live cell imaging with fluorescent indicators is its ability to optically measure a wide range of cellular parameters using dyes that have been designed to change some aspect of their fluorescence (intensity, excitation/emission wavelength, or fluorescence lifetime) in proportion to changes in physiological factors in the cell. For example, fluorescent indicators that report cytosolic Ca^{2+}, Na^{+}, K^{+}, Cl^{-}, pH, membrane potential and cell viability were first available in the 1980s and have since then been used extensively. Although a review of these probes is beyond the scope of this lecture, an excellent starting point is the freely available Molecular Probes® Handbook [1] and related online resources provided these vendors.

Whereas fluorescence imaging and synthetic fluorescent probes are well established tools for cell physiology, they are primarily suited to short term experiments (< 1 hr) that are carried out under *in vitro* conditions in thin samples. There are a number of reasons why such techniques work better *in vitro* and these can be simply organized as relating to: 1) the difficulties associated with labelling cells in intact tissue and their poor cytosolic retention at physiological temperatures, and 2) the more general optical limitations of conventional fluorescence microscopy that prevent imaging in thick samples. These issues will be briefly discussed and used to introduce some of the new genetically encoded fluorescent proteins sensors that permit the imaging of cell physiology *in vivo* over long periods of time. Then, some of the limitations of fluorescence microscopy will be reviewed to introduce multiphoton microscopy, a specific type of nonlinear fluorescence microscopy that allows the imaging of intact tissues and animals. Finally, some examples of the research underway in our laboratory will briefly presented to show the potential of these technologies for the study of pulsed electric field therapeutics on cancers *in vivo*.

GENETICALLY ENCODED INDICATORS AND OPTOGENETICS

As mentioned above, synthetic fluorescent indicators work well *in vitro*, but are not well retained in intact tissues at physiological temperatures. This is partially due to the diffusion of fluorescent molecules from cells down the concentration gradient, if they are cell permeable, and the active extrusion of cell impermeable dyes injected or loaded into cells with ester modifications. Dyes are extruded from cells via active processes requiring ATP by transporter protein complexes such as the multidrug resistance protein MDR1 or p-glycoprotein [2]. In addition to the leakage and active translocation of dyes from cells, another issue is the differential compartmentalization of fluorophores that occurs at physiological temperatures and that can result in reduced sensitivity of these indicators depending on the dye and cell type [3]. A further problem with synthetic indicators relates to the temperature sensitivity of the photophysical mechanisms of certain fluorescent molecules [4]. The latter is a particularly important point to consider when using fluorescent probes in experiments applying pulsed electric field treatments that may cause heating. Our group recently exploited the temperature sensitive property of the fluorophore Rhodamine B to measure thermal changes induced by pulsed electric fields at the cellular level [5]. Temperature effects resulting from pulsed electric fields have also been evaluated theoretically [6].

The fluorescent protein revolution

An elegant solution for many of the above issues with synthetic fluorophores came with the isolation, cloning and optimization of green fluorescent protein (GFP) from the jellyfish *Aequorea Victoria [7, 8]*. This advance initiated a revolution in genetically encoded fluorescent proteins that later led to the award of the Nobel Prize in Chemistry to Chalfie, Shinomura and Tsien in 2008. Following these advances, cells and entire biological organisms could be made to express genetically targeted fluorescent proteins using molecular techniques. There is now an extensive range of fluorescent proteins that have either been mutated from the original GFP or isolated from other organisms. Consequently, a wide palette of fluorescent proteins now exist with emissions wavelengths spanning the entire visible spectrum. In the last 10 years, several groups have focused on improving the brightness and photostability of these fluorescent proteins, as well as, engineering photoactivatable fluorescent proteins that can be used for marking cells with light [9, 10] and other applications in superresolution imaging [11]. The recent trend has been to engineer fluorescent proteins that are functional indicators of cell physiology to replace synthetic dyes.

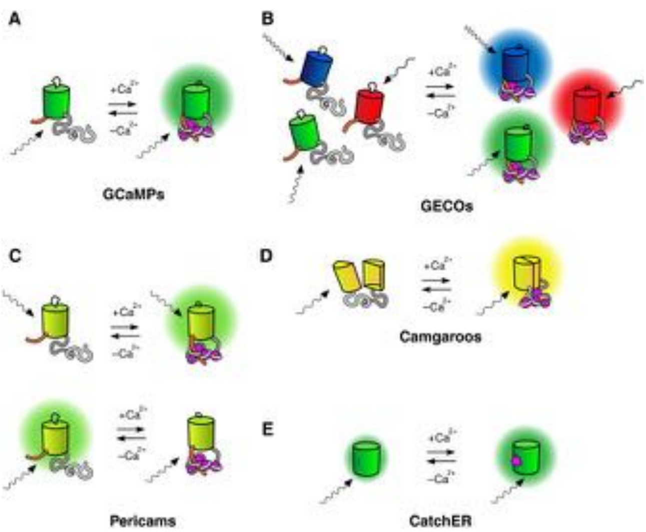

Figure 1: The family of genetically encoded Ca^{2+}indicators that are based on a single fluorescent protein. (reproduced from [21])

Genetically encoded calcium indicators

The Nobel Laureate, Roger Tsien, was responsible for the optimization of GFP and its mutation to increase brightness and shift its fluorescence properties to produce other colours. Incidentally, Tsien also invented many of the synthetic fluorescent ion indicators currently used in cell physiology [12-15]. More recently, Tsien [16] and others [17-20] have developed several fluorescent proteins that can report changes in cytosolic Ca^{2+}, thereby providing probes that give functional readout of cell physiology rather than merely acting as a structural markers or tag. Because these proteins can be genetically targeted to various cellular compartments or organelles, they can be used to measure highly local Ca^{2+} signals, for example, occurring in mitochondria, the endoplasmic reticulum, at the plasma membrane or in the nucleus.

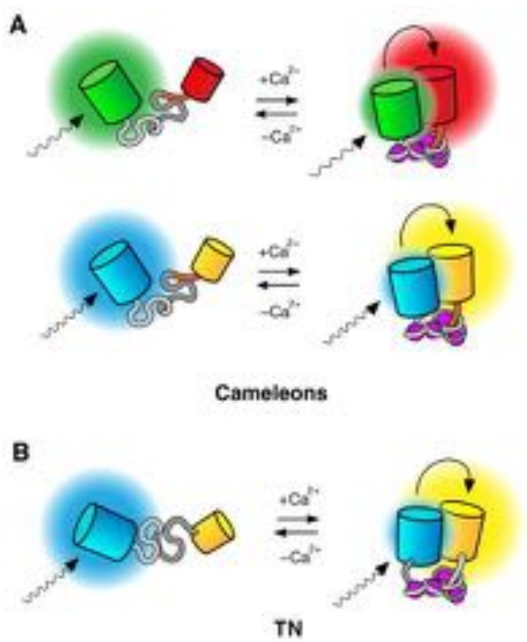

Figure 2: GECIs that are based on a design using two fluorescent proteins and Ca^{2+} binding elements. Here the change in fluorescence results from a FRET interaction between the donor and acceptor fluorescent proteins with the binding of Ca^{2+} to the complex (reproduced from [21])

A good recent review of the currently available GECI sensors is presented in [21]. GECIs can be classed into two groups by their mechanism for producing fluorescence in the presence of Ca^{2+}: 1) those which use a single fluorescent protein (GCaMPs, GECOs, Pericams, Camgaroos and CatchER), as shown in Fig. 1, and 2) those which use Förster resonance energy transfer (FRET) between two fluorescent proteins, as shown in Fig. 2. The general mechanism whereby GECIs detect Ca^{2+} is conferred by the fusion of a Ca^{2+} binding motif, like calmodulin, M13 or troponin C, with fluorescent proteins. The binding of Ca^{2+} to these elements in the engineered protein therefore leads to conformational changes in the protein(s) and alterations in the fluorescence properties of the sensor.

The sensitivity and brightness of GECIs now approaches or equals that of the synthetic Ca^{2+} indicators. Particular advances have come through large-scale efforts at the Janelia Research Campus of the Howard Hughes Medical Institute. There, a several groups have collaborated to obtain the crystal structure of the GCaMP GECIs (Fig. 3a) and then proceeded to mutate and manipulate the protein sequence to optimize the brightness and temporal responsiveness of these sensors for reporting neuronal Ca^{2+} signals associated with action potentials [22-24]. This approach has led to highly sensitive Ca^{2+} sensor exhibiting up to a 5-fold change in fluorescence and with other specific mutants designed for their fast temporal response (decay times of ~200 ms)[25].

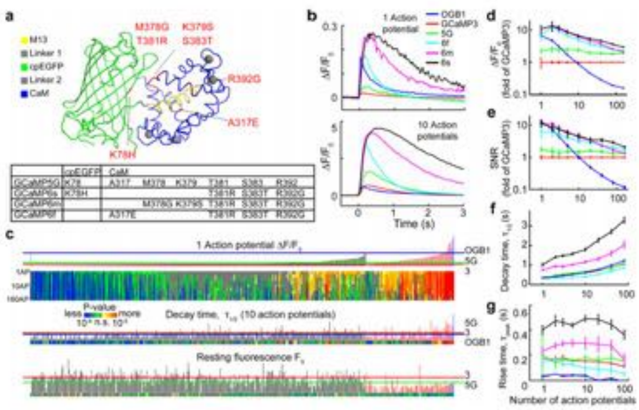

Figure 3: Ultrasensitive Ca^{2+} sensors from the 6th generation development cycle of GCaMPs designed at Janelia HHMI. The structure of GCaMP protein is shown in panel a. Panel b demonstrates the ability of the GCaMP6 series of GECIs to resolve a single action potential and their comparative performance with respect to GCaMP3 and the synthetic indicator Oregon Green Bapta (OGB1) (reproduced from [25]).

Optogenetics and the manipulation of cell permeability control of cell behaviour with light

In parallel to the advances in the design of fluorescent proteins sensors, there has been another revolution initiated by the discovery of microbial opsin proteins that can be used to manipulate membrane potential and cell physiology with light. This burgeoning field, known as optogenetics, developed from the study of proteins that detect light in the primitive eye spot of the algae *Chlamydomonas reinhardtii* and other microorganisms. The discovery that these proteins were directly light-gated ion channels [26, 27] and their immediate use to control membrane potential and excitability in mammalian neurons *in vitro* [28, 29] and *in vivo* [30] led to an explosion of applications in a number of fields ranging from systems and behavioural neuroscience, to prosthetic devices and human therapeutics.

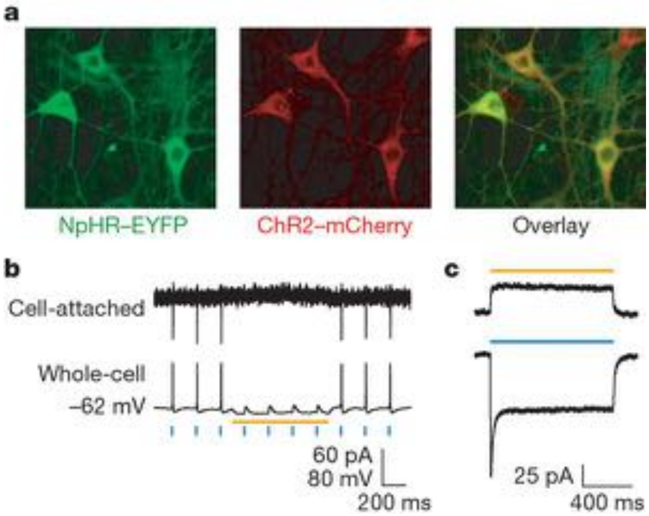

Figure 4: Optogenetics as a tool to control neuronal excitability. Here neurons are expressing both the yellow light-gated Cl^- channel NpHR and the blue light-gated Ca^{2+} channel ChR2, as shown by the overlays of fluorescent-fusion protein markers in panel a.. Panel b shows electrophysiological recordings of action potentials caused by 15ms pulses of blue light and the subsequent silencing of this neuronal activity by continuous pulse of yellow light. (reproduced from [31])

The challenge of causing a spatially selective, transient permeability of the plasma membrane to ions will be familiar to researchers with backgrounds in electroporation; however, the means and selectivity by which optogenetics accomplishes this end differs considerably. The expression of microbial opsin proteins in mammalian cells allows one to control specific currents depending on the particular opsin and the wavelength of light used. For example, a neuron can be made to express both Channelrhodopsin-2 (ChR2), a light gated ion channel primarily selective for Ca^{2+} and sensitive to 470 nm blue light, and the Halorhodopsin (NpHR), an ion channel that gates a Cl^- current and that is sensitive to 570 nm yellow light. Using either lasers or light emitting diodes, one can depolarize or hyperpolarize the membrane potential, thereby either exciting or silencing neuronal activity, respectively (Fig. 4)[31]. Further, using specific promoters to target genetically identical subsets of neurons in the brain, one can control populations of neurons that are heterogeneous and spatially proximal using pulses of different coloured light. The ability to genetically target microbial opsins, their differential selectivity to specific ions, and their precise spatial and temporal control by visible light, together make optogenetics a formidable approach for manipulating cell physiology *in vitro* and *in vivo*.

Whilst the initial uses of optogenetics over the last 10 years have been focused on the manipulation of cell excitability for the control of neurons, there are several recent applications of these tools in oncology research [32]. A comprehensive review of the field of optogenetics is beyond the scope of this paper; however, there are excellent reviews written on the optogenetic toolkit and its widespread applications [29, 33].

In the present context, a brief synopsis of optogenetics was also provided to introduce a new series of fluorescent proteins also derived from microbial opsins that report cellular membrane potential.

Genetically encoded voltage indicators

In the same spirit of GECI research, the development of genetically-encoded voltage indicators (GEVIs) has progressed significantly in the last 10 years due to advances in molecular engineering and the design of several sensors based on newly discovered voltage-sensitive proteins. Much like synthetic Ca^{2+} indicators, voltage-sensitive fluorescent indicators have been around for many years and were largely pioneered by an individual who worked through a great number of optical techniques for measuring the electrical activity of neurons [34]. Many further synthetic probes were developed over the last 30 years, but none are suitable for the measurement of *in vivo* over long periods of time.

As it stands, most of the faster voltage-sensitive indicators, like ANEPs and hemicyanine dyes (di-4-ANEPPS and di-8-ANEPPS, ANNINE-6) [35-37], exhibit small relative changes in fluorescence per mV, whilst dyes that show larger changes in fluorescence, such as carbocyanine and oxonol dyes [38], have slow response times. This is a simplistic explanation and there are more thorough descriptions of the strengths and weakness of these indicators elsewhere [39]. Fortunately, a similar trend in the neuroscience community is currently pushing GEVI technology forward as investigators seek to measure large networks of neurons by the optical readout of electrical activity. Meanwhile, the established potentiometric indicators have nonetheless proved to be highly useful tools in neurophysiology, as well as, in the specific study of pulsed electric fields effects on the plasma membrane potential in bioelectrics research [40-43].

GEVIs are typically engineered using voltage-sensing domains from either ion channels, voltage-sensitive phosphatases or microbial opsins. The first GEVI, FlaSH, was designed by fusing the shaker voltage-gated K^{+} channel to GFP [44]. However, rather than focusing on the progression GEVIs over the last 10 years, the current classes of GEVIs will be presented following the organization of a recent review that presents both historical and detailed mechanistic details of these sensors [45]. As shown in Fig. 5, GEVIs can be organized into several families, including the early sensors that were made by the insertion of fluorescent proteins into ion channels (FlaSH, SPARC, FlASH split), those that have isolated voltage-sensor domains coupled to a FRET-based sensor (VSFP1/2s), FRET-based butterfly sensors, circularly permuted VSFPs or single fluorescent proteins (VSFP3s). In each of these cases the voltage-sensors typically used were the S1-S6 or S1-S4 domains from Kv potassium channels or the voltage-sensitive domains from the Voltage-sensitive phosphatase of *Ciona intestinalis* [46], a similar voltage sensor without a native channel. In each of the above variants, the response time constants of these GEVIs are in the order of 1-2ms with associated relative changes of fluorescence in the order of 22% per 50 mV.

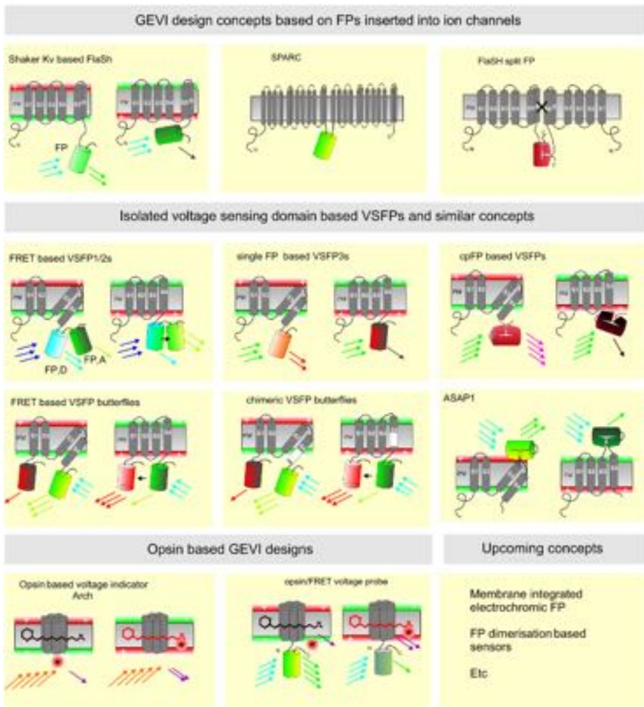

Figure 5: The classes of genetically-encoded voltage indicators (GEVIs) (reproduced from [45])

An interesting and very different set of GEVIs have been designed using the microbial opsin archaerhodopsin (ARCH) [47, 48]. These probes are more related to the previously discussed optogenetic opsin probes as they are derived from a light-gated proton channel with a mutated channel domain. This change led to a discovery of a voltage-sensitive fluorescence caused by a proton transfer in the transient excited state of the retinal chromophore [48]. Variants of these GEVIs, known as QuasAr1 and QuasAr2, are the fastest and brightest probes so far with on and off constants in the range of 100 µs and relative change in fluorescence of ~60% per 100 mV. A further strength of these tools is that they emit red fluorescence and can therefore be combined with the blue excited light-sensitive optogenetic channel ChR2 for an all optical pump and probe approach to electrophysiology [49]. Unfortunately, QuasArs are very dim and have a low quantum yield (~ 1/1000 that of GFP). Further, these probes cannot be used for *in vivo* imaging as they have poor two-photon cross sections and cannot be excited by infrared lasers (personal communication A. Cohen).

In summary, there are currently a number of very promising genetically-encoded fluorescent indicators for measuring Ca^{2+} signals and voltage that are bright, sensitive and suited to measurements at 37°C, as well as, tools for manipulating cell physiology with light. Altogether, in the current usage these GECIs, GEVIs and opsin light-activators are now described as Optogenetics tools in a highly dynamic area of research where many other sensors and actuators are under development (see for example the online resource with extensive links for acquiring molecular tools and hardware at http://www.openoptogenetics.org/).

IN VIVO IMAGING WITH MULTIPHOTON MICROSCOPY

With the current set of genetically-encoded indicators, it is now very feasible to perform imaging experiments over days, weeks and months. Whether the experiments are the optical recording electrical activity in the brain, or the measurement of Ca^{2+} dysregulation and membrane potential following the treatment of tumors with pulsed electric fields, it is now possible to study neuro- and pathophysiology under nearly *in vivo* conditions over long periods. However, in order to take advantage fluorescent sensors like GECIs and GEVIs *in vivo*, it is necessary to use a specific type of fluorescence microscopy suited to thick samples.

Light microscopy is typically limited to thin samples such as cells cultured on glass, *in vitro*, due to the absorption and scattering of visible light in thicker tissues. Fluorescence microscopy is therefore only practical in the upper layers of tissue (~150 µm). An optical window exists, however, where there is little absorption of light by tissue between 700 and 900 nm in the near infrared range (Fig. 6).

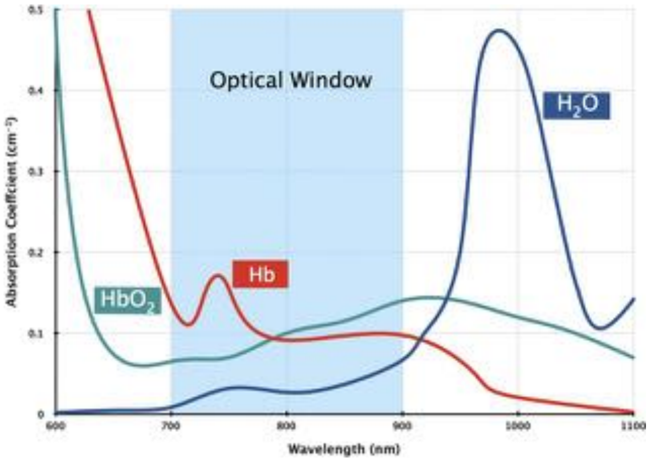

Figure 6: An optical transmission window exists in tissue is the near infrared between 700-900nm (reproduced from [50]).

Multiphoton excitation fluorescence microscopy

In 1990, Denk demonstrated a new type of fluorescence microscopy suited to deeper tissue imaging where fluorescent molecules were excited by a two-photon process using an ultrafast pulsed infrared laser in the near infrared range [51]. The two-photon absorption of fluorescent molecules can occur when a molecule is excited by two photons instead of a single photon having equivalent energy; for example, if a fluorophore like GFP is normally excited by a photon of blue light at 450 nm, the simultaneous absorption of two photons of 900 nm infrared light has the equivalent energy and can cause the same excitation process. The probability of such a two-photon process is low, but it increases when the photons arrive in intense ultrashort bursts from a mode-locked ~100 femtosecond pulsed Titanium Sapphire laser. This technique was very rapidly applied for the *in vivo* imaging of vasculature [52] and neurons in the intact brain [53], and has since been used in thousands of investigations in neuroscience with more recent adoption in immunology [50] and experimental oncology [54].

Two-photon absorption processes depend on the square of the photon flux [55], which therefore confines the excitation to a small volume at the focus of the objective. This confers an inherent optical sectioning capability and can be observed in Fig. 7, where the linear fluorescence excitation of a fluorescein sample in a cuvette leads to an excitation cone with a 488 nm laser. The two-photon excitation of the same sample by femtosecond pulsed 960 nm light shows only excitation at the focal point. Two-photon microscopy is therefore a highly useful multiphoton, nonlinear process and one of a number of other types of nonlinear microscopy including 2nd harmonic and CARS imaging [56]. The resolution is similar to that of confocal microscopy in the X-Y plane at ~300 nm, but is slightly less at ~0.9 μm in the Z dimension.

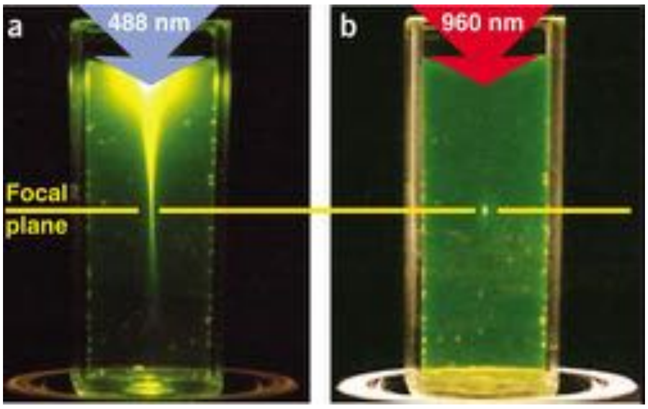

Figure 7: Linear excitation of fluorescein compared to the two-photon excitation of the same sample with a femtosecond pulsed infrared laser. Excitation only at the focal point gives two-photon excitation microscopy (reproduced from [56])

Multiphoton imaging with GECIs

Some of the pioneers of multiphoton imaging have been strong proponents of the development and use of GECIs [24], so it is not surprising that these tools have been rapidly adopted and showcased using these imaging techniques. At present, there are dozens of published examples showing how well GECIs perform with multiphoton imaging in *in vivo* in experiments performed in fly, zebrafish, worm and mouse transgenic lines expressing GECIs [24, 57, 58]. Plasmids and viral vectors for the delivery of these molecular tools are also readily available online at distribution resources like http://www.addgene.org/.

Multiphoton imaging in bioelectrics research

There are presently few examples of the application of multiphoton imaging to study pulsed electric field or electroporation related effects. It might be expected that this approach would be beneficial in applications where intravital *in vivo* imaging has previously provided insights [59-63] and where further resolution in the z-depth, 3D volume reconstruction or dynamic tracking is desired. It is important, however, to balance the added information gained using multiphoton imaging over conventional intravital imaging, since it comes with a significant instrumentation cost and other challenges associated with analysing large, complex 4D datasets.

Our group at XLIM are particularly interested in combining multiphoton imaging with GECIs and GEVIs in order to investigate changes in physiological parameters such as cytosolic Ca^{2+} and membrane potential in the solid tumor microenvironment with growth, angiogenesis and metastasis. In addition, we are actively using this imaging approach to study the response of vascularized tumor spheroids expressing GECIs to nanosecond pulsed electric fields.

Perspective and conclusion

The particular strengths of multiphoton imaging is its capacity to study 3D volumes with subcellular resolution and to visualize volumes in complex tissues over time. There are practical limits to the actual depth of imaging achievable with two-photon microscopy which are fixed ~650-700 μm due to the contribution of the out-of-focus fluorescent background. It is therefore unlikely that multiphoton imaging will displace other preclinical imaging modalities such as CT, MRI or ultrasound considering the reach of these techniques. Nevertheless, there are few techniques that give the dynamic structural and functional information at the cellular level that *in vivo* multiphoton imaging provides, and given the growing toolkit of genetically encoded indicators being developed, the future of optophysiology is exciting, even if bounded by questions posed in 500 μm^3 at a time.

REFERENCES

[1] L. Technologies and R. P. Haugland, Molecular Probes Handbook, A Guide to Fluorescent Probes and Labeling Technologies, 11th Edition: Life Technologies, 2010.

[2] L. Homolya, Z. Holló, U. A. Germann, I. Pastan, M. M. Gottesman, and B. Sarkadi, "Fluorescent cellular indicators are extruded by the multidrug resistance protein," Journal of Biological Chemistry, vol. 268, pp. 21493-21496, October 15, 1993 1993.

[3] D. Thomas, S. C. Tovey, T. J. Collins, M. D. Bootman, M. J. Berridge, and P. Lipp, "A comparison of fluorescent Ca2+ indicator properties and their use in measuring elementary and global Ca2+ signals," Cell Calcium, vol. 28, pp. 213-23, Oct 2000.

A. E. Oliver, G. A. Baker, R. D. Fugate, F. Tablin, and J. H. Crowe, "Effects of temperature on calcium-sensitive fluorescent probes," Biophys J, vol. 78, pp. 2116-26, Apr 2000.

[4] D. Moreau, C. Lefort, R. Burke, P. Leveque, and R. P. O'Connor, "Rhodamine B as an optical thermometer in cells focally exposed to infrared laser light or nanosecond pulsed electric fields," Biomedical Optics Express, vol. 6, pp. 4105-4117, 2015/10/01 2015.

[5] T. Kotnik and D. Miklavcic, "Theoretical evaluation of the distributed power dissipation in biological cells exposed to electric fields," Bioelectromagnetics, vol. 21, pp. 385-94, Jul 2000.

[6] M. Chalfie, Y. Tu, G. Euskirchen, W. W. Ward, and D. C. Prasher, "Green fluorescent protein as a marker for gene expression," Science, vol. 263, pp. 802-5, Feb 11 1994.

[7] R. Y. Tsien, "The green fluorescent protein," Annu Rev Biochem, vol. 67, pp. 509-44, 1998.

[8] J. Lippincott-Schwartz and G. H. Patterson, "Fluorescent proteins for photoactivation experiments," Methods Cell Biol, vol. 85, pp. 45-61, 2008.
[9] K. A. Lukyanov, D. M. Chudakov, S. Lukyanov, and V. V. Verkhusha, "Innovation: Photoactivatable fluorescent proteins," Nat Rev Mol Cell Biol, vol. 6, pp. 885-91, Nov 2005.
[10] E. Betzig, G. H. Patterson, R. Sougrat, O. W. Lindwasser, S. Olenych, J. S. Bonifacino, et al., "Imaging Intracellular Fluorescent Proteins at Nanometer Resolution," Science, vol. 313, pp. 1642-1645, September 15, 2006 2006.
A. Minta, J. P. Kao, and R. Y. Tsien, "Fluorescent indicators for cytosolic calcium based on rhodamine and fluorescein chromophores," J Biol Chem, vol. 264, pp. 8171-8, May 15 1989.
[11] Minta and R. Y. Tsien, "Fluorescent indicators for cytosolic sodium," J Biol Chem, vol. 264, pp. 19449-57, Nov 15 1989.
[12] M. Poenie and R. Tsien, "Fura-2: a powerful new tool for measuring and imaging [Ca2+]i in single cells," Prog Clin Biol Res, vol. 210, pp. 53-6, 1986.
[13] R. Y. Tsien, T. Pozzan, and T. J. Rink, "Calcium homeostasis in intact lymphocytes: cytoplasmic free calcium monitored with a new, intracellularly trapped fluorescent indicator," J Cell Biol, vol. 94, pp. 325-34, Aug 1982.
A. Miyawaki, J. Llopis, R. Heim, J. M. McCaffery, J. A. Adams, M. Ikura, et al., "Fluorescent indicators for Ca2+ based on green fluorescent proteins and calmodulin," Nature, vol. 388, pp. 882-7, Aug 28 1997.
[14] O. Garaschuk, O. Griesbeck, and A. Konnerth, "Troponin C-based biosensors: a new family of genetically encoded indicators for in vivo calcium imaging in the nervous system," Cell Calcium, vol. 42, pp. 351-61, Oct-Nov 2007.
[15] N. Heim and O. Griesbeck, "Genetically encoded indicators of cellular calcium dynamics based on troponin C and green fluorescent protein," J Biol Chem, vol. 279, pp. 14280-6, Apr 2 2004.
[16] J. Nakai, M. Ohkura, and K. Imoto, "A high signal-to-noise Ca(2+) probe composed of a single green fluorescent protein," Nat Biotechnol, vol. 19, pp. 137-41, Feb 2001.
[17] Y. Zhao, S. Araki, J. Wu, T. Teramoto, Y. F. Chang, M. Nakano, et al., "An expanded palette of genetically encoded Ca(2)(+) indicators," Science, vol. 333, pp. 1888-91, Sep 30 2011.
[18] V. Perez Koldenkova and T. Nagai, "Genetically encoded Ca(2+) indicators: properties and evaluation," Biochim Biophys Acta, vol. 1833, pp. 1787-97, Jul 2013.
[19] J. Akerboom, T. W. Chen, T. J. Wardill, L. Tian, J. S. Marvin, S. Mutlu, et al., "Optimization of a GCaMP calcium indicator for neural activity imaging," J Neurosci, vol. 32, pp. 13819-40, Oct 3 2012.
[20] J. Akerboom, J. D. Rivera, M. M. Guilbe, E. C. Malave, H. H. Hernandez, L. Tian, et al., "Crystal structures of the GCaMP calcium sensor reveal the mechanism of fluorescence signal change and aid rational design," J Biol Chem, vol. 284, pp. 6455-64, Mar 6 2009.
[21] L. Tian, S. A. Hires, T. Mao, D. Huber, M. E. Chiappe, S. H. Chalasani, et al., "Imaging neural activity in worms, flies and mice with improved GCaMP calcium indicators," Nat Methods, vol. 6, pp. 875-81, Dec 2009.
[22] T. W. Chen, T. J. Wardill, Y. Sun, S. R. Pulver, S. L. Renninger, A. Baohan, et al., "Ultrasensitive fluorescent proteins for imaging neuronal activity," Nature, vol. 499, pp. 295-300, Jul 18 2013.
[23] G. Nagel, D. Ollig, M. Fuhrmann, S. Kateriya, A. M. Musti, E. Bamberg, et al., "Channelrhodopsin-1: a light-gated proton channel in green algae," Science, vol. 296, pp. 2395-8, Jun 28 2002.
[24] G. Nagel, T. Szellas, W. Huhn, S. Kateriya, N. Adeishvili, P. Berthold, et al., "Channelrhodopsin-2, a directly light-gated cation-selective membrane channel," Proc Natl Acad Sci U S A, vol. 100, pp. 13940-5, Nov 25 2003.
[25] E. S. Boyden, F. Zhang, E. Bamberg, G. Nagel, and K. Deisseroth, "Millisecond-timescale, genetically targeted optical control of neural activity," Nat Neurosci, vol. 8, pp. 1263-8, Sep 2005.
[26] F. Zhang, L. P. Wang, E. S. Boyden, and K. Deisseroth, "Channelrhodopsin-2 and optical control of excitable cells," Nat Methods, vol. 3, pp. 785-92, Oct 2006.
[27] R. Arenkiel, J. Peca, I. G. Davison, C. Feliciano, K. Deisseroth, G. J. Augustine, et al., "In vivo light-induced activation of neural circuitry in transgenic mice expressing channelrhodopsin-2," Neuron, vol. 54, pp. 205-18, Apr 19 2007.
[28] F. Zhang, L. P. Wang, M. Brauner, J. F. Liewald, K. Kay, N. Watzke, et al., "Multimodal fast optical interrogation of neural circuitry," Nature, vol. 446, pp. 633-9, Apr 5 2007.
A. Ingles-Prieto, E. Reichhart, K. Schelch, H. Janovjak, and M. Grusch, "The optogenetic promise for oncology: Episode I," Molecular & Cellular Oncology, vol. 1, p. e964045, 2014/12/08 2014.
[29] L. Fenno, O. Yizhar, and K. Deisseroth, "The development and application of optogenetics," Annu Rev Neurosci, vol. 34, pp. 389-412, 2011.
[30] L. B. Cohen and B. M. Salzberg, "Optical measurement of membrane potential," Rev Physiol Biochem Pharmacol, vol. 83, pp. 35-88, 1978.
[31] E. Fluhler, V. G. Burnham, and L. M. Loew, "Spectra, membrane binding, and potentiometric responses of new charge shift probes," Biochemistry, vol. 24, pp. 5749-5755, 1985/10/01 1985.
[32] P. Fromherz, G. Hübener, B. Kuhn, and M. J. Hinner, "ANNINE-6plus, a voltage-sensitive dye with good solubility, strong membrane binding and high sensitivity," European Biophysics Journal, vol. 37, pp. 509-514, 07/10/accepted 2008.
[33] P. Yan, C. D. Acker, W.-L. Zhou, P. Lee, C. Bollensdorff, A. Negrean, et al., "Palette of fluorinated voltage-sensitive hemicyanine dyes," Proceedings of the National Academy of Sciences of the United States of America, vol. 109, pp. 20443-20448, 11/20 2012.
[34] T. Brauner, D. F. Hulser, and R. J. Strasser, "Comparative measurements of membrane potentials with microelectrodes and voltage-sensitive dyes," Biochim Biophys Acta, vol. 771, pp. 208-16, Apr 11 1984.
A. Grinvald, R. D. Frostig, E. Lieke, and R. Hildesheim, "Optical imaging of neuronal activity," Physiol Rev, vol. 68, pp. 1285-366, Oct 1988.
[35] G. Pucihar, T. Kotnik, and D. Miklavcic, "Measuring the induced membrane voltage with Di-8-ANEPPS," J Vis Exp, 2009.
[36] G. Pucihar, T. Kotnik, B. Valic, and D. Miklavcic, "Numerical determination of transmembrane voltage induced on irregularly shaped cells," Ann Biomed Eng, vol. 34, pp. 642-52, Apr 2006.

[37] J. A. White, U. Pliquett, P. F. Blackmore, R. P. Joshi, K. H. Schoenbach, and J. F. Kolb, "Plasma membrane charging of Jurkat cells by nanosecond pulsed electric fields," Eur Biophys J, vol. 40, pp. 947-57, Aug 2011.

A. Silve, S. Rocke, and W. Frey, "Image processing for non-ratiometric measurement of membrane voltage using fluorescent reporters and pulsed laser illumination," Bioelectrochemistry, vol. 103, pp. 39-43, Jun 2015.

[38] M. S. Siegel and E. Y. Isacoff, "A genetically encoded optical probe of membrane voltage," Neuron, vol. 19, pp. 735-41, Oct 1997.

[39] W. Akemann, C. Song, H. Mutoh, and T. Knöpfel, "Route to genetically targeted optical electrophysiology: development and applications of voltage-sensitive fluorescent proteins," Neurophotonics, vol. 2, pp. 021008-021008, 2015.

[40] Y. Murata, H. Iwasaki, M. Sasaki, K. Inaba, and Y. Okamura, "Phosphoinositide phosphatase activity coupled to an intrinsic voltage sensor," Nature, vol. 435, pp. 1239-43, Jun 30 2005.

[41] J. M. Kralj, A. D. Douglass, D. R. Hochbaum, D. Maclaurin, and A. E. Cohen, "Optical recording of action potentials in mammalian neurons using a microbial rhodopsin," Nat Methods, vol. 9, pp. 90-5, Jan 2012.

[42] Maclaurin, V. Venkatachalam, H. Lee, and A. E. Cohen, "Mechanism of voltage-sensitive fluorescence in a microbial rhodopsin," Proc Natl Acad Sci U S A, vol. 110, pp. 5939-44, Apr 9 2013.

[43] R. Hochbaum, Y. Zhao, S. L. Farhi, N. Klapoetke, C. A. Werley, V. Kapoor, et al., "All-optical electrophysiology in mammalian neurons using engineered microbial rhodopsins," Nat Methods, vol. 11, pp. 825-33, Aug 2014.

[44] T. G. Phan and A. Bullen, "Practical intravital two-photon microscopy for immunological research: faster, brighter, deeper," Immunol Cell Biol, vol. 88, pp. 438-44, May-Jun 2010.

[45] W. Denk, J. H. Strickler, and W. W. Webb, "Two-photon laser scanning fluorescence microscopy," Science, vol. 248, pp. 73-6, Apr 6 1990.

[46] Kleinfeld, P. P. Mitra, F. Helmchen, and W. Denk, "Fluctuations and stimulus-induced changes in blood flow observed in individual capillaries in layers 2 through 4 of rat neocortex," Proc Natl Acad Sci U S A, vol. 95, pp. 15741-6, Dec 22 1998.

[47] Helmchen, K. Svoboda, W. Denk, and D. W. Tank, "In vivo dendritic calcium dynamics in deep-layer cortical pyramidal neurons," Nat Neurosci, vol. 2, pp. 989-96, Nov 1999.

[48] J. Liu, "Two-photon microscopy in pre-clinical and clinical cancer research," Frontiers of Optoelectronics, vol. 8, pp. 141-151, 2015/06/01 2015.

[49] Helmchen and W. Denk, "Deep tissue two-photon microscopy," Nat Methods, vol. 2, pp. 932-40, Dec 2005.

[50] W. R. Zipfel, R. M. Williams, and W. W. Webb, "Nonlinear magic: multiphoton microscopy in the biosciences," Nat Biotechnol, vol. 21, pp. 1369-77, Nov 2003.

[51] Dana, T. W. Chen, A. Hu, B. C. Shields, C. Guo, L. L. Looger, et al., "Thy1-GCaMP6 transgenic mice for neuronal population imaging in vivo," PLoS One, vol. 9, p. e108697, 2014.

[52] A. Zariwala, B. G. Borghuis, T. M. Hoogland, L. Madisen, L. Tian, C. I. De Zeeuw, et al., "A Cre-dependent GCaMP3 reporter mouse for neuronal imaging in vivo," J Neurosci, vol. 32, pp. 3131-41, Feb 29 2012.

[53] F. M. Andre, J. Gehl, G. Sersa, V. Preat, P. Hojman, J. Eriksen, et al., "Efficiency of high- and low-voltage pulse combinations for gene electrotransfer in muscle, liver, tumor, and skin," Hum Gene Ther, vol. 19, pp. 1261-71, Nov 2008.

[54] E. Bellard, B. Markelc, S. Pelofy, F. Le Guerroue, G. Sersa, J. Teissie, et al., "Intravital microscopy at the single vessel level brings new insights of vascular modification mechanisms induced by electropermeabilization," J Control Release, vol. 163, pp. 396-403, Nov 10 2012.

[55] M. Cemazar, M. Golzio, J. M. Escoffre, B. Couderc, G. Sersa, and J. Teissie, "In vivo imaging of tumor growth after electrochemotherapy with cisplatin," Biochem Biophys Res Commun, vol. 348, pp. 997-1002, Sep 29 2006.

[56] M. Cemazar, M. Golzio, G. Sersa, P. Hojman, S. Kranjc, S. Mesojednik, et al., "Control by pulse parameters of DNA electrotransfer into solid tumors in mice," Gene Ther, vol. 16, pp. 635-44, May 2009.

[57] B. Markelc, E. Bellard, G. Sersa, S. Pelofy, J. Teissie, A. Coer, et al., "In vivo molecular imaging and histological analysis of changes induced by electric pulses used for plasmid DNA electrotransfer to the skin: a study in a dorsal window chamber in mice," J Membr Biol, vol. 245, pp. 545-54, Sep 2012.

ACKNOWLEDGEMENTS

This work was supported by LabEx SigmaLim, the French National Research Agency (ANR), Region Limousin and the CNRS. The research presented was conducted in the scope of LEA EBAM.

Rod O'Connor was born in Stirling, Scotland in the United Kingdom in 1971. He received his BSc and MSc in Neuroscience from Laurentian University in Canada. His PhD research was completed in Molecular Signalling and Cell Physiology at the Babraham Institute of the University of Cambridge, where he applied fluorescence microscopy techniques to study the cellular effects of visible light and radiofrequency electromagnetic fields. Thereafter, he held a Marie Curie fellowship on the application of multiphoton microscopy for imaging and manipulating the brain *in vivo* with femtosecond lasers (European Laboratory for Nonlinear Spectroscopy, Florence, Italy), and later developed fiber optic methods for stimulating the brain with light *in vivo* using optogenetics (Janelia Research Campus, HHMI, Ashburn,VA). He currently holds the Sigma-Lim LABEX Excellence Chair in Bioengineering at the XLIM Research Institute in Limoges, France.

NOTES

NOTES

NOTES

Electrical Impedance and Electroporation

Antoni Ivorra
Universitat Pompeu Fabra, Department of Information and Communication Technologies, Barcelona, Spain

Abstract: The electrical impedance of biological matter is also known as electrical bioimpedance or simply as bioimpedance. Although it is not physiologically relevant *per se*, electrical bioimpedance can indirectly reflect some conditions and events which are interesting for biomedicine. As a matter of fact, bioimpedance measurements depend on many physiological parameters and phenomena. This lack of specificity can be an important drawback of electrical impedance methods. On the other hand, impedance measurement is well suited for clinical applications because it is minimally invasive and it yields real-time data with simple and practical implementations. One of those potential applications can be monitoring of electroporation, both *in vitro* and *in vivo*, as a way to assess electroporation effectiveness. In this lecture, departing from basic concepts and minimizing technicalities taking into consideration the broad audience of the course, I will briefly overview the accumulated knowledge on this topic with particular emphasis on my own experimental results. A significant conclusion I have drawn from my experimental studies on the topic is that conductivity measured shortly after treatment may be correlated with electroporation effectiveness in terms of cell membrane permeabilization. That is, it has the potential to be used as an electroporation effectiveness indicator. On the other hand, dynamic conductivity during the electroporation pulses, which is much easier to be measured, does not seem to be correlated with electroporation effectiveness.

BASIC CONCEPTS

Most readers will be familiar with the concept of resistance. However, terms such as conductivity, permittivity, impedance and phase angle may be unfamiliar to others or may be barely remembered. The goal of this first section is to try to establish a common ground for all readers through a brief overview of basic concepts. Those familiar with electromagnetism or circuit theory can skip this section without hesitation.

If an electrically conductive path exists between two points (terminals) with different voltages (i.e. different levels of electric potential energy) then free electric charges will move from the high energy position to the low energy position. In this scenario, the electric current value indicates the amount of electric charge that goes through a cross-section of the electric path per second. That is, the flow of electric charges. Traditionally, an analogy with fluidic elements has been employed in order to illustrate the voltage and the electric current concepts: the hydrostatic pressure difference (analogy for the voltage difference) between two liquid tanks at different heights causes the liquid (analogy for the electrical charge) to flow through a pipe that connects both tanks. This analogy is also useful to explain the electrical resistance concept: flow will not only depend on pressure difference between the tanks but also on the viscosity of the liquid and on the pipe diameter and length; the shorter and wider the pipe is, the larger the flow is. A lot of materials exhibit a linear relationship between the electric current and the voltage difference. This relationship is known as the Ohm's law and the constant that relates both parameters is the resistance, R, which is expressed in ohms (Ω):

$$v = iR, \tag{1}$$

where v is the voltage difference between the two terminals of the conductor, expressed in volts (V), and i is the current, expressed in amperes (A), at any given time.

Figure 1: Circuit symbol for resistance.

Conductors in series (i.e. one after the other) exhibit a combined resistance, R_T, equal to the summation of their individual resistances, as pipes in a fluidic system would do:

$$R_T\big|_{in\ series} = R_1 + R_2 + \ldots + R_n, \tag{2}$$

whereas conductors in parallel (sharing input and output) exhibit a combined resistance equal to:

$$R_T\big|_{parallel} = R_1 // R_2 // \ldots // R_n = \frac{1}{\frac{1}{R_1} + \ldots + \frac{1}{R_n}}, \tag{3}$$

as parallel pipes in a fluidic system would do (by increasing the number of parallel pipes their combined resistance decreases).

The resistance depends on an intrinsic property of the material that forms the conductive path known as the resistivity, ρ, which is expressed in (Ω.m). In terms of the fluidic analogy, it can be though as analogous to the viscosity of the fluid. The relation between the resistance and the resistivity for a uniform wire would be:

$$R = \rho \frac{l}{A}, \tag{4}$$

where A is the cross section area of the wire (m^2) and l is the length of the wire (m). In general, for any conductor with an arbitrary geometry, the resistance and the resistivity will be related by a geometrical constant, k, expressed in (m^{-1}):[3]

$$R = \rho k, \tag{5}$$

This constant k is known as the cell constant because it depends on the geometry of the measurement cell in which a material is characterized. Measurement cells typically consist of two metallic flat electrodes across a cuvette in which the material is confined ($k = l/A$). However, two needle electrodes inserted into a living tissue also constitute a measurement cell. In this case, since the tissue is not confined and it can be approximated that it extends infinitely, the cell constant depends on the geometry of the electrodes rather than on the geometry of the sample. For a few simple geometries it is possible to find closed analytical expressions for obtaining k (similar to equation 4). In most cases, however, it will be necessary to compute the cell constant by numerical methods or to find it by measuring the resistance of a sample with a well known conductivity. For instance, in the field of bioimpedance the solution 0.9% NaCl is typically used because its composition and conductivity (1.44 S/m at 20ºC) are similar to those of blood plasma.

The Ohm's law can also be written in infinitesimal terms (i.e. for each point in a continuous material):

$$\mathbf{J} = \frac{1}{\rho}\mathbf{E}, \tag{6}$$

where the vector **J** is the current density, expressed in (A/m^2), and the vector **E** is the electric field, expressed in (V/m).

The resistance and the resistivity are the inverse of the conductance, G, and of the conductivity, σ, respectively.

Table 1: Resistance, resistivity, conductance and conductivity.

value	symbol(s)	unit(s)	expressions
resistance	R	Ω	$R = v/i$
resistivity	ρ	Ω.m	$\rho = R/k$
conductance	G	Ω^{-1}, S (siemens)	$G = 1/R$
conductivity	σ, κ	S/m	$\sigma = 1/\rho$

[3] It must be noted that in some studies the cell constant is instead defined as k=ρ/R (inverse of the definition used here) and it is expressed in (m).

Some materials rather than being able to conduct charge help to store charge. These materials are known as dielectrics.

Any conductor is able to store some charge but the storage capacity is much larger for the combination of two separated conductors. In particular, the charge storage capacity, known as capacitance, C, and expressed in farads (F), of two parallel flat conductors (Fig. 2) is:

$$C = \varepsilon \frac{A}{d} = \varepsilon_r \varepsilon_0 \frac{A}{d}, \tag{7}$$

where A is the area of the conductors, d is the separation distance between them and ε is the permittivity of the dielectric material between the two conductors. If no material is present (i.e. vacuum) the permittivity is ε_0 = 8.8541× 10^{-12} F/m. Dielectric materials have relative permittivity, ε_r, values above 1. For instance, the relative permittivity of water at 20 ºC is 80, that of glycerol is 47 and that of glass and most common synthetic plastics is between 2 a 10.

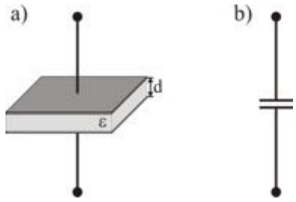

Figure 2: a) Two plate capacitor, b) circuit symbol for capacitance.

The structure formed by two conductors separated by a dielectric is known as capacitor and the charge, Q, accumulated into it is:

$$Q = CV, \tag{8}$$

where V is the voltage difference across the two conductors. In an ideal dielectric (i.e. infinite resistivity) no free charges will flow across the two conductors. However, if time varying voltage is applied, charge can flow in and out from the conductors thereby causing a time varying current that apparently goes through the capacitor:

$$Q = CV \Rightarrow \frac{dQ}{dt} = C\frac{dV}{dt} \Rightarrow i = C\frac{dV}{dt}, \tag{9}$$

This current is known as a displacement current and it must be noted that it does not correspond to an actual flow of charges through the dielectric, it corresponds to charge being stored and charge being released.

If the voltage applied across the capacitor has a sinusoidal dependence with time, t,

$$v(t) = V_p \sin(2\pi f t), \tag{10}$$

where V_p is the amplitude of the sinusoidal voltage and f is its frequency, then the displacement current through the capacitor will also be sinusoidal

$$i(t) = C\frac{dv(t)}{dt} = 2\pi fCV_p \sin(2\pi ft + \frac{\pi}{2}), \quad (11)$$

with an amplitude dependant on the frequency and on the capacitance ($2\pi fC$) and with a relative angle shift, ($\pi/2$), with respect to the applied voltage. In general, in any circuit composed of resistances and capacitances, when the excitatory signal is a sinusoidal current or voltage, all the resulting voltages and currents will be sinusoidal signals with the same frequency of the excitatory signal, only differences in magnitude (amplitude) and phase angle (angle shift ≈ delay) will be observed.

Now it is possible to define the impedance (**Z**). The impedance of an element at a certain frequency is defined as the relation between the sinusoidal voltage and the current for that frequency. Two relations will exist between voltage and current: 1) a relation of amplitudes, known as impedance magnitude or modulus |**Z**|, and 2) a relation of phases, known as phase angle of the impedance $\angle\mathbf{Z}$.

Note that according to equation 11 the impedance magnitude of a capacitance is

$$|\mathbf{Z}_C| = \frac{1}{2\pi fC}, \quad (12)$$

and that this implies that for high frequencies a capacitance will act as a short circuit whereas for low frequencies it will act as an open circuit. Up to a point, in the frequency domain, the behaviour of a capacitance can be assimilated to that of a resistance whose value inversely depends on the frequency.

Materials neither will be ideal conductors nor will be ideal dielectrics. That is, it will be possible to define a conductivity value, σ, and also a permittivity value, ε, for each frequency[4]. These two values are typically referred to as the passive electrical properties of the material. From impedance measurements performed with an electrode setup of known cell constant (k) it is possible to calculate both σ and ε. The expressions that relate these values are listed in table 2. It goes beyond the introductory scope of this section to properly justify these expressions because an overview of basic concepts on complex numbers would be required. Note that the impedance, **Z**, is noted in bold type not because it is a vector – as it was the case of **E** and **J** – but because it is a complex quantity. Readers not familiar with complex notation just need to keep in mind that complex numbers are a mere construct to represent two quantities (e.g. magnitude and phase) which is convenient for mathematical analysis.

Table 2: Expressions relating impedance and the passive electrical properties of materials according to different notations found in the literature.

value	symbol(s)	unit(s)	expressions
impedance magnitude	|**Z**|	Ω	$\lvert\mathbf{Z}\rvert = \sqrt{R^2 + X^2}$
impedance phase	$\angle\mathbf{Z}$	º, rad	$\angle\mathbf{Z} = \arctan(X/R)$
resistance	R	Ω	$R = \lvert\mathbf{Z}\rvert\cos(\angle\mathbf{Z})$
reactance	X	Ω	$X = \lvert\mathbf{Z}\rvert\sin(\angle\mathbf{Z})$
impedance	**Z**	Ω	$\mathbf{Z} = R + jX; \quad j = \sqrt{-1}$
impedivity	**z**	Ω.m	$\mathbf{z} = \mathbf{Z}/k$
admittance	**Y**	Ω^{-1}, S	$\mathbf{Y} = 1/\mathbf{Z}$
conductance	G	Ω^{-1}, S	$G = \lvert\mathbf{Y}\rvert\cos(\angle\mathbf{Y})$
susceptance	B	Ω^{-1}, S	$B = \lvert\mathbf{Y}\rvert\sin(\angle\mathbf{Y})$
admittivity	**y**	S/m	$\mathbf{y} = k\mathbf{Y}$
conductivity	σ, κ	S/m	$\sigma = kG$
permittivity	ε	F/m	$\varepsilon = kB/2\pi f$
complex conductivity	$\boldsymbol{\sigma}$, $\boldsymbol{\kappa}$	S/m	$\boldsymbol{\sigma} = \mathbf{y}\,; \boldsymbol{\sigma} = \sigma' + j\sigma''$
complex permittivity	$\boldsymbol{\varepsilon}$	F/m	$\boldsymbol{\varepsilon} = \boldsymbol{\sigma}/2\pi f\,; \boldsymbol{\varepsilon} = \varepsilon' + j\varepsilon''$

In the two-electrode measurement cells described above, the impedances of the electrodes and of the electrical connections to the electronic measurement system are in series with the impedance that it is intended to be measured. That may distort the measurement. The impedances of the electrical connections are generally negligible (<< 1 **Ω**) in the bioimpedance field but those of the electrodes may be relevant and produce large errors. Under small signal conditions (i.e. when a small voltage or current is applied for non-invasive measurement), an interface impedance appears between the electrode and the electrolyte (biological sample) which can be coarsely approximated by a capacitance in order of 10 μF/cm^2 for flat metallic electrodes[5]. This electrode/electrolyte impedance, which is generally uncontrollable[6] and which cannot be compensated mathematically[7], will

[4] Although σ and ε are defined for each frequency it must be noted that most homogeneous materials exhibit constant σ and ε across large bands of the frequency spectrum. On the other hand, σ and ε of composite materials, such as is the case of biological samples, significantly depend on frequency.

[5] The capacity can be boosted, and hence the impedance magnitude decreased, by increasing the surface area by roughening the electrodes, for instance, by sandblasting or by chemical methods.

[6] For instance this impedance depends on the local concentration of ionic species which is generally uncontrollable, particularly in the case of living tissues. Recently such dependence on ionic concentration has been analyzed in the context of electroporation of cell suspensions [29]

[7] Exception: if a broad impedance spectrogram is recorded with a high dynamic range, then it is possible to subtract the contribution of the electrode/electrolyte impedance from the measured impedance data by fitting the low frequency data to a model of the electrode/electrolyte impedance [30].

have a very significant impact at low frequencies (e.g. <10 kHz). Because of that, impedance measurements of cell suspensions and soft living tissues must be generally performed with the so-called four-electrode method, also referred to as the tetrapolar or Kelvin method, in which the impact of the impedances of the electrodes is minimized – ideally cancelled – by employing a pair of electrodes to inject the measurement current and employing another pair of electrodes for measuring the voltage across the sample.

It must be noted that the concerns and precautions of the above paragraph are only relevant when small voltages (or currents) are applied for measuring impedance before, in between or after the electroporation pulses. During the electroporation pulses large voltages are applied and those force electrochemical reactions to happen at the interface of the electrodes thereby changing the electrode behaviour from capacitive to conductive. That is, during the electroporation pulses the electrodes do not behave as a capacitance but as a low value resistance.

A comprehensive book on all the above concepts and on bioimpedance is [1].

BIOIMPEDANCE OF CELLS AND TISSUES

In 1925, two decades before the lipid bilayer was understood, Fricke [2] was able to hypothesize a reasonable value for the membrane thickness (30 nm instead of the actual 7 nm) by analyzing the passive electrical properties of red blood cells. His calculations were based on an electrical model for the cell and its environment in which the cell membrane was modeled as a dielectric layer and the extracellular and the intracellular media were modeled as conductive materials. The electrical model employed by Fricke is still considered to be a good approximation of the passive electrical properties of a single cell for frequencies up to several megahertz. In this model every infinitesimal portion of the extracellular and intracellular media can be modeled as a resistance and every infinitesimal portion of the membrane is modeled as a capacitance. Circuit theory allows all those elements to be combined to form a simple equivalent circuit as seen from the electrodes: a resistance representing the extracellular medium (R_e) in parallel with the series combination of a capacitance (C_m), which represents the membrane, and another resistance which represents the intracellular medium (R_i). In a tissue or cell suspension the impedance contribution from all cells is combined so that the same electrical model – obviously with different values – can be employed to characterize the impedance behavior as seen from the measurement electrodes.

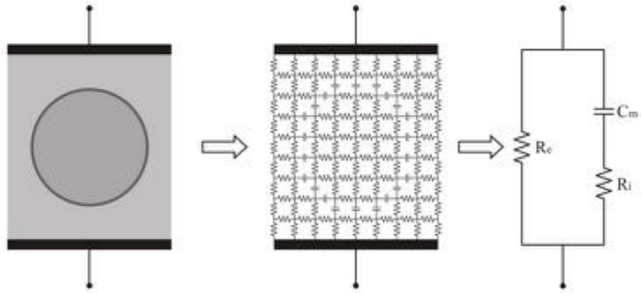

Figure 3: Electrical model for a cell in suspension as seen from the electrodes. Infinitesimal portions of the extracellular and intracellular media can be modeled as resistances and infinitesimal portions of the membrane can be modeled as capacitances. All those elements can be combined in an extracellular resistance (R_e) in parallel with the series combination of a membrane capacitance (C_m) and an intracellular resistance (R_i). The same three-element model can be employed to represent the behavior of tissues.

The resistive behavior of the extracellular and intracellular media is basically due to their contents of ions; both media are in fact ionic solutions (electrolytes). Most abundant ions in the extracellular medium are Na^+ and Cl^- whereas in the intracellular media K^+ is the most abundant ion. Blood plasma conductivity at 37 °C is 1.5 S/m (resistivity = 0.66 Ω.m). This is the value that most researchers chose for representing the extracellular conductivity. In some cases this same value is also employed for the intracellular conductivity, although most researchers prefer significantly lower values around 0.6 S/m [3].

The cell membrane consists primarily of a thin lipid bilayer. This film (~ 7 nm thick) is partially permeable to lipids and water molecules but it is almost impermeable to ions. Its intrinsic electrical conductance is very low and can be considered as a good dielectric. Therefore, the structure formed by the extracellular medium, the lipid bilayer and the intracellular medium is a conductor-dielectric-conductor and it behaves as a capacitance. Experimentally it has been found that such capacitance has a value of about 0.01 F/m^2.

Now, taking into account what has been learnt in the previous subsection about capacitance behavior in the frequency domain (i.e. it behaves as an open circuit at low frequencies and as a short-circuit at high frequencies) it can be understood that low frequency currents will not penetrate into the cell whereas high frequency currents will flow freely through it (Fig. 4.a). Hence the impedance magnitude (i.e. opposition to current flow) will be higher at lower frequencies (i.e. $|Z|=R_e$) than at higher frequencies (i.e. $|Z|= R_e//R_i$) because the electrical paths at low frequencies are narrower. For intermediate frequencies a transitional behavior is manifested (Fig. 4.b). Typically, for most animal tissues, the transition between the low frequency behavior and the high frequency behavior occurs at frequency band from about 10 kHz to about 1 MHz.

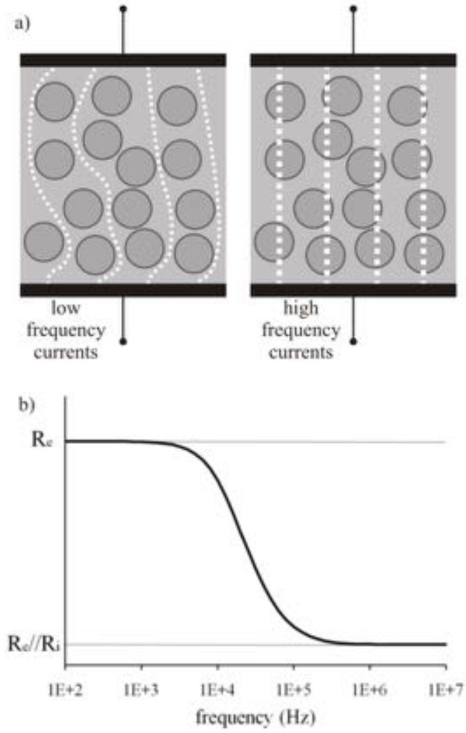

Figure 4: Low frequency currents are restricted to extracellular spaces whereas high frequency currents can flow freely through living tissues. a) Graphic representation of the passage of low frequency and high frequency currents through a cell suspension or tissue. b) Idealized graph of impedance magnitude versus frequency in a living tissue. Note that the scale for the frequency is logarithmic.

The above model corresponds to the following expression for the impedance:

$$Z = R_\infty + \frac{R_0 - R_\infty}{1 + j2\pi f\tau} = R_\infty + \frac{\Delta R}{1 + j2\pi f\tau}, \quad (13)$$

where τ ($=C_m R_i$) is the time constant of the model, R_∞ is $R_e//R_i$ and R_0 is R_e.[8] Impedance empirical data from single cells or diluted cell suspensions can be fitted nicely with this equation thus confirming the validity of the model [4]. However, for fitting dense cell suspensions or living tissues, it has been found that an alternative equation – known as the Cole equation – produces much better results:

$$Z = R_\infty + \frac{\Delta R}{1 + (j2\pi f\tau)^\alpha}, \quad (14)$$

where the α parameter typically has values from 0.7 to 0.9 (note that α = 1 implies that this equation is identical to equation 13). Observed in a semi log plot (Fig. 4) the impedance magnitude transitional behavior of Cole compatible data is slightly more gradual than the response plotted in Fig. 4. The physical meaning of the α parameter is still a matter of debate [5], [6]. Nevertheless, in the context of electroporation it has little significance because, as will be explained in next section, for monitoring electroporation it will be required to follow the behavior of R_0 rather than of the whole impedance spectrum. Therefore, for the sake of simplicity, only the simple model $R_e//(C_m+R_i)$ will be considered in this lecture.

If the expressions listed in table 2 are employed to extract the conductivity and permittivity values, it will be noticed that both change across the spectrum. However, it will also be noticed that the conductivity is constant for very low, σ_0, and for very high frequencies, σ_∞. These two values are directly related to R_0 and R_∞:

$$\sigma_0 = \frac{k}{R_0}, \quad \sigma_\infty = \frac{k}{R_\infty}, \quad (15)$$

IMPACT OF ELECTROPORATION

When electroporation occurs, cell membrane becomes more permeable and, according to the previous model, the cell membrane conductivity will increase thus producing a drop in the impedance magnitude at low frequencies (i.e. low frequency current will be able to flow through the cell). This indeed has been empirically corroborated by different means. As a matter of fact, it must be noted that the first description of the electroporation phenomenon as a disturbance of the cell membrane permeability which can be reverted was obtained by performing resistance measurements [7].

The cell membrane is not a perfect dielectric. Embedded within the lipid bilayer there are different sorts of protein assemblies which are porous structures that allow some ions to flow through the membrane. In addition, a few ions can leak through defects in the lipid bilayer even in the absence of embedded proteins. Hence the electrical model displayed in Fig. 4 needs to be modified slightly in order to include these short-circuiting effects. In other words, R_0 is not exactly equal to R_e but to $R_e//(R_i+R_m)$ where R_m is the leak resistance through the membrane (Fig. 5). Electroporation creates extra conductive paths across the membrane which can be modeled also as a resistance R_{EP}. It must be noted that Fig. 5 is not to scale: R_{EP} can be much, much lower than R_m; when electroporation occurs, cell membrane conductivity can increase a thousand-fold [8].

[8] Note that the ∞ in R_∞ indicates that that is the impedance magnitude observed at infinite frequency. Similarly the 0 in R_0 indicates that that is the impedance magnitude at low frequencies (ideally at 0 Hz).

According to the model, and to empirical data [9], the effect of electroporation is not immediately observable by impedance measurements at high frequencies. This has an important practical implication: for monitoring electroporation it will be required to perform impedance measurements at a low frequency so that $|\mathbf{Z}| \sim R_0$, which is the impedance parameter directly dependant on electroporation. Indeed, typically frequencies below 1 kHz or 10 kHz are employed for monitoring electroporation and it is implicitly assumed that $R_0' = |\mathbf{Z}|$ and from R_0' a conductivity value, σ_0', is extracted (equation 15). Strictly, this value σ_0' is not conductivity but admittivity magnitude. Although σ_0' is not equal to σ_0, it may be a very good approximation of it if the measurement frequency is low enough (e.g. 1 kHz) as shown in [10].

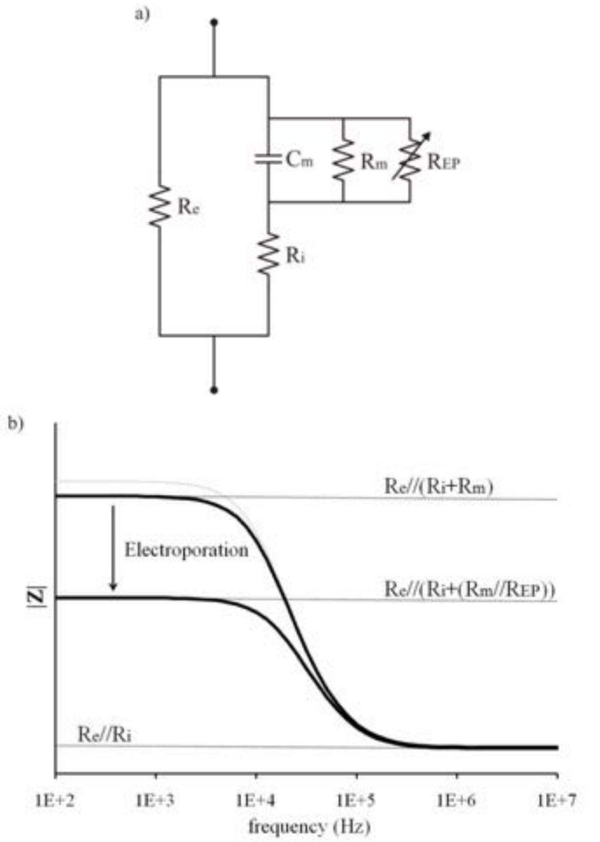

Figure 5: a) Enhanced electrical model for a living cell (and for tissues): R_m represents the short-circuiting resistance across the membrane due to ionic channels and leakage through the lipid bilayer and R_{EP} represents the increased conductance due to the electroporation phenomenon (the arrow denotes that it is variable). b) Plot of impedance magnitude versus frequency for the enhanced electrical model. Electroporation causes a significant drop in impedance magnitude at low frequencies. (The doted gray trace corresponds to the model with $R_0 = R_e$).

During the electroporation pulse

In Fig. 6 it can be observed a typical behavior of the current signal when a rectangular electroporation pulse is applied to a living tissue or a very dense cell suspension. This example does not correspond to an actual experiment but it shows the main features that can be noticed in actual measurements in tissues [11], [12] or dense cell suspensions [13]: after an initial peak due to cell membrane charging, current increases exponentially and afterwards it seems to increase much slower in a quite linear fashion or it stops increasing. The initial abrupt change in conductance, masked by the membrane charging process, is most likely the manifestation of immediate membrane permeabilization. The later exponential rise shows that membrane conductance increases slowly and moderately during the pulse.

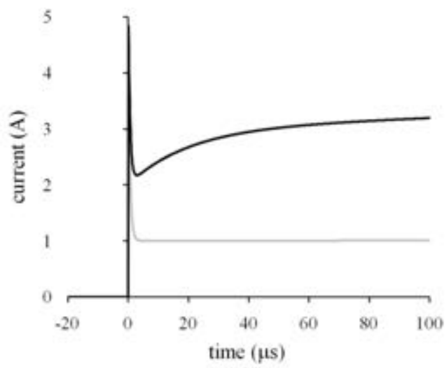

Figure 6: Plausible recording (black line) of current during delivery of a 100 µs high voltage pulse (e.g. 1000 V) to a soft tissue by means of parallel plate electrodes (e.g. 1 cm × 1 cm electrodes at a separation distance of 1 cm). The gray line indicates what would be the response if electroporation did not occur: after a peak in current due to cell membrane charging, current would increase very slightly (almost unappreciable in the graph) because of resistive heating.

The gray line in Fig. 6 shows what would be the behavior of the tissue in case the electroporation phenomenon did not exist. After the peak due to the membrane charging process, tissue conductivity would increase moderately, almost inappreciably, due to resistive heating. This tissue conductivity increase due to Joule heating is related to the fact that the conductivity of ionic solutions shows a positive dependence on the temperature[9]. In the particular case of physiological fluids is estimated that the conductivity increases about 2% per each °C [14]. In

[9] Conductivity depends on the amount of free charges and the mobility of those charges in the material. In metals the concentration of free charges – electrons – is huge. By increasing the temperature, electron collision rate is increased thereby reducing their mobility and consequently decreasing the conductivity of the metal (superconductors, $\rho = 0\ \Omega$.m, are possible at extremely low temperatures). In diluted ionic solutions, such as is the case of biological fluids and tissues, the amount of free charge – ions – is low and they rarely collide. By increasing the temperature water viscosity is reduced thus increasing mobility and conductivity.

the above example the resulting increase of conductivity due to thermal heating is not significant, however, this phenomenon should be kept in mind as it can be significant in other cases [13].

Since the voltage (v_{PULSE}) is constant during the rectangular pulse, it is possible to define a resistance and a conductance during the pulse from current recordings ($i_{PULSE}(t)$):

$$R_{PULSE}(t) = \frac{v_{PULSE}}{i_{PULSE}(t)} \quad G_{PULSE}(t) = \frac{1}{R_{PULSE}}, \qquad (16)$$

and from them, if the cell constant, k, is known, it is possible to define the resistivity, $\rho_p(t)$, and the conductivity during the pulse, $\sigma_p(t)$. These resistivity and conductivity values are referred to as dynamic or quasi-dc resistivity and conductivity. Strictly, the dynamic conductivity is not a true conductivity because, when dc measurements are not possible, as it is the case, the conductivity can only be extracted from impedance measurements at certain frequency so that both the conductivity and the permittivity contributions can be isolated. However, after the first very few microseconds in which the cell membrane charges, $\sigma_p(t)$ can be considered to be a good approximation of $\sigma_0(t)$. In reality, no alternatives are available: to superimpose an ac signal to obtain σ_0 would not be practical because low frequencies would be required (f <1 kHz, T > 1 ms) and, therefore, dynamic changes during the pulse would be not recorded because pulse durations are typically < 100 µs.

For different field magnitudes and three different tissues, Fig. 7 displays the ratio between the dynamic conductivity at 100 µs after the electroporation (σ_p) pulse onset and the original tissue conductivity (σ_0). It can be observed that the ratio seems to saturate for large field magnitudes. The maximum ratio (σ_p/σ_0) is in all cases close to the ratio σ_∞/σ_0 measured before electroporation. This is in agreement with the electrical model of electroporation depicted in Fig. 5: in principle, the minimum resistance that can be reached by electroporation must be equal to the minimum impedance magnitude that can be obtained by applying high frequencies (R_∞); in both cases the cell membrane is "short-circuited". Therefore, at 100 µs, for large field magnitudes, cell membrane has become so permeable to ions that its resistance is insignificant when compared to the resistance of the intracellular and extracellular media. Such statement does not imply that membrane is completely disrupted; only a tiny fraction of the membrane area needs to be opened (<1%) in order to achieve such irrelevance in terms of resistance [15].

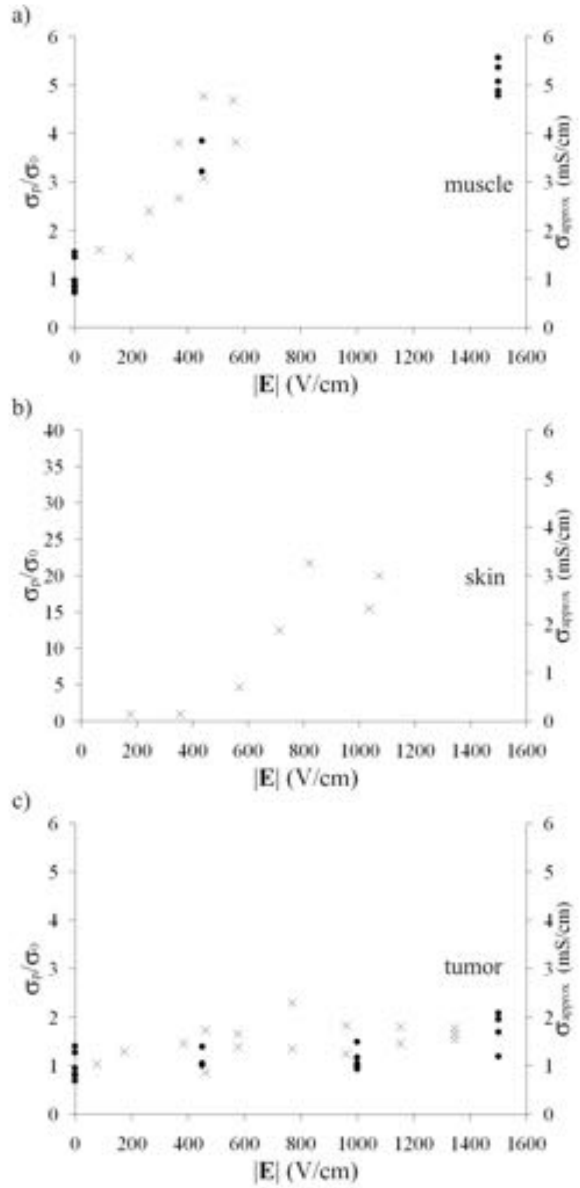

Figure 7: For three different animal tissues (rat transversal skeletal muscle, rat skin and sarcoma tumor implanted in mice), relative conductivity (σ_p/σ_0) at 100 µs after the beginning of the pulse. The approximate absolute conductivity is also represented on the secondary vertical axis (right). The symbol × indicates data from [16] whereas the symbol • indicates data collected by the author [9], [17].

After the electroporation pulse

There are some studies on isolated membranes [18] and on cells [13], [19]–[26] in which the electrical conductance is measured after the application of the electroporation pulses or in between the application of multiple pulses. From all these studies some interesting general observations can be extracted:

1) After cessation of the high voltage pulse, conductance drops very fast (<<1 ms) to a value which is much smaller than the conductance during the pulse (σ_p) but significantly larger than the conductance value before the pulse (σ_0). This

phenomenon is presumably linked to the resealing of hypothesized short-lived pores and resembles the fast increase in conductance that is observed when the high voltage pulse is applied.

2) After the fast conductance drop, the conductance of the sample keeps falling slowly towards the original conductance value. Conductance drop during this stage can be modeled with two or three exponential decays with time constants in the order of tens or hundreds of milliseconds [26]. This slow recovery of the membrane resistance is presumably associated with the existence of long-lived membrane defects which could last for minutes. In the case of dense cell suspensions (e.g. cell pellets), the decrease in conductance, may even yield values significantly below that original value. This puzzling observation is explained as being the result of osmotic imbalance induced by the permeabilization: water rushes into the cells and causes them to swell so that the extracellular spaces are significantly compressed and, therefore, the resistance at low frequencies increases notably [21]. Of course, if the pulse is large or long enough, some degree of permeabilization will be irreversible and the original membrane resistance will never be reached.

3) Conductance changes due to multiple electroporation pulses show a memory effect, that is, the conductance increase caused by each pulse depends on the pulses that were applied before.

4) A generally observed phenomenon is that post-pulse membrane conductance increases gradually pulse after pulse. This agrees with the fact that electroporation effectiveness, as assessed by other methods, increases pulse after pulse.

In diluted cell suspensions the immediate increase in conductance caused by an electroporation pulse may be unappreciable ($R_e << R_i$) whereas a later slow increase conductance may be observed [13]. This sustained slow increase in conductance is due to the release of intracellular contents into the extracellular medium by diffusion after electroporation. Up to a point, this phenomenon can be considered as an artifact and must be avoided by performing only fast measurements shortly after the pulses.

The above phenomena can also be observed in a few studies in which living tissue conductance is assessed after or in between the pulses [11], [9], [27], [28], [10], [17].

Due to the large ratio between cell volume and extracellular volume in tissues, the conductance increase caused by electroporation in tissues is much more noticeable than in cell suspensions and the impact of post-treatment intracellular release does not seem to be significant. On the other hand, the osmotic effect observed cell pellets seems to have a very significant impact. As a consequence, impedance measurements must be performed shortly after treatment (e.g. 50 ms) for preventing that this osmotic effect masks the conductivity increase produced by cell membrane permeabilization.

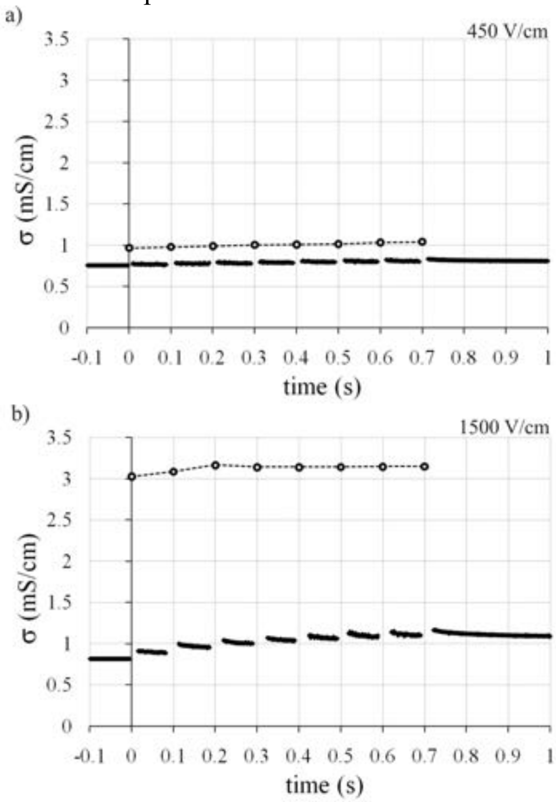

Figure 8: Two examples of conductivity evolution during *in vivo* electroporation of rat liver. The points marked with circles and joined by a dashed line represent the conductivity values obtained at the end of the electroporation pulses (in-pulse dynamic conductivity, σ_p). The electroporation protocol consisted of 8 rectangular pulses of 100 µs at 10 Hz. In a) the magnitude of the electric field was 450 V/cm and in b) it was 1500 V/cm.

For illustration, Fig. 8 displays the result of an experimental *in vivo* study in which rat livers were subjected to multi-pulse electroporation (8 pulses of 100 µs at 10 Hz) [10]. When the electric field magnitude is 450 V/cm the conductivity ($\sigma_0^{'}$) slightly increases pulse after pulse up to a value 1.08 times the original one. The dynamic conductivity at the end of the 100 µs pulses (σ_p) (represented with a single circle) is significantly higher than the conductivity just before or just after each pulse but also shows a quite linear progressive increase. On the other hand, when the magnitude is 1500 V/cm the dynamic in-pulse conductivity seems to saturate at a value (3.2 mS/cm) which is quite close to the pre-treatment admittivity magnitude at high frequencies ($\sim \sigma_\infty$) [10]. In this case the conductivity ($\sigma_0^{'}$) increase induced by each pulse is quite significant and it accumulates up to a conductivity value a 42% higher than the original conductivity.

The above example (Fig. 8) conveys one of the main take-home messages from this lecture: dynamic in-pulse conductivity measurements do not seem to be correlated with electroporation efficacy whereas post-pulse conductivity maybe is. Note that, in Fig. 8.b, according to in-pulse conductivity electroporation efficacy would be null, or even lower, after the third pulse whereas the post-pulse conductivity would indicate that electroporation efficacy increases pulse after pulse although the incremental efficacy diminishes, as it is known to happen when electroporation efficacy is assessed by other methods such as dye cellular uptake or cell killing by irreversible electroporation.

The previous message is further reinforced by the results of the study presented in [17] which are partially displayed in Fig. 9. Briefly, for electroporation protocols known to be reversible and for protocols known to be irreversible in the tissue sample under study (subcutaneously implanted sarcomas in mice), it was compared the increase in conductivity as obtained from measurements taken 50 ms after treatment (σ_0') and from measurements at the end of the last electroporation pulse (σ_p). As it can be observed, the dynamic conductivity at the last pulse (b) seems to be related with the field magnitude of the applied pulses but it produces similar values for protocol 1 at 3500 V/cm – which is known to be a reversible protocol – and for protocols 3 and 4 – which are known to be irreversible. That is, form those measurements it is not possible to distinguish the outcome of irreversible and reversible electroporation protocols. On the other hand, it is possible to clearly distinguish irreversible and reversible protocols from conductivity measurements taken 50 ms after treatment (b).

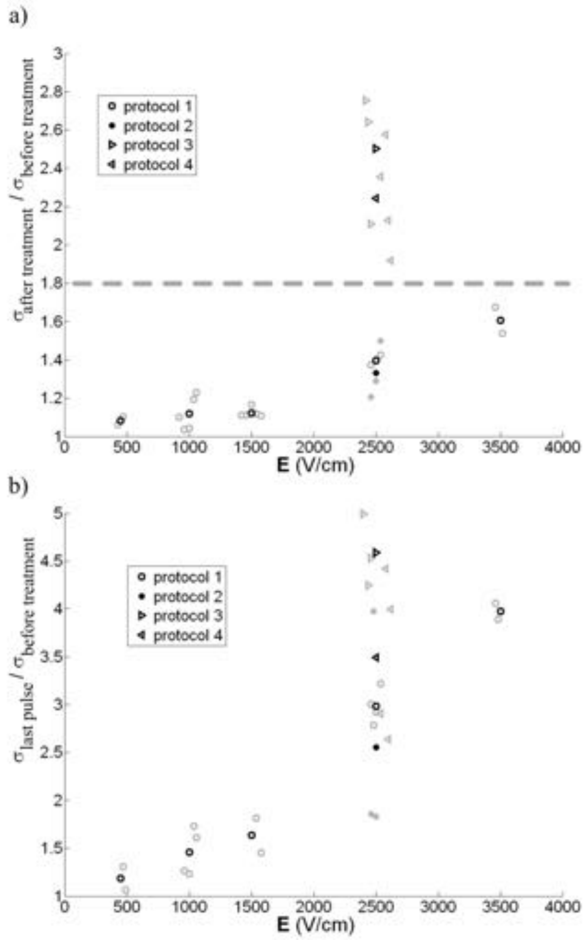

Figure 9: Comparison between relative increases in tissue conductivity determined from measurements 50 ms after treatment (a) and from measurements at the end of the last electroporation pulse (b) for electroporation protocols known to be irreversible (3 and 4) and protocols known to produce reversible electroporation (1 and 2) in subcutaneously implanted sarcomas in mice. Protocol 1: 8 pulses of 100 µs at 10 Hz; protocol 2: 8 pulses of 100 µs at 1 Hz; protocol 3: 8 pulses of 1000 µs at 0.03 Hz; protocol 4: 80 pulses of 100 µs at 1 Hz. Black marks indicate the mean values for each protocol and field magnitude. Grey color marks indicate individual experiments. (The slight random differences in field magnitude were artificially introduced for representation purposes.)

REFERENCES

[1] S. Grimnes and Ø. G. Martinsen, *Bioimpedance and bioelectricity basics*. San Diego, Calif. ; London: Academic, 2000.

[2] H. Fricke, “A mathematical treatment of the electric conductivity and capacity of disperse systems II. The capacity of a suspension of conducting spheroids surrounded by a nonconducting membrane for a current of low frequency,” *Phys. Rev.*, vol. 26, pp. 678–681, 1925.

[3] G. Pilwat and U. Zimmermann, “Determination of intracellular conductivity from electrical breakdown measurements.,” *Biochim. Biophys. Acta*, vol. 820, pp. 305–314, 1985.

[4] K. S. Cole, *Membranes, ions, and impulses; a chapter of classical biophysics*, vol. 1. Berkeley: University of California Press, 1968, p. 569.

[5] G. H. Markx, C. L. Davey, and D. B. Kell, “To what extent is the magnitude of the Cole-Cole α of the β-dielectric dispersion of cell suspensions explicable in terms of the cell size distribution?,” *Bioelectrochemistry Bioenerg.*, vol. 25, no. 2, pp. 195–211, 1991.

[6] A. Ivorra, M. Genesca, A. Sola, L. Palacios, R. Villa, G. Hotter, and J. Aguilo, “Bioimpedance dispersion width as a parameter to monitor living tissues,” *Physiol. Meas.*, vol. 26, no. 2, pp. S165–73, 2005.

[7] R. Stämpfli, “Reversible electrical breakdown of the excitable membrane of a Ranvier node,” *An. Acad. Bras. Cienc.*, vol. 30, pp. 57–63, 1958.

[8] A. Ivorra, J. Villemejane, and L. M. Mir, “Electrical modeling of the influence of medium conductivity on electroporation.,” *Phys. Chem. Chem. Phys.*, vol. 12, no. 34, pp. 10055–64, Sep. 2010.

[9] A. Ivorra, L. Miller, and B. Rubinsky, “Electrical impedance measurements during electroporation of rat liver and muscle,” in *13th International Conference on Electrical Bioimpedance and the 8th Conference on Electrical Impedance Tomography SE - 36*, vol. 17, H. Scharfetter and R. Merwa, Eds. Springer Berlin Heidelberg, 2007, pp. 130–133.

[10] A. Ivorra and B. Rubinsky, “In vivo electrical impedance measurements during and after electroporation of rat liver,” *Bioelectrochemistry*, vol. 70, no. 2, pp. 287–295, May 2007.

[11] U. Pliquett, R. Elez, A. Piiper, and E. Neumann, “Electroporation of subcutaneous mouse tumors by rectangular and trapezium high voltage pulses,” *Bioelectrochemistry*, vol. 62, no. 1, pp. 83–93, 2004.

[12] D. Cukjati, D. Batiuskaite, F. Andre, D. Miklavcic, and L. M. Mir, “Real time electroporation control for accurate and safe in vivo non-viral gene therapy,” *Bioelectrochemistry*, vol. 70, no. 2, pp. 501–507, May 2007.

[13] M. Pavlin, M. Kanduser, M. Rebersek, G. Pucihar, F. X. Hart, R. Magjarevic, and D. Miklavcic, “Effect of cell electroporation on the conductivity of a cell suspension,” *Biophys. J.*, vol. 88, no. 6, pp. 4378–4390, Jun. 2005.

[14] E. Gersing, “Monitoring temperature-induced changes in tissue during hyperthermia by impedance methods,” *Ann. N. Y. Acad. Sci.*, vol. 873, pp. 13–20, 1999.

[15] M. Hibino, H. Itoh, and K. Kinosita, “Time courses of cell electroporation as revealed by submicrosecond imaging of transmembrane potential.,” *Biophys. J.*, vol. 64, pp. 1789–1800, 1993.

[16] N. Pavselj, Z. Bregar, D. Cukjati, D. Batiuskaite, L. M. Mir, and D. Miklavcic, “The course of tissue permeabilization studied on a mathematical model of a subcutaneous tumor in small animals,” *IEEE Trans. Biomed. Eng.*, vol. 52, no. 8, pp. 1373–1381, 2005.

[17] A. Ivorra, B. Al-Sakere, B. Rubinsky, and L. M. Mir, “In vivo electrical conductivity measurements during and after tumor electroporation: conductivity changes reflect the treatment outcome,” *Phys. Med. Biol.*, vol. 54, no. 19, pp. 5949–5963, Oct. 2009.

[18] R. W. Glaser, S. L. Leikin, L. V Chernomordik, V. F. Pastushenko, and A. I. Sokirko, “Reversible electrical breakdown of lipid bilayers: formation and evolution of pores,” *Biochim. Biophys. Acta*, vol. 940, no. 2, pp. 275–287, May 1988.

[19] K. Kinosita Jr and T. Y. Tsong, “Voltage-induced conductance in human erythrocyte membranes,” *Biochim. Biophys. Acta*, vol. 554, no. 2, pp. 479–497, Jul. 1979.

[20] K. Kinosita Jr, I. Ashikawa, N. Saita, H. Yoshimura, H. Itoh, K. Nagayama, and A. Ikegami, “Electroporation of cell membrane visualized under a pulsed-laser fluorescence microscope,” *Biophys. J.*, vol. 53, no. 6, pp. 1015–1019, Jun. 1988.

[21] I. G. Abidor, L. H. Li, and S. W. Hui, “Studies of cell pellets: II. Osmotic properties, electroporation, and related phenomena: membrane interactions,” *Biophys. J.*, vol. 67, pp. 427–435, 1994.

[22] M. Schmeer, T. Seipp, U. Pliquett, S. Kakorin, and E. Neumann, “Mechanism for the conductivity changes caused by membrane electroporation of CHO cell-pellets,” *Phys. Chem. Chem. Phys.*, vol. 6, no. 24, pp. 5564–5574, 2004.

[23] J. Suehiro, T. Hatano, M. Shutou, and M. Hara, “Improvement of electric pulse shape for electropermeabilization-assisted dielectrophoretic impedance measurement for high sensitive bacteria detection,” *Sensors Actuators, B Chem.*, vol. 109, pp. 209–215, 2005.

[24] J. Wegener, C. R. Keese, and I. Giaever, “Recovery of adherent cells after in situ electroporation monitored electrically,” *Biotechniques*, vol. 33, pp. 348–357, 2002.

[25] J. Glahder, B. Norrild, M. B. Persson, and B. R. R. Persson, “Transfection of HeLa-cells with pEGFP plasmid by impedance power-assisted electroporation.,” *Biotechnol. Bioeng.*, vol. 92, pp. 267–76, 2005.

[26] T. García-Sánchez, M. Guitart, J. Rosell-Ferrer, A. M. Gómez-Foix, and R. Bragós, “A new spiral microelectrode assembly for electroporation and impedance measurements of adherent cell monolayers,” *Biomed. Microdevices*, vol. 16, pp. 575–590, 2014.

[27] R. C. Lee, L. P. River, F. S. Pan, L. Ji, and R. L. Wollmann, “Surfactant-induced sealing of electropermeabilized skeletal muscle membranes in vivo,” *Proc. Natl. Acad. Sci. U. S. A.*, vol. 89, no. 10, pp. 4524–4528, May 1992.

[28] U. Pliquett, R. Langer, and J. C. Weaver, “Changes in the passive electrical properties of human stratum corneum due to electroporation,” *Biochim. Biophys. Acta*, vol. 1239, no. 2, pp. 111–121, Nov. 1995.

[29] D. E. Chafai, A. Mehle, A. Tilmatine, B. Maouche, and D. Miklavčič, “Assessment of the electrochemical effects of pulsed electric fields in a biological cell suspension,” *Bioelectrochemistry*, vol. 106, Part B, pp. 249–257, Dec. 2015.

[30] A. Silve, A. Guimerà Brunet, B. Al-Sakere, A. Ivorra, and L. M. Mir, "Comparison of the effects of the repetition rate between microsecond and nanosecond pulses: Electropermeabilization-induced electro-desensitization?," *Biochim. Biophys. Acta - Gen. Subj.*, vol. 1840, no. 7, pp. 2139–2151, Jul. 2014.

ACKNOWLEDGEMENT

This work was supported in part by the Spanish Ministry of Economy and Competitiveness, Grant TESC2014-52383-C3-2-R.

Antoni Ivorra (Barcelona 1974) is a Tenured Associate Professor and a Serra Húnter Fellow at the Universitat Pompeu Fabra (UPF), were he leads a team composed by 3 PhD students under his supervision and himself (http://berg.upf.edu/). Before to joining the UPF in 2010, he enjoyed a three-year postdoctoral position at the University of California at Berkeley (2005-2008) followed by an appointment as Assistant Research Engineer at the same institution for a year. Then he moved to Villejuif, France, for an eight-month postdoctoral position at the Centre National de la Recherche Scientifique (CNRS) - Institut Gustave Roussy. During 1998-2005, he was with the Biomedical Applications Group of the Centre Nacional de Microelectrònica, Bellaterra, Spain. He received a M.Sc. degree in electronics engineering from the Universitat Politècnica de Catalunya, Barcelona, Spain, in 1998 and a Ph.D. degree in electronics engineering from the same institution in 2005.

His research is mostly focused on bioelectrical phenomena and on exploring the use of these phenomena for implementing new methods and devices for biomedical applications. Specifically, his main research topics are electroporation, particularly for cancer treatments, electrical bioimpedance for medical diagnosis and electrical stimulation for neuroprosthetics. He is author or coauthor of 34 publications in peer-reviewed journals, 3 book chapters and more than 30 conference contributions. He has been inventor or co-inventor of 10 families of patent applications.

NOTES

NOTES

Non-endocytotic delivery of lipoplex complexes into living cells

Pouyan E. Boukany, Piotr Glazer

Delft University of Technology, Faculty of Applied Science, Delft, Netherlands

Abstract: Lipoplexes are popular non-viral carriers for gene and drug delivery. The cellular uptake of lipoplex systems occurs through the endocytosis process, in conventional transfection methods. The entrapment of lipoplex nanoparticles into endocytic vesicle is a major hurdle to achieve efficient gene silencing and expression. Recently, we developed an effective nano-channel electroporation (NEP) method to enhance the cellular uptake and release of siRNAs/DNAs from lipoplexe nanoparticles. In this work, we demonstrated that in a NEP device, lipoplex nanoparticles were injected directly into the cytoplasm of cell within several seconds. We showed that lipoplexes containing MCL-1 siRNA delivered by NEP can more efficiently down-regulate the expression of MCL-1 mRNA in A549 cancer cells than conventional transfection. Quantum dot-mediated Förster resonance energy transfer (QD-FRET) reveals that lipoplexes delivered through NEP platform can directly release siRNA in the cytosol without going through the endocytosis route. Furthermore, the advantage of combining NEP with lipoplex nanoparticles by the successful delivery of large plasmids such as pCAG2LMKOSimO, 13 kbp into cells was demonstrated. This approach creates new opportunity to produce healthy induced pluripotent stem (iPS) cell.

INTRODUCTION

Safe and efficient intracellular delivery of nucleic acids, including large plasmids for gene expression, and oligonucleotides (antisense DNA or interfering RNA) for protein regulations, holds a great promise for treating diseases such as cancer. Despite the promising potential of nucleic-acid-based therapeutics, their delivery is still challenging because highly negative charged biological molecules have difficulty to cross the cell membrane and are prone to degradation prior to cellular uptake in the physiological conditions [1-8].

To overcome these issues, much effort has been devoted to developing efficient and safe strategies to package antisense DNAs and siRNAs inside nanoscale delivery vehicles in ways that enhance their resistance against enzymatic degradation, that assist cellular targeting and uptake. In general, biological and chemical methods are adopted to make these nanovehicles and they are classified either as viral or nonviral vectors. Viral vectors offer very high transducing efficiency, but their application in humans raises many safety concerns. On the other hand, non-viral vectors have emerged as a safer alternative to viral vectors, though being less efficient. Typically, the uptake of lipoplexes by cells is investigated in the laboratory by exposing cells at bottom of a culture plate to a suspension of lipoplex-NPs inside the culture medium. In this in vitro test, positively charged NPs bind to the cell membrane and fuse with the cell membrane [9-14]. The complexes are internalized inside the cells through the endocytothetic pathways involving endosomes and lysosomes (Figure 1a). Several studies have shown that saturation of intracellular uptake of lipoplex NPs into cells within 4-5 hours (h) agreed with endocytosis process. In addition, the effect of released drugs such as siRNA on the cellular function is observed within at least 24 h, when the carries escape from endosomes and lysosomes successfully All these issues from aggregation, sedimentation and residence time of NPs in the culture medium, gradual cellular uptake, the endolysosomal escape of NPs to cell division are limiting the efficiency of intracellular delivery of NPs [14-18].

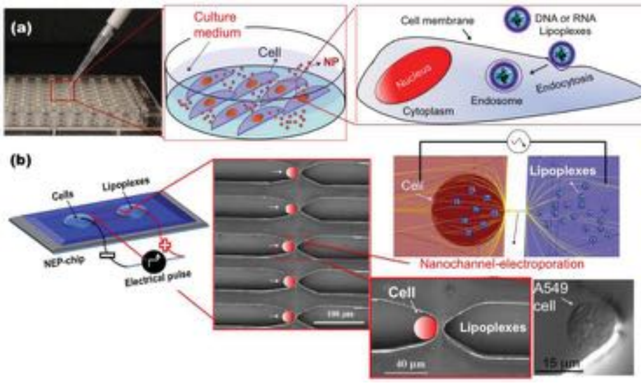

Figure. 1. (a) The conventional cellular uptake and (NEP delivery of lipoplex nanoparticles into the living cell. From Ref [20].

In this work, we proposed to electrophoretically shoot lipoplexes nano-carriers directly into cytosol by applying electrical pulses through a nanochannel (Figure 1b). Electric pulses are known to transiently permeable the cell membrane, which forces exogenous cargo to enter into cells and tissues. This process called electroporation (EP) has been routinely used for both in vitro and in vivo applications, due to technical simplicity, fast performance and almost no limitation on cell type and size. However, conventional EP suffers from several limitations: i) low cell viability, ii) non-uniform transfection, iii) gradual cellular uptake based on diffusion, iv) low transfection efficiency. In a recent work, we have developed a novel nanochannel electroporation (NEP) platform for precise drug and gene delivery without damaging the cell [19]. In contrast to conventional EP, our NEP technique has ability to produce a highly localized and focused electric field on the small area of cell membrane adjacent to the nanochannel. This treatment induces a strong electrophoresis at the nanoscale leading to drive and inject exogenous cargo instantly into the cell during nanoporation.

Recently, we showed that in a NEP device, siRNA lipoplexes were injected directly into the cytosol, after electrical pulses lasting milliseconds (ms) were applied [20]. Specifically, we have shown that siRNA (MCL-1) lipoplexes delivered with this approach can efficiently down-regulate the expression of MCL-1 protein in A549 lung cancer cell, in contrast to convectional delivery. To unravel the mechanism responsible for the efficient siRNA delivery in an NEP device, we integrated QDs mediated Förster resonance energy transfer (FRET) with nucleic acid loaded delivery lipoplexes and label endosomal compartments of A549 cells. The combination of QD-FRET and confocal microscopy allows us to explicitly track intracellular uptake, fate and unpacking kinetics of lipoplexes at cellular and sub-cellular level.

The DNA combing and polymer imprinting technique was employed to fabricate a NEP device made up of arrays of two microchannels connected by a nanochannel (with diameter of 120 nm) [21-22]. In this work, A549 cell line was selected as the representative model for lung cancer in humans. A custom made optical tweezer (OT) integrated with an inverted Fluorescent microscope (Olympus, IX-71) is used to isolate and maneuver single A549 cells inside the micro-channel. Single cells are positioned at the tip of nanochannel for NEP transfection (shown in Figure 1b, right).). Cationic lipoplexes with mean diameter by volume of ~65nm and zeta potential of 6.45±1.13mV were loaded in the other side of the nanochannel.

Cationic lipoplex nanoparticles containing FAM-labeled oligodeoxynucleotides (FAM-ODN) were first delivered to A549 cells using NEP, BEP, and the conventional transfection method (As shown in Figure 2). The FAM-ODN lipoplexes were mixed with A549 cells, cationic lipoplexes accumulated around the negatively charged cell membrane. After BEP, the lipoplexes were still located around the cell membrane, suggesting that BEP is not able to deliver lipoplexes efficiently. The similar phenomenon was also observed in conventional transfection. NEP, on the contrary, delivered lipoplexes directly into the cell cytoplasm and showed much higher fluorescence intensity than in conventional transfection and BEP.

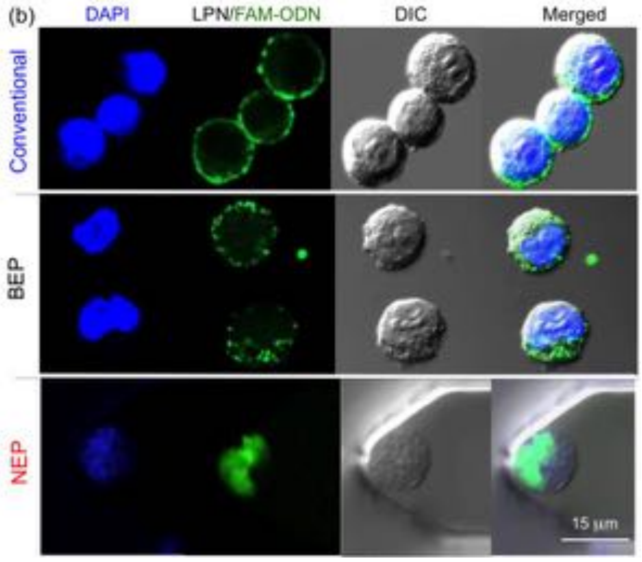

Figure 2. Delivery of Lipoplex Nanoparticles containing FAM-ODN into A549 cells by NEP, BEP and conventional transfection method. (Figure is adapted from Ref 20)

Then A549 cells were transfected by siRNA (MCL-1)-lipoplexes (with average particle size of 65 nm). In this work, siRNA (MCl-1) was selected, because MCL-1 protein is overexpressed in lung and leukemia cancer cells. It is well known that MCL-1 inhibits programmed cell death in these cancer cells (as shown schematically in Figure 3a). The control capability of NEP allows us to find the critical dosage required to kill A549 cells. We found that siRNA (MCL-1) induces apoptosis in all A549 cells within 18 h after transfection when three 5 ms pulses (pulse intervals = 0.1 s) at 220 V/2mm were delivered through NEP device. Similar NEP condition was applied to transfect A549 cells by scrambled siRNA-lipoplexes and all cells remain viable. Viability of transfected cells was measured by LIVE/DEAD assay 18 h after transfection.

To measure specific silencing of siRNA MCL-1, the evolution of MCL-1 mRNA expression relative to GAPDH (endogenous control gene) was monitored inside the transfected A549 cells. Two molecular beacons (MBs) probes were employed to detect MCL-1 and GAPDH mRNA simultaneously inside the single cells with FAM and Cy3 *fluorophores* respectively. MB is a probe with a fluorophore at one end and a quencher at the other end of a stem–hairpin structure. After hybridization with complementary RNA targets, the fluorescence is detectable by separating the fluorophore and the quencher, allowing to monitor the expression and localization of specific mRNA inside the cells. The molecular beacon against GAPDH (GAPDH– MB: 5′-Cy3-CGA CGG AGT

CCT TCC ACG ATA CCA CGT CG-BHQ2a-Q-3′) and MCL-1 (MCL-1 MB: 5′-FAM-CCT AGC TTG GCT TTG TGT CCT TGG CGG CTA GG-BHQ2a-Q-3′) were purchased from Eurofins MWG Operon.

The MCL-1 MB and GAPDH MB probes were delivered to the same cells to determine the MCL-1 mRNA and GAPDH mRNA expression levels at 1 h and 18 h post NEP transfection of lipoplex nanoparticles containing MCL-1 siRNA to A549 cells, (Figure 3 b, top). It is evident that the MCL-1 mRNA expression inside the cell was not affected by siRNA yet at 1 h post NEP transfection. However, 18 h post NEP transfection, we observed the loss of almost all MCL-1 mRNA expression, but no change in GAPDH mRNA expression. In the case of scrambled siRNA, no change of MCL-1 mRNA expression was observed (as shown in the bottom of Figure 3 b). The loss of MCL-1 mRNA expression (relative to GAPDH) after NEP transfection was compared and conventional transfection (Figure 3 c). In NEP treatment, the relative expression of MCL-1 mRNA was significantly reduced (~ 50%)within 12 h and all MCL-1 mRNA expression was almost silenced 24 h after NEP transfection. However, no detectable change in MCL-1 mRNA expression was observed until 20 h post transfection with conventional transfection. And only 50% down-regulation in the MCL-1 mRNA expression was observed 48 h post transfection. These results confirmed that NEP delivery route greatly affects the gene transfection process.

Then QD-FRET was employed to track the intracellular fate of lipoplexes in both NEP and conventional transfection. The QD-605 and Cy5-GTI2040 were encapsulated in the lipoplexes. When the lipoplexes are intact, the fluorescence from QD-FRET-mediated Cy5 is observed. When the lipoplexes break up, the QD-FRETmediated Cy5 would disappear. In addition, the endosomal compartments of A549 cells were labeled by transfecting the cells with the GFP-Rab7 plasmid using bulk electroporation to investigate the location of lipoplex nanoparticles (as shown in Figure 4). We used confocal microscopy to image the lipoplex nanoparticles containing QD605/Cy5 and the endosomal compartments. As shown in Figure 4 , the majority of QD605/Cy5 containing lipoplex nanoparticles were accumulated in the endosomes of A549 cells at 4 h after conventional transfection suggesting that the endocytosis process is the dominant mechanism for cellular uptake. However, in NEP treatment, the lipoplex nanoparticles were found inside a transfected cell only 10 min after poration, and most of the lipoplexes were found outside of the endosomes (Figure 4 b). The unique feature of NEP allows instant injection of lipoplexes inside the A549 cells, which allows bypassing the endocytosis route.

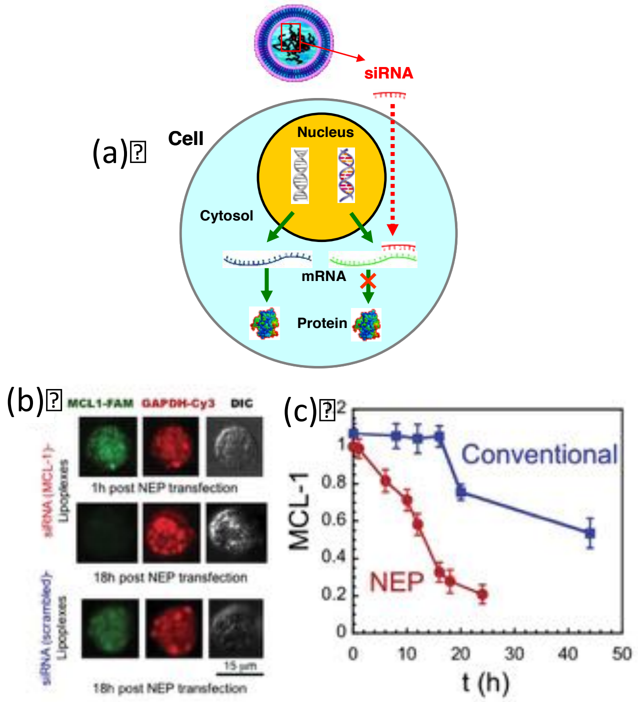

Figure 3. (a) Schematic representation of gene silencing mechanism by siRNA MCL-1. (b) Expression levels of MCL-1 and GAPDH mRNAs were detected by MCL-1 MB and GAPDH MB at 1 h and 16 h post NEP transfection of A549 cells with lipoplex nanoparticles containing MCL-1 siRNA (top) and lipoplex nanoparticles containing scrambled siRNA (bottom) (NEP condition: 220 V/2 mm, four 5 ms pulses). (c) The evolution of relative expression level of MCL-1 mRNA to GAPDH mRNA after NEP and conventional transfection by lipoplex nanoparticles containing MCL-1 siRNA. Error bars represent standard deviation. (Figure is adapted from Ref 20)

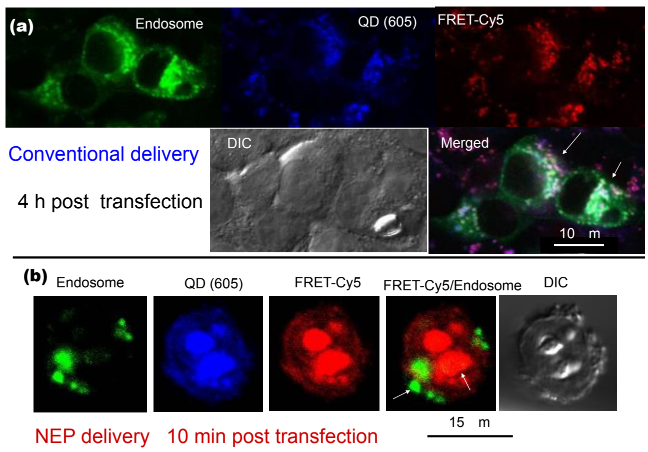

Figure 4. Delivery of lipoplex nanoparticles by a) conventional transfection and b) NEP transfection. Confocal fl uorescence images from left to right: Endosomes (green), QD-605 (blue), and QD-FRET-mediated Cy5 (red). Endosomes of A549 cells were labeled by transfection of GFP-rab 7 plasmid 24 h before NEP and conventional transfection. (Figure is adapted from Ref 20)

To provide more insight into the mechanism of delivery, we measured the intracellular unpacking kinetics of lipoplexes in both NEP and conventional transfection. QD-FRET in confocal fluorescence microscopy is a well-established tool to estimate the state of nanocomplexes in real time. [33,34]. A high FRET-mediated Cy5 signal implies that lipoplexes are intact and unperturbed inside the cells. Again, we compare NEP with conventional transfection.

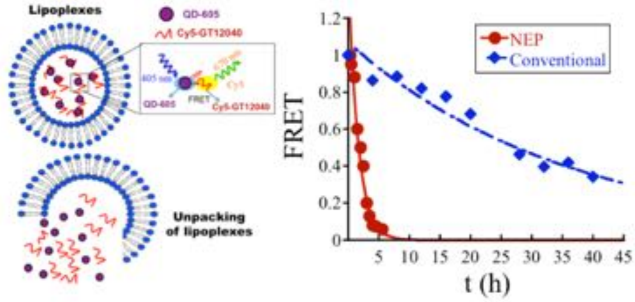

Figure 5. Left: sketch of the QD-FRET lipoplex complexes used to investigate the unpacking of lipoplex nanoparticles. QD605 and Cy5-GTI2040 were encapsulated in the lipoplexes. Upon excitation at 405 nm, the emission of QD-FRET-mediated Cy5 represented compact and intact lipoplex nanoparticles. (Right) Kinetics of release in NEP (circles) and conventional transfection method (diamonds). (Figure is adapted from Ref 20).

In NEP, the loss of QD-FRET signal was significantly faster than conventional transfection (as shown in Figure 5). Most of lipoplex nanoparticles were disassociated at 5 h, which was consistent with the observed fast and efficient down-regulation of siRNA by NEP. In conventional transfection, the fluorescence signal of QD-FRET-mediated Cy5 gradually decreased at 24–40 h post transfection, indicating the unpacking of lipoplex nanoparticles was a much slower process. In addition, many lipoplexes might not escape from endosomes successfully, and could be degraded in the lysosomes.

Intracellular delivery of large plasmids is crucial for cell reprogramming and engineering applications, but challenging by convectional delivery techniques. In this work, pCAG2LMKOSimO plasmid (13 kbp) was sued as a representative plasmid model with contour length of 2.5 µm and radius of gyration of about 200 nm for cell reprogramming applications. [35] Figure 6 a,b displays that transfection of CHO cells by pCAG2LMKOSimO plasmid was very poor via both BEP and NEP of naked plasmids. To overcome this issue, we formed smaller size of lipoplex nanoparticles containing pCAG2LMKOSimO plasmid (diameter: ≈140 nm and zeta potential: 30 ± 6 mV) for cytosolic delivery. These lipoplexes were delivered through a nanochannel (diameter:~ 155 nm) into CHO cells (NEP conditions: 250 V/2 mm, 4 pulses, 5 ms). Within 8 h after NEP delivery of lipoplex nanoparticles, strong mOrange fluorescence was observed in CHO cells confirming successful transfection (see Figure 6 c). In BEP delivery of lipoplex nanoparticles containing plasmids, a sharp reduction of cell viability and very low transfection were achieved.

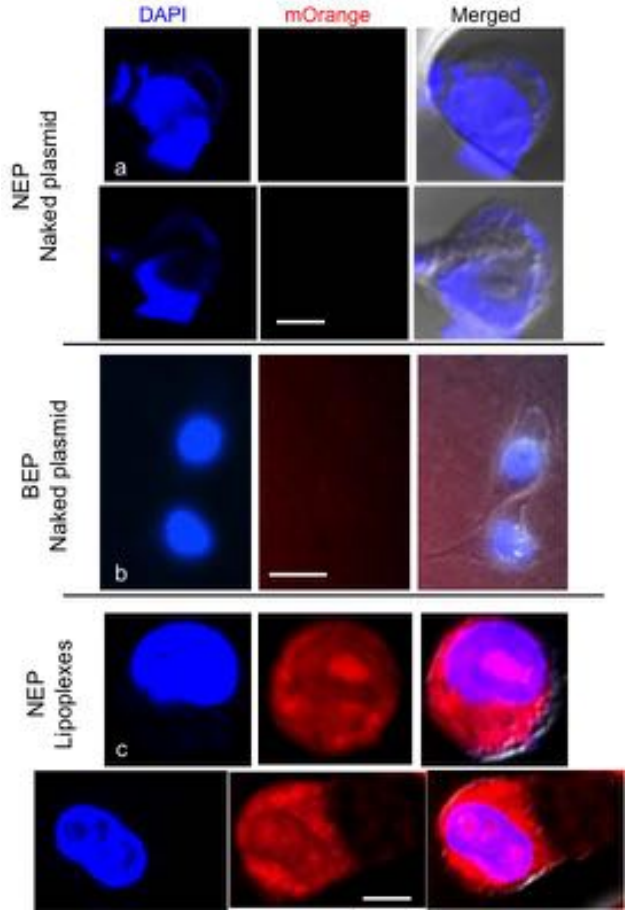

Figure 6. Expression of pCAG2LMKOSimO plasmids (13 kbp) in CHO cells. a) 10 h post NEP transfection of naked plasmids (250 V/2 mm, 5 pulses 5 ms) (scale bar: 5 µ m). b) 24 h post BEP transfection of naked plasmids (scale bar: 10 µm). c) 10 h post NEP transfection of lipoplex nanoparticles containing pCAG2LMKOSimO plasmids (scale bar: 5 µm). The cell nuclei were stained by DAPI (blue) and transfected cell by plasmid expressed mOrange fluorescent protein (red). (Figure is adapted from Ref 20)

Conclusions and Perspectives

Currently, micro/nano-fluidic technology holds a huge potential to revolutionize fundamental biology and health care applications. In this work, we showed that NEP enables fast/efficient delivery of lipoplex nanoparticles containing a wide range of biomolecules into A549 and CHO cells without going through the endocytosis pathway. It was found that NEP transfection of lipoplex nanoparticles containing MCL-1 siRNA resulted in efficient and fast down-regulation of MCL-1 mRNA compared to conventional transfection. The responsible mechanism for this efficient delivery was unraveled by QD-FRET measurements. Furthermore, successful delivery of large pCAG2LMKOSimO plasmid (13 kbp) into the CHO cell via NEP transfection of lipoplex nanoparticles was achieved. This novel strategy will provide a convenient, safe, and efficient approach for in vitro nucleic acid delivery in regulating gene expression. In addition, we are developing next generation of NEP device that can handle high population of cells. NEP provides new opportunity in advancing fundamental biological science and modifying cells for regenerative medicine and therapeutic cell engineering [23].

REFERENCES

[1] Fire, A., Xu, S., Montgomery, M. K., Kostas, S. A., Driver, S. E., Mello, C. C. Potent and specific genetic interference by doublestranded RNA in Caenorhabditis elegans. Nature, 391 (1998).

[2] de Fougerolles, A., Vornlocher, H.P., Maraganore J, Lieberman, J. Interfering with disease: a progress report on siRNAbased therapeutics. Nat Rev Drug Discov 6(6), (2007).

[3] Elbashir, S.M., Lendeckel, W., Tuschl, T. RNA interference is mediated by 21and 22 nucleotide RNAs. Gene Dev 15, 188200 (2001).

[4] Vargason, J.M., Szittya, G., Burgyan, J., Hall, T.M. Size selective recognition of siRNA by an RNA silencing suppressor. Cell 115, 799â^811 (2003).

[5] Davis ME, et al. Evidence of RNAi in humans from systemically administered siRNA via targeted nanoparticles. Nature 464(7291):1067U1140 (2010).

[6] Luo, D., Saltzman,W.M. Synthetic DNA delivery systems. Nat Biotechnol 18(1):3337 (2000).

[7] Kootstra, N.A. Verma, I.M. Gene therapy with viral vectors. Annu Rev Pharmacol 43:413439 (2003).

[8] Torchilin VP Recent approaches to intracellular delivery of drugs and DNA and organelle targeting. Annu Rev Biomed Eng 8:343375 (2006).

[9] Santel A, et al. A novel siRNAlipoplex technology for RNA interference in the mouse vascular endothelium. Gene Ther 13(16):12221234 (2006).

[10] Schaffert D and Wagner E Gene therapy progress and prospects: synthetic polymer based systems. Gene Ther 15(16):11311138 (2008).

[11] Zhou JH, et al. PAMAM dendrimers for efficient siRNA delivery and potent gene silencing. Chem Commun (22):23622364 (2006).

[12] Alivisatos, A.P. Semiconductor clusters, nanocrystals, and quantum dots. Science 271(5251):933937 (1996)..

[13] Kam NW, O'Connell M, Wisdom JA, and Dai H. Carbon nanotubes as multifunctional biological transporters and near infrared agents for selective cancer cell destruction. Proc Natl Acad Sci U S A 102(33):1160011605 (2005).

[14] Hu M, et al. Gold nanostructures: engineering their plasmonic properties for biomedical applications. Chem Soc Rev 35(11):10841094 (2006).

[15] Elouahabi A and Ruysschaert J.M. Formation and intracellular trafficking of lipoplexes and polyplexes. Mol Ther 11(3):336347 (2005).

[16] Khalil IA, Kogure K, Akita H, and Harashima H. Uptake pathways and subsequent intracellular trafficking in nonviral gene delivery. Pharmacol Rev 58(1):3245 (2006).

[17] Wu Y, et al. Uptake and intracellular fate of multifunctional nanoparticles: a comparison between lipoplexes and polyplexes via quantum dot mediated Forster resonance energy transfer. Mol Pharm 8(5):16621668 (2011).

[18] Kim JA, Aberg C, Salvati A, and Dawson K.A. Role of cell cycle on the cellular uptake and dilution of nanoparticles in a cell population. Nat Nanotechnol 7(1):6268 (2012).

[19] Boukany PE, et al. Nanochannel electroporation delivers precise amounts of biomolecules into living cells. Nat Nanotechnol 6(11):747754 (2011).

[20] Boukany, P.E., et al. Nonendocytic Delivery of Lipoplex Nanoparticles into Living Cells Using Nanochannel Electroporation, Advanced Healthcare Materials, 3 (2014), 682–689.

[21] Guan J, Boukany, P. et al. Large laterally ordered nanochannel arrays from DNA combing and imprinting. Adv Mater 22(36):39974001 (2010).

[22] Glazer, P. P.J. Glazer, L. Bergen, L. Jennings, A. J. Houtepen, E. Mendes and Boukany, P.E., Generating Aligned Micellar Nanowire Arrays by Dewetting of Micro-patterned Surfaces, Small, 10, 1729-1734 (2014).

[23] Zhao, X., Huang, X., Wang, X., Wu, Y., Eisfeld, A.-K., Schwind, S., Gallego-Perez, D., Boukany, P. E., Marcucci, G. I. and Lee, L. J., Nanochannel Electroporation as a Platform for Living Cell Interrogation in Acute Myeloid Leukemia. Advanced Science, (2015).

ACKNOWLEDGEMENT

Funding of this work is provided by Marie Curie Career Integration Grant (CIG) and ERC-STG.

Pouyan Boukany was born in Tehran (Iran) in 1978. He obtained his M.Sc in Chemical Engineering (IUT). He received his Ph.D in Polymer Science from University of Akron (Ohio, USA). His doctoral work explored non-linear dynamics of DNA in Entangled fluids. He joined as a Postdoctoral Research Associate in the Center for Affordable Nanoengineering of Polymeric Biomedical Devices at the Ohio State University (Columbus, USA) in 2009. He is currently an assistant professor in Chemical Engineering Department at Delft University of Technology in the Netherlands. In 2013, he won ERC Starting Grant to understand and control the transport of DNA in electroporation at the molecular/sub-cellular level such that efficient and safe gene delivery can be achieved. More details on his group research interests in nanoengineering, rheology, living soft matter and biomedical applications thereof, are published on his website http://cheme.nl/ppe/boukany.

NOTES

NOTES

SHORT PRESENTATIONS

Computational Monte Carlo model of the electroporation process

Magdalena Żulpo[1*], Krystian Kubica[1]; [1]*Wroclaw University of Technology, Department of Biomedical Engineering, Plac Grunwaldzki 13, 50-377 Wroclaw, Poland;*

INTRODUCTION

Electroporation allows for delivering drugs (e.g. destroy cancer cells), genetic material (gene therapy), and markers (e.g. photosensitizers in photodynamic therapy) into the cells. It is particularly acute in multi-drug resistance - using this technique drug concentration inside the cell can be increased even hundreds of times (e. g. bleomycin). However, electroporation effectiveness depends on the selection of the appropriate parameters (such as the electric field strength and pulse duration) for the introduced substance. Despite many experimental and theoretical studies, correct definition of the electroporation parameters is no easy task, as there is still little known about its molecular mechanism- exact lipid molecules reaction to an external electric field [1]. To improve our understanding of molecular mechanisms we developed mathematical model based on the Monte Carlo (MC) technique. Performed simulations allows us to identify electroporation conditions, under which the formation of the pore is feasible, and determine the minimum and maximum pore diameters under various experimental and physico-chemical conditions.

METHODOLOGY

Developed author's model is based on Pink's model. Here, polar lipid heads were additionally taken into account. The lipid membrane is presented as triangular lattice consisting of two parallel layers. Each node is occupied by a hydrocarbon chain, and every two hydrocarbon chains have one polar part - a dipole. The Hamiltonian of the studied system consists of four terms: I) the energy of van der Waals interactions, II) the conformational energy, III) the energy of electrostatic interactions between the lipid heads and IV) the energy which describes the polar part interactions between the polar parts of lipid molecule (heads) and the electric field. To find the maximum size of stable pores in certain ambient conditions we have performed MC simulations for DPPC membrane in gel and fluid phase, surrounded by 10 and 100 mmol NaCl solution, exposed to the electric field from 10^5 to 10^8 V/m.

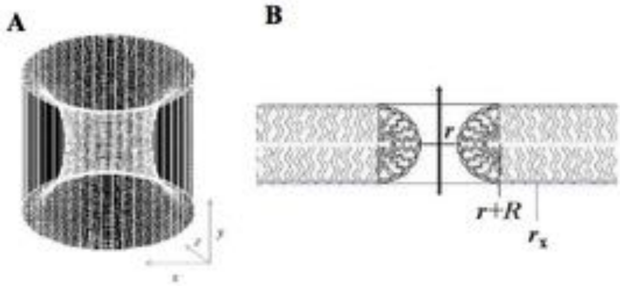

Figure 1. A) Representation of the geometry. B) Schematic representation of the process of pore formation in the DPPC lipid bilayer.

The system was equilibrated for the 200 - steps per node in 320 K (fluid phase), then 1000 steps per site were performed to find the average energy of the studied system.

RESULTS

We have found the relationship between energy of polar heads of lipids creating a pore in a lipid membrane, exposed to the electric field, and the pores size. If the electric field intensity is 10^6V/m potential energy is positive and rising with the hypothetical pore diameter . When we have added the positive energy of van der Waals interaction of lipid chains, we observed that in such conditions the pore is not stable. By increasing the electric intensity to 10^7 V/m the energy of polar part of a pore is negative (from d_a=3.68 nm) and for smaller pores the energy becomes positive (Fig. 2B). For larger values of the electric field (10^8 V/m) the energy of dipoles is negative and decreases with increasing in pore size. Considered chains are all in fluid conformation, for which the van der Waals and conformational energy are positive, despite of the negative energy of the polar part, the appearing pore could be stable only in small size (d_a=2.4 nm). The existence of larger stable pores requires conformational changes of lipid chains toward all-trans conformation.

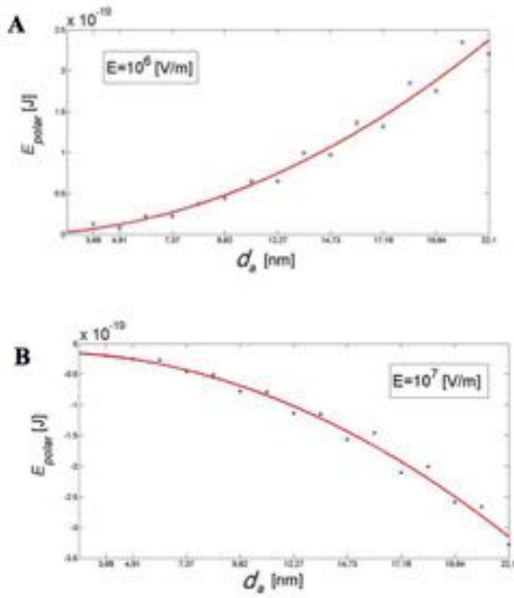

Figure 2. Dependence of the energy of polar part of pores formed in the membrane placed in an electric field of intensity A) 10^6V/m, B) 10^7V/m on pore diameter da. The standard deviation of the energy is of order 10^{-21}J.

REFERENCES

[1]C. Chen, S.W. Smye, M.P. Robinson, J.A. Evans, "Membrane electroporation theories: a review. Medical and Biological Engineering and Computing", *Med Biol Eng Comput*., vol.44(1-2), pp.5-14, 2006

Modelling of permeabilization during and after electroporation predicts mild dependence of electroporation effectiveness on cell radius

Borja Mercadal[1], P. Thomas Vernier[2], Antoni Ivorra[1]; [1]*Department of Information and Communication Technologies, Universitat Pompeu Fabra, Roc Boronat 138, Barcelona, SPAIN*
[2]*Frank Reidy Research Center for Bioelectrics, 4211 Monarch Way, Norforlk, VA 23508, USA*

INTRODUCTION

Although electroporation is not a bi-stable phenomenon and cell membrane permeabilization exhibits a gradual dependence on the local transmembrane voltage, the dependency is exponential and in practice so abrupt that it is widely accepted that electroporation occurs when the transmembrane voltage reaches a threshold. Such threshold is assumed to be nearly constant for any cell at the same conditions. Under this assumption, in order to trigger electroporation in a spherical cell, Schwan's equation leads to a proportionally inverse relationship between the cell radius and the minimum magnitude of the applied electric field. And, indeed, several publications report experimental evidences of an inverse relationship between the cell size and the field required to achieve electroporation. However this dependence is not always observed or is not so steep as predicted by Schwan's equation [1-3].

Observations are based on measurable effects of electroporation (e.g. uptake of ions). While these effects are related with changes over the whole membrane, Schwan's equation only stands for electroporation of a single point and is no longer valid after electroporation begins. Therefore we hypothesized that by modeling changes in conductivity during the electroporation pulse and posterior uptake of species by diffusion we might explain the experimentally observed behaviors.

MATERIALS AND METHODS

We used COMSOL Multiphysics 4.4 for simulating electroporation of a cell in suspension. In particular, we used a membrane conductivity model to describe permeabilization dependency on transmembrane voltage (V_m) [4]:

$$\sigma_m = \sigma_{m0} + K(e^{\beta|V_m|} - 1) \tag{1}$$

where σ_{m0} is the initial conductivity of the membrane and K and β are two constants.

Results allowed us to calculate the average conductivity of the cell membrane at the end of the applied pulse. Then the relative area occupied by the pores, $\overline{S_p}$, was obtained as:

$$\overline{S_p} = \frac{\overline{\sigma_m} - \sigma_{m0}}{\sigma_{pores}} \tag{2}$$

Simulations were run to calculate the minimum field magnitude (critical field) required to obtain a certain pore area as a function of cell radius.

In addition, we computed the field magnitude required to reach a certain intracellular concentration of ions by uptake of extracellular ions through diffusion after the pulse. To account for pore resealing, the effective diffusion surface was approximated as an exponential decrease of the pore area at the end of the pulse. Under this approximation the end intracellular concentration of ions is:

$$c_i = c_e\left(1 - \mathrm{e}^{-\frac{DS_{p1}}{Vh\tau}}\right) \tag{3}$$

where (c_e) is the external concentration, D is the diffusion constant in the pore, S_{p1} is the pore area at the end of the pulse, V is the cell volume, h is membrane thickness and τ is the time constant for pore resealing (30 ms).

RESULTS

Preliminary results from simulations (Figure 1) show that dependency of critical field on cell radii is less steep for the two models that incorporate permeabilization than for the model based on Schwan's equation.

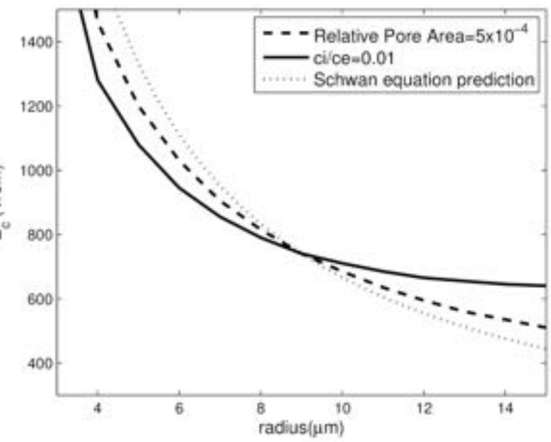

Figure 1: Necessary applied field from simulations to obtain a relative pore area of 5×10^{-4} (dashed line), and an intracellular concentration of 1% the extracellular concentration of a given ion (solid line); electric field for a constant voltage predicted by a simple, Schwan's equation based, model (dotted line).

REFERENCES

[1] B. E. Henslee, A. Morss, X. Hu, G. P. Lafyatis, and L. J. Lee, "Electroporation dependence on cell size: Optical tweezers study," *Anal. Chem.*, vol. 83, no. 11, pp. 3998–4003, 2011.

[2] L. Towhidi, T. Kotnik, G. Pucihar, S. M. P. Firoozabadi, H. Mozdarani, and D. Miklavčič, "Variability of the Minimal Transmembrane Voltage Resulting in Detectable Membrane Electroporation," *Electromagn. Biol. Med.*, vol. 27, no. 4, pp. 372–385, 2008.

[3] S. Hojo, K. Shimizu, H. Yositake, M. Muraji, H. Tsujimoto, and W. Tatebe, "The relationship between electropermeabilization and cell cycle and cell size of Saccharomyces cerevisiae," *IEEE Trans. Nanobioscience*, vol. 2, no. 1, pp. 35–39, 2003.

[4] A. Ivorra, J. Villemejane, and L. M. Mir, "Electrical modeling of the influence of medium conductivity on electroporation," *Phys. Chem. Chem. Phys.*, vol. 12, no. 34, p. 10055, 2010.

Spore inactivation by pulsed electron beam

Camille Lamarche[1], Houda Baaziz[2], Marie-Pierre Rols[2], Gauthier Demol[1], Flavien Pillet[2],
[1]*International Technologies for High Pulsed Power (ITHPP), Hameau de Drèle 46500 Thégra, France;* [2]*IPBS/CNRS (Institut de Pharmacologie et de Biologie Structurale), BP64182, 205 route de Narbonne 31077 Toulouse Cedex04, France*

INTRODUCTION

Electron beam is a promising technology to sterilize packaging in food or pharmaceutical industries. The pulsed electron beam at low energy allows sterilization by ionization of a large area.

Here, we first study the efficiency of pulsed electron beam on bacteria (vegetative form and spore) and yeast. Then, we investigate if an adaptive mechanism of spores to electron beam is present. Finally, we tried to explain mechanisms involved in the killing effect.

METHODS

Different numbers of pulses were tested with the following parameters: U=250 kV; I=5 kA; τ=10 ns; f=100 Hz. To estimate the logarithmic decrease, colony counting was performed on PCA (Plate Count Agar).

To study spores' resistance, two spots of 100 µL of *Bacillus pumilus* spore (10^9 CFU/mL) were put on Petri dishes: one spot for the Wild Type (WT) and another one which undergoes a number of ionisation before. Between each serie of radiation (10 pulses), the surviving spore were cultivated in DIFCO medium, concentrated and filed on Petri dish for the next treatment.

The genotoxicity of the spores treated by electron beam was tested on cancer cell HCT116 and on healthy cell HDFn. The spore treated with 20 pulses was recovered and filtered. The solution was put in contact with cell (50 000 cells by well). The genotoxicity was measure by the rate of phosphorylated histone H2AX. The phosphorylation of H2AX is the most sensitive marker that can be used to examine the DNA damage.[1][2]

The viability is quantified by Reddot staining, which label live cell nuclear

RESULTS

In Table 1, the logarithmic decrease obtained for different microorganisms allows to confirm that *Bacillus pumilus* (ATCC 27142) spore is the most resistant strain for irradiation technologies. The next experiments were made for this strain.

The influence of frequencies on the efficiency was tested. For the two frequency 50 Hz and 100 Hz, the logarithmic reduction was the same on *Bacillus pumilus* spore. The better efficiency is for 5 Hz and can be explain by a higher value of current, so a higher dose.

After 10 generations, spores do not developed a mechanism of resistance. Indeed, the logarithmic decrease is the same for the WT and the n+10 generation.

The viability and the genotoxicity of cancer cell HCT116 were not affected by the treatment. The same experiment was done on human fibroblast HDFn and the same result was observed.

Strain	Number of pulses	Logarithmic decrease
Saccharomyces cerevisiae	1	4.1 $\log_{10}$
Escherichia coli	1	> 6 $\log_{10}$
***Bacillus subtilis* (vegetative form)**	1 2	2 $\log_{10}$ > 5.7 $\log_{10}$
***Bacillus subtilis* (spore)**	10	4.47 $\log_{10}$
***Bacillus pumilus* (spore)**	10	4.1 $\log_{10}$

Table 1: Efficiency of pulsed electron beam on different strains

CONCLUSIONS

The results obtained confirm the high efficiency of the technology on yeast and bacteria. Indeed, for *Bacillus pumilus* spore, 4 logarithmic reductions were obtained within 100 ms. In addition, it was demonstrated that the treatment does not induce an adaptive mechanism which increases the resistance for survival *Bacillus pumilus*, even after 10 generations. Moreover, the treatment of *Bacillus pumilus* do not induced the creation of genotoxic agents for HCT116 cell and for human fibroblast HDFn.

Further experiments will consist on the observation of the cell wall of *Bacillus pumilus* spore by AFM to visualize the integrity of the bacteria. In addition, the study of proteins and DNA integrity should be investigate to understand the mechanism involved in the killing effect of pulsed electron beam.

ACKNOWLEDGEMENTS

I would like to thank the LEA EBAM which allows me to present my work and which gives me access to their facilities to learn more about electroporation.

REFERENCES

[1] A. Sharma, K. Singh and A. Almasan, "Histon H2AX phosphorylation: a marker for DNA damage" *Methods Mol Biol*., **DNA** Repair Protocols,613, 2012.

[2] Audebert M, Dolo L, Perdu E, Cravedi J-P, Zalko D. Use of the γH2AX assay for assessing the genotoxicity of bisphenol A and bisphenol F in human cell lines. Arch Toxicol. Nov 2011;85(11):1463-73.

Thermal effect of nanosecond pulsed electric fields

David Moreau[1], Claire Lefort[1], Ryan Burke[1], Philippe Leveque[1], Rod O'Connor[1]; [1] *Univ. Limoges, CNRS, XLIM, UMR 7252, F-87000 Limoges, France*

INTRODUCTION

Nanosecond pulsed electric fields (nsPEFs) are a tool with an increased interest used for cancer treatment [1]. nsPEFs can be used to make the plasma membranes of cells permeable in a transient way [2]. In spite of having high peak power, these ultrashort pulses are considered to be non-thermal since they have a very short duration, making them delivering low average energy density. However, it has been interestingly shown analytically that the electrical effects of the application of nsPEFs to cells could be accompanied by thermal effects at the local scale due to Joule heating [3,4].

Here we highlight the local thermal effects involved in the application of nsPEFs by using the Rhodamine B (RhB). RhB is a fluorophore with the particularity to have its quantum yield dependent on the temperature.

EXPERIMENTAL SETUP

The setup is presented in figure 1. We used a wide field epifluorescence microscope to detect the RhB fluorescence intensity. The LED with a wavelength centered at λ=549 nm performed the excitation of RhB. We used a dichroic mirror centered at 565 nm to deliver this light to the cells, and a 20X objective to focus this same light from the LED in the petri dish containing the cells loaded with RhB. The fluorescence emission light (centered at λ=576 nm) of RhB passed through the dichroic mirror and was detected with a 16 bits electron-multiplying charge-coupled device camera. All the elements of the setup were controlled and synchronized by the freely available software Winfluor and by the use of an analog output from digital acquisition (DAQ) board.

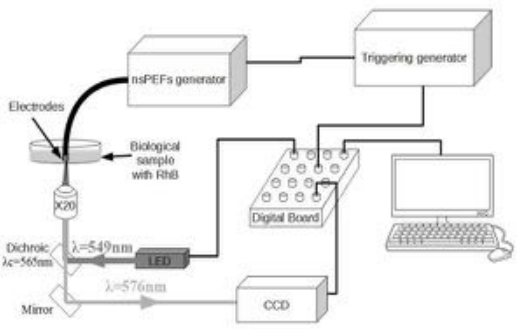

Figure 1: Experimental Setup

To study the impact of nsPEFs on local temperature, the nsPEF delivery system was based on a nanosecond pulse generator that delivered 10 ns pulses. This generator was triggered by a function generator controlled by a custom Labview program. The trigger signal was constituted by square pulses (duty cycle of 10 %) and was recorded during all the experiments. The electrical pulses were delivered to the cells by two electrodes, separated by a distance of 1.5 mm.

RESULTS

Different parameters of the exposure of biological cells to nsPEFs were tested. In the first set of experiments, we used 100 pulses with a frequency of 10 Hz, and we varied the voltage of the source to finally have an electric field varying from 5.5 to 44 kV/cm, according to FDTD simulations. The results are presented in table 1.

Table 1: Temperature increase depending on nsPEFs amplitude

nsPEF amplitude (kV/cm)	5.5	11	17	22	34	44
Temperature increase (°C)	0	0.2	0.4	0.7	1.5	2

In the second set of experiments, we fixed the electric field at 44 kV/cm, and we varied the number of pulses and their frequency. The results are shown in table 2.

Table 2: Temperature increase depending on frequency and number of nsPEFs

		NUMBER OF PULSES		
		1	10	100
FREQUENCY (HZ)	10	0°C	0.6°C	2.1°C
	100	0°C	0.6°C	4.8°C

In our experiments, we demonstrated the increase of local temperature at the cellular level in biological samples exposed to nsPEFs with a duration of 10 ns. The results presented here suggest that temperature changes should also be considered in nsPEFs effects, as well as electrical effects, particularly at higher electric fields, application frequencies and repetition rates.

AKNOWLEDGEMENTS:

The research was conducted in the scope of LEA EBAM.

REFERENCES

[1] X.H. Chen, S.J. Beebe, and S.S. Zheng, "Tumor ablation with nanosecond pulsed electric fields," *Hepatobil. Pancreatic Diseases Int.*, vol. 11, pp. 122–124, 2012.

[2] A.G. Pakhomov, J.F. Kolb, J.A.,White, R.P. Joshi, S. Xiao, and K.H. Schoenbach, "Long-lasting plasma membrane permeabilization in mammalian cells by nanosecond pulsed electric field (nsPEF).," *Bioelectromagn.*, vol. 28(8), pp. 655–663, 2007.

[3] J. Song, R.P. Joshi, and K.H. Schoenbach, "Synergistic effects of local temperature enhancements on cellular responses in the context of high intensity, ultrashort electric pulses," *Med. Biological Eng. Computing*, vol. 49(6), pp. 713–718, 2011.

[1] [4] T. Kotnik, D. Miklavčič, "Theoretical evaluation of the distributed power dissipation in biological cells exposed to electric fields," *Bioelectromagnetics* vol.21, pp. 385-394, 2000.

Nanosecond electroporator with diode opening switch and Silicon Carbide MOSFET

Eva Pirc, Matej Reberšek; *Faculty of Electrical Engineering, University of Ljubljana, Tržaska 25, SI-1000 Ljubljana, SLOVENIA*

INTRODUCTION

Electroporation is a technique in which an electrical field is applied to cells in order to increase the permeability of their membranes. The application requires electroporator and electrodes. An electroporator is a high voltage pulse generator that generates pulses of specific shape, amplitude, duration, number and pulse repetition frequency.

Our goal was to design a 10 kV few nanoseconds pulse generator with 200 A output current. We focused on Silicon Carbide MOSFET technology, which we believe is the most suitable for our application. In nanosecond electroporator design the main challenge is, the construction of a generator that delivers very short high power pulses.

METHODS AND MATERIALS

We evaluated and compared new Silicon Carbide (SiC) MOSFET with most commonly used technologies. According to our application we are looking for an element that allows us to generate the highest possible load current in this very short nanosecond time. It should be capable of switching at high voltages and currents. In testing we confirm our assumption, that SiC MOSFET's are the most appropriate for this application, we also noticed, that a square pulse generator is inappropriate because of double pulse phenomenon. Further on we focus on designing a diode opening switch generator, with Marx bank circuit. In order to achieve desired output voltage and current, we have two by two SiC MOSFET-s in a series - parallel arrangement (Figure 1). Pulse is formed by a diode that must be forward and reverse pumped with adequate sinusoidal current. Diode should stop conducting when the majority of the total energy is stored in L_2. That means a current must be maximized at the time of switching. All requirements can be ensured with appropriate matching of capacitors and inductors values in LC oscilator [1, 2].

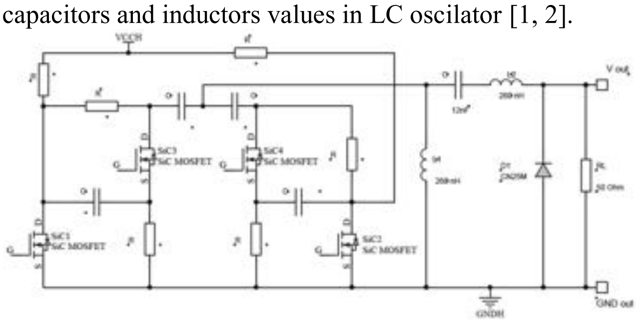

Figure 1: Basic schematic of pulse generator.

RESULTS AND DISCUSSION

Analysis and design of the final product are still in progress. For now our electroporator has not yet reached our goals (10 kV, few nanoseconds pulse, 200 A). The device generates 3.8 kV pulses of Gaussian shape and 10 ns duration on a 50 Ω load. We measured output voltage on two deferent loads, the first one was 100 Ω and the second one 50 Ω (Figure 2). The output voltage in case of 50 Ω load is not proportionally lower. Inductor (L_2) current reaches expected value 180 A, but output current is only 76 A. We can assume the diode switching time in not optimal. The amount of the output current is significantly higher, that means that the generator operates more efficiently with 50 Ω load. Transistors being operating in saturation region at slightly lower input voltages then expected. Maximum input voltage was 800 V, transistor drain source breakdown voltage is 1200 V, so we plan changes to use their full potencial.

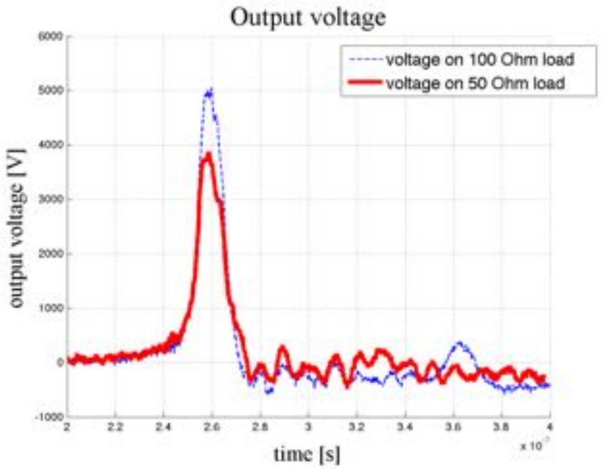

Figure 2: Output voltage on 100 Ω and 50 Ω load.

CONCLUSION

For better results it is necessary to adjust values in LC oscilator and change diode matrix.

REFERENCES

[1] J. M. Sanders, A. Kuthi, Yu-Hsuan Wu, P.T. Vernier, and M.A. Gundersen, "A linear, single-stage, nanosecond pulse generator for delivering intense electric fields to biological loads," in *Dielectrics and Electrical Insulation, IEEE*, vol. 16, August 2009.

[2] M. Kranjc, M. Reberšek, D. Miklavčič, "Numerical simulations aided development of nanosecond pulse electroporators," in *6th European Conference on Antennas and Propagation (EUCAP) 2012, IEEE,* pp. *344 – 347*.

ACKNOWLEDGEMENTS

This study was supported by the Slovenian Research Agency (ARRS) and conducted within the scope of the European Associated Laboratory on the Electroporation in Biology and Medicine (LEA-EBAM)

Calcium-independent disruption of microtubule growth following nanosecond pulsed electric field exposure in U87 human glioblastoma cells

Lynn Carr, Sylvia Bardet, Malak Soueid, Delia Arnaud-Cormos, Philippe Leveque, Rodney O'Connor;
Xlim Research Institute and LABEX "Sigma-LIM", University of Limoges and CNRS, 123, Avenue Albert Thomas, F-87060 Limoges, FRANCE

INTRODUCTION

High powered, nanosecond duration pulsed electric fields (nsPEF) have been proposed as a minimal side-effect, electrical cancer therapy, unlikely to result in resistance. They induce apoptotic death in cancerous cells and reduce tumour size by a currently unknown mechanism [1,2].

Microtubule depolymerisation is an intrinsic, early event in normally occurring apoptosis and electric fields have been shown to disrupt microtubule polymerisation [3,4]. Given this, it is therefore possible that nsPEF cause microtubule depolymerisation, which initiates apoptosis.

METHODS

U87 EB3-GFP cells were observed by epifluorescence using a Leica DMI6000 microscope with a 100x objective. Changes in intracellular calcium were measured in U87 cells loaded with 1.25 µM Fura Red, AM (Life Technologies). Standard HBSS containing either 1.8 mM of calcium or 4 mM EGTA (calcium free) were used as imaging buffers. Intracellular calcium stores were depleted by incubating cells for 30 minutes in calcium free imaging buffer containing 1 µM thapsigargin. 100, 10 ns, pulses with an electric field strength of 44 kV/cm were applied to cells at a frequency of 10 Hz using an nsPEF generator with 50 Ω output impedance and an electrode delivery system comprising of two steel electrodes, separated by a gap of 1.2 mm and with a 50 Ω impedance in parallel.

RESULTS

Live cell imaging of the microtubule plus end tracking protein EB3-GFP in U87 cells showed that 100, 10 ns pulses delivered at 10 Hz caused a rapid disruption of microtubule growth (figure 1). This disruption occurred within 3 minutes of pulse application, shown by a statistically significant decrease in EB3 fluorescence in nsPEF treated samples, as compared to non-pulsed controls ($t=2.64$, $p=0.02$, $n=11$). A post-pulse increase in intracellular calcium was measured in Fura Red, AM loaded U87 cells. This increase was due to both an influx of calcium from the imaging buffer and release from internal stores.

As calcium is known to depolymerise microtubules we sought to identify if it was the source of the observed microtubule disruption. U87 EB3-GFP cells, with depleted internal calcium stores, were pulsed in calcium free imaging buffer and a post-pulse decrease in microtubule growth, similar to that seen with calcium, was observed (figure 1). Cellular swelling, as a result of nsPEF induced membrane poration, is another possible cause of the microtubule disruption. However, cells pulsed in an isotonic sucrose buffer, to prevent swelling, showed a similar post-pulse decrease in EB3 fluorescence to those pulsed in normal buffer (figure 1).

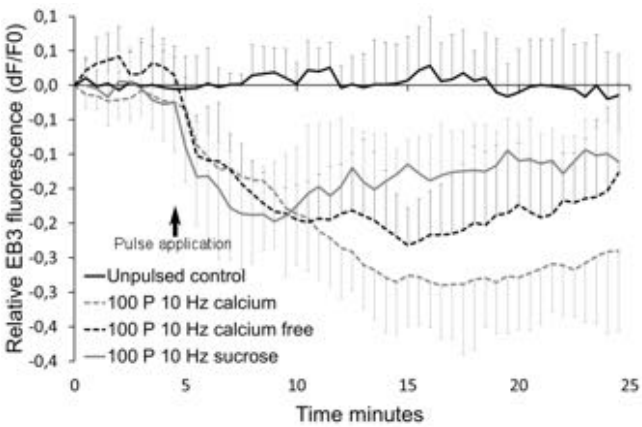

Figure 1: Disruption of microtubule growth, in U87 cells, following nsPEF treatment is independent of increases in intracellular calcium and cellular swelling.

CONCLUSIONS

We show that nsPEF induced microtubule disruption is independent of both changes in intracellular calcium levels and swelling. This suggests the involvement of an alternative mechanism, such as a direct destabilizing action of nsPEF on microtubules or modulation of one of the many microtubule-associated proteins that are linked to microtubule stability. Given the essential role of microtubules in apoptosis execution we propose that their depolymerisation could be an important factor in nsPEF-induced apoptosis.

REFERENCES

[1] Beebe, S. J. *et al*. Nanosecond, high-intensity pulsed electric fields induce apoptosis in human cells. *FASEB J*. 17**,** 1493–5, 2003

[2] Nuccitelli, R. *et al*. First-in-human trial of nanoelectroablation therapy for basal cell carcinoma: Proof of method. *Exp. Dermatol*. 23, 135–137, 2014

[3] Moss, D. K. & Lane, J. D. Microtubules: forgotten players in the apoptotic execution phase. *Trends Cell Biol*. 16, 330–8, 2006

[4] Ramalho, R. R. *et al*. Microtubule behavior under strong electromagnetic fields. *Mater. Sci. Eng. C*, 27**,** 1207–1210, 2007

ACKNOWLEDGEMENTS

This research was conducted in the scope of LEA EBAM

Small Molecule Transport Through Electropermeabilized Live Cells

Esin B. Sözer[1], and P. Thomas Vernier[1], [1] *Frank Reidy Research Center for Bioelectrics, Old Dominion University, Norfolk, VA USA*

INTRODUCTION

Studies of electropermeabilization (electroporation) often monitor the transport of normally impermeant fluorescent dyes across the cell membrane [1-5]. . Results are typically based on average fluorometric responses of cell populations or descriptive and geometric analyses of fluorescence microscope images of single cells. After decades of effort, however, the detailed molecular mechanisms underlying electropermeabilization in living cells remain obscure, and models are predictive only to a very limited extent.

MATERIALS AND METHODS

Single 6 ns, 20 MV/m pulses from an FID pulse generator [FPG 10-10NK] were delivered to cells in suspension in cover glass chambers [Thermo Scientific™ Nunc™ Lab-Tek™ II] through parallel tungsten wire electrodes with a separation of 100 µm, positioned in the chamber with a micromanipulator [6]. U937 (human histiocytic lymphoma monocyte; ATCC CRL-1593.2) cells were cultured in RPMI-1640 medium (Corning® glutagro™ 10-104-CV) with 10% fetal bovine serum (Corning, 35-010-CV), and 1% penicillin/streptomycin mixture (10000U/mL penicillin and 10 mg/mL Streptomycin) at 37 °C in a humidified, 5% CO_2 atmosphere. Cells were washed and suspended at approximately 5×10^5 cells/mL in fresh medium containing 2 µM YO-PRO-1 for experiments.

RESULTS AND FUTURE WORK

Our results of quantification of the total influx of YO-PRO-1 into U937 cells after **single 6 ns pulse exposure** reveal a slow and continuous uptake of the molecule over 10 minutes (180 molecules per cell per second).

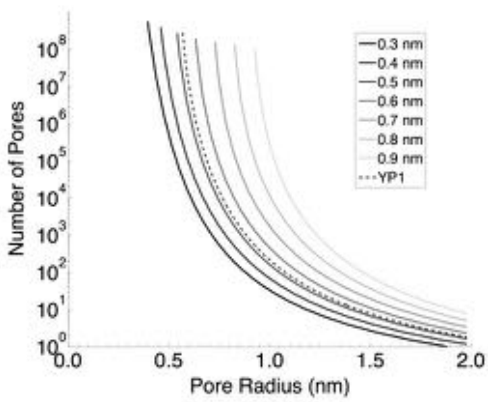

Figure 1: Number of pores versus pore radius for different solute sizes calculated based on the experimental measurements.

If we assume simple drift and diffusion model for the transport, we can calculate a range of number of pores versus pore size based on the experimentally measured uptake as seen in figure 1.

These experimental observations taken together with corresponding molecular dynamics simulations challenge the simple "drift and diffusion through a pore" model for small molecule transport. Comparative studies of small molecule electropermeabilization of U937 cells after 6 ns and 220 µs pulses using the fluorescent dyes YO-PRO-1, propidium, calcein, and Lucifer yellow are in progress.

These molecules of comparable size but different chemical properties exhibit large differences in localization of fluorescence and fluorescence increase dynamics after single or multiple 6 ns and 220 µs pulsed electric field exposures.

REFERENCES

[1] M. R. Prausnitz, J. D. Corbett, J. A. Gimm, D. E. Golan, R. Langer, and J. C. Weaver, "Millisecond measurement of transport during and after an electroporation pulse.," *Biophys. J.*, vol. 68, no. 5, p. 1864, 1995.

[2] B. Gabriel and J. Teissié, "Time courses of mammalian cell electropermeabilization observed by millisecond imaging of membrane property changes during the pulse," *Biophys. J.*, vol. 76, no. 4, pp. 2158–2165, 1999.

[3] S. M. Kennedy, Z. Ji, J. C. Hedstrom, J. H. Booske, and S. C. Hagness, "Quantification of Electroporative Uptake Kinetics and Electric Field Heterogeneity Effects in Cells," *Biophys. J.*, vol. 94, no. 12, pp. 5018–5027, Jun. 2008.

[4] M. M. Sadik, J. Li, J. W. Shan, D. I. Shreiber, and H. Lin, "Quantification of propidium iodide delivery using millisecond electric pulses: Experiments," *Biochim. Biophys. Acta - Biomembr.*, vol. 1828, no. 4, pp. 1322–1328, Apr. 2013.

[5] A. G. Pakhomov, E. Gianulis, P. T. Vernier, I. Semenov, S. Xiao, and O. N. Pakhomova, "Multiple nanosecond electric pulses increase the number but not the size of long-lived nanopores in the cell membrane.," *Biochim. Biophys. Acta*, vol. 1848, no. 4, pp. 958–966, Apr. 2015.

[6] Y.-H. Wu, D. Arnaud-Cormos, M. Casciola, J. M. Sanders, P. Leveque, and P. T. Vernier, "Moveable wire electrode microchamber for nanosecond pulsed electric-field delivery.," *IEEE Trans. Biomed. Eng.*, vol. 60, no. 2, pp. 489–496, Feb. 2013.

Change in propidium iodide (PI) fluorescence intensity of MEC- 1 Cells due to treatment with microsecond electric pulses

Alaaddin Coskun, Handan Kayhan[2], Ayse G. Canseven[1] [1]*Department of Biophysics, Faculty of Medicine, Gazi University, Ankara, TURKEY,* [2]*Department of Internal Medicine, Division of Hematology, Faculty of Medicine, Gazi University, Ankara, TURKEY*

INTRODUCTION

Cell electroporation is a physical method that facilitates the passage of various molecules (DNA, drug, non-permanent ion, etc) into cells by applying high electric field pulses inducing sufficently high transmembrane voltage (0.5-1 V) by formation of pores on the cell membrane. A few kV/cm of electric field and several microseconds are required to induce reversible or irreversible breakdown of the cell plasma membrane [1,2]. For the estimations of cell permeabilization in vitro Propidium Iodide (PI) has been used [3,4]. The aim of this study is to determine the appropriate electric field strength that is needed to electropermeabilize MEC-1 cells for 100 µs pulse duration by evaluating florescence intensity of PI by flow cytometry.

MATERIALS AND METHODS

In-vitro experiments were performed on MEC-1 cell line derived from B-chronic lymphocytic leukemia (B-CLL) cells to determine membrane permeabilization. A programmable high-voltage squarewave electric pulse generator BTX ECM 830 wave electroporator was used for generation of electric pulses. Eight square wave pulses with a frequency of 1 Hz, an electric field strength of 0 to 1250 V/cm, a duration of 100 µs were used as pulse parameters. Experiments were performed in electroporation cuvettes containing parallel steel stainless electrodes with a distance of 4 mm (electrode gap). PI uptake was used to evaluate cell permeabilization of MEC -1 cells due to electric pulses. Flow cyrometry was used to assess PI uptake into the pulsed cells.

RESULTS

Fluorescence intensity depending on the electric field intensity was evaluated. Figure 1 shows the variation of the total fluorescence intensity (TFI) as a function of electric field intensity at a duration of 100 µs. Increase in amplitude of electric pulse resulted in increase of fluorescence intensity. It was observed that increase of total fluorescence intensity showing electropermeabilized cell count increases with the electric field intensity.

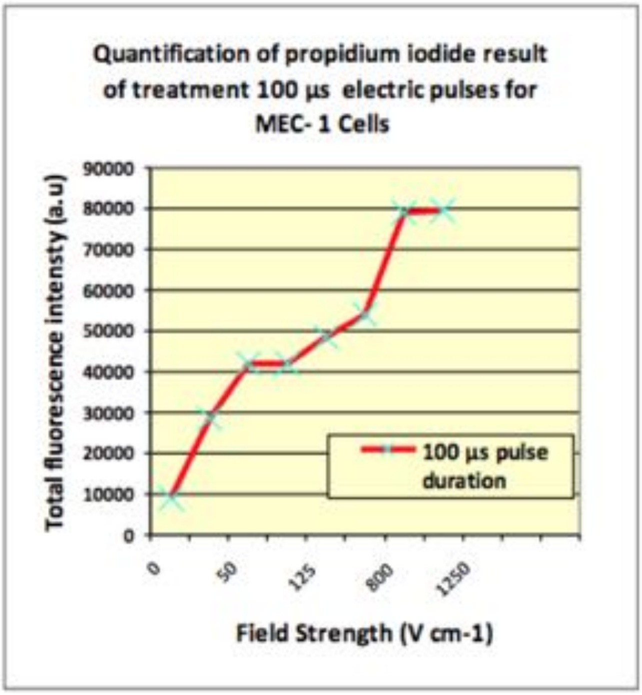

Figure 1. Quantification of propidium iodide result of treatment with eight electric pulses (100 µs) for MEC- 1 cells in vitro

REFERENCES

[1] Zimmermann, U. (1996) in Electromanipulation of Cells (Zimmermann, U. and Neil, G., eds.), pp. 1-106, CRC Press, Boca Raton,FL.
[2] S. Kee, J. Gehl, E.W. Lee, Clinical Aspects of Electroporation, Springer, New York, 2011.
[3] M.P. Rols, C. Delteil, M. Golzio, P. Dumond, S. Cros and J.Teissié. In vivo electrically mediated protein and gene transfer in murine melanoma. Nat.Biotechnol., 16, 168-171, 1998.
[4] David C. Bartoletti, Gail I. Harrison and James C. Weaver.The number of molecules taken up by electroporated cells: quantitative determination. Federation of European Biochemical Societies., Volume 256, number 1,2, 4-10.

Voltage-gated ion channel antagonists inhibit nsPEF-induced membrane depolarization in U87 glioblastoma cells

Ryan C. Burke, David Moreau, Delia Arnaud-Cormos, Phillipe Leveque & Rod O'Connor, Xlim Research Institute and LABEX "Sigma-LIM", University of Limoges and CNRS, 123, Avenue Albert Thomas, Limoges F-87060, France.

INTRODUCTION

nsPEFs influence cell physiology by a number of mechanisms including the permeabilization of the plasma membrane [1,2]. Few studies have considered the influence of nsPEF on excitable cells or voltage-gated ion channels [3,4]. This is an important consideration given that several types of voltage-gated ion channels are known to be expressed in cancers like glioblastoma [5].

METHODS

U87 glioblastoma cells were incubated at 37°C at 5% CO2 for a period of 30 minutes in Live Cell Imaging solution (with 5.5 mM glucose) and the voltage sensitive dye (PMPI at a concentration of 0.5 µL/mL). Fluorescence images were collected using a 100x oil immersion objective. Fluorescent excitation/emission was 475 nm and 615 nm, respectively, and measurements were recorded every 30 seconds. Cells were exposed to a single, monopolar 10 ns pulse using a commercially available nsPEF generator with a 50 Ω output impedance. Pulses were applied to cells by positioning an electrode delivery system with a micromanipulator. The electric field strength of the applied pulse was 34.2 kV/cm as simulated by FDTD.

RESULTS

In investigating the various cation currents involved in nsPEF effects, we observed that the tetraethylammonium cation (TEA), a potassium channel blocker, prevented the depolarization in membrane potential caused by a single nsPEF. Experiments were performed to determine the specific potassium channel involved. At high concentrations [100 mM] TEA blocks BK channels and SK channels, whereas at low concentrations [5 mM] TEA is known only to block SK channels. Significant nsPEF inhibition was observed only when high concentrations of TEA were used. Penitrem A is known as a selective and potent BK channel blocker and had a similar effect at [10 uM] on nsPEF membrane depolarization as high concentrations of TEA. Since the BK channel is a calcium-dependent voltage-gated potassium channel, calcium-free media was used where equimolar amounts of EGTA [1.8 mM] replaced the calcium. In this condition a similar inhibitory effect was observed on nsPEF membrane depolarization as the other conditions. Finally, nifedipine [10 uM] was used to investigate the effects of an L-type calcium channel inhibitor on nsPEF-induced membrane depolarization in order to see if this effect was specific to the BK channel as the results had suggested up to this point. Although an inhibitory effect was observed, the effect was significantly less than observed using BK channel inhibitors.

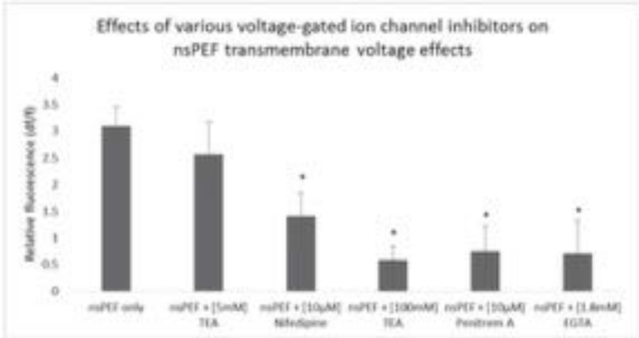

Figure 1: The effects of calcium-free media and various voltage-gated ion channel inhibitors on nsPEF-induced membrane depolarization (Error bars represent +/-2SE). *indicates statistically significant difference, α=0.05

CONCLUSIONS

Here we have demonstrated that membrane depolarization from a single nsPEF can be inhibited using various voltage-gated antagonists. Whereas inhibition of voltage-gated calcium channels did reduce the depolarizing effect, it was significantly less effective than BK channel inhibition directly or through calcium removal from the media. Together these results suggest that nsPEF membrane depolarization by a single pulse appears to be acting directly on voltage-gated channels as opposed to electroporation of the membrane. Although non-specific, this effect appears to be mediated primarily through BK channels.

REFERENCES

[1] Pakhomov, A. G., et al. (2007). Long-lasting plasma membrane permeabilization in mammalian cells by nanosecond Pulsed Electric Field (nsPEF). Bioelectromagnetics, 28, 655–663.

[2] Chopinet, L., & Rols, M.-P. (2014). Nanosecond electric pulses: A mini-review of the present state of the art. Bioelectrochemistry. doi:10.1016/j.bioelechem.2014.07.008

[3] Craviso, G. L., et al. (2010). Nanosecond electric pulses: A novel stimulus for triggering Ca2+ influx into chromaffin cells via voltage-gated Ca2+ channels. Cellular and Molecular Neurobiology, 30(8), 1259–1265.

[4] Semenov, I., et al. (2015). Cell stimulation and calcium mobilization by picosecond electric pulses. Bioelectrochemistry, 105, 65–71.

[5] Ducret, T., Vacher, A.-M., & Vacher, P. (2003). Voltage-dependent ionic conductances in the human malignant astrocytoma cell line U87-MG. Molecular Membrane Biology, 20, 329–343.

Acknowledgments: This research was conducted in the scope of LEA EBAM

Effects of Applied Voltage on Electropermeabilization of SH-SY5Y Neuroblastoma (NB) and MCF-7 human breast carcinoma cells

Meric Arda Esmekaya[1], Handan Kayhan[2], Ayse G. Canseven[1]; [1]*Department of Biophysics, Faculty of Medicine, Gazi University, Ankara, TURKEY*, [2]*Department of Internal Medicine, Division of Hematology, Faculty of Medicine, Gazi University, Ankara, TURKEY*

INTRODUCTION

Electrochemotherapy is a type of chemotherapy that allows delivery of drugs into the cell. It is based on the local application of short and intense electric pulses that transiently permeabilize the cell membrane, thus allowing transport of drugs that are not permitted by the membrane. When a biological cell is exposed to an electric field of sufficient strength, an increase in the transmembrane voltage is generated, which leads to rearrangements of the cell membrane structure. These changes result in an increase of the cell membrane permeability which allows drugs to enter the cell. This phenomenon is called electroporation and is becoming widely used to improve anticancer drug delivery into cells [1,2].

Electropermeabilization of cells depends on magnitude of pulse, pulse duration, number of pulses, cell type, geometry and etc [3,4]. To achieve reversible membrane permeabilization, electrical pulse applied to cell must have an appropriate value. For this reason, it is very important to choose amplitude of critical electrical pulse parameters. In this study, we investigated critical electroporation voltages for electropermeabilization of SH-SY5Y Neuroblastoma (NB) and MCF-7 human breast carcinoma cells.

MATERIALS AND METHODS

Cells were cultured in 75 ml culture flasks in Dulbecco's modified Eagle's medium (DMEM D5546-500ML- Sigma). Electroporation was performed in disposable electroporation cuvettes containing parallel plate electrodes with a distance of 4 mm (electrode gap). The cell suspension was placed in electrode chamber between the electrodes. Eight square wave pulses with a frequency of 1 Hz, electrical voltage up to 800 V, and duration of 100 µs were used as pulse parameters. The percentage of fluorescence intensity of PI and permeabilised cells were determined from histogram obtained by flow cytometry (Becton-Dickinson). At least 10.000 cells were measured from each sample.

RESULTS

PI fluorescence intensity versus electrical voltage for SH-SY5Y and MCF-7 was given in figures 2 and3 3. As seen in figures, higher pulse amplitude increased cell permeabilization in both cell type. Moreover, SH-SY5Y cells were more resistant to electrical pulses. These results showed that critical electric pulse voltages to achieve membrane permeabilization depend on both electrical pulse magnitude and type of cell.

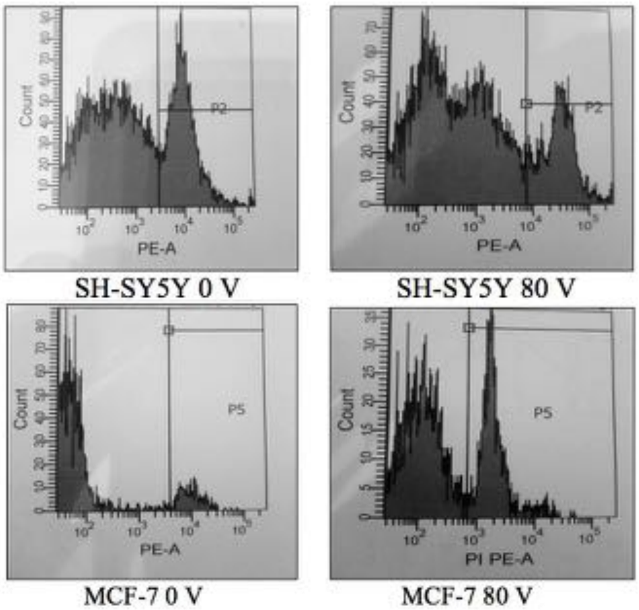

Figure 1: Mean fluorescence intensity of PI

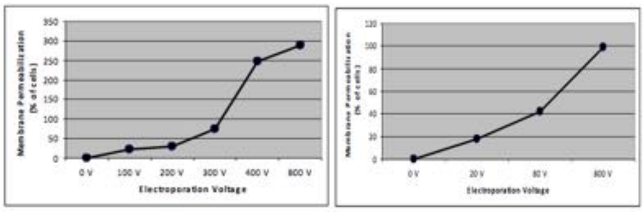

Figure 2: Percentage of electropermeabilizated cells in SH-SY5Y (right) and MCF-7 (left) cells.

REFERENCES

[1] Pucihar G, Kotnik T, Miklavcic D, Teissié J. Kinetics of transmembrane transport of small molecules into electropermeabilized cells. Biophys J. 2008 15;95(6):2837-48.

[2] Pavlin M, Kanduser M, Rebersek M, Pucihar G, Hart FX, Magjarevic R, Miklavcic D. Effect of cell electroporation on the conductivity of a cell suspension. Biophys J. 2005 88(6):4378-90.

[3] De Vuyst E1, De Bock M, Decrock E, Van Moorhem M, Naus C, Mabilde C, Leybaert L. In situ bipolar electroporation for localized cell loading with reporter dyes and investigating gap junctional coupling. Biophys J. 2008 15;94(2):469-79.

The Influence of Electroporation on the Cellular Morphology of Selected Cell Lines

Jolanta Saczko[1], Nina Rembiałkowska[1], Anna Choromańska[1], Julita Kulbacka[1], [1]*Department of Medical Biochemistry, Medical University of Wroclaw, Chałubińskiego 10, 50-368 Wroclaw, POLAND*

INTRODUCTION

Electroporation (EP) of cells is widely applied in cell biology. biotechnology and medicine. This method is based on the action of electric field on the cells. The pulses of the high voltage creates temporary pores in the cell membrane, which opens additional way for various compounds into the cells [1, 2]. The mechanism of EP is still not fully understood. Presently EP is used in cell culture as the purest available method of gene transfection and drug transport in chemotherapy called electrochemotherapy [3, 4]. Even though EP is useful in facilitating molecular transport, the intracellular effects of its application have not been sufficiently studied [1]. The main goal of the our investigation was examination of EP influence on cell morphology in selected normal and malignant by inverted light and electron transmission microscopy. The present paper shows unique studies of the EP influence on cell morphology.

MATERIAL AND METHODS

All experiments were performed on selected malignant cells in vitro (human breast adenocarcinoma resistant to doxorubicin, MCF-7/DOX). The cells after electroporation in various conditions were observed in inverted light microscopy and were prepared to evaluate in transmission electron microscopy (TEM).

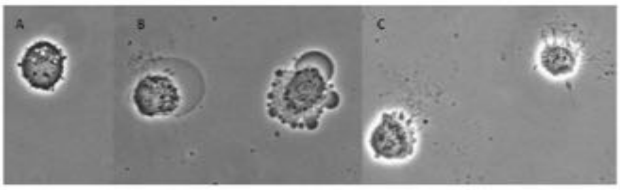

Figure 1: Phase contrast images of breast carcinoma cells MCF-7/DOX. **A**. No electric field applied; **B**. after electroporation at 1000 V – blebs in the membrane indicate unsealing of the membrane; **C**. after electroporation at 1200 V – release of the intracellular material through the pores [5].

RESULTS AND CONCLUSIONS

After electroporation at 1000 V/cm (8 pulses, 100 µs, 1Hz) blebs were observed (Fig.1)[5] occurring on the surface of the cellular membrane, which indicate poration of the membrane. After stronger electric field release of the intracellular material through the pores occurred. In lower electric field the same alternation appeared. Not significant ultrastructural changes were noticed in cells (Fig. 2) [1]. The degree of the morphological changes at the level of an inverted microscope, phase contrast has been dependent on the conditions of electroporation (current, amplitude, number of pulses) and the cell type. Cells after electroporation characterized vacuolisation, presence of bubbles on the membrane surface and irregular shape of the nucleus.

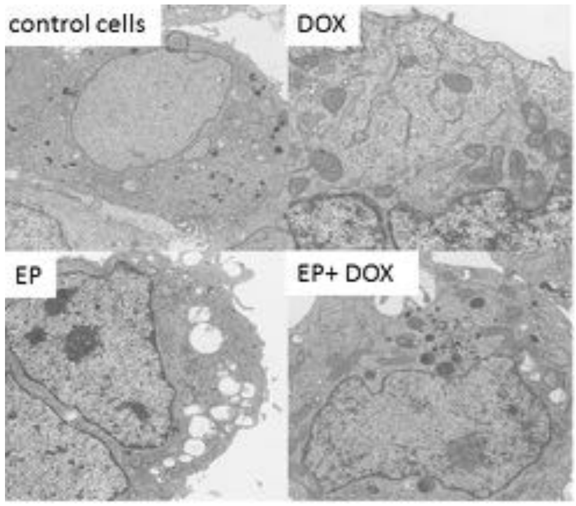

Figure 2: The ultrastructure of MCF-7/DOX cells [1].

Acknowledgments: This work was supported by the grant PBmn-132 and Statutory Funds of UMED ST-882

REFERENCES

[1] N. Skołucka, J. Saczko, M. Kotulska, M. Kulbacka, A. Choromańska, "Elektroporacja i jej zastosowanie". *Pol Mer Lek.*, (2010) XXVIII, pp 168-173.
[2] N. Skołucka M. Daczewska, J. Saczko, A. Chwiłkowska, A. Choromańska, M. Kotulska, I. Kamińska, J, "ETM study of electroporation influence on cell morphology in human malignant melanoma and human primary gingival fibroblast". *Asian Pac J Trop Biomed*. *Apr*; (2011) 1(2), pp: 94–98.
[3] J.C. Weaver, "Electroporation of Cells and Tissues" IEEE *Transactions on plasma Science*, (2000) 28, pp: 24-33.
[4] M. L Yarmush, A, Goldberg, G. Sersa, T. Kotnik and D. Miklavcic, " Electroporation-Based Technologies for Medicine: Principles, Applications, and Challenges", *Ann. Rev. Biomed. Eng,* (2014) 16, pp:295–320.
[5] J. Kulbacka, M. Nowak, N. Skołucka, J. Saczko, M. Kotulska. The influence of electroporation on in vitro photodynamic therapy of human breast carcinoma cells. *Folia Biol (Praha)*. 2011; 57(3): 112-118.

Evaluation of bystander effect in *in vitro* electroporation

Ajda Prevc[1], Apolonija Bedina-Zavec[2], Maja Cemazar[1, 3], Gregor Sersa[1]; [1]*Institute of Oncology Ljubljana, Zaloska 2, SI-1000 Ljubljana, SLOVENIA* [2]*National Institute of Chemistry, Hajdrihova 19, SI-1000 Ljubljana SLOVENIA* [3]*Faculty of Health Sciences, University of Primorska, Polje 42, SI-6310 Izola, SLOVENIA*

INTRODUCTION

Bystander effect (BE) is a known phenomenon in radiotherapy. It represents the damage of cells, which are not directly irradiated but are in the vicinity of the irradiated cells [1]. This damage is thought to be mediated through signals released by the irradiated cells. Among these signals are membrane vesicles i.e. microvesicles which are considered to contain proteins, RNA and other agents which can activate various signaling pathways in the target cells, including pathways leading to carcinogenesis or immune responses [2]. BE in electroporation (EP) has not yet been described. Therefore, our aim was to determine whether BE is present in *in vitro* EP and whether the electroporated cells produce microvesicles which could contribute to BE.

MATERIALS AND METHODS

The CMeC-1 canine melanoma cells [3] were electroporated using parallel plate electrodes with 2 mm gap. Eight square wave pulses of amplitude 80–320 V (amplitude over distance ratio (electric field intensity) 400–1600 V/cm), duration 100 µs and frequency 1 Hz were applied. After the EP, the cells were incubated for 5 hours, then the electroporated-cell conditioned medium (ECCM) was harvested and the cells were trypsinized and plated for the viability assay. After 24 hour incubation, we transferred the ECCM to the non-electroporated cells [4] and after 24 hours performed the viability assay using PrestoBlue reagent (Thermo Fisher Scientific, MA, USA) to determine the occurrence of BE. In addition, we measured the amount of microvesicles in the ECCM using Altra Flow Cytometer (Beckman Coulter Inc., CA, USA).

RESULTS

The results of the PrestoBlue assay showed no significant difference in viability of the control cells (without EP and with fresh medium) and the cells which were exposed to EP or ECCM of any electric field intensity (Table 1).

Table 1: Cell viability after electroporation with different electric field intensities or after medium transfer normalised to the control group (AM ± SEM).

Electric field intensity [V/cm]	cell viability [%]	cell viability after medium transfer [%]
0 (control)	100.0 ± 3.3	100.0 ± 0.7
400	100.2 ± 4.3	99.2 ± 0.7
800	99.8 ± 3.8	101.6 ± 2.1
1000	103.4 ± 3.6	99.7 ± 1.4
1200	100.7 ± 4.7	100.9 ± 1.4
1400	102.1 ± 5.0	99.1 ± 0.7
1600	98.6 ± 6.7	99.3 ± 0.6

Accordingly, the results of preliminary flow cytometry measurement of microvesicles, indicated no significant difference in the amount of microvesicles in the control cell medium and in the ECCM (Figure 1).

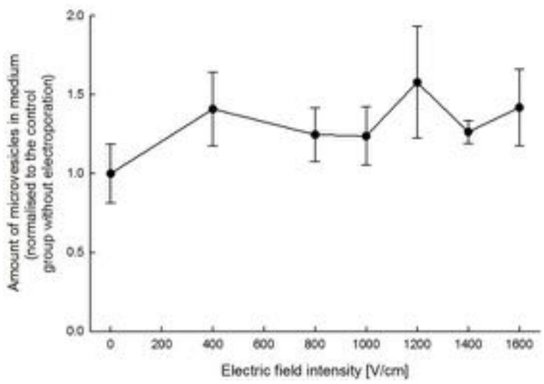

Figure 1: The amount of microvesicles in media from the cells exposed to different electric field intensities. The data represent AM ± SEM of three independent experiments.

CONCLUSION

Our preliminary results indicate that bystander effect is not present in *in vitro* EP and that there is no increase in formation of microvesicles by the electroporated cells, which could contribute to bystander effect.

ACKNOWLEDGEMENTS

ARRS, COST and LEA EBAM for the financial support.

REFERENCES

[1] A. Marín, M. Martín, O. Liñán, F. Alvarenga, M. López, L. Fernández, D. Büchser, L. Cerezo, "Bystander effects and radiotherapy," *Reports of Practical Oncology and Radiotherapy*, vol. 20, pp. 12–21, 2015.

[2] K.K. Jella, S. Rani, L. O'Driscoll, B. McClean, H.J. Byrne, F.M. Lyng, "Exosomes are involved in mediating radiation induced bystander signalling in human keratinocyte cells," *Radiation Research*, vol. 181, pp. 138–145, 2014.

[3] K. Inoue, E. Ohashi, T. Kadosawa, S.H. Hong, S. Matsunaga, M. Mochizuki, R. Nishimura, N. Sasaki, "Establishment and characterization of four canine melanoma cell lines," *Journal of Veterinary Medical Science*, vol. 66, pp. 1437–1440, 2004.

[4] C. Mothersill and C. Seymour, "Medium from irradiated human epithelial cells but not human fibroblasts reduces the clonogenic survival of unirradiated cells," *International Journal of Radiation Biology*, vol. 71, pp. 421–427, 1997.

Dependence of DNA electrotransfer efficiency to cells *in vitro* on the time-lag between low- and high-voltage pulses

Milda Jakutavičiūtė, Aurelija Kazlauskaitė, Paulius Ruzgys, Saulius Šatkauskas, *Biophysical research group, Faculty of Natural Sciences, Vytautas Magnus University, Vileikos 8, Kaunas, LT-44404, Lithuania*

INTRODUCTION

The method of electroporation uses high-voltage electric pulses (HV) that allow high and low molecular mass molecules to enter the inside of the cell [1,2]. However, it is also known that the efficiency of DNA electrotransfection increases when low-voltage electric pulses (LV) are used after permeabilizing HV pulses to increase the electrophoretic movement of DNA *in vivo* [3] and, at low plasmid concentrations, *in vitro* [4]. This work attempted to investigate the role of time-lag between HV and LV pulses and the amount of DNA used on the efficiency on DNA electrotransfection to cells.

METHODS

The experiments were conducted *in vitro* on Chinese Hamster Ovary (CHO) cells. 1 HV pulse of 1200 V/cm amplitude and 100 µs duration and 1 LV pulse of 100 V/cm amplitude and 100 ms duration were used. Plasmids encoding firefly luciferase and green fluorescent protein (GFP) were used with 10 µg/ml, 50 µg/ml and 100 µg/ml concentrations. Time-lags between 1 HV and 1 LV pulses were 1 µs, 10 µs, 100 µs, 1 ms, 10 ms, 100 ms and 1 s. The efficiency of luciferase coding plasmid electrotransfer was determined measuring luciferase activity 24 hours after plasmid electrotransfer and the efficiency of GFP coding plasmid electrotransfer was determined by counting GFP-positive cells under a fluorescent microscope and by using flow cytometry. Cell viability was determined using clonogenic assay. Statistical significance was calculated using Student's t-test. Results are represented as mean±SEM.

RESULTS AND CONCLUSIONS

It is known that, *in vivo*, DNA electrotransfection efficiency is higher when lower voltage and longer duration LV pulses are applied after higher voltage and short duration HV pulses. We applied that knowledge to *in vitro* system and tested the effect of plasmid concentration and the duration of time-lag between HV and LV pulses.

First of all, we tested the effect of time-lag duration (1 µs to 1 s) between HV and LV pulses while transfecting the cells with different concentrations of luciferase coding plasmid. As expected, increasing plasmid concentration increased electrotransfer efficiency. With all plasmid concentrations tested, highest transfection efficiency was observed with shorter time-lag durations. However, in higher concentration groups, decrease from maximum transfection efficiency was observed after longer time-lags between HV and LV pulses. Notably, use of shorter time-lags between pulses caused a drop in cell viability. We repeated the experiments using GFP coding plasmid and got similar results: the efficiency of DNA electrotransfer was highest using shortest time-lag between HV and LV pulses, and increased plasmid concentration lengthened the maximum time-lag observed before a drop in electrotransfer efficiency.

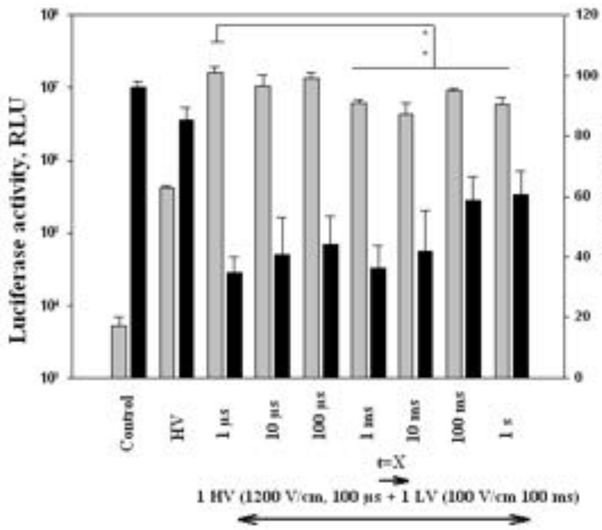

Figure 1: The effect of time-lag between high-voltage (HV, 1200 V/cm, 100 µs) and low-voltage (LV, 100 V/cm, 100 ms) electric pulses on the efficiency of DNA electrotransfection, evaluated from luciferase activity 24 hours after luciferase coding plasmid (end concentration 100 µg/ml, presented to cell suspension prior electroporation) electrotransfer to CHO cells. Grey bars show the luciferase activity, black bars show the cell viability. A decrease in electrotransfection efficiency is observed when time-lag duration is increased above 1 µs.

REFERENCES

[1] J.C Weaver, Y.A. Chizmadzhev, "Theory of electroporation: A review," *Bioelectroch Bioenerg*, vol. 41, pp. 135-160, 1996.
[2] M.P. Rols, J. Teissie, "Electropermeabilization of mammalian cells. Quantitative analysis of the phenomenon," *Biophys J*, vol. 58, pp. 1089–1098, 1990.
[3] S. Satkauskas *et al.*, "Mechanisms of in vivo DNA electrotransfer: respective contributions of cell electopermeabilization and DNA electrophoresis," *Mol Ther*, vol. 5, pp. 133-140, 2002.
[4] M. Kanduser, D. Miklavcic., M. Pavlin, "Mechanisms involved in gene electrotransfer using high- and low-voltage pulses: an in vitro study," *Bioelectrochemistry*, vol. 74, pp. 265-271, 2009.

Canine Oral Melanoma - Electrochemotherapy Combined with Standard and CO_2 Laser Surgeries as a Palliative Treatment – Case Report

Julita Kulbacka[1], Joanna Paczuska[2], Nina Rembiałkowska[1], Jolanta Saczko[1]; Zdzisław Kiełbowicz[2], Wojciech Kinda[2], Bartłomiej Liszka[2], Małgorzata Kotulska[3], Natasa Tozon[4], Maja Cemazar[5],

[1]Department of Medical Biochemistry, Medical University of Wroclaw, Chałubińskiego 10, 50-368 Wroclaw, POLAND;[2]Department of Surgery, Wroclaw University of Environmental and Life Sciences, Norwida 31; 50-375 Wrocław, POLAND; [3]Department of Biomedical Engineering, Wroclaw University of Technology, Wybrzeże Wyspiańskiego 27, 50-370 Wroclaw, POLAND; [4]University of Ljubljana, Veterinary Faculty, Small Animal Clinic, Cesta v Mestni log 47, SI-1000 Ljubljana, SLOVENIA; [5]Institute of Oncology, Zaloska 2, SI-1000 Ljubljana, SLOVENIA

INTRODUCTION

Oral melanomas commonly occur in older dogs with darkly pigmented areas of the mouth, tongue and gums. Melanoma is a very aggressive disease and tumours are often very large, frequently invading the surrounding bones of the oral cavity before they are even detected by an owner or veterinarian. The average lifespan of a dog following diagnosis of the most aggressive stage of malignant melanoma is five to eight months. The complete removal of the tumour is difficult and often a part of the dog's jaw has to be removed [1]. Tumour recurrence and metastasis is common with malignant oral tumours. In order to treat aggressive stages of melanoma, oncologists often apply surgical procedures to remove as much of the tumour as possible, as well as any cancerous bone growth. Because the chance of cancer recurrence and rapid metastasis is so high, chemotherapy, immunotherapy or electrochemotherapy (ECT) could be suggested [2]. The available studies indicate that ECT with cytostatics is an effective treatment of various tumours in animals. ECT is quite a simple method with short duration of treatment sessions, low chemotherapeutic doses and insignificant side-effects [3, 4].

ANIMAL

An 11-year-old male crossbreed dog (weight 30 kg) was diagnosed with malignant melanoma of the jaw. Tumour mass filled the whole jaw. There was noted deformation of the jaw and bleeding observed for 2 months. RTG and CT indicated enlarged and distorted submandibular lymph nodes. The patient was diagnosed for stage IV of the disease with spread of metastasis. The dog could not be diagnosed previously because of its high aggressiveness. After a week, when the dog stopped eating, the owner decided for the medical control. The study was performed with approval from the dog owner.

SURGERY-ECT TREATEMENT

The dog was subjected to complete anaesthesia. A primarily standard surgery was performed in order to remove most of the tumour tissue and enable ECT treatment. Then CO_2 laser surgery was performed to limit continuous bleeding. Electrochemotherapy included intravenous and intratumoral administration of bleomycin (Bleomedac, medac Gesellschaft für klinische Spezialpräparate mbH) and exposure of the tumour nodules to electric pulses. Bleomycin was dissolved in physiological saline and applied at concentration of 0.3 mg/kg intravenously and at 3 mg/ml intratumorally. The interval after bleomycin administration before the application of electric pulses was 8 minutes. Two types of electrodes were applied: 1) two-Needle Array (BTX model 532) and 2) Petri Dish Electrode (BTX model 45-0100). In each application of electrodes 8 square wave pulses of 100 µsec, 1Hz were delivered, with the electric field intensity set as 1300 V/cm (302V for petri electrode and 650V for needle electrodes) . After the treatment, the dog was kept in the clinic for about 2 hours. After that, the animal was examined every two weeks in order to evaluate the treatment effectiveness and possible local and systemic side-effects.

RESULTS

Fig.1 presents the dog before and during ECT procedure.

Figure 1: Oral melanoma in dog: **A**) before treatment; **B**) Two-Needle Array electrodes; **C**) during ECT; **D**) ECT with petri dish electrode.

ECT enhanced surgical effect, stopped bleeding during surgery and enabled faster recovery to physiological activities. The protocol combining ECT and surgery seems to be promising in palliative melanoma treatment.

Acknowledgments: This work was supported by the grant PBmn-131 and Statutory Funds of UMED ST-882.

REFERENCES

[1] K. Bowlt, M. Starkey, S. Murphy. Oral malignant melanoma in dogs, *Vet.Times* No.:36, pp:27-29, 2013.
[2] P.J. Bergman. Canine oral melanoma. *Clin Tech Small Anim Pract*. 22(2):55-60, 2007.
[3] M. Cemazar, Y. Tamzali, G. Sersa, N. Tozon, L.M. Mir, D. Miklavcic, R. Lowe, J. Teissie. Electrochemotherapy in veterinary oncology. *J Vet Intern Med*. 22(4): 826-831. 2008.
[4] N. Tozon, V. Kodre, G. Sersa, M. Cemazar. Effective treatment of perianal tumors in dogs with electrochemotherapy. *Anticancer Res*. 25(2A): 839-845, 2005.

Expression of cytosolic DNA sensors after gene electrostransfer of plasmid gWIZ Blank into different tumor cell types

Katarina Žnidar[1], Masa Bošnjak[2], Loree C. Heller[3], Maja Čemazar[1,2]; [1] *Faculty of Health Sciences, University of Primorska, Polje 42, SI-6310 Izola, SLOVENIA* [2] *Department of Experimental Oncology, Institute of Oncology Ljubljana, Zaloska 2, SI-1000 Ljubljana, SLOVENIA* [3] *Frenk Reidy Research Center for Bioelectrics, Old Dominion University Norfolk, VA 23529, USA*

INTRODUCTION

In our preclinical murine tumor models the complete tumor regression, after gene electrotransfer (GET) of control blank plasmid, was observed [1]. This could be due to activation of Pattern recognition receptors (PRRs) by damage-associated molecular patterns (DAMPs) and pathogen associated molecular patterns (PAMPs). PRR signaling can further lead to expression of inflammatory mediators (such as interferon type 1) and consequently to inflammatory response and cell death [2,3].

The aim of this study was to evaluate the effect of empty plasmid gWiz Blank after GET on the expression of DNA PRRs in two different tumor cell types (carcinoma and melanoma), using electroporation.

MATERIALS AND METHODS

After GET (electric pulse generator GT-01, Faculty of Electrical Engineering, University of Ljubljana, Slovenia, 8 pulses, 600 V/cm, 5 ms duration at frequency 1 Hz, plate parallel electrodes with 2 mm gap in between) of plasmid gWiz Blank (2 mg/ml, Aldevron, North Dakota, USA) or plasmid DNA encoding enhanced green fluorescent protein (1 mg/ml, pEGFP, BD Bioscience, Clontech, California, USA) into murine melanoma (B16-F10) and mammary adenocarcinoma (TS/A) cells the transfection efficiency, cytotoxicity and expression of PRRs (RIG-1, DDX60, TLR9, DHX9, DHX36, DAI, p202, AIM, cGAS, DDX41) and cytokine interferon β1 (IFNβ1) was determined.

RESULTS

GET of plasmid pEGFP increased both fluorescent cell number and gene expression level in TS/A cells. GET of pEGFP into B16-F10 cells led to a significant, fivefold greater increase in the number of transfected cells, as well as in a greater median fluorescence intensity than in case of TS/A cells transfection (Fig. 1).

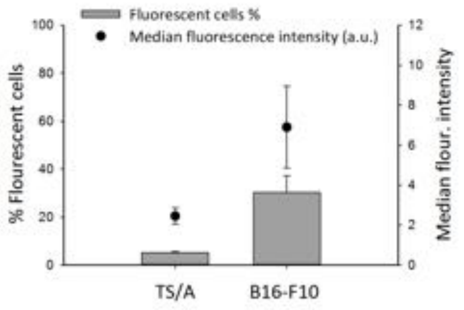

Figure 8: Transfection of B16-F10 and TS/A cells using plasmid pEGFP. *p < 0.05.

Cell survival of both cell types was significantly reduced after GET of different concentrations of plasmid gWiz Blank into the cells (Fig 2.). Compared to TS/A cells, the survival of B16-F10 melanoma cells was significantly lower at all concentrations tested.

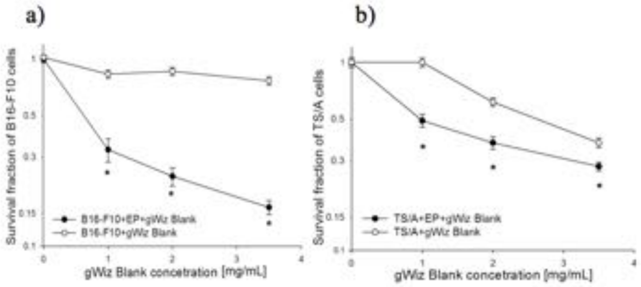

Figure 2: Cell survival curves of B16F10 (a) and TS/A (b) cells after treatment with plasmid gWiz Blank alone or in combination with EP. *p < 0.05.

Increased expression of DNA PRRs mRNAs was observed in both B16-F10 (DDX60, DAI) and TS/A (DDX60, DHX36, DAI) cell lines. In both cell lines, mRNA levels of interferon β1 were also significantly increased.

CONCLUSION

Taken together, GET of an empty plasmid DNA can lead to the increased expression of specific PRRs and cytokine IFNβ1 in B16-F10 and TS/A tumor cells *in vitro*, and could further lead to the reduction of cell survival .

REFERENCES

[1] L. Heller, V. Todorovic, M. Cemazar, Electrotransfer of single-stranded or double-stranded DNA induces complete regression of palpable B16.F10 mouse melanomas. Cancer Gene Ther vol. 20 pp. 695-700, 2013.
[2] CJ. Desmet, KJ. Ishii. Nucleic acid sensing at the interface between innate and adaptive immunity in vaccination. Nat Rev Immunol; vol. 12 pp. 479-491, 2012.
[3] SR. Paludan, AG. Bowie. Immune sensing of DNA. Immunity; vol. 38 pp. 870-880, 2013.

AKNOWLEDGMENT

The research was supported by Slovenian Research Agency and conducted in the scope of LEA EBAM and is a result of networking efforts within the COST TD1104 Action.

Bioflavonoids and menadione mixtures - novel systemic-friendly approach on cancer

Valentin Popescu[1,2], Bogdan Mastalier[2], Irina Baran[1]; [1] *"Carol Davila" University of Medicine and Pharmacy, Department of Biophysics, 8 Eroii Sanitari, 050474 Bucharest, ROMANIA* [2] *Colentina Clinical Hospital, Department of General Surgery, 19-21 Stefan cel Mare Blv., 020125 Bucharest, ROMANIA.*

INTRODUCTION

The potential benefit of using biomaterials that can slowly release quercetin (QC) for treating malignant tumors could revolutionize the treatment of cancer. Quercetin possesses chemo-preventive, anti-cancer, anti-mutagenic, anti-inflammatory, anti-allergenic and anti-microbial properties [1–7]. Menadione (MD) enhances antitumoral properties of quercetine. In this decade, microspheres have become one of the methods to obtain a selective localized drug delivery system for tumor therapies, without or with minimal surgical intervention site.

EXPERIMENTAL METHODS

1. Cell cultures
2. Clonogenic survival assay
3. Fluorescence spectroscopy, for evaluation of oxidative stress,
4. Flow cytometry for evaluating cell apoptosis.
5. QC absorbtion on PCL, and collagen coating of the PCL microspheres [9]

RESULTS AND DISCUSSION

This project is planed in 3 phases: biological proof of the molecular action, development of a nanocarrier able to sustain the optimal mixture at the area of interest in the human body, applying the treatment in clinical trials

QC and MD can be used as potent apoptogens in human leukemia Jurkat cells with an apoptotic cell fraction of 78.3 ± 15% within 48 h following the treatment with QC 15 μM + MD 15 μM. We found a strong synergic interaction between MD and QC leading to efficient cell destruction rate: MD:QC at concentrations 15 μM : 15 μM proved to be highly effective, by inducing a high apoptotic fraction and a clonogenic survival of 1.2% .

The second phase of the study is just in a incipient stage, where our team is searching a partner to make quercetin loaded polycaprolactone microspheres using solvent evaporation method. The complete coating of the surface through adsorption process has the potential of an enhanced effect on improving the bio-integration or compatibility of the implants.

CONCLUSION AND PERSPECTIVES

Natarajan et al obtained an entrapment efficiency of the quercetin onto the PCL-QC microspheres of 62.42 ± 0.55% whereas in collagen coated PCL-QC microspheres was 58.61%. The result indicates the 4% QC loss in the collagen coating process. Combining our results obtained with quercetin and menadione with Natarajan's method of obtaining a microparticulate implant or other method which could embed menadione in the implant could lead to the development of stealth micro/nano injectables as well as implants in that could be targeted and localized drug delivery systems. Our goal is to obtain an implant that can be delivered in to/near the tumor and induce selective apoptosis.

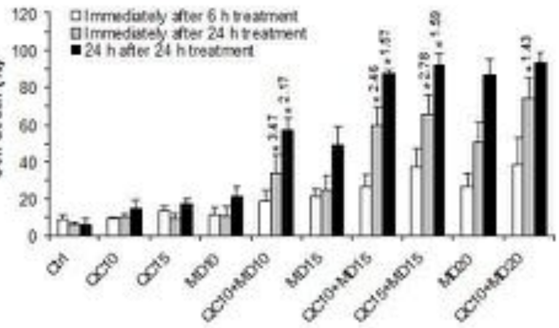

REFERENCES

[1] Murakami A, et al . Multitargeted cancer prevention by quercetin. Cancer Lett 2008;269:315-325.
[2] Chen G, et al Preferential killing of cancer cells with mitochondrial dysfunction by natural compounds. Mitochondrion 2010;10:614-625.
[3] Kelly GS. Quercetin. Altern Med Rev 2011;16:172-194.
[4] Russo M, et al The flavonoid quercetin in disease prevention and therapy: facts and fancies. Biochem Pharmacol 2012;83:6-15.
[5] Chen D, et al Dietary flavonoids as proteasome inhibitors and apoptosis inducers in human leukemia cells. Biochem Pharmacol 2005;69:1421-1432.
[6] Rao YK, et al. Antioxidant and cytotoxic activities of naturally occurring phenolic and related compounds: A comparative study. Food Chem Toxicol 2007;45:1770-1776.
[7] Jeong JH, et al Effects of low dose quercetin: cancer cell-specific inhibition of cell cycle progression. J Cell Biochem 2009;106:73-82.
[8] T.K. Dash, V.B. Konkimalla, J. Control Release (2011), doi:10.1016/j.jconrel.2011.09.064.
[9] V. Natarajan et al. Collagen adsorption on quercetin loaded polycaprolactone microspheres: Approach for "stealth" implant International Journal of Biological Macromolecules *50 (2012) 1091– 1094*

Polymeric membranes in the form of giant lamellar vesicles as possible carrier of functional membrane proteins into viable cells via electrofusion

Gianluca Bello[1], Tina B. Napotnik[2], Lea Rems[2], Damijan Miklavcic[2], Eva K. Sinner[1]; [1] *University of Natural Resources and Life Sciences, BOKU, Institute of Synthetic Bioarchitectures, Department of Nanobiotechnology, DNBT, Muthgasse 11, A-1190 Vienna, AUSTRIA* [2] *Faculty of Electrical Engineering, University of Ljubljana, Trzaska 25, SI-1000 Ljubljana, SLOVENIA*

INTRODUCTION

Many human diseases are related to the malfunction of membrane proteins (MPs) within the cells [1]. MPs can be successfully inserted into polymeric vesicles, so called polymersomes (PS), via cell free protein expression (CFPS) [2], generating proteo-PS. We were able to porate PS without proteins using nanosecond electric field pulses, meaning it might be possible to fuse them with living cell. Consequently the fusion process between proteo-PSs and cells could result in the regeneration of the protein activity in the impaired cell. This innovative methodology presents an alternative method to the genetic modification of cells.

Such a challenging goal requires, first of all, the successful electrofusion of cells and PSs. This process must be achieved by finely tuning the electric field, the buffer conditions and by providing a close contact between cells and PSs.

MATERIALS AND METHODS

We use the amphiphilic copolymer Poly(butadiene)-b-Poly(ethylene oxide) (BdEO) (**Error! Reference source not found.**A) to produce PSs with diameters in the micrometer range via electroformation (EFO) [3]. The large size of PSs allows for their direct visualization by common optical microscopy.

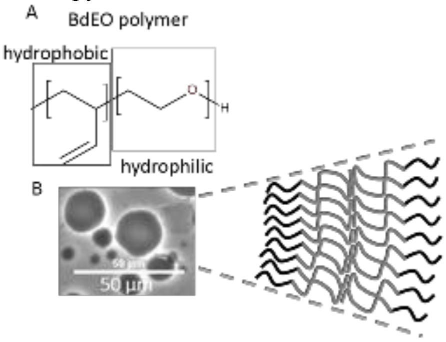

Figure 9 A) diblock copolymer structure B) vesicles of BdEO: hydrophobic (grey) and hydrophilic (black) parts

The PSs are loaded with the fluorescent dye Calcein in order to display the electroporation event. The BdEO polymer is also chemically functionalized with the Dansyl fluorescent dye which will give the possibility to track the fusion of the polymeric bilayer with the cell membrane. P19 and CHO cells will be used to attempt the first electrofusion between polymeric membranes and cells.

RESULTS

The buffers used for the poration of PSs contain different concentrations of Saccharose and NaCl which help to decrease the electric field strength by adjusting the osmotic pressure and the conductivity. Although high solutes concentrations prevent PS formation via EFO, PSs have been successfully produced in such buffers (**Error! Reference source not found.**B).

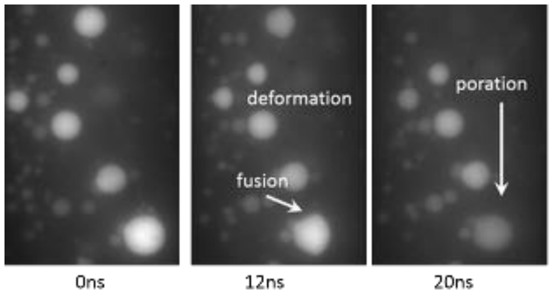

Figure 10 Fusion, deformation and electroporation of PSs filled with Calcein exposed to nanosecond electric pulses

The poration and fusion of polymeric vesicles has been shown (**Error! Reference source not found.**) in preliminary experiments with Calcein-filled PSs. Moreover the close contact between PSs and CHO cells has been achieved by dielectrophoresis.

CONCLUSIONS

PSs present a durable, compatible [4] and novel bilayer system for the electrofusion with living cells. Their poration is a promising result and the fusion with the cells will be attempted with proteo-PSs as well. MPs insertion into polymeric bilayer is and attractive biomedical application for the regeneration of the lost MPs function in impaired cells without genetic modification.

REFERENCES

[1] C.R. Sanders, J.K. Myers, "Disease-related misassembly of membrane proteins", *Annu. Rev. Biophys. Biomol. Struct.*, vol.33, pp 25–51, 2004.

[2] S. May, E.K. Sinner, "In Vitro Expressed GPCR Inserted in Polymersome Membranes for Ligand-Binding Studies", *Angew. Chem.*, vol.52, pp 749-53, 2013

[3] P. Walde, P. Stano,P. "Giant Vesicles: Preparations and Applications",*Chembiochem*, vol.11, pp 848–65, 2010.

[4] S. Li, "Self-Assembled Poly(butadiene)-b-Poly(ethylene oxide) Polymersomes as Paclitaxel Carriers", *Biotech. Prog.*, vol.23, pp 278-85, 2007

REFERENCES

Austrian-Slovenian Lead Agency Joint Project: Electroporation as Method for Inserting Functional Membrane Proteins in Mammalian Cells- funded by Austrian Science Fund (FWF), Austria and Slovenian Research Agency (ARRS), Slovenia.

Is the novel platelet-derivative component viable for non-transfusion use? Challenges and perspectives for a Blood Bank

Ana P Sousa[1], Luís M Redondo [2]; [1]*Portuguese Blood and Transplant Institute, Lisbon, PORTUGAL*
[2]*Lisbon Eng. Sup. Inst., ISEL/GIAAPP, PORTUGAL*

INTRODUCTION

The application of nsPEF in biologic systems is possible although it might induce concerns regarding cell viability and biologic activity as well as potential negative long-term effects (apoptosis). It has been demonstrated that the application of nsPEF behaves as an agonist for platelet activation, inducing morphological changes and stimulating aggregation (1,2). Also, the electric stimulation triggers growth factors release at the same (or higher level) compared with bovine thrombine (3). Those growth factors are involved in wound healing and tissue regeneration (4). Could we propose this approach for producing a new blood component for non-transfusion use?

METHODOLOGY

In our experiment we applied different voltage pulse protocols, consisting on a single pulse each as seen in Table 1, to different platelet samples: Platelet Pools (Pool_LD_AS) and Apheresis Platelets (Aph_LD_AS), introduced in the 0.8 ml electroporation cuvettes, at a distance of 0.4 cm between the electrodes. We measured the voltage and the current for each protocol and subsequently we observed the platelets under a contrast phase microscope at a magnification of x800 (times). We also performed a platelet histogram.

Table 1: Electric protocols.

Protocol n°	U [V]	I [A]	E [V/cm]	t [µs]	W [J]	ΔT [°C]
1	5	0.18	12.5	$30*10^6$	27	8
2	3500	250	8750	5	4.4	1.3
3	2000	140	5000	50	14	4.1

RESULTS

Even though the differences between using these protocols with Pools and Apheresis Platelets were not significant we did take note of a few alterations. In Aph_LD_AS we observed a 48% increase in the MPV and an apparent decrease in the PLT content when applied a continuous voltage. The histogram indicates an increase of large PLTs. Considering the application of protocols 1 and 2 we observed an increase in MPV of 26% and the phase microscope micrographs show evidence of some microaggregates. Considering the Pool_LD_AS and continuous (1) voltage there was a 40% reduction in the number of PLTs and 5% increase in the MPV. In the protocols 2 and 3 we identified a 7% increase in the MPV and a rise in PLC-R.

CONCLUSION

None of these parameters (except the volume/concentration) are mandatory by the 34/CE/2004 Directive or recommended by EDQM (European Directorate for the Quality of Medicines and Healthcare). Probably, considering the ex-vivo manipulation of platelets, new requirements might be defined.

REFERENCES

[1] P Sousa, Marcos T Pereira, Luis M Redondo. "Impact of Pulsed Electric Fields in Standard Platelet Components", 11^{th} International Bioelectrics Symposium, Columbia, 2014
[2] Jue Zhang *et al*. "Nanosecond pulse electric field (nanopulse): A novel non-ligand agonist for platelet activation, Archives of Biochemistry and Biophysics 471 (2008) 240-248
[3] Andrew S Torres *et al*. "Platelet activation using electric pulse stimulation: growth factor profile and clinical implications", J Trauma Acute Care Surg., 77, 3, Supplement 2
[4] Laura Mazzucco *et al*." Platelet-Derived factors involved in Tissue Repair-From signal to function", Transfusion Medicine Reviews, 24, 3, 2010:218-234

Use of Pulsed Electric Fields and Ultrasound for the Microbial Inactivation of an Enzymatic Preparation from Porcine Pancreas

Paula Navarro[1], James G. Lyng[1], Paul Whyte[2], Michael O'Sullivan[1]; [1] *School of Agriculture and Food Science, University College Dublin, Belfield Campus, IRELAND*. [2] *School of Veterinary Medicine, University College Dublin, Belfield Campus, IRELAND*.

INTRODUCTION

Porcine pancreas is the main source of a digestive enzyme preparation called 'pancreatin' that is widely used as a 'dietary supplement' for people suffering from pancreatic insufficiency. In recent years much of the research effort has focused on improving the efficiency of the production process used for this product (i.e. reducing processing times, enhancing yield, reducing initial microbial loads on starting material, controlling microbial load increases during extraction and reducing or even eliminating the use of organic solvents associated with its extraction). Novel technologies such as high voltage pulsed electric fields (PEF) and high intensity ultrasound (US) could also have a role to play in this regard. Both can induce physical disruption at a cellular level though by very different mechanisms (electroporation and acoustic cavitation, respectively). These technologies are widely accepted for microbial control (vegetative cells particularly) in liquids [1] though reports of their ability to inactivate enzymes have also been reported [2, 3]. Interestingly, recent attempts in University College Dublin (UCD) to inactivate pancreatic enzymes using PEF have shown poor results in this regard, which would very useful in the current context. PEF could then be used to control microorganisms during the extraction of these enzymes while retaining enzyme activity. The principal objective of this project is to evaluate the use of PEF and US on the microbial quality of active enzyme preparations from porcine pancreas.

MATERIAL AND METHODS

Porcine pancreas are provided in a frozen state by an approved abattoir (Ireland) and stored frozen at -20 °C in UCD.

The pancreatin extract is prepared by standard homogenisation/extraction procedure in bicarbonate buffer following a modified version of the procedure discovered by El Abboudi *et al*. [4].

Microbial characterisation of the porcine pancreases and pancreatin extracts prepared therefrom, will be determined using a range of standardised methods for the detection, isolation and enumeration of at least, the following microbial genera/species: *Bacillus cereus* (ISO7932), *Clostridium perfringens* (ISO7937), *Listeria monocytogenes* (ISO11290-1), *Escherichia coli* (ISO16649), Enterobacteriaceae (ISO 21528), *Salmonella* spp. (ISO6579) and total mesophilic aerobic count (IS06579). This will provide baseline information that will enable subsequent studies to be carried out to assess the impact of novel processing technologies on microbial profiles of extracts.

Porcine pancreases and extracts prepared from these specimens will be inoculated with defined populations of common microbial contaminants found in these tissues. Samples will be treated with PEF and US using a range of parameters and the effects on levels of these bacteria will be assessed and compared with non-processed samples.

RESULTS

Work on this project has recently commenced. Standard methods for detecting and enumerating target microorganisms have been selected. Optimisation of enzyme extraction techniques and parameters for PEF and US are currently underway. Preliminary data will be generated over the coming months.

CONCLUSIONS – FUTURE IMPACT

A successful outcome of recovering microbiologically safe functional protein co-products from meat processing streams will represent a significant opportunity to enhance the economic performance and improve the environmental impact of the Irish meat Industry. It will also generate technical know-how to develop functional co-products with applications in food, beverage, health and biomedical engineering.

ACKNOWLEDGEMENTS

This work forms part of the ReValueProtein Research Project (Grant Award No. 11/F/043) supported by the Department of Agriculture, Food and the Marine (DAFM) under the National Development Plan 2007–2013 funded by the Irish Government.

REFERENCES

[1] P. Mañas and R. Pagán, "Microbial inactivation by new technologies of food preservation" *Journal of Applied Microbiology*, vol. 98, pp. 1387-1399, 2005.

[2] S. Min, G. Akdemir and H .Q. Zhang, "Pulsed Electric Fields: Processing System, Microbial and Enzyme Inhibition, and Shelf Life Extension on Foods" *IEEE Transactions on Plasma Science*, vol. 35, pp. 59-73, 2007.

[3] M. N. Islam, M. Zhang and B. Adhikari, "The inactivation of enzymes by ultrasound-a review of potential mechanism" *Food Reviews International*, vol. 30, pp. 1-2, 2014.

[4] M. El, Abboudi, M. Beaulieu and F. Bellavance, "Method for producing pancreatin which contains low amounts of residual organic solvent and product thereof," U.S. Patent 5861291, Jan. 19, 1999.

Faculty members

Damijan Miklavčič

University of Ljubljana, Faculty of Electrical Engineering, Tržaška 25, SI-1000 Ljubljana, Slovenia

E-mail: damijan.miklavcic@fe.uni-lj.si

Lluis M. Mir

UMR 8532 CNRS-Institut Gustave-Roussy, 39 rue Camille Desmoulins, F-94805 Villejuif Cédex, France

E-mail: Luis.MIR@gustaveroussy.fr

Marie-Pierre Rols

IPBS UMR 5089 CNRS, 205 route de Narbonne, F-31077 Toulouse, France

E-mail: marie-pierre.rols@ipbs.fr

Gregor Serša

Institute of Oncology, Zaloška 2, SI-1000 Ljubljana, Slovenia

E-mail: gsersa@onko-i.si

Mounir Tarek

UMR CNRS 7565 Nancy –Université, BP 239 54506 Vandœuvre-lès-Nancy Cedex,France

E-mail: mounir.tarek@univ-lorraine.fr

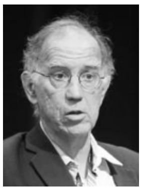

Justin Teissié

IPBS UMR 5089 CNRS, 205 route de Narbonne, F-31077 Toulouse, France

E-mail: justin.teissie@ipbs.fr

P. Thomas Vernier

Old Dominion University, Frank Reidy Center for Bioelectrics, 442 Research Park Ii, Norfolk, VA 23529, USA

E-mail: pvernier@odu.edu